
Markov Processes linking Thermodynamics and Turbulence

Dissertation

Institut für Physik
Fakultät für Mathematik und Naturwissenschaften
Carl von Ossietzky Universität Oldenburg

Dipl.-Phys. Daniel Nickelsen

geboren am 15.01.1983 in Bredstedt

Erstgutachter: **Prof. Dr. Andreas Engel**

Zweitgutachter: **Prof. Dr. Joachim Peinke**

Tag der Disputation: **05.08.2014**

Abstract

This thesis deals with Markov processes in stochastic thermodynamics and fully developed turbulence.

In the first part of the thesis, a detailed account on the theory of Markov processes is given, forming the mathematical fundament. In the course of developing the theory of continuous Markov processes, stochastic differential equations, the Fokker-Planck equation and Wiener path integrals are introduced and embedded into the class of discontinuous Markov processes. Special attention is paid to the difficulties that arise in the case of multiplicative noise.

Referring to the paradigm of Brownian motion, the thermodynamic quantities work, heat and entropy, and the accompanied first law and second law, are formulated on the level of individual trajectories using stochastic differential equations.

One of the prominent results of stochastic thermodynamics are so-called fluctuation theorems which reveal an intimate relation between entropy production and irreversibility. Using the path integral formulation, fluctuations theorems are derived in a formal setting.

Applications of fluctuation theorems to thermodynamic systems are dependent on a reliable statistics of rare events. To access the statistics of rare events, an asymptotic method is developed. The first order asymptotics is derived for the general case of multiplicative noise, the second order asymptotics for the simpler case of additive noise. The application of the asymptotic method is demonstrated for work distributions in physically relevant models.

The second part of the thesis carefully introduces the concept of fully developed turbulence and gives an account on established theories. These theories can be reformulated in terms of Markov processes. An overview of these Markov representations is compiled, including a few new approaches.

In view of the results of stochastic thermodynamics, implications for the Markov representation are exploited. Fluctuation theorems are derived and applied to experimental data. In an experimental as well as theoretical analysis, fluctuation theorems are found to be sensitive to intermittent small-scale fluctuations. The above mentioned asymptotic method is used to assess these fluctuations.

In closing the thesis, the discussed approaches to fully developed turbulence are contrasted with each other using their Markov representations, and an interpretation of the respective Markov processes is offered.

Zusammenfassung

Diese Dissertation beschäftigt sich mit Markov Prozessen in stochastischer Thermodynamik und voll entwickelter Turbulenz.

Der erste Teil der Arbeit führt ausführlich in die Theorie der Markov Prozesse ein. Die Darstellung dieses mathematischen Grundgerüsts schließt stochastische Differentialgleichungen, die Fokker-Planck Gleichung und Wiener Pfadintegrale ein. Diese dadurch beschriebenen stetigen Markov Prozesse werden in die Formulierung unstetiger Markov Prozesse eingebettet. Ein besonderes Augenmerk ist dabei auf die Komplikationen gerichtet, die sich für den Fall multiplikativen Rauschens ergeben.

In Bezug auf das Musterbeispiel Brown'scher Bewegung werden aus stochastischen Differentialgleichungen Arbeit, Wärme und Entropie, und die damit einhergehenden ersten beiden Hauptsätze der Thermodynamik auf der Ebene individueller Trajektorien eingeführt.

Herausragende Ergebnisse stochastischer Thermodynamik sind sogenannte Fluktuationstheoreme, die die enge Beziehung zwischen Entropieproduktion und Irreversibilität deutlich machen. Die Fluktuationstheoreme werden formal aus der Pfadintegral-Formulierung hergeleitet.

Die Anwendungen der Fluktuationstheoreme auf thermodynamische Systeme ist abhängig von einer zuverlässigen Statistik seltener Ereignisse. Um die Statistik seltener Ereignisse zugänglich zu machen, wird eine asymptotische Methode entwickelt. Die Asymptotik erster Ordnung wird für den allgemeinen Fall multiplikativen Rauschens hergeleitet, die Asymptotik zweiter Ordnung für additives Rauschen. Die Anwendung der asymptotischen Methode wird für Arbeitsverteilung in physikalisch relevanten Modellen demonstriert.

Der zweite Teil der Arbeit führt sorgfältig in das Konzept voll entwickelter Turbulenz ein und verschafft einen Überblick über etablierte Theorien. Diese Theorien können auch als Markov Prozesse formuliert werden. Es wird eine Zusammenstellung dieser Markov Darstellungen angefertigt, die auch ein paar neue Ansätze einschließt.

In Hinblick auf Ergebnisse der stochastischen Thermodynamik wird ihre Bedeutung für die Markov Darstellung ausgewertet. Fluktuationstheoreme werden berechnet und auf experimentelle Daten angewandt. Sowohl hinsichtlich einer experimentellen als auch einer theoretischen Untersuchung stellt sich heraus, dass Fluktuationstheoreme dem Auftreten intermittenter klein-skaliger Fluktuationen Rechnung tragen. Unter Benutzung der oben genannten asymptotischen Methode werden diese Fluktuationen beurteilt.

Abschließend werden die besprochenen Theorien voll entwickelter Turbulenz anhand ihrer Markov Darstellung gegenübergestellt, und eine Interpretation der entsprechenden Markov Prozesse wird unterbreitet.

Contents

Introduction	1
I Stochastic Thermodynamics	5
I.1 Markov Processes (MPs)	7
I.1.1 Stochastic differential equations (SDEs)	8
I.1.2 The Fokker-Planck equations (FPE)	16
I.1.3 Wiener path integrals (WPIs)	23
I.1.4 Discontinuous Markov processes	28
I.2 Thermodynamic interpretation of continuous MPs	37
I.2.1 Energy balance and the first law	38
I.2.2 Entropies and the second law	45
I.2.3 Fluctuation theorems and irreversibility	55
I.2.4 Applications	67
I.3 Asymptotic analysis	75
I.3.1 Gauß approximation (GA)	75
I.3.2 The asymptotic method	77
I.3.3 Euler-Lagrange equations	79
I.3.4 The pre-exponential factor	80
I.4 Conclusions	103
II Universal features of turbulent flows	107
II.1 General theory	109
II.1.1 The Navier-Stokes equation (NSE)	109
II.1.2 Turbulence generation and decay	112
II.1.3 Energy budget	115
II.2 Fully developed turbulence	117
II.2.1 Homogeneity, Isotropy, Stationarity	117
II.2.2 Energy cascade	124
II.2.3 Scaling laws	128

II.2.4	Small-scale intermittency	133
II.3	Markov analysis	149
II.3.1	Interpretation as stochastic process	149
II.3.2	Drift and diffusion	154
II.3.3	Experimental investigations	167
II.4	Fluctuation theorems and irreversibility	173
II.4.1	Experimentally estimated versus K62	173
II.4.2	Beyond K62 scaling	183
II.5	Asymptotic analysis	193
II.5.1	Realisations of extreme entropy	193
II.5.2	Asymptotic $p(u, r)$ and ζ_n	198
II.6	Closing discussion	207
II.6.1	Classification	207
II.6.2	Interpretation	209
II.6.3	Possible future studies	213

Conclusions **217**

A Technical details of continuous MPs **243**

A.1	Itô calculus	245
A.2	Transformation of time in a SDE	249
A.3	Derivation of FPE from SDE	253
A.4	Derivation of WPI from SDE	259
A.5	Overview of SDE, FPE and WPI	267

Introduction

In the preceding century, two branches of physics¹ have been advanced considerable.

One branch is the theory of Brownian motion, pushed forward by Einstein, Smoluchovski and Langevin in the beginning of the preceding century, and from which in the last 20 years the developing field of stochastic thermodynamics emerged.

The other branch is studying universal features of turbulent flows, initiated by Kolmogorov and Obhukov who addressed scaling laws for the statistics of fluctuations of flow velocity and coined the conception of cascading turbulent structures.

The motion of a Brownian particle suspended in a fluid is a continuous Markov process, which means that the current state of the particle only depends on the most recent event. The events in Brownian motion are collisions between particle and fluid molecules, provoking an irregular and random motion of the particle. Brownian motion is observable for tiny particles for which it is not unlikely that fluid molecules collide predominantly with only one side of the particle, kicking the particle to the other side. For large particles, too many molecules are involved in the collisions, such that a possible excess of collisions on one side of the particle is negligible.

The incidents in which the small particles are kicked forward constitute to a local rectification of thermal noise, cooling down the fluid molecules involved in the collision, and thus *consuming* entropy. On the other hand, fast particles collect significant more collisions on its front side than on its backside, provoking a friction that slows down the particle. Due to this friction, decelerating particles entail a local heating of the fluid, and thus *produce* entropy. The balance between entropy consuming and entro-

¹And many others, of course.

py producing collisions are quantified by so-called *fluctuation theorems*, which are prominent results of *stochastic thermodynamics*.

Stochastic thermodynamics is the thermodynamics of nanoscopic systems which may be arbitrarily far from equilibrium. The smallness of the systems is crucial in order to observe the entropy consuming events as exemplified for the Brownian particle, and non-equilibrium can be imposed by driving the particle with an external force or preparing a non-equilibrium initial state. Stochastic thermodynamics extends the first law and the second law to the level of individual trajectories of nanoscopic systems with non-equilibrium dynamics.

The fluctuation theorems are used to extract equilibrium information from non-equilibrium measurements, a procedure being dependent on a sufficient occurrence of the entropy consuming events in the system. Methods to assess the entropy consuming events, or to correct for an insufficient sampling of the rare events, are focus of current research.

Universal features of turbulent flows are traditionally sought in the scaling properties of the moments of velocity fluctuations in the flow. Less than 20 years ago, a new approach to characterise turbulent flows has been suggested, in which spatial fluctuations of flow velocity are modelled by a Markov process. These Markov processes address the repeated break-up of turbulent structures due to the non-linear interactions in the flow. The individual trajectories are probes of the spatial structures of the flow, or more specific, velocity fluctuations on different spatial scales. The evolution of these structures towards smaller scales is captured by the conception of *turbulent cascades*.

Though valid on a macroscopic scale, stochastic thermodynamics does usually not provide more insights when applied to macroscopic systems. Therefore, since turbulent flows are of rather macroscopic dimension, the implications of the results of stochastic thermodynamics for the Markovian approach to turbulent flows are rather unexplored. However, it has proved recently that fluctuation theorems implied by the Markov representation of turbulent cascades do apply for a surprisingly small ensemble of probes.

The formulation of turbulent cascades as Markov processes raise intriguing questions. Acquire the formal expressions for entropy productions a meaningful form for turbulent cascades? What is the statement of the

associated second law? What do the entropy consuming trajectories look like? Under what conditions do entropy consuming trajectories arise sufficiently often to allow a practical use of fluctuation theorems? What are possible applications of fluctuation theorems for characterisations of turbulent flows? Can the rare events in a turbulent flow be assessed?

The aim of this thesis is to find answers to such questions.

The first part of the thesis introduces the relevant aspects of the theory of Markov processes, and elucidates the thermodynamic interpretation of Markov processes in the framework of stochastic thermodynamics.

The second part introduces to the basic theory of turbulence and compiles the Markov representation of established approaches to turbulence, combining a survey of existing results and a report of novel Markov representations. On the basis of the introduced Markov representations, the above questions are tackled.

Each part is divided into chapters, which are in turn divided into sections.

To be able to transfer results of stochastic thermodynamics to turbulence, the involved concepts have to be well understood. In contradiction to the usual thermodynamic setting, the Markov representations of turbulent cascades are always characterised by a diffusion that depends on the current state of the process, which entails ambiguities and technical difficulties. A special focus of the first part of the thesis is therefore the implications of state dependent diffusion, and consequently, the theory of stochastic thermodynamics is introduced on the abstract level of arbitrary diffusion. To maintain intuition, the paradigm of Brownian motion serves as an intuitive example whenever appropriate.

This thesis is publication based and includes three peer-reviewed publications [1–3]. Some aspects elucidated in the included publications are also discussed in the main text to allow a fluent introduction to stochastic thermodynamics and the theory of turbulence, and to maintain the central theme of the thesis.

Bringing together two rather distinct fields of research, each of which treated in a separate part of the thesis, the publications are included into the respective parts. The central results are given by the publications, a couple of minor, unpublished results are included in the main text.

I Stochastic Thermodynamics

The properties of nanoscopic systems can not be described by equilibrium thermodynamics. Examples of nanoscopic systems include colloidal particles, biological cells and nanoscopic devices. Characteristic for nanoscopic systems is the stochasticity in their degrees of freedom. The developing field of stochastic thermodynamics addresses the thermodynamic properties of these systems, taking into account the stochasticity and, in addition, remains valid in situations arbitrarily far from equilibrium. In the last 20 years, stochastic thermodynamics has put forth intriguing results, a prominent example being the relation between entropy production and irreversibility on the level of individual trajectories.

The mathematical fundament of stochastic thermodynamics is the theory of Markov processes which will be introduced in the first chapter of this part. The second chapter explicates the thermodynamic interpretation of Markov processes, including the first and second law of thermodynamics, and an account on applications of the so-called fluctuation theorems. The third chapter introduces an asymptotic method and exemplifies its use in models relevant for the application of fluctuation theorems.

I.1 Markov Processes (MPs)

In this chapter we introduce the theory of Markov processes (MPs) which forms the mathematical basis of this thesis. The basic material will mainly build on the books by Gardiner [4] and van Kampen [5] on stochastic processes, the book by Chaichian and Demichev on path integrals [6], and the article by Lau and Lubensky on state dependent diffusion [7].

A Markov process is a subclass of stochastic processes which involve a time dependent random variable $X(t)$. The random variable is not restricted to one dimension, but we will primarily consider Markov processes with one degree of freedom. A realisation of a stochastic process $X(t)$ is a sequence of measured values x_1, x_2, x_3, \dots at times $t_1 > t_2 > t_3 > \dots$, completely described by the joint probability density function (PDF)

$$p(x_1, t_1; x_2, t_2; x_3, t_3; \dots) . \quad (\text{I.1.1})$$

If the stochastic process is a MP, the necessary information to define the process uniquely reduces to univariate PDFs.

A stochastic process is qualified as a MP by the *Markov assumption*. The Markov assumption states that conditioned on having measured values y_1, y_2, \dots at times $\tau_1 \geq \tau_2 \geq \dots$, the probability of measuring x_1, x_2, \dots at later times $t_1 \geq t_2 \geq \dots$ will only depend on the most recent measured value y_1 :

$$p(x_1, t_1; x_2, t_2; \dots | y_1, \tau_1; y_2, \tau_2; \dots) = p(x_1, t_1; x_2, t_2; \dots | y_1, \tau_1) . \quad (\text{I.1.2})$$

This definition of a MP implies that we can write for the joint PDF

$$\begin{aligned} p(x_1, t_1; x_2, t_2; x_3, t_3; \dots x_n, t_n) & \quad (\text{I.1.3}) \\ &= p(x_1, t_1 | x_2, t_2) p(x_2, t_2 | x_3, t_3) \cdots p(x_{n-1}, t_{n-1} | x_n, t_n) p(x_n, t_n) , \end{aligned}$$

now defined solely by the conditional PDF $p(x_{i-1}, t_{i-1} | x_i, t_i)$ and the univariate PDF $p(x_n, t_n)$ with $t_{i-1} > t_i$.

A direct consequence of the Markov assumption is the *Chapman-Kolmogorov equation* (CKR)

$$p(x_1, t_1 | x_3, t_3) = \int p(x_1, t_1 | x_2, t_2) p(x_2, t_2 | x_3, t_3) dx_2 . \quad (\text{I.1.4})$$

The CKR states that the transition probability from time t_3 to t_1 can be subdivided into transition probabilities from t_3 to t_2 and then from t_2 to t_1 . Such a sequence of realisations (x_1, x_2, x_3, \dots) , in which each realisation x_i determines the probability to observe the next realisation x_{i+1} , is commonly referred to as a Markov chain.

Markov processes can be subdivided into continuous and discontinuous components. This distinction addresses the values of $X(t)$ at infinitesimal time steps which will be rendered more precisely in the course of this chapter.

Regarding the time variable t , the above introduction suggests that time is discrete. In fact, the model equations for Markov processes used in this thesis assume that time is continuous. This assumption does not hold for realistic MPs, since any real stochastic process will have a time scale t_{ME} below which the Markov assumption does not hold. We will call t_{ME} the *Markov-Einstein time scale*, for reasons which will be discussed in the following section.

We will start in section I.1.1 with Brownian motion, from which intuitively a stochastic differential equation (SDE) arises, the *Langevin equation* (LE). The thus motivated SDEs will then be formally defined and discussed. In sections I.1.2 and I.1.3, we introduce two equivalent formulations of MPs, the Fokker-Planck equation (FPE) and Wiener path integrals (WPI). Until then, only continuous MPs are considered. In section I.1.4 we will come back to the CKR and show how continuous MPs fit into the greater class of MPs that also involve discontinuous realisations. In the appendix, A.1-A.5, we provide additional material regarding continuous Markov processes.

I.1.1 Stochastic differential equations (SDEs)

The Langevin equation (LE) In 1908, Paul Langevin was the first to set up a SDE, in an attempt to simplify Albert Einstein's theory of Brownian motion [8], which Einstein formulated in 1905 [9]. Langevin considered spherical particles suspended in a medium (fluid), on which an external force F_{ex} acts (e.g. gravity). Denoting the centre of mass by x and ignoring effects of the medium, Newton's equation of motion reads

$$m\ddot{x}(t) = F_{\text{ex}}(x(t)) , \quad (\text{I.1.5})$$

where dots denote derivatives with respect to time t , and m is the mass of the particle.

For spherical particles in a fluid, it is known that the particles experience a frictional force F_{fr} proportional to the velocity of the particles ([10] p. 70ff),

$$F_{\text{fr}} = -\gamma \dot{x}, \quad \gamma := 6\pi\nu R. \quad (\text{I.1.6})$$

Here, ν is the dynamic viscosity and R is the radius of the particle. The above equation is known as *Stoke's law*, and γ is referred to as friction coefficient. Stoke's law holds at laminar flow conditions (that is, small Reynolds numbers $\text{Re} = R\dot{x}/\nu$).

It is clear that due to this friction, the particles will eventually come to rest. Sufficient small particles, however, exhibit an ongoing irregular motion, observed by Robert Brown in 1827, and is hitherto known as Brownian motion. The origin of this motion is the thermal energy of the fluid, due to which the fluid molecules hold a kinetic energy of the order of magnitude $k_{\text{B}}T$ where k_{B} is Boltzmann's constant and T is the temperature of the fluid. If the particles are small enough, the kinetic energy transferred by collisions from the fluid molecules to the particles results into an observable irregular motion.

In his approach to Brownian motion, Langevin considered a thermal force

$$F_{\text{th}} = \sqrt{2\gamma k_{\text{B}}T} \xi(t) \quad (\text{I.1.7})$$

acting on the particles, where $\xi(t)$ is a δ -correlated random variable sampled from a Gaussian distribution with zero mean and infinite variance. Due to its δ -correlation, $\xi(t)$ is also called Gaussian white noise. The pathological properties of $\xi(t)$ are elucidated in the appendix, and the main consequences will be discussed shortly.

Including the frictional and the thermal force into Newton's equation (I.1.5), we arrive at the *Langevin equation* (LE)

$$\ddot{x}(t) + \gamma \dot{x}(t) = -V'(x(t)) + \sqrt{2\gamma k_{\text{B}}T} \xi(t). \quad (\text{I.1.8})$$

Here we assumed that $F_{\text{ex}}(x)$ arises from a potential $V(x)$, $F_{\text{ex}}(x) = -V'(x)$, which can always be achieved in one dimension, and we set $m := 1$ (force is measured in units of acceleration). Note that the unit of $\xi(t)$ is $1/\sqrt{\text{s}}$.

The LE illustrates the interplay between damping of the particles due to frictional effects and energy injection to the particles by thermal kicks: The frictional effects withdraw kinetic energy from the particle, energy that is received by the fluid and in turn passed back to the particles as thermal fluctuations. Hence, even in the absence of an external force, Brownian particles exhibit an ongoing irregular motion.

The thermal energy $k_B T$ entering the thermal force is intuitive, whereas the occurrence of the friction coefficient γ , proportional to R and ν , see (I.1.6), is counter-intuitive. Whereas it is clear that for larger particles both the friction coefficient and the ability to absorb thermal fluctuations increase, it appears dubious that the fluid molecules should exert stronger forces on the Brownian particle for increased viscosity. We unravel this paradox² by arguing that with higher viscosity, the collisions between fluid molecules and Brownian particle become more inelastic, and consequently, more heat is transferred to the fluid, which, in order to maintain the constant temperature T , is in return received by the Brownian particle through an increased strength of kicks by the fluid molecules. This fast equilibration mechanism is coarse grained as Gaussian white noise, and γ should in that context merely be thought of a coupling coefficient between fluid and particle.

The assumption that $\xi(t)$ is on average zero, accounts for the fact that a resting particle experiences decelerating and accelerating collisions in equal measures. The excess of decelerating collisions for a moving particle is taken into consideration by the frictional force. As a rising temperature increases the decelerating and accelerating collisions in equal shares, the temperature does not enter the frictional force.

The above considerations suggest that fluctuating forces and dissipative forces have the same origin - the collisions with fluid molecules. This interrelation of fluctuation and dissipation is the essence of fluctuation-dissipation theorems, which in its simplest form is the Einstein relation

$$D = \frac{k_B T}{\gamma} , \tag{I.1.9}$$

²In Langevin's derivation the magnitude of the thermal force arises from satisfying the equipartition theorem [8].

where D is the diffusion constant [9]. The Einstein relation expresses that the diffusion of a particle is a result of both thermal fluctuations and frictional dissipation.

The diffusion of particles was subject of research before Einstein derived (I.1.9) from his theory of Brownian motion. In the course of that research, Adolf Fick derived in 1855 ([4] p. 336)

$$j(x, t) = -D \partial_x p(x, t) , \quad (\text{I.1.10})$$

where $j(x, t)$ measures the flux of particles per area and time, and $p(x, t)$ is the particle density. The determination of the diffusion constant by Einstein in 1905 given by (I.1.9) revealed the rather unexpected relation between friction and diffusion and was confirmed by Smoluchovski (1906) and by Langevin (1908). The more general fluctuation-dissipation theorems are part of response theory, we direct the interested reader to the recent overview article by Marconi et al. [11].

Fick's law (I.1.10) can be generalised to diffusing particles subject to external forces, which leads to an evolution equation for $p(x, t)$ where only force and diffusion enter. This equation is known as Fokker-Planck equation, to which we will come back in the next section.

We return to the LE. For particles with small mass, frictional effects prevail over inertial effects. In this so-called *overdamped limit*, the inertial term is negligible, and we obtain the *overdamped* LE

$$\gamma \dot{x}(t) = -V'(x(t)) + \sqrt{2\gamma k_B T} \xi(t) . \quad (\text{I.1.11})$$

The overdamped LE is often given in terms of velocities,

$$\begin{aligned} \dot{x}(t) &= -\Gamma V'(x(t)) + \sqrt{2k_B T \Gamma} \xi(t) \\ &= -\Gamma V'(x(t)) + \sqrt{2D} \xi(t) , \quad D = k_B T \Gamma , \end{aligned} \quad (\text{I.1.12})$$

where $\Gamma = 1/\gamma$ is the mobility of the particle, and $-\Gamma V'(x)$ is now the *drift velocity* and $\sqrt{2k_B T \Gamma} \xi(t)$ accounts for abrupt changes in velocity after collisions with fluid molecules. In this form, the occurrence of the mobility Γ in both the drift and diffusion term is intuitive, which in retrospect justifies the dependency of the thermal force $\sqrt{2\gamma k_B T} \xi(t)$ in (I.1.11) on γ .

It can be shown that the solutions of the LE (I.1.12) are continuous Markov processes ([4] p. 92). Brownian motion itself, however, is not a Markov

process on arbitrary time scales, since the Markov assumption does not hold for the detailed dynamics of the collisions. But the outcome of each collision does only depend on the initial condition of this collision, that is on only the most recent collision, which is precisely the Markov assumption. The time scale t_{ME} above which Brownian motion can be assumed to be Markovian is therefore of the same order of magnitude as the mean time between collisions. Referring to Einstein's theory of Brownian motion, the time scale t_{ME} above which a process is Markovian is often called *Markov-Einstein scale*.

Stochastic calculus Bridging Brownian motion to the theory of Markov processes brings us back to the formal level. We will return to the intuitive picture in chapter I.2.

On the formal level, $x(t)$ is now a continuous degree of freedom in a MP, and the LE is a *stochastic differential equation* (SDE). The general form of a SDE reads

$$\dot{x}_t = f(x_t, t) + g(x_t, t) \xi(t) , \quad x(t = t_0) = x_0 , \quad (\text{I.1.13a})$$

$$\langle \xi(t) \rangle = 0 , \quad \langle \xi(t) \xi(t') \rangle = \delta(t - t') , \quad (\text{I.1.13b})$$

where for clarity $x(t)$ is denoted by x_t . In view of the inherent time scale separation of realistic Markov processes, the white noise $\xi(t)$ is not exactly δ -correlated, but rather of the form

$$\langle \xi(t) \xi(t') \rangle \sim \frac{1}{t_{\text{ME}}} e^{-\frac{|t-t'|}{t_{\text{ME}}}} . \quad (\text{I.1.14})$$

In this case, the noise is called *coloured* noise. In the limit $t_{\text{ME}} \rightarrow 0$, the *white-noise limit*, the exponential function becomes the δ -function $\delta(t - t')$. Solving SDEs for time-steps $\Delta t < t_{\text{ME}}$ is therefore an interpolation of the real process to non-Markovian time scales.

By the attempt to solve a SDE, however, we encounter a problem. Naive integration yields

$$x(t) - x(t_0) = \int_{t_0}^t f(x_\tau, \tau) d\tau + \int_{t_0}^t g(x_\tau, \tau) \xi(\tau) d\tau . \quad (\text{I.1.15})$$

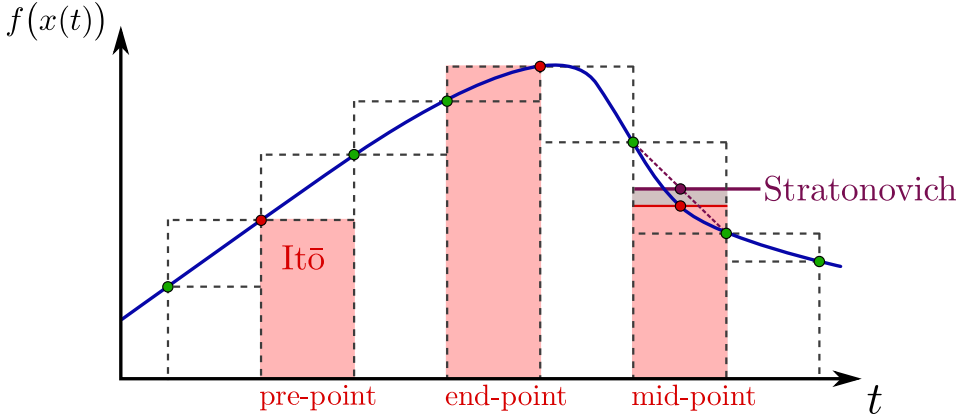


Figure I.1: Discretisation rules and conventions. The integrand of a stochastic integral is given as the blue line (for clarity, as a smooth function). The vertical and horizontal dashed lines indicate lower and upper sums. The coloured circles mark the discretisation intervals. The red circles exemplary designate points taken for pre-point, mid-point and end-point, the light-red coloured areas are the resulting rectangles to approximate the integral. The Itô convention is identical with the pre-point rule, and the Stratonovich convention, added as purple symbols, is identical with the trapezoidal rule.

Due to the stochastic variable $x(t)$, the above integrals are *stochastic integrals* for which the usual Riemann definition of an integral is not suitable. The consequence is that, in the continuous limit, the value of the stochastic integral is not unique, depending on whether we define the integral as a lower sum or upper sum. We will therefore parametrise the value of stochastic integrals with α , where $\alpha = 0$ corresponds to taking the value of the integrand at the beginning of each discretisation interval, $\alpha = 1$ to the end of each interval, and $0 < \alpha < 1$ to somewhere in-between. The two mostly used definitions of stochastic integrals are the *pre-point* rule ($\alpha = 0$) and the *mid-point* rule ($\alpha = 1/2$). See figure I.1 for an illustration.

It is clear that, since the stochastic integrals in (I.1.15) depend on α , also the solution of the SDE will depend on α . If we take, for instance, the SDE

$$\dot{x}_t = a x(t) + \sqrt{2b} x(t) \xi(t), \quad x(t = t_0) = x_0 \quad (\text{I.1.16})$$

which is known as *geometric Brownian motion* (GBM), we find that the solution reads for $x_0 x(t) > 0$ (cf. (A.1.12), (A.5.9))

$$x(t) = x_0 \exp \left[(a + (2\alpha - 1)b)(t - t_0) + \sqrt{2b} Z(t - t_0) \right] \quad (\text{I.1.17})$$

where $Z(t)$ is a Gaussian random variable with zero mean and variance t . We see that for mid-point, $\alpha = 1/2$, the deterministic parameter a of the SDE determines the mean, and the stochastic parameter b fixes the variance of $\ln x(t)/x_0$. On the other hand, for $a = 0$ but $\alpha \neq 1/2$, the mean of $\ln x(t)/x_0$ does not vanish, despite the vanishing deterministic parameter. Such a noise induced drift is generally referred to as *spurious drift*, in the sense that it does not arise physically but from the discretisation rule applied to the SDE.

The immediate consequence of the ambiguity of SDEs is that generally, along with the SDE itself, also the discretisation rule needs to be defined, otherwise the solution of the SDE is not unique. The definition of the discretisation rule is also referred to as an *interpretation* of the SDE, or as *convention*.

A crucial point is that for $\alpha \neq 1/2$ the usual rules of calculus are not applicable. A change of variable in the SDE or the integration rules for polynomials in $x(t)$, for instance, need to be modified. For $\alpha = 0$, such a modified calculus was developed by the mathematician Kiyoshi Itô, now known as *Itô calculus*. For an introduction to Itô calculus see appendix A.1, for further readings we recommend the books by Gardiner [4] or van Kampen [5]. The charm of the Itô convention is the mathematical feasibility of the rigorous theory. For practical purposes, the mid-point rule is often preferable, since then the ordinary rules of calculus apply. Defining the mid-point rule along with a SDE is usually referred to as *Stratonovich convention*, after the physicist Ruslan L. Stratonovich.³

The ambiguity of SDEs implies a dilemma. Suppose we want to describe a stochastic system with a SDE, and identify from the physics of the system the deterministic and stochastic influences as $f(x, t)$ and $g(x, t)$. So far

³More specific, contrary to the mid-point rule, the Stratonovich stochastic integral takes the average of beginning and end of the discretisation intervals ([4] p.96), see also figure I.1. A distinction that becomes irrelevant for small discretisation intervals.

so good, but how can we decide from physical arguments which convention is the correct one, such that we can expect that the SDE correctly predicts the outcome of experimental measurements? This dilemma is known as *Itô-Stratonovich dilemma*, and still debated in current research [12–18]. To deal with this dilemma, we will follow the argumentation by van Kampen [19] (see also [5] p.232), in which he distinguishes between *external* and *internal* noise. External noise refers to the case where the source of stochasticity is separate from the source of deterministic dynamics, whereas internal noise arises from an intertwined source of both stochastic and deterministic dynamics. In other words, external noise comes on top of a pure deterministic process and vanishes on average, internal noise is intrinsically present in the system and implies a non-vanishing average tendency.

Van Kampen claims that in the case of external noise, a SDE can be meaningfully set up, and Stratonovich convention has to be used. This is in accord with our previous observation regarding the example of GBM that $\langle x(t) \rangle \equiv x_0$ for $f(x, t) \equiv 0$ and $\alpha = 1/2$. Additional support for van Kampen’s claim follows from reverting to coloured noise as in (I.1.14). In this case, solutions of the SDE do not depend on α , and the Itô-Stratonovich dilemma is baseless. In the white noise limit, the solutions of the SDE with coloured noise reproduce the solutions of the SDE with white noise in the Stratonovich interpretation.

If the stochasticity of the processes arises from internal noise, van Kampen argues that a SDE is not the natural equation to describe the process. Instead a *master equation*, which we will discuss in chapter I.1.4, is advisable. Under certain conditions, a master equation can be recast as a Fokker-Planck equation which is formally equivalent to a SDE. The interpretation of the SDE is then simply a matter of taste, as long as the equivalence to the Fokker-Planck equation is retained. The defining functions $f(x, t)$ and $g(x, t)$ of the SDE will then depend on α , and it is tedious to attribute a meaning to $f(x, t)$ and $g(x, t)$ for various α . For thermodynamic diffusion processes, Lau and Lubensky argued that the choice $\alpha = 1$ is the most convenient one [7].

In closing, we mention that the practical significance of SDEs is to generate realisations $x(t)$ of a stochastic process $X(t)$. This can be achieved by solving the SDE explicitly and trace the randomness of $x(t)$ back to

random variables of known PDFs as we did in (I.1.17). The analytic solution of a SDE, however, can rarely be achieved. The numerical solution of SDEs is therefore the predominant practice when dealing with SDEs. The numerical results of this thesis are achieved by the first order integration scheme given by (A.3.8).

In the appendix A.5, we provide an overview of equivalent descriptions of continuous Markov processes that are defined via a SDE. We also demonstrate how a SDE in various interpretations can be reformulated to an equivalent SDE in a different interpretation.

I.1.2 The Fokker-Planck equations (FPE)

In the previous chapter we discussed SDEs which are the evolution equations for a stochastic variable $x(t)$. Instead of considering realisations $x(t)$, we can also describe the process by PDFs $p(x, t)$ of x for each instant of time t . The evolution equation for these PDFs is the *Fokker-Planck equation* (FPE), which we will discuss in this section.

Equivalence to SDEs In the appendix A.3, we demonstrate that the equivalent FPE of a SDE of the form (I.1.13) reads

$$\begin{aligned} \dot{p}(x, t) &= \partial_x \left[-f(x, t) - \alpha g'(x, t)g(x, t) + \partial_x \frac{1}{2}g(x, t)^2 \right] p(x, t) , \\ p(x, t = t_0) &= p_0(x) , \end{aligned} \quad (\text{I.1.18})$$

with the initial PDF $p_0(x)$. Note that the FPE depends on α , as was to be expected in view of the discussion regarding the interpretation of SDEs in the previous section. However, a FPE alone does not involve stochastic integrals and should as such not be plagued by the interpretation ambiguity. We therefore rewrite the FPE by defining

$$D^{(1)}(x, t) := f(x, t) + \alpha g'(x, t)g(x, t) , \quad (\text{I.1.19a})$$

$$D^{(2)}(x, t) := \frac{1}{2}g(x, t)^2 \quad (\text{I.1.19b})$$

as suggested by Lau and Lubensky [7]. The deterministic coefficient $D^{(1)}(x, t)$ is known as *drift* coefficient, and the *diffusion* coefficient $D^{(2)}(x, t)$ is the state and time dependent equivalent of the diffusion constant we

met in Fick's law (I.1.10) and the Einstein relation (I.1.9).⁴ In terms of $D^{(1,2)}(x, t)$, the FPE reads

$$\dot{p}(x, t) = \partial_x [-D^{(1)}(x, t) + \partial_x D^{(2)}(x, t)] p(x, t) , \quad p(x, t_0) = p_0(x) \quad (\text{I.1.20})$$

which is sometimes also referred to as the Itô form of the FPE, as for $\alpha = 0$ we have $D^{(1)}(x, t) = f(x, t)$.

By defining the probability current density

$$j(x, t) = -[-D^{(1)}(x, t) + \partial_x D^{(2)}(x, t)] p(x, t) , \quad (\text{I.1.21})$$

the FPE obtains the form of a continuity equation

$$\partial_t p(x, t) + \partial_x j(x, t) = 0 . \quad (\text{I.1.22})$$

As objected by Lau and Lubensky [7], however, setting $D^{(1)}(x, t) \equiv 0$ does not reproduce the correct generalisation of Fick's law (I.1.10) for state dependent diffusion. If we instead define

$$F(x, t) := D^{(1)}(x, t) - \partial_x D^{(2)}(x, t) \quad (\text{I.1.23a})$$

$$D(x, t) := D^{(2)}(x, t)^5 \quad (\text{I.1.23b})$$

and perform the derivative of $\partial_x D^{(2)}(x, t)$ in (I.1.20), the FPE and the current take the form

$$\dot{p}(x, t) = \partial_x [-F(x, t) + D(x, t) \partial_x] p(x, t) , \quad p(x, t_0) = p_0(x) , \quad (\text{I.1.24})$$

$$j(x, t) = F(x, t) p(x, t) - D(x, t) p'(x, t) , \quad (\text{I.1.25})$$

which is sometimes referred to as the Stratonovich form, although $F(x, t) = f(x, t)$ for $\alpha = 1$ (instead of $\alpha = 1/2$). If we now set $F(x, t) \equiv 0$, we obtain the correct generalisation of Fick's law (I.1.10). In I.2.1, we will see that $F(x, t)$ is the drift velocity in reaction to an external force, and the stationary distribution of the Stratonovich FPE coincides with the thermal equilibrium distribution. The connection to thermal equilibrium and

⁴The enumeration of drift as (1) and diffusion as (2) will become clear when discussing in I.1.4 how a FPE arises from a master equation.

⁵The superfluous definition of $D(x, t)$ is for convenience and a better distinction from $D^{(1,2)}(x, t)$.

the correct generalisation of Fick's law led Lau and Lubensky to call the choice $\alpha = 1$ the thermodynamic consistent convention.⁶ An overview of equivalent descriptions of continuous Markov processes defined by FPEs is provided in the appendix (A.5).

We note that an useful quantity is the local average velocity $\langle \dot{x}|x, t \rangle$ which allows to write the probability density current as the product

$$j(x, t) = \langle \dot{x}|x, t \rangle p(x, t) . \quad (\text{I.1.26})$$

We also note that for the initial PDF $p_0(x) = \delta(x - x_0)$, the solution of the FPE will be the conditional PDF $p(x, t|x_0, t_0)$, from which by

$$p(x, t) = \int p(x, t|x_0, t_0) p_0(x_0) dx_0 \quad (\text{I.1.27})$$

the solution of the FPE for any other initial PDF can be determined. Therefore, $p(x, t|x_0, t_0)$ is the Green's function of a FPE.

Moment equation Often of interest are the moments of a PDF instead of the PDF itself. We define the moments of $p(u, r)$ as

$$S_x^n(t) := \langle x^n \rangle_{p(x,t)} = \int x^n p(x, t) dx . \quad (\text{I.1.28})$$

If $p(u, r)$ is the solution of a FPE, we find by multiplying the FPE with x^n and integrating with respect to x ,

$$\begin{aligned} \int x^n \dot{p}(x, t) dx &= \int x^n \partial_x [- D^{(1)}(x, t) + \partial_x D^{(2)}(x, t)] p(x, t) dx \quad (\text{I.1.29}) \\ &= - \int x^n \partial_x D^{(1)}(x, t) p(x, t) dx + \int x^n \partial_x^2 D^{(2)}(x, t) p(x, t) dx \\ &= n \left\langle x^{n-1} D^{(1)}(x, t) \right\rangle_{p(x,t)} + n(n-1) \left\langle x^{n-2} D^{(2)}(x, t) \right\rangle_{p(x,t)} \end{aligned}$$

where the last line follows from repeated integration by parts and vanishing boundary terms due to the normalisation condition of $p(x, t)$.

⁶More specific, they argued that the definition $F(x, t) = f(x, t) + (\alpha - 1)g'(x, t)g(x, t)$ is thermodynamic consistent, in which $\alpha = 1$ is the most convenient choice.

Since x is in (I.1.29) a independent variable and not to be confused with the time-dependent path $x(t)$ as we had in the context of SDEs, we immediately obtain for the n -th moment $S_x^n(t)$ the ODE

$$\dot{S}_x^n(t) = n \left\langle x^{n-1} D^{(1)}(x, t) \right\rangle_{p(x,t)} + n(n-1) \left\langle x^{n-2} D^{(2)}(x, t) \right\rangle_{p(x,t)}. \quad (\text{I.1.30})$$

For polynomial $D^{(1,2)}$ in u , the averages on the right hand side of (I.1.29) reduce to a combination of moments $S_x^m(t)$ of different order m , and consequently, the integration of (I.1.29) to obtain $S_x^n(t)$ requires in general the knowledge of moments of order $m \neq n$.

For the special case $D^{(1)}(x, t) = d_1(t)x$ and $D^{(2)}(x, t) = d_2(t)x^2$, however, we get

$$\begin{aligned} \dot{S}_x^n(t) &= n \left\langle x^{n-1} d_1(t)x \right\rangle_{p(x,t)} + n(n-1) \left\langle x^{n-2} d_2(t)x^2 \right\rangle_{p(x,t)} \\ &= [n d_1(t) + n(n-1) d_2(t)] S_x^n(t), \end{aligned} \quad (\text{I.1.31})$$

with the solution

$$S_x^n(t) = S_x^n(t_0) \exp \left[\int_{t_0}^t (d_1(t) - d_2(t))n + d_2(t)n^2 dt \right]. \quad (\text{I.1.32})$$

The $S_x^n(t)$ are the moments of a log-normal distribution with mean $\mu = \int_{t_0}^t (d_1(t) - d_2(t)) dt$ and variance $\sigma^2 = 2 \int_{t_0}^t d_2(t) dt$.

For the simple choice $d_1(t) \equiv a + 2\alpha b$ and $d_2(t) \equiv b$, which, as we see from (I.1.18), is equivalent to GBM defined in (I.1.16) for arbitrary convention α , we obtain $\mu = (a + (2\alpha - 1)b)(t - t_0)$ and $\sigma^2 = 2b(t - t_0)$, which are indeed mean and variance of $\ln x(t)$, where $x(t)$ is the solution (I.1.17) of the SDE (I.1.16) of GBM. This simple example demonstrates the equivalence of SDEs and FPEs for arbitrary α .

Stationary solution An important characteristic of a FPE is its stationary solution $p^{\text{st}}(x)$. For a stationary process, that is $F(x, t) = F(x)$ and $D(x, t) = D(x)$ are time independent, the stationary distribution $p^{\text{st}}(x)$ is invariant under the dynamics defined by the FPE and can be determined by

$$0 \stackrel{!}{=} \partial_x [-F(x) + D(x)\partial_x] p^{\text{st}}(x). \quad (\text{I.1.33})$$

By writing the above equation in terms of the Fokker-Planck operator

$$\hat{\mathcal{L}}_{\text{FP}} = \partial_x [-F(x) + D(x)\partial_x] , \quad \hat{\mathcal{L}}_{\text{FP}} p^{\text{st}} = 0 p^{\text{st}} , \quad (\text{I.1.34})$$

it becomes apparent that $p^{\text{st}}(x)$ is the eigenfunction corresponding to zero eigenvalue, and hence the time evolution of every initial distribution $p_0(x)$ will in most cases converge to that stationary distribution $p^{\text{st}}(x)$.

For the case of time dependent $F(x, t)$ and $D(x, t)$, an *instantaneous* stationary distribution $p^{\text{st}}(x, t)$ can be defined. With 'instantaneous' is meant that the time variable t in $F(x, t)$, $D(x, t)$ and $p^{\text{st}}(x, t)$ is treated as a parameter which can be fixed to a certain value, whereas the time t in $p(x, t)$ and $\dot{p}(x, t)$ is the evolving time. To clarify this point, we temporarily introduce the constant parameter κ and write for the FPE

$$\dot{p}(x, t) = \partial_x [-F(x; \kappa) + D(x; \kappa)\partial_x] p(x, t) \quad (\text{I.1.35})$$

with now $F(x; \kappa)$ and $D(x; \kappa)$ being constant in time. The stationary distribution $p^{\text{st}}(x; \kappa)$ also depends on κ and by setting $\dot{p}^{\text{st}}(x; \kappa) = 0$ in the FPE (I.1.20), we arrive at the conditional equation for $p^{\text{st}}(x; \kappa)$,

$$0 = \partial_x [F(x; \kappa) - D(x; \kappa)\partial_x] p^{\text{st}}(x; \kappa) . \quad (\text{I.1.36})$$

Integration with respect to x yields

$$c(\kappa) = F(x; \kappa) p^{\text{st}}(x; \kappa) - D(x; \kappa) \partial_x p^{\text{st}}(x; \kappa) \quad (\text{I.1.37})$$

with a constant $c(\kappa)$. Referring to (I.1.21), we identify the integration constant to be the stationary probability current, $c(\kappa) = j^{\text{st}}(\kappa)$. In one dimension and for no periodic boundary conditions, we demand that $j^{\text{st}}(\kappa) \equiv 0$ to ensure $\dot{p}^{\text{st}}(x; \kappa) = 0$.

Upon isolation of $p^{\text{st}}(x; \kappa)$ and integration, we obtain

$$p^{\text{st}}(x; \kappa) = \exp \left[- [\varphi(x; \kappa) - \mathcal{G}(\kappa)] \right] , \quad (\text{I.1.38})$$

defining

$$\varphi(x; \kappa) = - \int_{-\infty}^x \frac{F(x'; \kappa)}{D(x'; \kappa)} dx' , \quad (\text{I.1.39a})$$

$$\mathcal{G}(\kappa) = - \ln Z(\kappa) = - \ln \int \exp [- \varphi(x; \kappa)] dx , \quad (\text{I.1.39b})$$

where $Z(\kappa)$ is the normalisation constant included into the exponential of $p^{\text{st}}(x; \kappa)$ in terms of $\mathcal{G}(\kappa)$.

For each value of κ and any initial distribution $p_0(x)$, the solution of the FPE will in general become $p^{\text{st}}(x; \kappa)$ in the limit $t \rightarrow \infty$. By writing again time t instead of parameter κ , $p^{\text{st}}(x, t)$ hence is the stationary distribution for any instance of time t at which we keep $F(x, t)$ and $D(x, t)$ fixed and let the dynamics evolve. Instead of simply $\kappa = t$, we could also outsource the time-dependency of $F(x, t)$ and $D(x, t)$ by leaving $\kappa(t)$ unspecified. The *protocol* $\kappa(\cdot)$ can take any functional form, of which $\kappa(t) = t$ is just the simplest choice. We will come back to the notion of protocols in the context of fluctuation theorems in section I.2.3.

If the system is in a steady state, i.e. $p(x, t) = p^{\text{st}}(x)$, the appendant probability current $j^{\text{st}}(x)$ must necessarily be constant in time which is a direct consequence of the continuity equation (I.1.22). Except for periodic boundary conditions, the current $j^{\text{st}}(x)$ must vanish at its boundaries to preserve probability. Hence the probability current must vanish in a steady state, $j^{\text{st}}(x) \equiv 0$.

If, however, the MP takes place in higher dimensions, i.e. $\mathbf{X}(t) \in \mathbb{R}^n$ with $n \geq 2$, the continuity equation becomes

$$\dot{p}(\mathbf{x}, t) + \nabla \cdot \mathbf{j}(\mathbf{x}) = 0, \quad (\text{I.1.40})$$

from which it is evident that it now is sufficient to require that the stationary probability current is divergence free, i.e. $\nabla \cdot \mathbf{j}^{\text{st}}(\mathbf{x}) = 0$. This requirement implies that the vector field \mathbf{j}^{st} is a pure curl, it is therefore natural to divide $\mathbf{F}(\mathbf{x})$ into a conservative part deriving from the scalar potential $\varphi(\mathbf{x}, t)$ and an additional non-conservative vector-field $\mathbf{A}(\mathbf{x}, t)$,

$$\mathbf{F}(\mathbf{x}, t) = \mathbf{D}(\mathbf{x}, t) [-\nabla \varphi(\mathbf{x}, t) + \mathbf{A}(\mathbf{x}, t)], \quad (\text{I.1.41})$$

where we now have a diffusion matrix $\mathbf{D}(\mathbf{x}, t)$ instead of a scalar diffusion coefficient.

The FPE and the probability current now read

$$\dot{p}(\mathbf{x}, t) = -\nabla \cdot [\mathbf{F}(\mathbf{x}, t) - \mathbf{D}(\mathbf{x}, t) \nabla] p(\mathbf{x}, t), \quad (\text{I.1.42})$$

$$\mathbf{j}(\mathbf{x}, t) = \mathbf{F}(\mathbf{x}, t) p(\mathbf{x}, t) - \mathbf{D}(\mathbf{x}, t) \nabla p(\mathbf{x}, t). \quad (\text{I.1.43})$$

We further write the stationary distribution as

$$p^{\text{st}}(\mathbf{x}, t) = \exp \left[-\phi(\mathbf{x}, t) \right] , \quad (\text{I.1.44})$$

where it has to be stressed that the non-equilibrium potential $\phi(\mathbf{x}, t)$ is distinct from $\varphi(x, t)$ defined in (I.1.39a) in the sense that $\mathbf{F}(\mathbf{x}, t) \neq \mathbf{D}(\mathbf{x}, t) \nabla \phi(\mathbf{x}, t)$ due to the non-conservative part of $\mathbf{F}(\mathbf{x}, t)$ in (I.2.78). In fact, the analytic determination of $\phi(\mathbf{x}, t)$ is only in particularly simple cases possible.

Substituting $p^{\text{st}}(\mathbf{x}, t)$ from (I.1.44) and $\mathbf{F}(\mathbf{x}, t)$ from (I.2.78) into (I.1.43), we get for the stationary current

$$\mathbf{j}^{\text{st}}(\mathbf{x}, t) = \mathbf{D}(\mathbf{x}, t) \mathbf{A}(\mathbf{x}, t) p^{\text{st}}(\mathbf{x}, t) \quad (\text{I.1.45})$$

and consequently for the stationary local mean velocity

$$\langle \dot{\mathbf{x}} | \mathbf{x}, t \rangle_{\text{st}} = \mathbf{D}(\mathbf{x}, t) \mathbf{A}(\mathbf{x}, t) . \quad (\text{I.1.46})$$

Only for the case of no non-conservative forces, i.e. $\mathbf{A}(\mathbf{x}, t) \equiv 0$, we have a vanishing stationary current.

It is insightful to express the FPE in terms of the stationary distribution and stationary current. To this end, we plug $p^{\text{st}}(\mathbf{x}, t)$ from (I.1.44) into the current (I.1.43)

$$\mathbf{j}^{\text{st}}(\mathbf{x}, t) = \left[\mathbf{F}(\mathbf{x}, t) + \mathbf{D}(\mathbf{x}, t) \nabla \phi(\mathbf{x}, t) \right] e^{-\phi(\mathbf{x}, t)} , \quad (\text{I.1.47})$$

and solve for $\mathbf{F}(\mathbf{x}, t)$,

$$\mathbf{F}(\mathbf{x}, t) = e^{\phi(\mathbf{x}, t)} \mathbf{j}^{\text{st}}(\mathbf{x}, t) - \mathbf{D}(\mathbf{x}, t) \nabla \phi(\mathbf{x}, t) , \quad (\text{I.1.48})$$

to arrive at

$$\begin{aligned} \dot{p}(\mathbf{x}, t) &= -\nabla \left[e^{\phi(\mathbf{x}, t)} \mathbf{j}^{\text{st}}(\mathbf{x}, t) - \mathbf{D}(\mathbf{x}, t) \nabla \phi(\mathbf{x}, t) - \mathbf{D}(\mathbf{x}, t) \nabla \right] p(\mathbf{x}, t) \\ &= -\nabla \left[e^{\phi(\mathbf{x}, t)} \mathbf{j}^{\text{st}}(\mathbf{x}, t) - \mathbf{D}(\mathbf{x}, t) e^{-\phi(\mathbf{x}, t)} \nabla e^{\phi(\mathbf{x}, t)} \right] p(\mathbf{x}, t) \\ &= -\nabla \left[\langle \dot{\mathbf{x}} | \mathbf{x}, t \rangle p(\mathbf{x}, t) - \mathbf{D}(\mathbf{x}, t) p^{\text{st}}(\mathbf{x}, t) \nabla \frac{p(\mathbf{x}, t)}{p^{\text{st}}(\mathbf{x}, t)} \right] . \end{aligned} \quad (\text{I.1.49})$$

The Fokker-Planck operator can then be written as

$$\hat{\mathcal{L}}_{\text{FP}}(\mathbf{x}, t) = -\nabla \left[e^{\phi(\mathbf{x}, t)} \mathbf{j}^{\text{st}}(\mathbf{x}, t) - \mathbf{D}(\mathbf{x}, t) e^{-\phi(\mathbf{x}, t)} \nabla e^{\phi(\mathbf{x}, t)} \right], \quad (\text{I.1.50})$$

which shows that the dynamics can independently be fixed by choosing $\{\phi, \mathbf{D}, \mathbf{j}^{\text{st}}\}$. In particular, fixing ϕ and \mathbf{D} but varying the current \mathbf{j}^{st} (making sure it is still divergence free), we can define a family of dynamics with identical $\phi(\mathbf{x}, t)$ and $\mathbf{D}(\mathbf{x}, t)$ but distinct currents $\mathbf{j}^{\text{st}}(\mathbf{x})$. We will pick up this notion in the context of entropies in section I.2.2 and fluctuation theorems in section I.2.3.

More details regarding the FPE and its various applications can be found in the book by Risken [20].

I.1.3 Wiener path integrals (WPIs)

So far, we addressed continuous Markov processes $X(t)$ by evolution equations for realisations $x(t)$, SDEs, and an evolution equation for the PDF $p(x, t)$ of the random variable x at time t , the FPE. In this section, we introduce a third notion, which allocates to a certain realisation $x(t)$ a probability measure $P[x(\cdot)]$. To emphasise that we do not evaluate a function $x(t)$ at a certain time t but rather take the whole path from initial time t_0 to final time t , we will write $x(\cdot)$ for realisations of the continuous MP. The probabilistic description of sample paths $x(\cdot)$ is given by *Wiener path integrals* (WPIs), which were introduced by Norbert Wiener in the 1920s for Brownian motion (and related diffusion processes), and which we will recast here on a formal level. In doing so, we build on the book by Chaichian and Demichev [6], and the article by Lau and Lubensky [7].

The point of origin of WPIs is the Chapman-Kolmogorov relation (CKR) (I.1.4) which is of the form

$$p(x_3, t_3 | x_1, t_1) = \int p(x_3, t_3 | x_2, t_2) p(x_2, t_2 | x_1, t_1) dx_2. \quad (\text{I.1.51})$$

Here, (x_1, x_2, x_3) are subsequent measurements of a continuous MP at times $t_1 > t_2 < t_3$. In order to capture not only three points but the whole

path $x(\cdot)$, we combine $N-2$ CKRs and write the Green's function of a FPE as

$$p(x, t | x_0, t_0) = \int \left[\prod_{i=2}^{N-1} dx_i \right] \prod_{i=1}^{N-1} p(x_{i+1}, t_{i+1} | x_i, t_i) \quad (\text{I.1.52})$$

where $(x_1, t_1) = (x_0, t_0)$ and $(x_N, t_N) = (x, t)$. This is the prototype of a WPI.

The conditional probability $p(x_{i+1}, t_{i+1} | x_i, t_i)$ is called the *propagator*, in the sense that it propagates upon integration the probability of (x_i, t_i) to (x_{i+1}, t_{i+1}) .

Based on the SDE $\dot{x}_t = f(x_t, t) + g(x_t, t)\xi(t)$ in α -point and for small times $\Delta t = t_{i+1} - t_i$, the propagator can be well approximated by

$$p(x_{i+1}, t_{i+1} | x_i, t_i) \simeq \frac{1}{\sqrt{2\pi\Delta t g_{i\alpha}^2}} e^{-\Delta t s_i(x_i, x_{i+1})}, \quad (\text{I.1.53a})$$

$$s_i(x_i, x_{i+1}) := \frac{1}{2g_{i\alpha}^2} \left(\frac{x_{i+1} - x_i}{\Delta t} + f_{i\alpha} + \alpha g_{i\alpha} g'_{i\alpha} \right)^2 - \alpha f'_{i\alpha}. \quad (\text{I.1.53b})$$

Here, the index i_α denotes that $f_{i\alpha}$ and $g_{i\alpha}$ have to be evaluated in α -point. The detailed calculation that led to this result can be found appendix A.4, in essence, it arises from a probability transformation from $\xi(t)$ to $x(t)$. Substituting the above propagator into the repeated CKR (I.1.52) yields

$$p(x, t | x_0, t_0) \simeq \frac{1}{\sqrt{2\pi\Delta t g_{N\alpha}^2}} \int \left[\prod_{i=2}^{N-1} \frac{dx_i}{\sqrt{2\pi\Delta t g_{i\alpha}^2}} \right] \exp \left[-\epsilon \sum_{j=1}^{N-1} s_j(x_j, x_{j+1}) \right] \quad (\text{I.1.54})$$

In the continuous limit, $\Delta t \rightarrow 0$ and $N \rightarrow \infty$, the sum becomes the stochastic integral

$$\begin{aligned} \mathcal{S}[x(\cdot)] &:= \int_{t_0}^t \frac{[\dot{x}_\tau - F(x_\tau, \tau) + (2\alpha - 1)D'(x_\tau, \tau)]^2}{4D(x_\tau, \tau)} - J(x_\tau, \tau) d\tau, \\ J(x, t) &:= \alpha F'(x, t) + \frac{1}{2}D''(x, t) \end{aligned} \quad (\text{I.1.55})$$

and the remaining integration is symbolically abbreviated as

$$\int_{(x_0, t_0)}^{(x, t)} \mathcal{D}x(\cdot) := \frac{1}{\sqrt{4\pi D_N \Delta t}} \int \left[\prod_{i=2}^{N-1} \frac{dx_i}{\sqrt{4\pi D_i \Delta t}} \right] . \quad (\text{I.1.56})$$

Here, we already substituted $F(x, t) = f(x, t) + (\alpha - 1)g'(x, t)g(x, t)$ and $D(x, t) = \frac{1}{2}g(x, t)^2$ as defined in the context of a FPE, see (I.1.19) and (I.1.23). The functional $\mathcal{S}[x(\cdot)]$ is usually referred to as the *action* of the Wiener process, and $J(x, t)$ can be identified as a Jacobian of the underlying transformation from $\xi(t)$ to $x(t)$.

Using the above definitions for $\mathcal{S}[x(\cdot)]$ and $\mathcal{D}x(\cdot)$, we finally arrive at the WPI

$$p(x, t | x_0, t_0) = \int_{(x_0, t_0)}^{(x, t)} \mathcal{D}x(\cdot) P[x(\cdot) | x_0] , \quad (\text{I.1.57a})$$

$$P[x(\cdot) | x_0] = \exp \left[-\mathcal{S}[x(\cdot)] \right] , \quad (\text{I.1.57b})$$

with the probability density functional $P[x(\cdot) | x_0]$, which we will simply call *path probability*.

In appendix A.5, the action of WPIs is listed for continuous MPs defined via a SDE or a FPE.

The formulation of continuous MPs in terms of WPIs might seem cumbersome, but despite its formal complexity, it offers a great deal of intuition in practical applications which will partially unfold in section I.2.3 and I.3 in the context of fluctuation theorems and asymptotic approximations.

For now we note that a WPI is the sum of the probabilities of all possible paths $x(\cdot)$ that connect (x_0, t_0) with (x, t) . The functional $P[x(\cdot) | x_0]$ is to be understood as a *density* in function space, whereas the *probability* of a single path is rather $P[x(\cdot) | x_0] \mathcal{D}x(\cdot)$, bearing resemblance to a random variable x with PDF $p(x, t)$, for which the probability $p(x)dx$ is the product of the density $p(x)$ and an infinitesimal volume dx . In that sense, loosely speaking, the measure $\mathcal{D}x(\cdot)$ can be thought of as an infinitesimal tube that encloses the path $x(\cdot)$. However, $\mathcal{D}x(\cdot)$ remains to be a highly symbolic object.

The form of the action $S[x(\cdot)]$ can also be furnished with intuition. For this purpose, we take the Stratonovich convention $\alpha = 1/2$ in which we have no spurious drift. We observe that $S[x(\cdot)]$ is larger, the more $x(\cdot)$ deviates from the solution of the deterministic equation $\dot{x}_\tau - F(x_\tau, \tau)$, that is when the actual velocity \dot{x} deviates from the drift velocity $F(x, t)$. On the other hand, if $D(x, t)$ is large along $x(\cdot)$, the penalty for deviating from the deterministic motion, $(\dot{x}_\tau - F(x_\tau, \tau))^2$, gets mitigated; in other words, a high diffusivity implies a higher probability for large excursions. Thus, we retrieve the interplay between deterministic and stochastic dynamics. The occurrence of the diffusion coefficient in the denominator of $S[x(\cdot)]$ allows for another intuitive interpretation. Let us assume that we can factor out an overall diffusion magnitude d_0 and write $D(x, t) = d_0 \tilde{D}(x, t)$, where $\tilde{D}(x, t)$ is now dimensionless. For moderate values of d_0 , an ensemble of trajectories fluctuating around the deterministic solution contribute to the path integral. For small values of d_0 , the variety of contributing trajectories narrows down to slightly fluctuating trajectories close to the deterministic solution. In the limit $d_0 \rightarrow 0$, only the deterministic solution will survive. This limit is known as the *weak noise limit*, and approximations with d_0 as small parameter are called *weak noise approximations* ([4] p.169, [6] p.27). We note that the weak noise approximation is closely related to the stationary-phase approximation of Feynman path integrals in quantum mechanics ([6] p.169).

Quite analogous to WPIs, a Feynman path integral considers all paths that are *simultaneously* realised in the quantum mechanical regime, for instance in the double-slit experiment. This correspondence is not a coincidence, since the Schrödinger equation is a Fokker-Planck equation with imaginary diffusion coefficient proportional to \hbar . In the limit $\hbar \rightarrow 0$, only the classical path survives. The stationary-phase approximation is a semi-classical method in which small quantum fluctuations are considered that are characterised by actions large compared \hbar .

We return to the WPI. Per construction, the path probability $P[x(\cdot)|x_0]$ is still conditioned on the initial value x_0 . Augmenting $P[x(\cdot)|x_0]$ with the initial distribution $p_0(x)$

$$P[x(\cdot)] := p_0(x_0) P[x(\cdot)|x_0] , \quad (\text{I.1.58})$$

and integration with respect to the initial value x_0 yields

$$p(x, t) = \int dx_0 \int_{(x_0, t_0)}^{(x_t, t)} \mathcal{D}x(\cdot) P[x(\cdot)] . \quad (\text{I.1.59})$$

The path probability $P[x(\cdot)]$ is normalised upon integration with respect to all paths connecting the initial and final points, and integration with respect to these points,

$$1 = \int dx_t \int_{(x_0, t_0)}^{(x_t, t)} dx_0 \int \mathcal{D}x(\cdot) P[x(\cdot)] . \quad (\text{I.1.60})$$

Building on this normalisation condition, we can write for the average of an integral observable $Y = \mathcal{Y}[x(\cdot)]$,

$$\langle Y \rangle = \int dx_t \int_{(x_0, t_0)}^{(x_t, t)} dx_0 \int \mathcal{D}x(\cdot) P[x(\cdot)] \mathcal{Y}[x(\cdot)] , \quad (\text{I.1.61})$$

as the analogue of $\langle y(x) \rangle_{p(x,t)} = \int y(x) p(x) dx$. Here, the path probability $P[x(\cdot)]$ weights each path according to the chance of its realisation. Note that the above average $\langle \rangle$ defined in terms of a path integral is equivalent to the *ensemble average* of values for Y resulting from a representative (in principle infinite large) ensemble of realisations $x(\cdot)$.

We can also write the PDF of the observable Y as a WPI,

$$P(Y) = \int dx_t \int_{(x_0, t_0)}^{(x_t, t)} dx_0 p_0(x_0) \int \mathcal{D}x(\cdot) P[x(\cdot)|x_0] \delta(Y - \mathcal{Y}[x(\cdot)]) . \quad (\text{I.1.62})$$

Due to the δ -function, the integration space is restricted to paths that obey $Y - \mathcal{Y}[x(\cdot)]$, thus the WPI collects the probabilities of all paths that give rise to the desired value Y . We will come back to the WPI representation of a PDF in chapter I.3, in which we will approximate the above WPI with an asymptotic method formally equivalent to the weak noise

approximation.

Finally, we note that the formalism of WPIs can be generalised to higher dimensions. We refrain from giving an account on this generalisation and refer the interested reader to [21].

I.1.4 Discontinuous Markov processes

In the previous three sections, we were concerned with continuous MPs. In this section, we will embed the continuous subclass of MPs into the larger context of MPs that also allow discontinuous realisations ([4] p. 45ff).

We begin with formulating the continuity condition

$$\lim_{\Delta t \rightarrow 0} \frac{1}{\Delta t} \int_{|z-x|>\epsilon} p(z, t+\Delta t | x, t) dz = 0 \quad \forall \epsilon > 0 \quad (\text{I.1.63})$$

to define the borderline between continuous and discontinuous MPs. In words, the continuity condition requires that the probability for arbitrary small jumps in the process, $|z-x| > \epsilon$, has to approach zero *faster* than the time step Δt . Building on the above continuity condition, we distinguish continuous from discontinuous MPs by formulating the following three defining conditions,

$$\lim_{\Delta t \rightarrow 0} \frac{1}{\Delta t} p(z, t+\Delta t | x, t) =: \chi(z | x, t) , \quad (\text{I.1.64a})$$

$$\lim_{\Delta t \rightarrow 0} \frac{1}{\Delta t} \int_{|z-x|<\epsilon} (z-x) p(z, t+\Delta t | x, t) dz =: A(x, t) + \mathcal{O}(\epsilon) , \quad (\text{I.1.64b})$$

$$\lim_{\Delta t \rightarrow 0} \frac{1}{2\Delta t} \int_{|z-x|<\epsilon} (z-x)^2 p(z, t+\Delta t | x, t) dz =: B(x, t) + \mathcal{O}(\epsilon) . \quad (\text{I.1.64c})$$

Here, $\chi(z | x, t)$ measures the violation of the continuity condition (I.1.63) via jumps x to z at time t and is referred to as the *jump measure*. The coefficients $A(x, t)$ and $B(x, t)$ are related to the mean and variance of the

MP. For that reason, a non-zero $\chi(z|x, t)$ is responsible to the generation of discontinuous realisations, whereas $A(x, t)$ and $B(x, t)$ are connected with continuous realisations. B and χ must be positive.

The crucial question is, why are $A(x, t)$ and $B(x, t)$ sufficient to capture the continuous part of the MP. The question is equivalent to asking why the noise $\xi(t)$ in SDEs must be Gaussian in order to have continuous solutions. The answer is that one can indeed prove that ([4] p. 47f)

$$\lim_{\Delta t \rightarrow 0} \frac{1}{\Delta t} \int_{|z-x|<\epsilon} (z-x)^n p(z, t+\Delta t | x, t) dz = \mathcal{O}(\epsilon) \quad \forall n \geq 3, \quad (\text{I.1.65})$$

which follows from estimating the cubic equivalent of (I.1.64c) against $B(x, t)$, the quartic form against the cubic, and so on.

The master equation Having set up the above classification, the next step is to pursue an evolution equation for $p(x, t)$ that, in contrast to the FPE, also includes discontinuous realisation of the MP. This equation is the differential form of the CKR. The starting point to derive the differential CKR is the time derivative of the expectation of a test function $h(x)$, $\partial_t \int h(x)p(x, t) dx$. By writing the time derivative as the limit of a difference quotient, substituting the CKR, making use of conditions (I.1.64) and upon integration by parts, we can read off the differential CKR as the effect of the CKR on the test function $h(x)$ as

$$\begin{aligned} \partial_t p(x, t) = & -\partial_x A(x, t)p(x, t) + \partial_x^2 B(x, t)p(x, t) \\ & + \int \chi(x|z, t)p(z, t) - \chi(z|x, t)p(x, t) dz. \end{aligned} \quad (\text{I.1.66})$$

We note that all solutions of the differential CKR satisfy the CKR, and all MPs obey the CKR, but not all solutions of the differential CKR are necessarily Markovian. However, the cases in which the solutions of the differential CKR are not Markovian build on pathological choices for $\chi(z|x, t)$ which we do not consider here.

By setting one or two of the coefficients $A(x, t)$, $B(x, t)$ and $\chi(x|z, t)$ to zero, different subclasses of MPs are described. By assuming, e.g., a vanishing probability of jumps in the process, $\chi(x|z, t) \equiv 0$, we recover the

Fokker-Planck equation (I.1.20) with drift $A(x, t) = D^{(1)}(x, t)$ and diffusion $B(x, t) = D^{(2)}(x, t)$ describing a continuous MP. Also the deterministic case $B = 0$ and $\chi(x|z, t) \equiv 0$ can be considered as a MP ([4] p.54,353), and is then referred to as a Liouville process, in which the only randomness arises from sampling the initial values of the process from an initial PDF $p_0(x)$.

The simplest discontinuous case is setting drift $A(x, t) \equiv 0$ and diffusion $B(x, t) \equiv 0$, for which we find

$$\begin{aligned} \partial_t p(x, t) &= \int \chi(x|z, t)p(z, t) - \chi(z|x, t)p(x, t) \, dz \\ p_0(x) &= p(x, t = t_0) . \end{aligned} \quad (\text{I.1.67})$$

The above evolution equation is known as *master equation*.

The master equation can be interpreted: The probability $p(x, t)$ of a state x increases by jumps from states z to x and decreases by jumps from state x to states z .

Since $p(x, t)$ in the second term does not depend on z , we can rewrite the master equation as

$$\partial_t p(x, t) = \int \chi(x|z, t)p(z, t) \, dz - \varrho(x, t)p(x, t) , \quad (\text{I.1.68})$$

where we have defined the *escape rate*

$$\varrho(x, t) = \int \chi(z|x, t) \, dz . \quad (\text{I.1.69})$$

Note that using an appropriate $\chi(x|z, t)$, a pure jump process can be set up in which only discrete jumps occur, although the MP $X(t)$ does not need to be restricted to discrete values. If, however, the state-space is discrete, we have instead of $X(t)$ the time-dependent random variable $N(t) \in \mathbb{Z}$ with realisations $n(t)$, and the master equation for the PDF of measuring n at time t becomes

$$\partial_t p(n, t) = \sum_m [\chi(n|m, t)p(m, t) - \chi(m|n, t)p(n, t)] \quad (\text{I.1.70a})$$

$$= \sum_m [\chi(n|m, t)p(m, t)] - \varrho(n, t)p(n, t) , \quad (\text{I.1.70b})$$

$$\varrho(n, t) = \sum_m \chi(m|x, t) \, dz, \quad p_0(n) = p(n, t = t_0). \quad (\text{I.1.70c})$$

In this case, we are bound to have a pure jump process.

We mention that a useful property of jump processes is that for time independent jump measures $\chi(z|x)$, the time Δt between jumps is exponentially distributed, $p(\Delta t, x) = \exp[-\varrho(x)\Delta t]$ ([4] p. 52). This fact allows for simple simulation algorithms to generate realisations of jump processes, for instance the Gillespie algorithm [22].

The Kramers-Moyal expansion The master equation for a pure jump process can be expanded in the moments of the jump measure. This expansion is known as the *Kramers-Moyal expansion* (KME) ([4] p. 275). To derive it, we define the jump density

$$\theta(y; x, t) := \chi(x+y|x, t). \quad (\text{I.1.71})$$

In terms of $\theta(y; x, t)$, the master equation (I.1.67) reads

$$\partial_t p(x, t) = \int \theta(y; x-y, t) p(x-y, t) - \theta(y; x, t) p(x, t) \, dy. \quad (\text{I.1.72})$$

By expanding the integrand

$$\begin{aligned} \theta(y; x-y, t) p(x-y, t) &= \theta(y; x, t) p(x, t) \\ &+ \sum_{k=1}^{\infty} \frac{(-1)^k}{k!} \frac{\partial^k}{\partial x^k} [\theta(y; x, t) p(x, t)] y^k \end{aligned} \quad (\text{I.1.73})$$

and substitution into the master equation (I.1.72), we get the KME

$$\begin{aligned} \partial_t p(x, t) &= \int \sum_{k=1}^{\infty} \frac{(-1)^k}{k!} \frac{\partial^k}{\partial x^k} [\theta(y; x, t) p(x, t)] y^k \, dy \\ &= \sum_{k=1}^{\infty} \frac{(-1)^k}{k!} \frac{\partial^k}{\partial x^k} [\Psi^{(k)}(x, t) p(x, t)], \end{aligned} \quad (\text{I.1.74})$$

where we defined the moments of the jump density as

$$\begin{aligned}\Psi^{(k)}(x, t) &:= \int y^k \theta(y; x, t) \, dy \\ &= \int (z-x)^k \chi(z|x, t) \, dz .\end{aligned}\tag{I.1.75}$$

Truncating the KME after the second term, we obtain a FPE with drift $D^{(1)}(x, t) = \Psi^{(1)}(x, t)$ and diffusion $D^{(2)}(x, t) = \frac{1}{2}\Psi^{(2)}(x, t)$ which is often used to approximate the jump process defined by the jump density $\theta(y; x, t)$ as a continuous process ([20] p. 70ff).

The KME in the form (I.1.72) rules a pure jump process. To include an underlying continuous MP into the expansion, we substitute the KME (I.1.73) into the full differential CKR (I.1.66) and find the expansion

$$\begin{aligned}\partial_t p(x, t) &= -\partial_x [A(x, t) + \Psi^{(1)}(x, t)] p(x, t) \\ &\quad + \partial_x^2 [B(x, t) + \frac{1}{2}\Psi^{(2)}(x, t)] p(x, t) \\ &\quad + \sum_{k=3}^{\infty} \frac{(-\partial_x)^k}{k!} [\Psi^{(k)}(x, t) p(x, t)] \\ &= \sum_{k=1}^{\infty} (-\partial_x)^k [D^{(k)}(x, t) p(x, t)]\end{aligned}\tag{I.1.76}$$

with

$$D^{(1)}(x, t) := A(x, t) + \Psi^{(1)}(x, t) ,\tag{I.1.77a}$$

$$D^{(2)}(x, t) := B(x, t) + \frac{1}{2}\Psi^{(2)}(x, t) ,\tag{I.1.77b}$$

$$D^{(k)}(x, t) := \frac{1}{k!}\Psi^{(k)}(x, t) \quad \text{for } k \geq 3 .\tag{I.1.77c}$$

This expansion is also known as a KME, and we will refer to the $D^{(k)}(x, t)$ as *Kramers-Moyal coefficients* (KMCs).

If the conditional PDFs of a MP are known, we see by (I.1.64) that the KMCs can be obtained from

$$D^{(k)}(x, t) = \lim_{\Delta t \rightarrow 0} \frac{1}{k! \Delta t} M^{(k)}(x, t; \Delta t) ,\tag{I.1.78a}$$

$$M^{(k)}(x, t; \Delta t) = \int (z-x)^k p(z, t+\Delta t | x, t) \, dz ,\tag{I.1.78b}$$

where we defined the conditional moments $M^{(k)}(x, t; \Delta t)$. The above prescription is often used to estimate $D^{(k)}(x, t)$ from experimental measurements by estimating the conditional moments $M^{(k)}(x, t; \Delta t)$ for various Δt . In this context, the knowledge of the Markov-Einstein time scale Δt_{ME} , which we discussed in section I.1.1, is of relevance, since the formulae of prescription (I.1.78) rely on the Markov assumption which only holds for $\Delta t > \Delta t_{\text{ME}}$. To obtain an estimate for Δt_{ME} from experimental data, the time-constant of the auto-correlation function of the measured $x(t)$ may serve. In the simplest approach, the limit in (I.1.78a) can be substituted by $D^{(k)}(x, t) = M^{(k)}(x, t; \Delta t_{\text{ME}})$ ([5] p. 195), but many more sophisticated procedures have been established [23–27], commonly regarded to as *Markov analysis*.

It is important to keep in mind that the $\Psi^{(k)}(x, t)$ in (I.1.75) are defined as the moments of the jump measure $\chi(z|x, t)$, whereas using the prescription (I.1.78) to estimate $D^{(k)}(x, t)$ from experimental data rests upon the conditional distribution $p(z, t+\Delta t | x, t)$ being insensitive to the formal distinction between the continuous and discontinuous components of the process $X(t)$.

To clarify our point, let us discuss the correspondence from (I.1.77),

$$D^{(1)}(x, t) = A(x, t) + \Psi^{(1)}(x, t) , \quad (\text{I.1.79a})$$

$$D^{(2)}(x, t) = B(x, t) + \frac{1}{2}\Psi^{(2)}(x, t) , \quad (\text{I.1.79b})$$

$$D^{(\geq 3)}(x, t) = \frac{1}{k!}\Psi^{(\geq 3)}(x, t) . \quad (\text{I.1.79c})$$

In the case of a continuous process $X(t)$, i.e. $\Psi^{(k)}(x, t) \equiv 0$, it follows from (I.1.79) that by estimating $D^{(1,2)}(x, t)$ we find the drift and diffusion coefficients of the FPE ruling $X(t)$. In the case of an underlying jump process, however, $D^{(1,2)}(x, t)$ includes also the first two moments of the jump density, and the FPE is a mere approximation of the true process. Realistic MPs taken to be continuous will always have an underlying jump process, the $D^{(1,2)}(x, t)$ as above will therefore never equal $A(x, t)$ and $B(x, t)$ exactly. However, in many applications, the discontinuous component of a MP can be neglected ([26], [20] p. 77ff). In the major part of this thesis, when considering continuous MPs, we will therefore drop the distinction between $A(x, t)$, $B(x, t)$ and $D^{(1,2)}(x, t)$.

If we were to decide whether $X(t)$ is approximately continuous, we could in principle estimate $D^{(k)}(x, t)$ for an even $k \geq 4$ (a symmetric distribution has vanishing odd moments) and, if $D^{(k)}(x, t) \equiv 0$, argue that $\chi(z|x, t) \equiv \delta(z - x)$ which assigns zero probability to non-zero jump widths. We can also formulate this finding as that “for a positive $p(z, t + \Delta t | x, t)$, the KME may stop after the first or the second term, and if it does not stop after the second term, it must contain an infinite number of terms” (Risken, p. 70). This statement is known as the *theorem of Pawula*, originally proved by applying a generalised Schwarz inequality to a combination of conditional moments [28].

However, restricting ourselves to the fourth coefficient as being, due to experimental and statistical limitations, the statistically easiest accessible, it is not possible to show that exactly $D^{(4)}(x, t) \equiv 0$. Instead, it can only be found that $D^{(4)}(x, t) \approx 0$ within a certain error margin, or that $D^{(4)}(x, t)$ is negligible small compared to $D^{(2)}(x, t)$, both of which does not mean that the $D^{(k)}(x, t)$ for $k > 4$ are negligible too. In that sense, the KME is not a systematic expansion in a small parameter ([4] p. 276, [5] p. 199). An improved expansion is the *system size expansion* suggested by van Kampen, which coincides with the KME in the weak noise limit ([4] p. 276ff, [5] p. 199ff).

From the FPE we derived an equation for the moments $S_x^n(t)$ of the PDF $p(x, t)$. Integrating the KME (I.1.76), we can also obtain a moment equation for MPs involving both continuous and discontinuous components,

$$\begin{aligned}
 \dot{S}_x^n(t) &= \sum_{k=1}^{\infty} \int x^n (-\partial_x)^k [D^{(k)}(x, t)p(x, t)] dx \\
 &= \sum_{k=1}^n \int \frac{n!}{(n-k)!} [x^{n-k} D^{(k)}(x, t)p(x, t)] dx \\
 &= \sum_{k=1}^n \frac{n!}{(n-k)!} \langle x^{n-k} D^{(k)}(x, t) \rangle \\
 &= n \langle x^{n-1} A(x, t) \rangle + n(n-1) \langle x^{n-2} B(x, t) \rangle \\
 &\quad + \sum_{k=1}^n \binom{n}{k} \langle x^{n-k} \Psi^{(k)}(x, t) \rangle .
 \end{aligned} \tag{I.1.80}$$

Note that now the sum involves a finite number of terms, in contrast to the infinite sum in the KME. The consequence is that, apart from drift and diffusion, only the n first moments of the jump density contribute to the n -th moment of $p(u, r)$.

For the special case that $A(x, t) = a(t)x$, $B(x, t) = b(t)x^2$ and $\Psi^{(k)}(x, t) = d^{(k)}(t)x^k$, we obtain a closed equation for the moments,

$$\dot{S}_x^n(t) = \left[na(t) + n(n-1)b(t) + \sum_{k=1}^n \binom{n}{k} d^{(k)}(t) \right] S_x^n(t) . \quad (\text{I.1.81})$$

The solution of this equation reads

$$S_x^n(t) = S_x^n(t_0) \exp \left[\int_{t_0}^t na(t) + n(n-1)b(t) + \sum_{k=1}^n \binom{n}{k} d^{(k)}(t) dt \right] . \quad (\text{I.1.82})$$

Summary We close this chapter with a summary of MPs.

MPs are stochastic processes where each event depends solely on the most recent one. Realistic MPs are only Markovian above a certain time scale, the Markov-Einstein time scale t_{ME} . A paradigmatic example is Brownian motion which arises from collisions of nanoscopic particles with fluid molecules, and the outcome of each collision depends only on the outcome of the previous collision. Here, t_{ME} is the average collision time. An intuitive approach the Brownian motion is the Langevin equation.

The Langevin equation is a SDE. We have seen that solutions of SDEs are realisations $x(t)$ of continuous MPs, determined by a deterministic and by a stochastic component, where the stochastic component arises from a Gaussian white noise $\xi(t)$. Due to the Markov assumption, $\xi(t)$ is δ -correlated. Instead of addressing the realisations $x(t)$ itself, a FPE is an evolution equation for the PDF $p(x, t)$ and defined by drift and diffusion coefficients, $D^{(1)}(x, t)$ and $D^{(2)}(x, t)$. The FPE is advantageous with regard to the calculation of moments $\langle x(t)^n \rangle$ and allows to determine the instantaneous stationary distribution $p^{\text{st}}(x, t)$, to which the process tries to relax at each instant of time. In the representation of WPIs, we defined the probability density functional $P[x(\cdot)]$ for paths $x(\cdot)$. The advantage of path integrals will unfold in the following chapter.

If the white noise $\xi(t)$ is not Gaussian, MPs are discontinuous, characterised by a jump density $\theta(y; x, t)$. In this case, a description via a FPE or WPI is not possible, or in some cases only an approximation. The evolution equation for $p(x, t)$ is the master equation, formally equivalent to the KME involving the KMCs $D^{(k)}(x, t)$. For a discontinuous MPs, all even $D^{(k)}(x, t)$ are non-zero, and for continuous MPs, the first two $D^{(k)}(x, t)$ are drift and diffusion of the FPE, the remaining $D^{(k)}(x, t)$ vanish. From the definition of the KMCs, an estimation of drift and diffusion from experimental data is possible.

The drift and diffusion coefficients $D^{(1,2)}(x, t)$ arise formally from the KME and are directly related to the moments of the jump density. In a thermodynamic setting, more relevant is the drift velocity $F(x, t) = D^{(1)}(x, t) - \partial_x D^{(2)}(x, t)$, as it arises from the physical potential that defines thermal equilibrium. The thermodynamic interpretation of continuous MPs is the subject of the following chapter.

I.2 Thermodynamic interpretation of continuous MPs

In the previous chapter we were mainly concerned with the formal definition and implications of Markov processes with barely physical reference. In this chapter, we will imbue the theory of continuous Markov processes with life by offering a thermodynamic interpretation. This interpretation will build on the equivalence between the stationary solution of the Fokker-Planck equation and the canonical equilibrium distribution.

In the first section of this chapter, I.2.1, we remark on thermodynamic consistency in the case of multiplicative noise, and will then identify expressions for heat and work from the Langevin equation and discuss the appendant first law. In section I.2.2, we use the FPE to establish the bridge to the Gibbs entropy together with the second law. In section I.2.3, we will approach the irreversibility of non-equilibrium processes using Wiener path integrals and elucidate the relation to entropy.

The distinctive feature of the thermodynamic interpretation will be its formulation on the level of individual realisations $x(t)$ of processes arbitrarily far from equilibrium. Non-equilibrium can be imposed by a time dependent external force, or by preparing the initial state of the process off equilibrium⁷. The former are *driven processes*, the latter are *relaxation processes*. The signature of non-equilibrium is in both cases that the solution of the FPE, $p(x, t)$, does not coincide with the stationary solution $p^{\text{st}}(x, t)$. The combination of stochasticity and non-equilibrium is the scope of *stochastic thermodynamics*.

In order to be transferable to other fields of application, we will leave the defining coefficients of the Markov process, e.g. $F(x, t)$ and $D(x, t)$, unspecified whenever possible. To maintain an intuitive level, however, we will occasionally come back to Brownian motion in which $F(x, t) = -\Gamma V'(x(t))$ arises from an external potential and $D = k_B T \Gamma$ is defined by the Einstein relation (I.1.9), and we will also on the formal level refer to the picture of particle and fluid.

More details to the material presented in this chapter can be found in a

⁷Also non-equilibrium constraints, such as multiple noise-terms (reservoirs), impose non-equilibrium, which will play a minor role in what follows.

recent review article by Seifert [29]. For an appealing introduction to the field of stochastic thermodynamics we recommend the overview article [30] by the same author.

1.2.1 Energy balance and the first law

Before we begin with identifying heat and work from the Langevin equation, we recap the stationary solution of the FPE and discuss its relation to equilibrium for various forms of the diffusion coefficient.

Thermodynamic consistency We start with ordinary Brownian motion subject to an external force, for which we derived in (I.1.1) the Langevin equation from Newton's equation of motion, (I.1.11), which involved a frictional force, an external force and a thermal force,

$$\gamma \dot{x}(t) = -V'(x(t)) + \sqrt{2\gamma k_B T} \xi(t) . \quad (\text{I.2.1})$$

Here, $V(x, t)$ is a potential that gives rise to the external force. The attendant canonical equilibrium distribution to $V(x, t)$ (the Boltzman distribution) reads

$$p^{\text{eq}}(x, t) = \frac{1}{Z(t)} \exp \left[-\beta V(x, t) \right] \quad (\text{I.2.2})$$

with $\beta := 1/k_B T$ and partition sum $Z(t) = \int \exp \left[-\beta V(x, t) \right] dx$. On the other hand, recall that the FPE (I.1.24)

$$\dot{p}(x, t) = \partial_x \left[-F(x, t) + D(x, t) \partial_x \right] p(x, t) , \quad p(x, t_0) = p_0(x) , \quad (\text{I.2.3})$$

implies a stationary distribution (I.1.39) of the form

$$p^{\text{st}}(x, t) = \exp \left[-\varphi(x, t) + \mathcal{G}(t) \right] \quad (\text{I.2.4})$$

with

$$\varphi(x, t) = - \int_{-\infty}^x \frac{F(\tilde{x}, t)}{D(\tilde{x}, t)} d\tilde{x} \quad (\text{I.2.5a})$$

$$\mathcal{G}(t) = - \ln \int \exp \left[-\varphi(x, t) \right] dx \quad (\text{I.2.5b})$$

By taking drift velocity $F(x, t)$ and diffusion coefficient $D(x, t)$ to be

$$F(x, t) = -\Gamma V'(x, t) , \quad (\text{I.2.6a})$$

$$D = k_B T \Gamma , \quad (\text{I.2.6b})$$

where $\Gamma = 1/\gamma$ is the mobility, we establish the equivalency of the FPE to the LE from Newton's equation of motion as stated above in (I.2.1) (cf. also (A.5.5)). The stationary distribution then coincides with the equilibrium distribution (I.2.1),

$$\varphi(x) = - \int_{-\infty}^x \frac{-\Gamma V'(x')}{k_B T \Gamma} dx' = \beta V(x) . \quad (\text{I.2.7})$$

In the above example, in which the diffusion coefficient is constant, $D = k_B T \Gamma$, the interpretation ambiguity of the LE with regard to the rule of discretisation is irrelevant. In cases in which the diffusion coefficient does not depend on x , the noise is called *additive noise*, as $\xi(t)$ enters the LE for $x(t)$ additively. In contrast, a state dependent diffusion coefficient implies a multiplication of $\xi(t)$ with $x(t)$, accordingly, in this case the noise is referred to as *multiplicative noise*. Therefore, the interpretation ambiguity of the LE arises only for multiplicative noise.

The ambiguity for multiplicative noise raises the question how the above discussed correspondence between the stationary distribution and thermal equilibrium is affected. In view of the Einstein relation, $D = k_B T \Gamma$, multiplicative noise may occur for position dependent mobility $\Gamma(x)$ or in the presence of a temperature gradient $T(x)$. We discuss both cases shortly.

The mobility of Brownian particles typically depend on their position in the presence of geometrical confinement, see the article by Lau and Lubensky [7]. The LE (I.1.12) derived from Newton's equation of motion becomes

$$\dot{x}_t = -\Gamma(x_t) V'(x_t, t) + \sqrt{2k_B T \Gamma(x_t)} \xi(t) . \quad (\text{I.2.8})$$

This is now a typical case of internal noise as discussed by van Kampen [19], since $\Gamma(x_t)$ influences both the deterministic and the stochastic component. Or in other words, in absence of the external force, $V'(x, t) \equiv 0$, the deterministic component of the process does not vanish, which can

immediately be seen from drift velocity and diffusion coefficient of the equivalent FPE (A.5.1c),

$$F(x, t) = -\Gamma(x)V'(x, t) - (1 - \alpha)k_B T \Gamma'(x_t) , \quad (\text{I.2.9a})$$

$$D(x, t) = k_B T \Gamma(x) . \quad (\text{I.2.9b})$$

If we dealt with external noise, we could take the above LE in the Stratonovich convention, $a = 1/2$. Instead, we choose $\alpha = 1$, since we then retain thermal equilibrium,

$$\varphi(x) = - \int_{-\infty}^x \frac{-\Gamma'(x')V'(x')}{k_B T \Gamma(x')} dx' = \beta V(x) , \quad (\text{I.2.10})$$

as $\Gamma(x)$ cancels for arbitrary dependency on x .

The starting point of this consideration was a naive generalisation of the LE. To avoid the resulting interpretation ambiguity, it is advisable to base the considerations on the FPE. The appropriate $F(x, t)$ and $D(x, t)$ follow then from a comparison of the FPE with the generalised Fick's law which indeed results into (I.2.9) for $\alpha = 1$ [7]. The equivalent LE to this FPE reads (A.5.5b)

$$\dot{x}_t = -\Gamma(x_t)V'(x_t, t) + (1 - \alpha)k_B T \Gamma'(x_t) + \sqrt{2k_B T \Gamma(x_t)} \xi(t) , \quad (\text{I.2.11})$$

for which no interpretation ambiguity arises since the dynamics is the same for any choice of α . The accordance with Fick's law and thermal equilibrium of the above LE (I.2.11) for any α (or the LE (I.2.8) for $\alpha = 1$) is what Lau and Lubensky mean by thermodynamic consistency [7].

The case where a temperature gradient causes multiplicative noise is intricate. If we again naively modify the LE as above with now constant mobility Γ and position dependent temperature $T(x)$, the equivalent FPE is defined by (A.5.1c),

$$F(x, t) = -\Gamma V'(x) - (1 - \alpha)\Gamma k_B T'(x_t) , \quad (\text{I.2.12a})$$

$$D(x, t) = \Gamma k_B T(x) , \quad (\text{I.2.12b})$$

and instead of $\varphi(x) = \beta V(x, t)$, the stationary distribution is now defined by

$$\begin{aligned} \varphi(x) &= \int_{-\infty}^x \frac{V'(x') + (1 - \alpha)k_B T'(x')}{k_B T(x')} dx' \\ &= (1 - \alpha) \ln T(x) + \int_{-\infty}^x \frac{V'(x')}{k_B T(x')} . \end{aligned} \quad (\text{I.2.13})$$

At this point it is not clear which α to choose, since the dynamics of suspended particles in fluids under the influence of a temperature gradient, known as thermophoresis, is still subject to current research [31–35, 14]. It is debatable whether a naively modified LE constitutes a fruitful approach to thermophoresis.

Heat, work and the first law We now turn to the energy balance implied by the LE due to its derivation from Newton’s equation of motion. We start again with ordinary Brownian motion, and then mention the difficulties that arise in the case of multiplicative noise.

To obtain the energy balance of Brownian motion, we multiply the LE with an infinitesimal piece of trajectory dx_t and obtain

$$\left[\gamma \dot{x}_t - \sqrt{2k_B T \gamma} \xi(t) \right] dx_t = -V'(x_t, t) dx_t. \quad (\text{I.2.14})$$

On the left hand side of (I.2.14), we find the energy loss due to motion against the friction force minus the energy received from collisions with fluid molecules (which may also be negative), which in total is the heat transferred into the fluid along dx_t . If the heat capacity of the fluid is much larger than the Brownian particles, we can assume that the fluid maintains a constant temperature T and serves as an ideal heat bath. Denoting the infinitesimal amount of dissipated heat by $\dot{Q}(t)$, the total heat dissipated by a particle along the trajectory $x(\cdot)$ in a time-interval $\tau = t_0 \dots t$ reads

$$Q[x(\cdot)] = \int_{t_0}^t \dot{Q}(\tau) d\tau = - \int_{t_0}^t V'(x_\tau, \tau) \dot{x}_\tau d\tau. \quad (\text{I.2.15})$$

Substitution of the total derivative of $V(x, t)$, that is $d_\tau V(x_\tau, \tau) = \dot{V}(x_\tau, \tau) + V'(x_\tau, \tau) \dot{x}_\tau$, reveals that $Q[x(\cdot)]$ can be split into an integral and a boundary term,

$$\begin{aligned} Q[x(\cdot)] &= \int_{t_0}^t \dot{V}(x_\tau, \tau) - d_\tau V(x_\tau, \tau) d\tau \\ &= \int_{t_0}^t \dot{V}(x_\tau, \tau) d\tau - [V(x_t, t) - V(x_0, t_0)]. \end{aligned} \quad (\text{I.2.16})$$

It is reasonable to identify the integral term as the work done on the system, as it constitutes a transfer of energy to a resting particle by externally lifting its potential energy, in contrast to heat dissipation which

takes place only for the moving particle. In view of the canonical equilibrium distribution (I.2.1), we identify the boundary term as the equilibrium difference in energy.

By denoting the work done on the particle as

$$W[x(\cdot)] = \int_{t_0}^t \dot{V}(x_\tau, \tau) \, d\tau \quad (\text{I.2.17})$$

and the equilibrium energy difference as

$$\Delta U = V(x_t, t) - V(x_0, t_0) , \quad (\text{I.2.18})$$

the first law on the level of individual trajectories follows from (I.2.16) as

$$\Delta U = W[x(\cdot)] - Q[x(\cdot)] . \quad (\text{I.2.19})$$

Hence, the equilibrium difference of energy between initial point and final point of the particle is the work done on the particle minus the dissipated heat. This derivation of the first law from Langevin dynamics was first noted by Sekimoto [36].

From the canonical point of view, we identify the Brownian particles as a *system* coupled to an *equilibrium heat bath* at constant temperature. We assume this heat bath to be the ambient medium, that is the fluid into which the particles are suspended. The assumption that the fluid is an ideal heat bath implies an instantaneous thermal equilibration for any value of $x(t)$. In fact, this equilibration takes place in finite time and is the fast dynamics on time scales $t < t_{\text{ME}}$ at which the Markov assumption does not hold. Hence, the inclusion of only the outcomes of collisions as white noise into the LE constitutes a coarse-graining of the fast dynamics to the slow dynamics modelled explicitly by the LE. Identifying the fast dynamics as the dynamics of the fluid molecules, and the slow dynamics as the dynamics of the particle, we may also regard $Q[x(\cdot)]$ in (I.2.15) as the transfer of heat from slow dynamics to fast dynamics, and the work $W[x(\cdot)]$ as the energy externally injected into the system by influencing the slow dynamics directly.

Due to the friction force $\gamma \dot{x}_t$, the derivation of the first law (I.2.19) takes explicitly non-equilibrium effects into account. To separate equilibrium

from non-equilibrium contributions to the first law (I.2.19), consider the canonical equilibrium distribution in the form

$$\begin{aligned} -\ln p^{\text{eq}}(x, t) &= \beta V(x, t) + \ln Z(t) \\ &= \frac{1}{k_{\text{B}}T} \left[V(x, t) - \mathcal{F}(t) \right] \end{aligned} \quad (\text{I.2.20})$$

with Helmholtz free energy

$$\mathcal{F}(t) = k_{\text{B}}T \ln Z(t) = k_{\text{B}}T \int e^{-\beta V(x, t)} . \quad (\text{I.2.21})$$

For reversible transition from equilibrium states x_0 at time t_0 to states x at time t , the reversible work $\Delta\mathcal{F} = \mathcal{F}(t) - \mathcal{F}(t_0)$ is the only work done on the system, and hence $-\Delta Q_{\text{rev}} = (\Delta U - \Delta\mathcal{F})$ is the heat reversibly received from the heat bath.⁸ Denoting by $W_{\text{diss}}[x(\cdot)]$ the work done in addition to the equilibrium work $\Delta\mathcal{F}$, and by $Q_{\text{irr}}[x(\cdot)]$ the heat transferred to the medium in addition to the reversible heat Q_{rev} , we rewrite the first law as (I.2.19)

$$\begin{aligned} W[x(\cdot)] &= \Delta\mathcal{F} + W_{\text{diss}}[x(\cdot)] \\ &= \Delta U + Q_{\text{rev}} + Q_{\text{irr}}[x(\cdot)] . \end{aligned} \quad (\text{I.2.22})$$

Limiting ourselves at first to quasi-steady process control, we see that spending the work $W[x(\cdot)]$, the internal energy of the system is increased by ΔU , and heat Q_{rev} is generated that is instantaneously transferred to the heat bath. Reversing the process, still in the case of quasi-steady process control, we can gain the free energy difference $\Delta\mathcal{F}$ as useful work by making direct use of lowering the internal energy by ΔU and retrieving Q_{rev} from the heat bath.

In the general (not quasi-steady) case, the additional heat $Q_{\text{irr}}[x(\cdot)]$ is dissipated, which in contrast to the quasi-steady case can not be retrieved from the heat bath in the reversed process, and the extra work $W_{\text{diss}}[x(\cdot)]$ has to be spent in order to compensate that heat loss. We will refer to $Q_{\text{irr}}[x(\cdot)]$ as irreversible heat, and to $W_{\text{diss}}[x(\cdot)]$ as dissipative work. Note

⁸In the context of stochastic thermodynamics it is common to denote by Q the heat delivered to the heat bath, in contrast to classical thermodynamics where Q is the heat received from the heat bath.

that in contrast to equilibrium state variables which only depend on initial and final state, the process functionals $Q_{\text{irr}}[x(\cdot)]$ and $W_{\text{diss}}[x(\cdot)]$ depend explicitly on the trajectory $x(\cdot)$ that connects initial and final state.

Depending on the process control, Q_{rev} can be retrieved or dissipated by the system, and the associated equilibrium entropy difference $\Delta S^{\text{eq}} = -Q_{\text{rev}}/T$ of the system can be positive or negative. Taking system and heat bath together, however, ΔS^{eq} of the system cancels with $-\Delta S^{\text{eq}}$ in the heat bath, and we are left with the irreversible entropy production (EP) $S_{\text{irr}}[x(\cdot)] = Q_{\text{irr}}[x(\cdot)]/T$ which is, according to the second law, on average non-negative. We will demonstrate in the next section, how $S_{\text{irr}}[x(\cdot)]$ arises along with other entropies from the FPE.

But before we turn to entropies arising from the FPE, let us briefly discuss the first law derived from the LE for multiplicative noise. For the case of state dependent mobility $\Gamma(x)$, or friction $\gamma(x) = 1/\Gamma(x)$, the energy balance based on the LE derived from Newton's equation of motion now reads

$$\left[\gamma(x_t) \dot{x}_t - \sqrt{2k_B T \gamma(x_t)} \xi(t) \right] dx_t = \left[-V'(x_t, t) - \frac{k_B T}{2} \frac{\gamma'(x_t)}{\gamma(x_t)} \right] dx_t. \quad (\text{I.2.23})$$

Here, we have taken the thermodynamic consistent LE (I.2.11) which reproduces for any convention α the canonical equilibrium distribution in the stationary state and chosen $\alpha = 1/2$ to resort to ordinary calculus. By following the same lines as for additive noise, we arrive at the modified first law

$$\Delta U + \Delta G = W[x(\cdot)] - Q[x(\cdot)] \quad (\text{I.2.24})$$

with the extra boundary term

$$\Delta G := k_B T \ln \sqrt{\frac{\Gamma(x_t)}{\Gamma(x_0)}}. \quad (\text{I.2.25})$$

We note that the quantity $T\Delta G$ is reminiscent of an entropy difference. For the case of a temperature gradient, which may even be time-dependent, we have the energy balance

$$\left[\gamma \dot{x}_t - \sqrt{2\gamma k_B T(x_t, t)} \xi(t) \right] dx_t = \left[-V'(x_t, t) - \frac{k_B T}{2} T'(x_t, t) \right] dx_t. \quad (\text{I.2.26})$$

In this case, all ingredients of the first law are augmented by thermophoretic terms

$$\Delta U \mapsto \left[V(x_\tau, \tau) + \frac{k_B}{2} T(x_\tau, \tau) \right]_{t_0}^t, \quad (\text{I.2.27a})$$

$$W[x(\cdot)] \mapsto \int_{t_0}^t \dot{V}(x_\tau, \tau) + \frac{k_B}{2} \dot{T}(x_\tau, \tau) \, d\tau, \quad (\text{I.2.27b})$$

$$Q[x(\cdot)] \mapsto \int_{t_0}^t \left[-V'(x_\tau, \tau) - \frac{k_B}{2} T'(x_\tau, \tau) \right] \dot{x}(\tau) \, d\tau, \quad (\text{I.2.27c})$$

where the second term in ΔU accounts for the difference in thermal energy between initial and final position, the extra term in $W[x(\cdot)]$ is due to lifting the thermal energy level of the particle externally (work-like), and for $Q[x(\cdot)]$ also the thermophoretic force proportional to the temperature gradient $T'(x)$ is considered.

We refrain from attempting a further interpretation of these results for the multiplicative case, and refer the interested reader to [37, 38, 14].

I.2.2 Entropies and the second law

In the previous section, we formulated the first law on the level of single stochastic trajectories in non-equilibrium. In doing so, we separated equilibrium state variables from non-equilibrium process functionals, the former only dependent on initial and final state, the latter on the specific trajectory. The introduced non-equilibrium functionals are dissipative work $W_{\text{diss}}[x(\cdot)]$ and irreversible heat dissipation $Q_{\text{irr}}[x(\cdot)]$, where $W_{\text{diss}}[x(\cdot)]$ has to be spent to compensate $Q_{\text{irr}}[x(\cdot)]$, hence, $W_{\text{diss}}[x(\cdot)] = Q_{\text{irr}}[x(\cdot)]$. The irreversibly dissipated heat is energy that can not be transformed into useful work. As a measure for useless energy, *entropy* is defined as irreversibly dissipated heat divided by the temperature of the heat bath that receives the heat. We will refer to the entropy change as *entropy production* (EP), which may also include equilibrium entropy differences. We denote the *total* EP of the compound of system and heat bath, that is the irreversible EP associated with $Q_{\text{irr}}[x(\cdot)]$, by $S_{\text{irr}}[x(\cdot)] = Q_{\text{irr}}[x(\cdot)]/T$. Perceiving the compound of system and bath as an isolated system, the second law applies for the total EP, $S_{\text{irr}}[x(\cdot)] > 0$.

The aim of this section is to identify $S_{\text{irr}}[x(\cdot)]$ from the FPE, along with

equilibrium EP, and two distinct EPs for non-equilibrium steady states (NESSs) that separately obey the second law. We will also demonstrate the equivalence of two established notions of EP.

As a preliminary, consider the probability current density $j(x, t) = F(x, t)p(x, t) - D(x, t)p'(x, t)$ defined in (I.1.25). In equilibrium, the current must vanish, $j^{\text{eq}}(x, t) \equiv 0$, which implies a basic condition to be satisfied in order for an equilibrium state to exist. Equivalent to demanding $j^{\text{eq}}(x, t) \equiv 0$ is the condition

$$F(x, t) - D(x, t) \frac{p^{\text{eq}'}(x, t)}{p^{\text{eq}}(x, t)} = \frac{j^{\text{eq}}(x, t)}{p^{\text{eq}}(x, t)} = \langle \dot{x} | x, t \rangle_{\text{eq}} \stackrel{!}{=} 0 . \quad (\text{I.2.28})$$

Substituting $p^{\text{eq}}(x, t) = \exp(-\varphi(x, t) - \mathcal{G}(t))$, this condition becomes

$$F(x, t) + D(x, t)\varphi'(x, t) = 0 , \quad (\text{I.2.29})$$

known as the *detailed balance condition* [39].

To satisfy the detailed balance condition, the external force must arise from a potential, $F(x, t) = -D(x, t)\varphi'(x, t)$, which can always be achieved in one dimensional processes. For the Brownian particle, i.e. $\varphi(x, t) = \beta V(x, t)$ and $F(x, t) = -\Gamma V'(x, t)$, the detailed balance equation becomes the Einstein relation (I.1.9), $\beta D = \Gamma$. Note that the two generalisations for multiplicative noise discussed in the previous section (position-dependent mobility and temperature gradient) also respect the detailed balance condition.

The general form (I.2.28) of the detailed balance condition, along with the local average of velocity $\langle \dot{x} | x, t \rangle$, will be important in the considerations of this section.

Trajectory based EP We now turn to entropic terms in a FPE. A reasonable definition for the system entropy on the formal level of a FPE is the Gibbs entropy

$$S(t) = \int p(x, t) s(x, t) \, dx = \langle s(x, t) \rangle , \quad (\text{I.2.30a})$$

$$s(x, t) = -k_{\text{B}} \ln p(x, t) , \quad (\text{I.2.30b})$$

where $p(x, t)$ is the solution of the FPE. In the following we will follow common practice and set $k_B := 1$, for which entropy becomes dimensionless and temperature is measured in units of energy.

In contrast to the thermodynamic quantities defined from the LE in the previous section, $S(t)$ and $s(x, t)$ are a-priori not defined on the level of individual trajectories $x(\cdot)$. To establish the formulation for individual $x(\cdot)$, we simply evaluate $s(x, t)$ along the trajectory $x(\tau)$, that is $s(x(\tau), \tau)$. Implicit and explicit differentiation with respect to τ yields

$$\dot{s}(\tau) = - \left. \frac{p'(x, t)}{p(x, t)} \right|_{x=x(\tau)} \dot{x}(\tau) - \left. \frac{\dot{p}(x, t)}{p(x, t)} \right|_{x=x(\tau)}, \quad (\text{I.2.31})$$

where we have written for short $d_\tau s(x(\tau), \tau) = \dot{s}(\tau)$. Integration of the EP rate $\dot{s}(\tau)$ with respect to τ recovers the notion of EPs as in the previous section.

To include the FPE (I.1.24) into our considerations, we use the current $j(x, t)$ defined in (I.1.25) and rewrite the FPE as

$$\frac{p'(x, t)}{p(x, t)} = - \frac{j(x, t)}{D(x, t)p(x, t)} + \frac{F(x, t)}{D(x, t)}. \quad (\text{I.2.32})$$

Substitution of the above form of the FPE into (I.2.31) yields $\dot{s}(\tau)$ in terms of $F(x, t)$ and $D(x, t)$,

$$\begin{aligned} \dot{s}(\tau) &= \frac{j(\tau)}{D(\tau)p(\tau)} \dot{x}(\tau) - \frac{F(\tau)}{D(\tau)} \dot{x}(\tau) - \frac{\dot{p}(\tau)}{p(\tau)} \\ &= \frac{\langle \dot{x} | \tau \rangle - F(\tau)}{D(\tau)} \dot{x}(\tau) - \frac{\dot{p}(\tau)}{p(\tau)}, \end{aligned} \quad (\text{I.2.33})$$

where we have written for short $p(\tau) = p(x(\tau), \tau)$ (analogous for the other quantities).

The first term is of the form “force times velocity”, in which, in the case of Brownian particles, the force becomes $\gamma \langle \dot{x} | \tau \rangle + V'(\tau)$. In view of (I.2.14), we see that this force is analog to the thermal force in the equivalent LE, and we may interpret $(\gamma \langle \dot{x} | \tau \rangle + V'(\tau)) \dot{x}(\tau)$ as the average energy received along $x(\tau)$ by the particle undergoing collisions with the fluid molecules. The second term of I.2.33 contributing to $\dot{s}(\tau)$ is the EP due to temporal change of $p(x, t)$, which is found in cases where the system is off equilibrium, that is for time dependent $D(x, t)$ or $F(x, t)$, or for an initial

distribution $p_0(x) \neq p^{\text{eq}}(x)$.

To obtain the EP rate in the steady state, we substitute $p^{\text{st}}(x, t)$ from (I.2.3),

$$\dot{s}^{\text{st}}(\tau) = -\frac{F(\tau)}{D(\tau)} \dot{x}(\tau) + (\dot{\varphi}(\tau) - \dot{\mathcal{G}}(\tau)) \quad (\text{I.2.34})$$

which upon integration becomes the difference of entropy between the stationary initial and final states,

$$\begin{aligned} \Delta S^{\text{st}} &= \int_{t_0}^t \varphi'(\tau) \dot{x}(\tau) + \dot{\varphi}(\tau) - \dot{\mathcal{G}}(\tau) \, d\tau \\ &= \Delta\varphi - \Delta\mathcal{G} \, , \end{aligned} \quad (\text{I.2.35})$$

irrespective of particular trajectories $x(\cdot)$. For the Brownian particle we recover the equilibrium EP,

$$\Delta S^{\text{st}} = \frac{-Q[x(\cdot)] + W[x(\cdot)] - \Delta\mathcal{F}}{T} = \frac{\Delta U - \Delta\mathcal{F}}{T} = \Delta S^{\text{eq}} \quad (\text{I.2.36a})$$

$$= \frac{-(Q_{\text{irr}}[x(\cdot)] + Q_{\text{rev}}) + W_{\text{diss}}[x(\cdot)]}{T} = -\frac{Q_{\text{rev}}}{T} = \Delta S^{\text{eq}} \, , \quad (\text{I.2.36b})$$

which is, again, valid for *arbitrary* individual trajectories $x(\cdot)$. We thus can determine the equilibrium entropy difference ΔS^{eq} between two states at time t_0 and t from non-equilibrium measurements of Q and W or Q_{irr} and W_{diss} , provided, of course, that we know the free energy difference $\Delta\mathcal{F}$.

Having identified the equilibrium EP from the FPE, we turn to the irreversible EP that obeys the second law which states that in an *isolated* and *macroscopic* system the entropy must increase. The specification 'macroscopic' is important in our considerations, since we deal with *individual* realisations. The bridge to macroscopic thermodynamics is established by considering the thermodynamic quantities in the *ensemble average* of in principle infinite many realisations. This macroscopic limit is equivalent to the thermodynamic limit in which the number of involved particles approaches infinity.

We introduced the Gibbs EP as the EP of the system. Being coupled to a heat bath, the system is not isolated, and accordingly, the system entropy

does not need to obey the second law. Instead, as already indicated in the previous section, we consider the compound of system and heat bath as an isolated system.

We denote by $\dot{s}_m(\tau)$ the EP in the medium, and by

$$\dot{s}_{\text{tot}}(\tau) = \dot{s}(\tau) + \dot{s}_m(\tau) \quad (\text{I.2.37})$$

the total EP of the compound of system and heat bath, which we expect to obey the second law. Availing ourselves of the picture of the Brownian particle and arguing that the EP in the medium is brought about by the heat $Q[x(\cdot)]$, we identify by comparison of (I.2.36a) with (I.2.34) the formal EP rate of the heat bath as

$$\dot{s}_m(\tau) := \frac{F(\tau)}{D(\tau)} \dot{x}(\tau) . \quad (\text{I.2.38})$$

Substituting the system EP rate $\dot{s}(\tau)$ from (I.2.33), we find for the total EP rate

$$\begin{aligned} \dot{s}_{\text{tot}}(\tau) &= \dot{s}(\tau) + \dot{s}_m(\tau) \\ &= \frac{\langle \dot{x} | \tau \rangle}{D(\tau)} \dot{x}(\tau) - \frac{\dot{p}(\tau)}{p(\tau)} , \end{aligned} \quad (\text{I.2.39})$$

or, in integrated form the total EP,

$$S_{\text{tot}}[x(\cdot)] = \Delta S + S_m[x(\cdot)] . \quad (\text{I.2.40})$$

We will show in the next section, see (I.2.71), that $S_{\text{tot}}[x(\cdot)]$ is indeed non-negative in the ensemble average. The identification of the total EP from the FPE we discussed here has been achieved by Seifert in [40].

In addition to defining the EP $S_m[x(\cdot)]$ by comparing (I.2.36a) with (I.2.34) as done above, we may also define the entropic equivalent of work, $R[x(\cdot)]$,

$$S_m[x(\cdot)] = - \int_{t_0}^t \varphi'(\tau) \dot{x}(\tau) \, d\tau , \quad (\text{I.2.41a})$$

$$R[x(\cdot)] := \int_{t_0}^t \dot{\varphi}(\tau) \, d\tau , \quad (\text{I.2.41b})$$

With the definitions above and substituting the total differential $d_\tau \varphi(\tau) = \varphi'(\tau)\dot{x}(\tau) + \dot{\varphi}(\tau)$ into (I.2.40), we can relate $S_{\text{tot}}[x(\cdot)]$ with $R[x(\cdot)]$,

$$S_{\text{tot}}[x(\cdot)] = R[x(\cdot)] - (\Delta\varphi - \Delta S) . \quad (\text{I.2.42})$$

Note that in these considerations we did not demand the process to start and end in a steady state. If we do so, however, the equations for the total EP simplify to

$$S_{\text{tot}}[x(\cdot)] = \Delta S^{\text{st}} + S_{\text{m}}[x(\cdot)] \quad (\text{I.2.43a})$$

$$= R[x(\cdot)] - \Delta\mathcal{G} . \quad (\text{I.2.43b})$$

In view this simplification, we mention that a formulation in terms of the Kullback-Leibler divergence $(-\ln(p/p^{\text{st}}))$ instead of the Gibbs entropy $(-\ln p)$ is advantageous.

Spatial averaged EP The discussion of entropies presented so far was based on evaluating EP rates $\dot{s}(x, t)$ along trajectories $x(\tau)$ to get EP rates $\dot{s}(\tau) = \dot{s}(x(\tau), \tau)$ and EPs $S[x(\cdot)]$ on the level of single $x(\cdot)$. This formulation in terms of functionals is of advantage when addressing EPs using WPIs, as will be discussed in the next section. In contrast to the *functional* formulation, it is also common to consider the *spatial average* of $\dot{s}(x, t)$, as suggested by Esposito and van den Broeck [41, 42, 39]. For completeness, we briefly demonstrate the correspondence of both formulations.

Starting point is again the Gibbs EP

$$\begin{aligned} \dot{S}(t) &= -d_t \int p(x, t) \ln p(x, t) dx \\ &= - \int \dot{p}(x, t) \ln p(x, t) dx - \int \dot{p}(x, t) dx . \end{aligned} \quad (\text{I.2.44})$$

Substituting $\dot{p}(x, t) = -j'(x, t)$, integrating by parts and substituting $p'(x, t)$ from the definition of $j(x, t)$ in (I.1.25), we find the splitting

$$\begin{aligned}\dot{S}(t) &= - \int j(x, t) \frac{p'(x, t)}{p(x, t)} dx \\ &= \int \frac{j(x, t)^2}{D(x, t)p(x, t)} dx - \int \frac{F(x, t)j(x, t)}{D(x, t)} dx .\end{aligned}\quad (\text{I.2.45})$$

The first term is the total irreversible EP and corresponds to $S_{\text{tot}}[x(\cdot)]$, and the second term is the EP in the heat bath and corresponds to $S_{\text{m}}[x(\cdot)]$. To clarify this correspondence, we rewrite

$$\dot{S}(t) = \int p(x, t) [\dot{s}_{\text{i}}(x, t) - \dot{s}_{\text{e}}(x, t)] dx \quad (\text{I.2.46})$$

in terms of the EP fields

$$\dot{s}_{\text{i}}(x, t) := \frac{\langle \dot{x}|x, t \rangle^2}{D(x, t)} - \frac{\dot{p}(x, t)}{p(x, t)} \quad (\text{I.2.47a})$$

$$\longleftrightarrow \quad \dot{s}_{\text{tot}}(\tau) = \frac{\langle \dot{x}|\tau \rangle}{D(\tau)} \dot{x}(\tau) - \frac{\dot{p}(\tau)}{p(\tau)}$$

$$\dot{s}_{\text{e}}(x, t) := \frac{F(x, t)}{D(x, t)} \langle \dot{x}|x, t \rangle \quad (\text{I.2.47b})$$

$$\longleftrightarrow \quad \dot{s}_{\text{m}}(\tau) = \frac{F(\tau)}{D(\tau)} \dot{x}(\tau)$$

in correspondence to (I.2.39) and (I.2.38). Note that we included the second term in (I.2.44) into $\dot{s}_{\text{i}}(x, t)$ which vanishes under spatial average due to probability conservation.

On spatial average, we arrive at the average EP rate discussed by Esposito and van den Broeck [41, 42, 39]

$$\dot{S}_{\text{i}}(x, t) = \int \frac{j(x, t)^2}{D(x, t)p(x, t)} dx \quad (\text{I.2.48a})$$

$$\dot{S}_{\text{e}}(x, t) = \int \frac{F(x, t)}{D(x, t)} j(x, t) dx \quad (\text{I.2.48b})$$

$$\dot{S}(x, t) = \dot{S}_{\text{i}}(x, t) - \dot{S}_{\text{e}}(x, t) \quad (\text{I.2.48c})$$

In view of (I.2.47) and (I.2.48), we make three comments.

- (i) The total EP is non-negative for all times t , $\dot{S}_i(x, t) \geq 0$, and is the irreversible EP that obeys the second law.
- (ii) On the trajectory level, we have besides the local average velocity along a trajectory, $\langle \dot{x} | \tau \rangle$, also the velocity of the trajectory itself, $\dot{x}(\tau)$, a distinction that is lost in the spatially averaged formulation of the Gibbs EP.
- (iii) The term \dot{p}/p in the irreversible EP rate only contributes on the trajectory level which suggests that \dot{p}/p accounts for a local balance between EPs that cancel in the spatial average.

Multidimensional generalisation So far, we limited ourselves to one-dimensional continuous MPs. In higher dimensions, i.e. $\mathbf{X}(t) \in \mathbb{R}^n$ with $n \geq 2$, the stationary solution of the FPE does not necessarily coincide with thermal equilibrium, the system is then referred to be in a *non-equilibrium steady state* (NESS). The defining property of a NESS is that the stationary probability current does no longer vanish, but acquires a constant value in time. The non-vanishing current in a steady state is possible because in higher dimensions a particle can run in closed loops, repeating each loop under the same conditions. Thus, in a NESS, the probability of observing a particle at time t at a position \mathbf{x} will be constant in time and the probability current $\mathbf{j}^{\text{st}}(\mathbf{x}, t)$ will be divergence free.

We discussed this multidimensional setting already in terms of a FPE in section I.1.2 after (I.1.40). The multidimensional drift velocity reads (I.2.78)

$$\mathbf{F}(\mathbf{x}, t) = \mathbf{D}(\mathbf{x}, t) [-\nabla \varphi(\mathbf{x}, t) + \mathbf{A}(\mathbf{x}, t)] . \quad (\text{I.2.49})$$

The forces that drive the particles in loops must be non-conservative, which we included into $\mathbf{F}(\mathbf{x}, t)$ in terms of a divergence free vector field $\mathbf{A}(\mathbf{x}, t)$. For a Brownian particle is

$$\mathbf{D}_{ij}(\mathbf{x}, t) \equiv \Gamma / \beta \delta_{ij} \quad (\text{I.2.50a})$$

$$\mathbf{A}(\mathbf{x}, t) = \beta \mathbf{F}_{\text{nc}}(\mathbf{x}, t) \quad (\text{I.2.50b})$$

$$\varphi(\mathbf{x}, t) = \beta V(\mathbf{x}, t) \quad (\text{I.2.50c})$$

$$\mathbf{F}(\mathbf{x}, t) = \Gamma [-\nabla V(\mathbf{x}, t) + \mathbf{F}_{\text{nc}}(\mathbf{x}, t)] \quad (\text{I.2.50d})$$

and \mathbf{F}_{nc} the non-conservative force.

The non-zero current in a NESS has consequences for the EP. Although in a steady state, the persistent motion of the particle dissipates energy and the system needs a continuous intake of energy to compensate that heat loss. The continuous dissipated heat into the medium is called *house-keeping heat* Q_{hk} , in the sense that its compensation maintains the NESS. The heat transferred to the medium that comes in addition to Q_{hk} is the so-called *excess heat* Q_{ex} . Distinguishing the two EPs associated with these two heat fluxes into the medium, we split the EP in the medium

$$(I.2.51)$$

$$S_{\text{m}}[\mathbf{x}(\cdot)] = S_{\text{hk}}[\mathbf{x}(\cdot)] + S_{\text{ex}}[\mathbf{x}(\cdot)] \quad (I.2.52)$$

into the two contributions

$$S_{\text{hk}}[\mathbf{x}(\cdot)] = \int_{t_0}^t \dot{\mathbf{x}}(\tau) \mathbf{D}^{-1}(\tau) \langle \dot{\mathbf{x}} | \tau \rangle_{\text{st}} \, d\tau \quad (I.2.53a)$$

$$S_{\text{ex}}[\mathbf{x}(\cdot)] = - \int_{t_0}^t \dot{\mathbf{x}}(\tau) \nabla \phi(\tau) \, d\tau \quad (I.2.53b)$$

with the stationary mean local velocity $\langle \dot{\mathbf{x}} | \tau \rangle_{\text{st}}$ from (I.1.46) and the non-equilibrium potential $\phi(\mathbf{x}, t) = -\ln p^{\text{st}}(\mathbf{x}, t)$ from (I.1.44). This splitting was introduced by Oono and Paniconi [43] and picked up by Hatano and Sasa [44], Speck and Seifert [45, 46] and Chernyak, Chertkov and Jarzynski [21] and many others [47–51].

The housekeeping EP $S_{\text{hk}}[\mathbf{x}(\cdot)]$ is non-negative in the ensemble average, whereas $S_{\text{ex}}[\mathbf{x}(\cdot)]$, like $S_{\text{m}}[\mathbf{x}(\cdot)]$, can remain positive on average, as it also includes reversible entropy transfer. To obtain the irreversible part of $S_{\text{ex}}[\mathbf{x}(\cdot)]$, we follow the same strategy as for $S_{\text{tot}}[\mathbf{x}(\cdot)]$ and find the non-negative EP ([29] p. 14)

$$\begin{aligned} S_{\text{ex}}^{\geq}[\mathbf{x}(\cdot)] &:= \Delta S + S_{\text{ex}}[\mathbf{x}(\cdot)] \\ &= \Delta S - \Delta \phi + \int_{t_0}^t \dot{\phi}(\tau) \, d\tau \\ &= -\ln \frac{p(\tau)}{p^{\text{st}}(\tau)} \Big|_{t_0}^t + \int_{t_0}^t \dot{\phi}(\tau) \, d\tau \end{aligned} \quad (I.2.54)$$

In the absence of non-conservative forces, $\mathbf{A}(\mathbf{x}, t) \equiv 0$, we have $\phi(\mathbf{x}, t) = \varphi(\mathbf{x}, t) - \mathcal{G}(t)$ (and $S_{\text{hk}}[\mathbf{x}(\cdot)] \equiv 0$) and are left with $S_{\text{ex}}^{\geq}[\mathbf{x}(\cdot)] = S_{\text{tot}}[\mathbf{x}(\cdot)]$. Taking it all together, in the presence of NESSs we have three non-negative EPs, the total EP

$$S_{\text{tot}}[\mathbf{x}(\cdot)] = S_{\text{hk}}[\mathbf{x}(\cdot)] + S_{\text{ex}}^{\geq}[\mathbf{x}(\cdot)] \geq 0 \quad (\text{I.2.55})$$

which is composed of the entropy $S_{\text{hk}}[\mathbf{x}(\cdot)] \geq 0$ produced for keeping up the stationary current $j^{\text{st}}(\mathbf{x}, t)$ in the “instantaneous” NESS $p^{\text{st}}(\mathbf{x}, t)$, and the entropy $S_{\text{ex}}^{\geq}[\mathbf{x}(\cdot)] \geq 0$ produced when not being in the NESS as in a relaxation process or a driven process.

The splitting into S_{hk} and S_{ex}^{\geq} can also be written in terms of spatial averaged EPs,

$$\begin{aligned} \dot{S}_{\text{na}}(t) &:= \int p(\mathbf{x}, t) \left[\frac{\mathbf{J}(\mathbf{x}, t)}{p(\mathbf{x}, t)} - \frac{\mathbf{j}^{\text{st}}(\mathbf{x}, t)}{p^{\text{st}}(\mathbf{x}, t)} \right] \mathbf{D}^{-1}(\mathbf{x}, t) \left[\frac{\mathbf{J}(\mathbf{x}, t)}{p(\mathbf{x}, t)} - \frac{\mathbf{j}^{\text{st}}(\mathbf{x}, t)}{p^{\text{st}}(\mathbf{x}, t)} \right] d^n x \\ &= - \int p(\mathbf{x}, t) \ln \frac{p(\mathbf{x}, t)}{p^{\text{st}}(\mathbf{x}, t)} d^n x \end{aligned} \quad (\text{I.2.56a})$$

$$\dot{S}_{\text{a}}(t) := \int p(\mathbf{x}, t) \frac{\mathbf{j}^{\text{st}}(\mathbf{x}, t)}{p^{\text{st}}(\mathbf{x}, t)} \mathbf{D}^{-1}(\mathbf{x}, t) \frac{\mathbf{j}^{\text{st}}(\mathbf{x}, t)}{p^{\text{st}}(\mathbf{x}, t)} d^n x \quad (\text{I.2.56b})$$

$$\dot{S}_{\text{i}}(t) = \dot{S}_{\text{na}}(t) + \dot{S}_{\text{a}}(t) \quad (\text{I.2.56c})$$

where it can be shown using the chain rule and the FPE that the mixed term of the quadratic form in $\dot{S}_{\text{na}}(t)$ vanishes,

$$\begin{aligned} &\int p(\mathbf{x}, t) \left[\frac{\mathbf{j}^{\text{st}}(\mathbf{x}, t)}{p^{\text{st}}(\mathbf{x}, t)} \right] \mathbf{D}^{-1}(\mathbf{x}, t) \left[\frac{\mathbf{J}(\mathbf{x}, t)}{p(\mathbf{x}, t)} - \frac{\mathbf{j}^{\text{st}}(\mathbf{x}, t)}{p^{\text{st}}(\mathbf{x}, t)} \right] d^n x \\ &= - \int \nabla \left[p(\mathbf{x}, t) \frac{\mathbf{j}^{\text{st}}(\mathbf{x}, t)}{p^{\text{st}}(\mathbf{x}, t)} \right] d^n x = 0 \end{aligned}$$

and therefore the splitting (I.2.56c) holds.

Due to the quadratic forms it is apparent that $\dot{S}_{\text{na}}(t) \geq 0$ and $\dot{S}_{\text{a}}(t) \geq 0$ for all times t . The EP $\dot{S}_{\text{na}}(t)$ is the analog of $S_{\text{ex}}^{\geq}[\mathbf{x}(\cdot)]$, and $\dot{S}_{\text{a}}(t)$ the analog of $S_{\text{hk}}[\mathbf{x}(\cdot)]$. The index of S_{na} stands for “non-adiabatic”, and in S_{a} for “adiabatic”, where “adiabatic” refers to the quasi-steady limit of process control. In that sense, $\dot{S}_{\text{na}}(t)$ is the irreversible entropy produced despite

of adiabatic process control, which is non-zero if non-conservative forces are involved [41].

Instead of non-conservative forces giving rise to NESSs, also in the case of multiple heat baths at different temperature we encounter NESSs. The simplest example is the heat transport from one heat bath to a second at lower temperature. In general, we can think of concurrent processes driven by different heat baths, each of which trying to impose their temperature on the system. This setting was analysed by Esposito and van den Broeck for continuous MPs [39] and discontinuous MPs [41, 42].

The analysis of EP can also be rather analogously extended to discontinuous MPs, which we consider beyond the scope of this thesis and direct the interested reader to the comprehensive article by Harris and Schütz [52] and part 6 of [29] for a brief introduction.

I.2.3 Fluctuation theorems and irreversibility

In the previous section, we mentioned the relation between entropy and irreversibility: If a transition from state A to state B produces entropy in finite time, no transition from B to A will be able to entirely consume this entropy, resulting in a net increase of *irreversible* entropy after completing the cycle. This irreversibly produced amount of entropy is a measure of the loss of useful energy, typically in the form of dissipated heat.

In this section, we aim at further exploring the connection of entropy and irreversibility. This connection will be stated in terms of fluctuation theorems (FTs), a rather new finding in the framework of stochastic thermodynamics, which were first observed 1993 by Evans et al. for entropy fluctuations in a shear driven fluid in contact with a heat bath [53, 54], and two years later proved to hold for a subclass of dissipative dynamical systems [55, 56]. In the sequel, FTs have been intensively studied and proved for many other settings. We will focus on FTs for continuous MPs, and give a short account on their applications in the next section.

Recent review articles on the relation between fluctuation theorems and irreversibility haven been written by van den Broeck [57] and Jarzynski [58], and is also covered by Seifert's review article [29].

Entropy and irreversibility As already mentioned, we ask the question at what entropic cost the consequences of a individual trajectory $x(\cdot)$ can be undone. This is best understood by parametrising the time dependency of the dynamics in terms of a protocol $\kappa(\cdot)$, i.e. $F(x; \kappa(\tau))$, $D(x; \kappa(\tau))$. The protocol $\kappa(\tau)$ takes different values when time evolves from t_0 to t . To assess the probability of individual trajectories $x(\cdot)$, we employ the WPIs introduced in section I.1.3. There, we defined the path probability

$$P[x(\cdot)|x_0; \kappa(\cdot)] = e^{-S[x(\cdot); \kappa(\cdot)]} \quad (\text{I.2.57})$$

in terms of the action functional

$$S[x(\cdot); \kappa(\cdot)] = \int_{t_0}^t \frac{(\dot{x}_\tau - F(x_\tau; \kappa_\tau))^2}{4D(x_\tau; \kappa_\tau)} + J(x_\tau; \kappa_\tau) d\tau \quad (\text{I.2.58})$$

$$J(x, t) = \frac{1}{2}F'(x, t) + \frac{1}{4}D''(x, t) . \quad (\text{I.2.59})$$

Here, we use the Stratonovich convention in order to use ordinary calculus, cf. (I.1.55) or (A.5.5d) for $\alpha = 1/2$.

To measure irreversibility, consider the time-reversal of dynamics, $\bar{\tau} = t - \tau + t_0$, $d\bar{\tau} = -d\tau$. Imagine we fix a starting point x_0 and observe a trajectory $x(\cdot)$, to which we can assign the path-probability $P[x(\cdot)|x_0; \kappa(\cdot)] \mathcal{D}x(\cdot)$. As a conjugate process, we define the time-reversed process by $\tau \mapsto \bar{\tau}$, i.e. use the protocol $\bar{\kappa}(\tau) = \kappa(t - \tau + t_0)$ instead of $\kappa(\tau)$. The path-probability of the time-reversed dynamics then reads $P[x(\cdot)|\bar{x}_0; \bar{\kappa}(\cdot)] \mathcal{D}x(\cdot)$.

In general, for a reversible trajectory $x(\cdot)$, the path probability of the time-reversed trajectory $\bar{x}(\cdot)$ under the time-reversed dynamics should be equal to the observed trajectory $x(\cdot)$ in the original dynamics, $P[\bar{x}(\cdot)|\bar{x}_0; \bar{\kappa}(\cdot)] = P[x(\cdot)|x_0; \kappa(\cdot)]$. For arbitrary trajectories, but in a reversible process, we will still have $P[\langle \bar{x}(\cdot) \rangle |\bar{x}_0; \bar{\kappa}(\cdot)] = P[\langle x(\cdot) \rangle |x_0; \kappa(\cdot)]$ for the average realisation $\langle x(\cdot) \rangle$. For trajectories in an irreversible process, however, the path probabilities $P[\bar{x}(\cdot)|\bar{x}_0; \bar{\kappa}(\cdot)]$ and $P[x(\cdot)|x_0; \kappa(\cdot)]$ will in general be distinct, since it is the very nature of an irreversible process that the original state can not be retrieved upon reversal of process control. This suggests, in analogy to the Gibbs entropy, to consider as a measure for irreversibility

$$\ln \frac{P[x(\cdot)|x_0; \kappa(\cdot)]}{P[\bar{x}(\cdot)|\bar{x}_0; \bar{\kappa}(\cdot)]} = \mathcal{S}[\bar{x}(\cdot); \bar{\kappa}(\cdot)] - \mathcal{S}[x(\cdot); \kappa(\cdot)] , \quad (\text{I.2.60})$$

that is, the difference of the respective actions.

To calculate this difference explicitly, we make use of the substitution $\bar{\tau} = t - \tau + t_0$ to rewrite

$$\begin{aligned} \mathcal{S}[\bar{x}(\cdot); \bar{\kappa}(\cdot)] &= \int_{t_0}^t \frac{(\dot{\bar{x}}_\tau - F(\bar{x}_\tau; \bar{\kappa}_\tau))^2}{4D(\bar{x}_\tau; \bar{\kappa}_\tau)} + J(\bar{x}_\tau; \bar{\kappa}_\tau) \, d\tau \\ &= - \int_t^{t_0} \frac{(-\dot{\bar{x}}_{\bar{\tau}} - F(\bar{x}_{\bar{\tau}}; \bar{\kappa}_{\bar{\tau}}))^2}{4D(\bar{x}_{\bar{\tau}}; \bar{\kappa}_{\bar{\tau}})} + J(\bar{x}_{\bar{\tau}}; \bar{\kappa}_{\bar{\tau}}) \, d\bar{\tau} \\ &= \int_{t_0}^t \frac{(\dot{x}_\tau + F(x_\tau; \kappa_\tau))^2}{4D(x_\tau; \kappa_\tau)} + J(x_\tau; \kappa_\tau) \, d\tau . \end{aligned} \quad (\text{I.2.61})$$

The Jacobian cancels and only the mixed term of the square remains,

$$\begin{aligned} \mathcal{S}[\bar{x}(\cdot); \bar{\kappa}(\cdot)] - \mathcal{S}[x(\cdot); \kappa(\cdot)] &= \int_{t_0}^t \frac{(\dot{x}_\tau + F(x_\tau; \kappa_\tau))^2 - (\dot{x}_\tau - F(x_\tau; \kappa_\tau))^2}{4D(x_\tau; \kappa_\tau)} \, d\tau \\ &= \int_{t_0}^t \frac{\dot{x}_\tau F(x_\tau; \kappa_\tau)}{D(x_\tau; \kappa_\tau)} \, d\tau \\ &= S_m[x(\cdot)] , \end{aligned} \quad (\text{I.2.62})$$

and we recover as the measure of irreversibility, on the level of individual trajectories, the EP in the medium,

$$S_m[x(\cdot)] = \ln \frac{P[x(\cdot)|x_0; \kappa(\cdot)]}{P[\bar{x}(\cdot)|\bar{x}_0; \bar{\kappa}(\cdot)]} . \quad (\text{I.2.63})$$

Any trajectory $x(\cdot)$ connecting initial and final point with an EP $S_m[x(\cdot)] > 0$ is not as likely to be observed in the time-reversed process.

There seems, however, to be a flaw in that argumentation, since S_m also includes the reversible heat transfer from system to heat bath, implying that a realisation $x(\cdot)$ can be reversible despite $S_m[x(\cdot)] = -\Delta S^{\text{st}} \neq 0$ (ΔS^{st} is the reversible EP in the system, and consequently $-\Delta S^{\text{st}}$ the EP in the heat bath). This flaw gets unravelled by noting that the stationary EP S^{st} is not a process functional but a state variable and as such only depends on initial and final points x_0 and x_t , whereas $S_m[x(\cdot)]$ only accounts for the EP by connecting a given initial and final state. In other words,

the path probability $P[x(\cdot)|x_0; \kappa(\cdot)]$ does not account for the probability $p_0(x_0)$ of the initial value x_0 , and the associated entropy, $-\ln p_0(x_0)$, can not enter our considerations.

Augmenting the conditioned path-probabilities with the initial distribution for the forward process, $p_0(x)$, and the solution of the FPE as the initial distribution for the reverse process, $p_t(x) := p(x, t)$, we indeed recover the total, irreversible EP

$$\begin{aligned} \ln \frac{p_0(x_0) P[x(\cdot)|x_0; \kappa(\cdot)]}{p_t(\bar{x}_0) P[\bar{x}(\cdot)|\bar{x}_0; \bar{\kappa}(\cdot)]} &= -\ln \frac{p_t(x_t)}{p_0(x_0)} + S_m[x(\cdot)] \\ &= \Delta S + S_m[x(\cdot)] = S_{\text{tot}}[x(\cdot)] \end{aligned} \quad (\text{I.2.64})$$

derived in the context of the corresponding FPE (I.2.40).

We readily convince ourselves that the above augmentation with the initial distributions indeed resolves the flaw discussed in view of (I.2.63): For the case that the process starts in a steady state and for quasi-steady process control, we have $p_0(x) = p^{\text{st}}(x, t_0)$ and $p_t(x) = p^{\text{st}}(x, t)$ and therefore $\Delta S = \Delta s^{\text{eq}}$ and $S_{\text{tot}}[x(\cdot)] = \Delta s^{\text{eq}} - \Delta s^{\text{eq}} = 0$. For any irreversible realisation $x(\cdot)$, we will have $S_{\text{tot}}[x(\cdot)] \neq 0$ which can be due to start off equilibrium (relaxation process) or non-equilibrium process control (driven process) or both. In this way, the path integral formulation and the notion of time-reversal elucidates the intimate relation between entropy and irreversibility.

The EP $S_{\text{tot}}[x(\cdot)]$ features a time-reversal symmetry. This symmetry becomes evident when using (I.2.64) to write $S_{\text{tot}}[x(\cdot)]$ in the form

$$S_{\text{tot}}[x(\cdot)] = \mathcal{S}[\bar{x}(\cdot); \bar{\kappa}(\cdot)] - \ln p_t(x_t) - (\mathcal{S}[x(\cdot); \kappa(\cdot)] - \ln p_0(x_0)) \quad (\text{I.2.65})$$

and then express the EP of the reversed trajectory under the time-reversed dynamics, $\bar{S}_{\text{tot}}[\bar{x}(\cdot)]$, in terms of the original EP,

$$\begin{aligned} \bar{S}_{\text{tot}}[\bar{x}(\cdot)] &= \mathcal{S}[\bar{\bar{x}}(\cdot); \bar{\bar{\kappa}}(\cdot)] - \ln \bar{p}_t(\bar{x}_t) - (\mathcal{S}[\bar{x}(\cdot); \bar{\kappa}(\cdot)] - \ln \bar{p}_0(\bar{x}_0)) \\ &= \mathcal{S}[x(\cdot); \kappa(\cdot)] - \ln p_0(x_0) - (\mathcal{S}[\bar{x}(\cdot); \bar{\kappa}(\cdot)] - \ln p_t(x_t)) \\ &= -S_{\text{tot}}[x(\cdot)] \end{aligned} \quad (\text{I.2.66})$$

Building on (I.2.66) and (I.2.64), we can express the forward path-probability

in terms of the reversed path-probability

$$P[x(\cdot)|x_0] = \frac{p_t(x_t)}{p_0(x_0)} \bar{P}[\bar{x}(\cdot)|x_t] e^{-\bar{S}_{\text{tot}}[\bar{x}(\cdot)]} \quad (\text{I.2.67})$$

where we have written for short $\bar{P}[\bar{x}(\cdot)|x_t] = P[\bar{x}(\cdot)|x_t; \bar{\kappa}(\cdot)]$. The above relation can be interpreted as the detailed balance condition on the level of single realisations, broken if the realisation irreversibly produces entropy, i.e. $S_{\text{tot}}[x(\cdot)] > 0$.

This kind of observation is the starting point to the derivation of so-called *fluctuation theorems* (FTs). We use (I.1.62) to express the probability density of the integral value $S_{\text{tot}} = S_{\text{tot}}[x(\cdot)]$ in terms of a WPI and substitute (I.2.67) to derive

$$\begin{aligned} p(S_{\text{tot}}) &= \int dx_t \int dx_0 p_0(x_0) \int_{(x_0, t_0)}^{(x_t, t)} \mathcal{D}x(\cdot) P[x(\cdot)|x_0] \delta(S_{\text{tot}} - S_{\text{tot}}[x(\cdot)]) \\ &= \int dx_t \int dx_0 \int_{(x_0, t_0)}^{(x_t, t)} \mathcal{D}x(\cdot) e^{-\bar{S}_{\text{tot}}[\bar{x}(\cdot)]} p_t(x_t) \bar{P}[\bar{x}(\cdot)|x_t] \delta(S_{\text{tot}} + \bar{S}_{\text{tot}}[\bar{x}(\cdot)]) \\ &= e^{S_{\text{tot}}} \int dx_0 \int dx_t p_t(x_t) \int_{(x_t, t)}^{(x_0, t_0)} \mathcal{D}\bar{x}(\cdot) \bar{P}[\bar{x}(\cdot)|x_t] \delta(S_{\text{tot}} + \bar{S}_{\text{tot}}[\bar{x}(\cdot)]) \\ &= e^{S_{\text{tot}}} \bar{p}(-S_{\text{tot}}) \end{aligned} \quad (\text{I.2.68})$$

For the third line we used the δ -function to write $e^{S_{\text{tot}}}$ before the integral, and we performed the variable transformation $x(\cdot) \mapsto \bar{x}(\cdot)$ of which the Jacobian is the identity as the transformation merely corresponds to a reversal of integration order (cf. the discrete definition of a WPI in (I.1.54)). The resulting relation,

$$\frac{p(S_{\text{tot}})}{\bar{p}(-S_{\text{tot}})} = e^{S_{\text{tot}}} , \quad (\text{I.2.69})$$

is known as a *detailed fluctuation theorem* (dFT), in this case for the irreversible EP S_{tot} . The dFT relates the probability of observing a *production*

of entropy to the probability of observing the *consumption* of entropy in the time-reversed process. The statement is that the odds of a consumption of entropy S_{tot} in the time-reversed process compared to the probability of a production of entropy S_{tot} in the forward process goes down exponentially with the entropy S_{tot} itself. In contrast to addressing the concept of irreversibility in terms of a WPI, as done in (I.2.64), the dFT is a probabilistic formulation of irreversibility in terms of the PDF $p(S_{\text{tot}})$. This probabilistic formulation can be further reduced by integration of (I.2.69),

$$\int e^{-S_{\text{tot}}} p(S_{\text{tot}}) dS_{\text{tot}} = \langle e^{-S_{\text{tot}}} \rangle = 1, \quad (\text{I.2.70})$$

which is known as an *integral fluctuation theorem* (iFT). Along similar lines as for the derivation of the dFT in (I.2.69), this iFT can also be derived in terms of a WPI by using the normalisation condition of the WPI as introduced in (I.1.60). Note that the iFT goes without the notion of time-reversal, implying that the mere existence of time-reversal rather than its explicit form is enough for the iFT to hold.

The iFT and dFT for the total EP S_{tot} was derived from the path integral representation by Seifert [40].

In the previous chapter, we postponed the proof that upon ensemble average it is $\langle S_{\text{tot}}[x(\cdot)] \rangle \geq 0$. This proof follows now immediately by applying the inequality $\langle \exp x \rangle \geq \exp \langle x \rangle$ to the iFT

$$\begin{aligned} 1 &= \langle e^{-S_{\text{tot}}[x(\cdot)]} \rangle \geq e^{-\langle S_{\text{tot}}[x(\cdot)] \rangle} \\ &\Rightarrow \langle S_{\text{tot}} \rangle \geq 0. \end{aligned} \quad (\text{I.2.71})$$

Remarkably, considering that the second law is an inequality and the iFT an equality, we reproduced the second law from the iFT. Or, in other words, in equilibrium thermodynamics we have $\langle S_{\text{tot}}[x(\cdot)] \rangle = 0$, whereas in non-equilibrium thermodynamics we find $\langle \exp [-S_{\text{tot}}[x(\cdot)]] \rangle = 1$. In that sense, the iFT refines the second law. Note that in order to observe the iFT to hold true for a limited number of realisations, the exponential average, $\langle \exp [-S_{\text{tot}}[x(\cdot)]] \rangle$, requires a sufficient portion of realisations $S_{\text{tot}}[x(\cdot)] < 0$.

Having retrieved the second law of classical thermodynamics from the iFT in the framework of stochastic thermodynamics, we discuss the scope of applicability of an iFT. To do so, we restate that stochastic thermodynamics differs from classical thermodynamics with respect to two defining properties: *Nanoscopic* systems, implying an inherent stochasticity, and *non-equilibrium*, brought about by driving the process or by preparing an initial state off equilibrium. Accordingly, we distinguish the following situations.

i) Nanoscopic, non-equilibrium thermodynamics, being the scope of stochastic thermodynamics. The realisations $x(\cdot)$ are stochastic and due to this stochasticity, the total EP $S_{\text{tot}}[x(\cdot)]$ is not restricted to non-negative values, and the exponential in the iFT, $\langle \exp[-S_{\text{tot}}[x(\cdot)]] \rangle$, approaches for a reasonable number of realisations its theoretical value of one. Due to the non-equilibrium conditions, the total EP will on average be strictly positive, $\langle S_{\text{tot}}[x(\cdot)] \rangle > 0$.

ii) Nanoscopic, equilibrium thermodynamics. The realisations $x(\cdot)$ remain stochastic and the resulting realisations of $S_{\text{tot}}[x(\cdot)]$ still may be negative. In the ensemble average, the total EP will be zero, $\langle S_{\text{tot}}[x(\cdot)] \rangle = 0$, implying that negative and positive realisations of $S_{\text{tot}}[x(\cdot)]$ are in exact balance and the validity of the iFT is observed for very few realisations.

iii) Macroscopic, equilibrium thermodynamics. Instead of individual trajectories, the trajectories $x(\cdot)$ represent the evolution of collective degrees of freedom of macroscopic systems which do not display a notable stochasticity. In other words, all realisations $x(\cdot)$ are practically identical. Due to equilibrium conditions, the EP will be zero, $S_{\text{tot}}[x(\cdot)] \equiv 0$, and the iFT is satisfied trivially.

iv) Macroscopic, non-equilibrium thermodynamics. The realisations $x(\cdot)$ remain practically identical, but due to the non-equilibrium condition, the total EP is strictly positive, $S_{\text{tot}}[x(\cdot)] > 0$. The iFT still holds in principle, but needs an infinite number of realisations (thermodynamic limit) which also includes the practically impossible realisations with negative EP.

We will discuss in the next section that the trade-off between non-equilibrium and stochasticity is vital for the application of FTs.

General methodology The procedure determining the dFT in (I.2.69) is a special case of a general methodology to determine a variety of FTs. To allow for a better insight into that procedure, and to derive two more important dFTs, we present a more abstract derivation of a dFT. In this derivation, the key point is to devise a conjugate dynamics from the original dynamics, and to define a transformation to be applied to trajectories $x(\cdot)$. The conjugate dynamics gives rise to a modified path-probability, which we denote by $\tilde{P}[x(\cdot)|x_0]$, and also includes an altered initial distribution, $\tilde{p}_0(x)$. For the transformed trajectories we will write $x^*(\cdot)$, evolving in time t^* .

In the derivation of the dFT for S_{tot} in (I.2.69), the conjugate dynamics was the time-reversed dynamics which originated from reversing the protocol, $\tilde{P}[x(\cdot)|x_0] = P[x(\cdot)|x_0; \bar{\kappa}(\cdot)]$, and the initial distribution, $\tilde{p}_0(x) = p_t(x)$, and likewise for the transformation of trajectories, $x^*(\cdot) = \bar{x}(\cdot)$.

We now turn to the more abstract level and define the observable

$$\mathcal{Y}[x(\cdot)] := \ln \frac{P[x(\cdot)|x_0] p_0(x_0)}{\tilde{P}[x^*(\cdot)|x_0^*] \tilde{p}_0(x_0^*)} . \quad (\text{I.2.72})$$

In most cases, the transformation of the dynamics is an involution (i.e. its own inverse), and the transformation applied to the trajectories is either the identity or the time-reversal (which both are involutions). We therefore restrict ourselves to these cases and find, analogous to (I.2.66), the symmetry

$$\tilde{\mathcal{Y}}[x^*(\cdot)] = -\mathcal{Y}[x(\cdot)] , \quad (\text{I.2.73})$$

which enables us to express $P[x(\cdot)|x_0]$ in terms of the transformed trajectories in the conjugate dynamics,

$$P[x(\cdot)|x_0] = \frac{\tilde{p}_0(x_0^*)}{p_0(x_0)} \tilde{P}[x^*(\cdot)|x_t^*] e^{-\tilde{\mathcal{Y}}[x^*(\cdot)]} \quad (\text{I.2.74})$$

and to obtain the dFT for Y along similar lines as in (I.2.68),

$$\begin{aligned}
 p(Y = \mathcal{Y}[x(\cdot)]) &= \int dx_t \int_{(x_0, t_0)}^{(x_t, t)} dx_0 p_0(x_0) \int \mathcal{D}x(\cdot) P[x(\cdot)|x_0] \delta(Y - \mathcal{Y}[x(\cdot)]) \\
 &= e^Y \int dx_t^* \int_{(x_0^*, t_0^*)}^{(x_t^*, t^*)} dx_0^* \tilde{p}_0(x_0^*) \int \mathcal{D}x^*(\cdot) \tilde{P}[x^*(\cdot)|x_0^*] \delta(Y + \tilde{\mathcal{Y}}[x^*(\cdot)]) \\
 &= e^Y \tilde{p}(-Y = \tilde{\mathcal{Y}}[x^*(\cdot)]) .
 \end{aligned} \tag{I.2.75}$$

Note that in the second line we did not only use (I.2.74) to substitute $P[x(\cdot)|x_0]$ but also used the symmetry (I.2.73) to substitute $\mathcal{Y}[x(\cdot)]$ in the δ -function, with the result that the complete integrand is written as a function of the integration variable $x^*(\cdot)$. The discussion of FTs on this abstract level is pursued in greater detail by Verley and Lacoste in their article [50], a unification of practically all FTs based on this abstract formulation was achieved by Seifert in his overview article [29].

From the path integrals in (I.2.75) we can also read off the general prescription to apply an iFT or dFT to a simulation or experiment:

To determine $p(Y) = p(Y = \mathcal{Y}[x(\cdot)])$, we need a set of realisations $\{x(\cdot)\}$ of the stochastic process fixed by the coefficients $F(x, t)$ and $D(x, t)$ and the initial distribution $p_0(x)$ which define $P[x(\cdot)]$. The set $\{x(\cdot)\}$ can be obtained by simulating the corresponding LE using, e.g., the integration scheme (A.3.10), or, the other way around, find $p_0(x)$, $F(x, t)$ and $D(x, t)$ that describes an already existing set of $\{x(\cdot)\}$ we got, e.g., from an experiment. To each realisation $x(\cdot)$, we determine $Y = \mathcal{Y}[x(\cdot)]$ from (I.2.72). From the resulting set $\{Y\}$ we can readily verify the iFT

$$\langle e^{-Y} \rangle = 1 . \tag{I.2.76}$$

If we have furthermore access to the set of realisations $\{x^*(\cdot)\}$ that obey the conjugate dynamics as used in the second path integral in (I.2.75), we can obtain from the functional $\tilde{\mathcal{Y}}[x^*(\cdot)]$ the set of values $\{Y_c\}$, where the index c declares that the Y_c were determined from the conjugate dynamics, and are distinguished from the set $\{Y\}$ obtained from the original dynamics. From the set $\{Y\}$ we produce a histogram to approximate $p(Y)$,

and likewise, we build from $\{Y_c\}$ a histogram to approximate $\tilde{p}(Y)$. Making use of a suitable interpolation method to plot $\ln(p(Y)/\tilde{p}(-Y))$ versus Y , we will, according to the dFT

$$\frac{p(Y)}{\tilde{p}(-Y)} = e^Y \quad (\text{I.2.77})$$

get a straight line of slope one.

Non-equilibrium steady states Having established the general formalism to set up observables that obey a dFT, we can readily discuss two more important FTs. To this end, recall that in the case of more than one degree of freedom, i.e. $\mathbf{X} \in \mathbb{R}^n$ with $n \geq 2$, non-conservative forces that do not arise from a scalar potential entail non-equilibrium steady states (NESSs). The distinguishing property of a NESS is that its probability current $\mathbf{j}^{\text{st}}(\mathbf{x})$ does not vanish, instead it is divergence free, $\nabla \cdot \mathbf{j}^{\text{st}}(\mathbf{x}) = 0$. In (I.2.78), we divided the drift velocity into a conservative part deriving from the scalar potential $\varphi(\mathbf{x}, t)$ and an additional non-conservative force arising from the vector-field $\mathbf{A}(\mathbf{x}, t)$,

$$\mathbf{F}(\mathbf{x}, t) = \mathbf{D}(\mathbf{x}, t) \left[-\nabla \varphi(\mathbf{x}, t) + \mathbf{A}(\mathbf{x}, t) \right]. \quad (\text{I.2.78})$$

In view of the Fokker-Planck operator in the form (I.1.50),

$$\hat{\mathcal{L}}_{\text{FP}}(\mathbf{x}, t) = -\nabla \left[e^{\phi(\mathbf{x}, t)} \mathbf{j}^{\text{st}}(\mathbf{x}, t) - \mathbf{D}(\mathbf{x}, t) e^{-\phi(\mathbf{x}, t)} \nabla e^{\phi(\mathbf{x}, t)} \right], \quad (\text{I.2.79})$$

we found that the triple $\{\phi, \mathbf{D}, \mathbf{j}^{\text{st}}\}$ fixes the dynamics of the process, and by varying \mathbf{j}^{st} at fixed φ and \mathbf{D} , we can define a family of dynamics with identical ϕ and \mathbf{D} but distinct currents, where the non-equilibrium potential $\phi(\mathbf{x}, t)$ fixes the stationary distribution $p^{\text{st}}(\mathbf{x}, t) = \exp(-\phi(\mathbf{x}, t))$.

A particular meaningful modification of the original dynamics is found by reversing the current, $\{\phi, \mathbf{D}, -\mathbf{j}^{\text{st}}\}$. In this dynamics, particles will run the loops in opposite direction, as is evident from equation (I.1.49) since the velocity $\langle \dot{\mathbf{x}} | \mathbf{x}, t \rangle$ acquires the opposite sign. In the current reversed dynamics the Fokker-Planck operator now reads

$$\hat{\mathcal{L}}_{\text{FP}}^\dagger(\mathbf{x}, t) = \nabla \left[e^{\phi(\mathbf{x}, t)} \mathbf{j}^{\text{st}}(\mathbf{x}, t) + \mathbf{D}(\mathbf{x}, t) e^{-\phi(\mathbf{x}, t)} \nabla e^{\phi(\mathbf{x}, t)} \right] \quad (\text{I.2.80})$$

or, equivalently, instead of $\mathbf{F}(\mathbf{x}, t)$ from (I.2.78), we may use the current reversed drift velocity

$$\begin{aligned}\mathbf{F}^\dagger(\mathbf{x}, t) &= -e^{\phi(\mathbf{x}, t)} \mathbf{j}^{\text{st}}(\mathbf{x}, t) - \mathbf{D}(\mathbf{x}, t) \nabla \phi(\mathbf{x}, t) \\ &= -(\mathbf{F}(\mathbf{x}, t) + 2\mathbf{D}(\mathbf{x}, t) \nabla \phi(\mathbf{x}, t)) .\end{aligned}\quad (\text{I.2.81})$$

At this point, it suggests itself to take the current reversed dynamics as the conjugate dynamics and consider the observable

$$\mathcal{Y}[\mathbf{x}(\cdot)] = \ln \frac{P[\mathbf{x}(\cdot)|\mathbf{x}_0] p_0(\mathbf{x}_0)}{P^\dagger[\mathbf{x}(\cdot)|\mathbf{x}_0] p_0(\mathbf{x}_0)} \quad (\text{I.2.82})$$

Note that current reversal does not affect the initial distributions. For the transformation of trajectories we chose the identity, as the system is in the same steady state for both dynamics (using the time reversed trajectories in the denominator would in fact result into $\mathcal{Y}[\mathbf{x}(\cdot)] \equiv 0$ for all $\mathbf{x}(\cdot)$).

Verifying that current reversal is an involution,

$$\begin{aligned}\hat{\mathcal{L}}_{\text{FP}}^{\dagger\dagger}(\mathbf{x}, t) &= \nabla \left[e^{\phi(\mathbf{x}, t)} (-\mathbf{j}^{\text{st}}(\mathbf{x}, t)) + \mathbf{D}(\mathbf{x}, t) e^{-\phi(\mathbf{x}, t)} \nabla e^{\phi(\mathbf{x}, t)} \right] \\ &= -\nabla \left[e^{\phi(\mathbf{x}, t)} \mathbf{j}^{\text{st}}(\mathbf{x}, t) - \mathbf{D}(\mathbf{x}, t) e^{-\phi(\mathbf{x}, t)} \nabla e^{\phi(\mathbf{x}, t)} \right] \\ &= \hat{\mathcal{L}}_{\text{FP}}(\mathbf{x}, t)\end{aligned}\quad (\text{I.2.83})$$

is the only requirement needed to state that Y obeys the FTs (I.2.76) and (I.2.77). The interesting bit is to see whether $\mathcal{Y}[\mathbf{x}(\cdot)]$ as defined in (I.2.82) has a physical meaning. Carrying out the necessary calculations⁹, we indeed end up with the housekeeping heat from (I.2.53a),

$$\begin{aligned}\mathcal{Y}[\mathbf{x}(\cdot)] &= \int_{t_0}^t \dot{\mathbf{x}}(\tau) \mathbf{D}^{-1}(\tau) \langle \dot{\mathbf{x}} | \tau \rangle_{\text{st}} d\tau \\ &= S_{\text{hk}}[\mathbf{x}(\cdot)] ,\end{aligned}\quad (\text{I.2.84})$$

which is nothing else than the entropy produced irreversibly while keeping the NESS up. This makes perfect physical sense, as the statement is that the odds to observe the same realisation in the current reversed dynamics as in the original dynamics goes down exponentially with the entropy

⁹Details can be found in [21] along with the multidimensional formulation of WPIs.

$S_{\text{hk}}[\mathbf{x}(\cdot)]$ produced by this realisation. It further confirms that $S_{\text{hk}}[\mathbf{x}(\cdot)]$ indeed obeys the second law $\langle S_{\text{hk}}[\mathbf{x}(\cdot)] \rangle \geq 0$ in the ensemble average. The iFT for the housekeeping heat was first derived by Speck and Seifert [45]. Having this in mind, it may not be surprising that taking the time reversal as conjugate dynamics and reversing also the trajectories, we recover the EPs given by (I.2.51), (I.2.53) and (I.2.55),

$$\ln \frac{P[\mathbf{x}(\cdot)|\mathbf{x}_0]}{\bar{P}[\bar{\mathbf{x}}(\cdot)|\bar{\mathbf{x}}_0]} = S_{\text{m}}[\mathbf{x}(\cdot)] = S_{\text{ex}}[\mathbf{x}(\cdot)] + S_{\text{hk}}[\mathbf{x}(\cdot)] \quad (\text{I.2.85a})$$

$$\ln \frac{P[\mathbf{x}(\cdot)|\mathbf{x}_0] p_0(\mathbf{x}_0)}{\bar{P}[\bar{\mathbf{x}}(\cdot)|\bar{\mathbf{x}}_0] p_t(\mathbf{x}_t)} = S_{\text{tot}}[\mathbf{x}(\cdot)] = S_{\text{ex}}^{\geq}[\mathbf{x}(\cdot)] + S_{\text{hk}}[\mathbf{x}(\cdot)] \quad (\text{I.2.85b})$$

where $S_{\text{m}}[\mathbf{x}(\cdot)]$ is the EP in the medium, $S_{\text{tot}}[\mathbf{x}(\cdot)]$ is the total, irreversible EP, and $S_{\text{ex}}[\mathbf{x}(\cdot)]$ and $S_{\text{ex}}^{\geq}[\mathbf{x}(\cdot)]$ are the excess entropies, being the respective equivalents to $S_{\text{m}}[\mathbf{x}(\cdot)]$ and $S_{\text{tot}}[\mathbf{x}(\cdot)]$ for dynamics without non-conservative forces.

To retrieve also the irreversible EP $S_{\text{ex}}^{\geq}[\mathbf{x}(\cdot)]$, associated with the entropy produced when not being in a steady state (e.g. in a relaxation process and/or driven process), we combine both time reversal and current reversal for the conjugate dynamics and obtain

$$\begin{aligned} \ln \frac{P[\mathbf{x}(\cdot)|\mathbf{x}_0] p_0(\mathbf{x}_0)}{\bar{P}^{\dagger}[\bar{\mathbf{x}}(\cdot)|\bar{\mathbf{x}}_0] p_t(\mathbf{x}_t)} &= \bar{S}^{\dagger}[\bar{\mathbf{x}}(\cdot)] - \ln \bar{p}_t(\bar{\mathbf{x}}_t) - (\mathcal{S}[\mathbf{x}(\cdot)] - \ln p_0(\mathbf{x}_0)) \\ &= \bar{S}^{\dagger}[\bar{\mathbf{x}}(\cdot)] - \ln \bar{p}_t(\bar{\mathbf{x}}_t) - (\mathcal{S}[\mathbf{x}(\cdot)] - \ln p_0(\mathbf{x}_0)) \\ &\quad - \bar{S}[\bar{\mathbf{x}}(\cdot)] + \bar{S}[\bar{\mathbf{x}}(\cdot)] \\ &= \bar{S}[\bar{\mathbf{x}}(\cdot)] - \ln \bar{p}_t(\bar{\mathbf{x}}_t) - (\mathcal{S}[\mathbf{x}(\cdot)] - \ln p_0(\mathbf{x}_0)) \\ &\quad - (\bar{S}[\bar{\mathbf{x}}(\cdot)] - \bar{S}^{\dagger}[\bar{\mathbf{x}}(\cdot)]) \\ &= S_{\text{tot}}[\mathbf{x}(\cdot)] - S_{\text{hk}}[\mathbf{x}(\cdot)] = S_{\text{ex}}^{\geq}[\mathbf{x}(\cdot)] . \end{aligned} \quad (\text{I.2.86})$$

We hence have, for systems with non-conservative forces, three non-negative entropies that obey a FT, the total EP S_{tot} , the housekeeping EP S_{hk} and the non-negative excess EP S_{ex}^{\geq} . The dFT for S_{ex}^{\geq} is also known as Hatano-Sasa relation [44]. A comprehensible presentation of how S_{hk} and S_{ex}^{\geq} arise from the path integral formulation was achieved by Chernyak, Chertkov and Jarzynski [21]. A derivation of the three FTs and the corresponding

second laws in the framework of a master equation was achieved by Esposito and van den Broeck [41, 42].

I.2.4 Applications

In this chapter we give a brief account on various forms of FTs, their applications, and arising difficulties.

Steady-state FT The FT that was first observed by Evans et al. [53] for entropy fluctuations in simulations of a two-dimensional shear-driven fluid belongs to the class of steady-state FTs which hold in a NESS for a fixed value of the protocol κ . Under certain chaotic assumptions, Gallavotti and Cohen proved that steady-state FTs hold in dissipative dynamical systems [55, 56].

In a NESS, reversal of time does not affect the dynamics, we therefore have the same path probability for the original and the time-reversed dynamics, and consequently, the same PDF for the observable that obeys the FT. For the total EP $S_{\text{tot}} = S_{\text{ex}}^{\geq} + S_{\text{hk}}$, the resulting dFT follows by combining (I.2.77) and (I.2.85b) as

$$\frac{p(S_{\text{tot}})}{p(-S_{\text{tot}})} = e^{S_{\text{tot}}} \quad (\text{I.2.87})$$

which is known as the Gallavotti-Cohen relation.

The Gallavotti-Cohen relation can conveniently be applied to experimental measurements as it only involves the knowledge of the PDF $p(S_{\text{tot}})$.

In early works involving the Gallavotti-Cohen relation, the EP in the medium, $S_{\text{m}} = S_{\text{ex}} + S_{\text{hk}}$ from (I.2.85a), was considered instead of S_{tot} . For large time intervals $t - t_0$, the Gallavotti-Cohen relation holds approximately for S_{m} , and asymptotically, that is in the limit $t - t_0 \rightarrow \infty$, even exact. This asymptotic validity can be attributed to the divergent property of S_{hk} , as, for large times, the contribution of S_{hk} to S_{m} dominates over the contribution from S_{ex} , such that the error made by using S_{ex} instead of S_{ex}^{\geq} becomes negligible. Taking it to extremes, it is sufficient to measure in an experiment a quantity Y that is somehow related to S_{hk} , such that the influence of S_{hk} prevails for large times, and then check whether

$\ln(p(Y)/p(Y-))$ takes a straight line for large measuring times. Examining the asymptotic validity of the Gallavotti-Cohen relation for entropy related quantities is a popular course of action to judge whether the system under consideration does in principle hold the symmetry of a dFT.

Estimation of $\Delta\mathcal{F}$ A widely used variant of the FTs for S_{tot} are so called work relations. The first work relation was proved by Jarzynski [59, 60], and is known as the Jarzynski relation. In our formulation, Jarzynski used the alternative form $S_{\text{tot}} = R - \Delta\mathcal{G}$ of the total EP, which we obtained in (I.2.43b) under the assumption that the initial state x_0 of the process is the steady state at initial time t_0 .¹⁰ The quantities R and $\Delta\mathcal{G}$ are the entropic equivalents of work W and free energy difference $\Delta\mathcal{F}$. In the usual thermodynamic setting, the diffusion coefficient follows from the Einstein relation (I.1.9), $D \equiv \Gamma/\beta$, we therefore have $R = \beta W$ and $\Delta\mathcal{G} = \beta\Delta\mathcal{F}$ and the FT for S_{tot} becomes the Jarzynski relation

$$\langle e^{-\beta W} \rangle = e^{-\beta\Delta\mathcal{F}}. \quad (\text{I.2.88})$$

A remarkable feature of the Jarzynski relation is that it relates work values W , measured in an arbitrary *non-equilibrium* transition from state A to state B, with the *equilibrium* free energy difference $\Delta\mathcal{F} = \mathcal{F}_B - \mathcal{F}_A$ between these two states. Since the derivation of the iFT for S_{tot} , (I.2.70), holds for arbitrary final distributions $p(x, t)$, the process needs only to be prepared to start from equilibrium initially, whereas the sampled trajectories giving rise to the work values W may be arbitrarily far from equilibrium. Practically, instead of *once* driving the transition *as slow as possible* in order to reach the final state in almost equilibrium and obtain the approximate free energy of the final state, \mathcal{F}_B , the Jarzynski relation enables the determination of $\Delta\mathcal{F}$ from *many* realisations of *arbitrarily fast* driven transitions.

Determining $\Delta\mathcal{F}$ from the Jarzynski relation (I.2.88) also entails a difficulty: The exponential average is dependent on negative-large realisations of W . Typically, these realisations are the rare realisations where $W < \Delta\mathcal{F}$,

¹⁰In fact, we assumed that also the final state is the corresponding steady state, but the Jarzynski relation holds for arbitrary final states, since in the derivation (I.2.70) of the iFT for S_{tot} only the initial distribution enters.

demonstrating that the second law, $W_{\text{diss}} = W - \Delta\mathcal{F} \geq 0$, can not directly be transferred to nanoscopic systems exhibiting pronounced stochasticity. In the literature, these relations are often referred to as transiently violating the second law, a misleading statement, since the second law is a result of macroscopic thermodynamics. Indeed, by applying again the inequality $\langle \exp x \rangle \geq \exp \langle x \rangle$ as we did to derive the second law from the iFT for S_{tot} in (I.2.71), we retrieve that in the ensemble average

$$\langle W \rangle \geq \Delta\mathcal{F} . \quad (\text{I.2.89})$$

The difficulty with the exponential average can be visualised by writing

$$\langle e^{-\beta W} \rangle = \int e^{-\beta W} P(W) dW , \quad (\text{I.2.90})$$

where $P(W)$ is the work distribution to be obtained from an ensemble of work values W . It is evident, that the factor $e^{-\beta W}$ incorporates a weight on large-negative W , shifting the work values that dominate the exponential average to the left tail of $P(W)$. A typical example is depicted in figure I.2. The exponential weight manifests itself in a slow convergence of the exponential average to the theoretical value $\exp(-\beta\Delta\mathcal{F})$, cf. figure I.3. In contrast to linear averages, the standard error of the set of realisations is not suited to judge the deviation from the true value of the average for a finite number of samples.

It arises the question, when it is feasible to employ the Jarzynski relation to estimate the free energy difference $\Delta\mathcal{F}$ between two states. The answer is, (i) in systems where the underlying potential $V(x, t)$ is not accessible, and (ii) in nanoscopic systems that exhibit work-fluctuations of the order of magnitude $W \sim \Delta\mathcal{F}$. Condition (i) is rather obvious, since $\Delta\mathcal{F}$ follows per definition (I.2.21) by integrating the Boltzmann factor $\exp[-\beta V(x, t)]$. In systems with many degrees of freedom, however, a high dimensional integration is needed, and the application of the Jarzynski relation may become advantageous despite an explicit knowledge of $V(\mathbf{x}, t)$. Condition (ii), $W \sim \Delta\mathcal{F}$, implies that frequent fluctuations $W < \Delta\mathcal{F}$ are realistic, and the convergence of the exponential average to $\exp(-\beta\Delta\mathcal{F})$ is to be expected for a reasonable number of work values.

The direct use of the Jarzynski relation to estimate $\Delta\mathcal{F}$ was only the starting point of many refinements in the procedure of $\Delta\mathcal{F}$ estimation. A

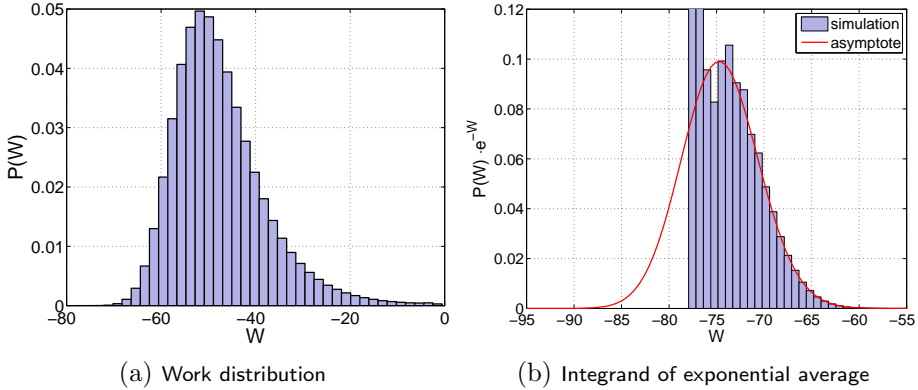


Figure I.2: Work distribution of a driven bistable system. The work values were obtained by simulating the LE with a time-dependent potential $V(x, t)$ that has initially a single minimum and becomes a double-well potential as time evolves, cf. (4.17) of [1] reprinted in section I.3.4. A number of $5 \cdot 10^7$ work values have been sampled in a time interval $t_0 = 0, t = 1$ and for $\beta = 1$. The resulting histogram of work values is shown in (a), the biased distribution that is needed to be integrated to obtain the exponential average (I.2.90) in the Jarzynski relation (I.2.88) is shown in (b). The red line is an asymptotic solution obtained in [1] which will be discussed in the next chapter, in particular in section I.3.4.

major improvement can be made, if also realisations of the reverse dynamics are accessible and the corresponding dFT of the Jarzynski relation can be employed,

$$\frac{P(W)}{\bar{P}(-W)} = e^{\beta(W - \Delta\mathcal{F})} \quad (\text{I.2.91})$$

which was first derived by Crooks [61, 62], along with a further generalisation to other observables, and is known as the Crooks FT. The improvement in $\Delta\mathcal{F}$ estimation via the Crooks FT is due to $P(W) = \bar{P}(-W)$ for $W = \Delta\mathcal{F}$, that is, the value of $\Delta\mathcal{F}$ can be estimated by determining the intersection point of work distribution $P(W)$ for the forward process and work distribution $\bar{P}(W)$ of the reverse process.

A further improvement of $\Delta\mathcal{F}$ estimation was achieved by Hummer and Szabo, who were able to derive in their article [63] a variant of the Jarzynski relation that does not only involve the free energy *difference* $\Delta\mathcal{F}$,

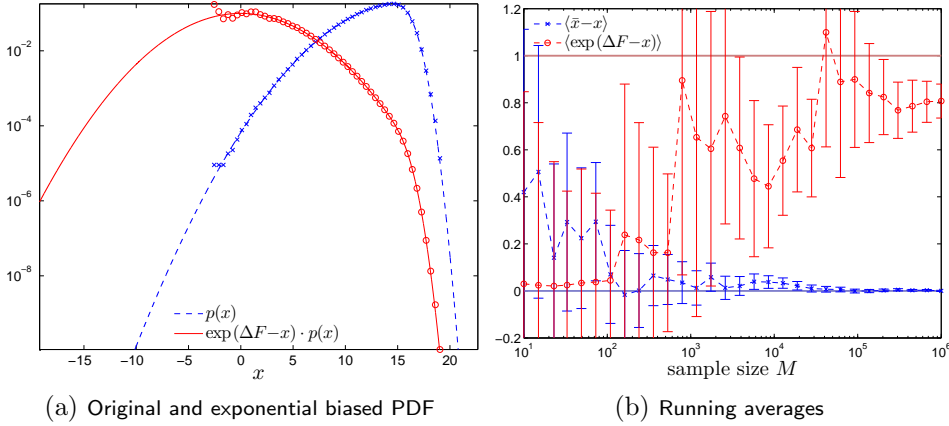


Figure I.3: Illustration of the difficulties of exponential averages compared to linear averages. A number of 10^6 samples have been drawn from an artificial distribution $p(x)$, depicted in (a) as a blue line together with the histogram resulting from the sampled values as symbols. The quantity ΔF is analytically determined such that the exponentially weighted distribution shown in red is normalised. The running averages for the deviation of the arithmetic average $\langle x \rangle$ to the exact mean \bar{x} and the exponential average that should give one due to the choice of ΔF are shown in (b) for an increasing number M of considered samples. The error bars are the corresponding standard errors. Note that for the linear average the true value is practically for all sample sizes within the error margin, whereas the convergence of the exponential average to its true value is hard to judge without knowing the true value.

but the free energy *landscape* $\mathcal{F}(\mathbf{x}_r)$ along a reaction coordinate \mathbf{x}_r .

A prominent example of using FTs for $\Delta \mathcal{F}$ estimation is force-spectroscopy of single biomolecules. In these experiments, single molecules are pulled along a reaction coordinate which forces the molecule to unfold, and then folded back to the original state by reversing the process. Monitoring the work needed to unfold the molecule and the work retrieved by re-folding the molecule enables an estimation of $\Delta \mathcal{F}$ from the Crooks FT after a sufficient number of repetitions of the experiment. In similar experiments, the Hummer-Szabo relation allows to determine the free energy landscape $\mathcal{F}(\mathbf{x}_r)$ of single biomolecules. Experimental realisations include RNA and DNA molecules [64–68] and other molecules [69–71].

Being an iFT, the Hummer-Szabo relation involves the same difficulties

regarding the convergence of the exponential average, and the bias generated by the fact that the exponential average equals $\exp(-\beta\Delta\mathcal{F})$ and not $\Delta\mathcal{F}$ itself. These issues are still keeping researchers busy, considerable progress was made by Ritort and co-workers [72, 73], Dellago and co-workers [74, 75] and Zuckerman and Woolf [76–78]. While the bias generated by taking the logarithm of the exponential average is tractable, the incomplete convergence of the exponential average persists to be a problem [79]. A possible approach is to deliberately bias the sampling of work values in order to improve the convergence of exponential average, and correct for the introduced bias in the final result, a technique that is known as umbrella sampling or importance sampling [76, 80, 74, 81]. Another approach is to augment $P(W)$ with an analytic expression for the left tail of $P(W)$ derived analytically from the specifics of the system under consideration [82, 1, 2]. The asymptotic method to determine the tails of observables in systems subject to stochastic dynamics is discussed in the next chapter. In general, FTs have been observed in a variety of experimental situations, prominent examples are colloidal particles [83–85], electrical circuits [86–88], quantum dots [89] and turbulent flows as discussed in [3] (chapter II.4) and references therein.

Dominant realisations In the context of the Crooks FT, Jarzynski discussed in his appealing article [90] *typical* and *dominant* realisations of the non-equilibrium process from which work values W are obtained. The typical realisations refer to realisations giving rise to work values from the centre of $P(W)$, whereas the dominant realisations give rise to the rare work values $W < \Delta\mathcal{F}$ that dominate the exponential average and hence are needed for the convergence of the Jarzynski relation. The statement made by Jarzynski is that the dominant realisations of the forward process are the typical realisations of the reverse process. In other words, the set of realisations of the forward process features a subset of realisations that undo the effects of the typical realisations and are responsible for the convergence of the exponential average. Or, vice versa, if for the dynamics of a certain system the validity of the Jarzynski relation is observable, then exists a subset of realisations that correspond to the time-reversed dynamics of the system.

The considerations regarding work W and free energy \mathcal{F} can be directly transferred to the total EP S_{tot} . From equation (I.2.43a) follows that the entropic equivalent to the condition $W \sim \Delta\mathcal{F}$, which indicates that dominant realisations are to be expected, reads $-S_{\text{m}} \sim \Delta S^{\text{eq}}$, where ΔS^{eq} is the equilibrium difference between the initial and the final states, and the minus sign is due to the convention that S_{m} is the EP in the medium. For entropy fluctuations of the order ΔS^{eq} , or equivalently but less significant, $S_{\text{tot}} \sim 0$, we can hence expect to observe $S_{\text{tot}} < 0$ which indicates that a subset of time-reversed realisations exists in the forward dynamics.

A complication arises for processes that are not initially in equilibrium. For these cases, we have resort to $S_{\text{tot}} = S_{\text{m}} + \Delta S$ which we derived in (I.2.40), where ΔS is the difference of Gibbs entropy between initial and final state which depends explicitly on the initial distribution of the process. We will come back to this kind of discussion of EPs in chapter II.4 in the context of cascade processes in fully developed turbulence.

In closing this chapter, we mention that the application of the above considerations to biological and nanoscopic machines is intriguing, since the microscopic fluctuations are not constrained by the second law, and mechanisms rectifying thermal noise are possible. On the macroscopic level, of course, the second law remains to hold true. It is a focus of current research to explore the possibilities of such nanoscopic devices [91–98]. In the course of this research, it proved that apart from work and entropy, a third thermodynamic quantity enters the picture, *information*. In particular the relation between entropy and information in nanoscopic devices is keeping researchers busy [99–107].

I.3 Asymptotic analysis

The discussed applications of FTs to nanoscopic systems in the previous section pointed up that the characterisation of rare fluctuations in the dynamics of nanoscopic systems is indispensable. These rare fluctuations typically give rise to a consumption of entropy, crucial for the functioning of biological machines and in designing nanoscopic devices, and required to estimate free energy profiles using FTs. The importance of rare fluctuations calls for a method to asymptotically analyse the PDFs of thermodynamic quantities. In this chapter, we develop such a method.

We will begin in section I.3.1 with a pedagogical one-dimensional example to give an understanding of the asymptotic method which will be introduced in the two subsequent sections I.3.2 and I.3.3. A major improvement of the method, along with applications to physically relevant toy-models including single molecule force-spectroscopy, is presented in section I.3.4, being the first two publications [1, 2] included into this thesis.

I.3.1 Gauß approximation (GA)

The asymptotic method to determine the tails of entropy or work distributions relies on the path integral representation discussed in chapter I.1.3. Before we turn to WPIs, let us consider a pedagogical example - the Γ -function.

The Γ -function is defined by

$$\Gamma(n+1) = \int_0^\infty e^{-x} x^n dx . \quad (\text{I.3.1})$$

Successive integrations by parts show that $n! = \Gamma(n+1)$. Knowledge of the asymptotic behaviour of the factorial is vital in statistical physics. A *Gaussian approximation* (GA) of the integral in (I.3.1) yields this asymptotic behaviour and is the one-dimensional equivalent of the method we will apply to WPIs in the next chapter. The GA is also known as *saddle-point approximation*, since the equivalent method in function theory, the method of steepest descent, deals with a saddle-point.

To perform the GA, we define the function

$$f(x) = x - n \ln x \quad (\text{I.3.2})$$

and rewrite the integrand of (I.3.1) as $e^{-f(x)}$. The Taylor expansion up to second order of this function at a point \bar{x} reads

$$f(x) \simeq f(\bar{x}) + f'(\bar{x})(x - \bar{x}) + \frac{1}{2}f''(\bar{x})(x - \bar{x})^2. \quad (\text{I.3.3})$$

The crux of the GA is to choose \bar{x} such that the linear term vanishes, and we are left with

$$f(x) \simeq f(\bar{x}) + \frac{1}{2}f''(\bar{x})(x - \bar{x})^2, \quad f'(\bar{x}) \stackrel{!}{=} 0, \quad (\text{I.3.4})$$

$$\Gamma(n+1) = \int_0^\infty e^{-f(x)} dx \simeq e^{-f(\bar{x})} \int_0^\infty e^{-\frac{f''(\bar{x})}{2}(x-\bar{x})^2} dx. \quad (\text{I.3.5})$$

The remaining integral is a Gaussian integral, thus the name of the method, which can be readily carried out, and we end up with¹¹

$$\Gamma(n+1) \simeq \frac{\sqrt{2\pi} e^{-f(\bar{x})}}{\sqrt{f''(\bar{x})}}. \quad (\text{I.3.6})$$

By solving $f'(\bar{x}) \stackrel{!}{=} 0$ we find $\bar{x} = n$, which substituted into the above GA formula yields Stirling's approximation of the factorial,

$$n! \simeq \sqrt{2\pi n} e^{n(\ln n - 1)}. \quad (\text{I.3.7})$$

Stirling's approximation is good for $n > 10$ and becomes excellent for $n > 100$, hence, it is indeed an asymptotic approximation for large n . But where did the asymptotic assumption enter?

To answer this question, we first note that $\bar{x} = n$ is a minimum of $f(x)$, and accordingly, a maximum of the integrand $e^{-f(x)}$. We then observe from the definition of $f(x)$, (I.3.2), that with increasing n the value of this maximum, $e^{-f(n)} \propto n^n$, increases exponentially. For large n , the integral in (I.3.1) is therefore dominated by the maximum and its immediate vicinity. Accordingly, for large n , the Gaussian integration captures the predominant contribution to the integral in (I.3.1). This is the desired situation of the GA.

¹¹This is, in fact, not entirely correct, since the integration covers not the whole \mathbb{R} . However, our approximation includes $\bar{x} \gg 0$, and the error we make is negligible considering the quality of the GA.

If only the far asymptotic behaviour is of interest, which is in this case $\ln n! \sim n(\ln n - 1)$, it is sufficient to replace the integral with the maximum value of the integrand. This 0-th order approximation spares us the Gaussian integration, which is in this simple example of course pointless, but represents a major simplification when applying the GA to more involved integrals like WPIs. In the following, we will refer to the factor $e^{-f(\bar{x})}$ as the *exponential factor*, and we will call the result of the Gaussian integration, $\sqrt{2\pi/f''(\bar{x})}$, the *pre-exponential factor*.

1.3.2 The asymptotic method

Having set the conceptional basis in the previous section, we now discuss the spirit of the GA of constrained WPIs, and will perform the explicit calculations in the next section.

We have seen in chapter I.1.3 that we can write the solution of a FPE as the WPI

$$p(x_t, t) = \int dx_0 p_0(x_0) \int_{(x_0, t_0)}^{(x_t, t)} \mathcal{D}x(\cdot) e^{-\mathcal{S}[x(\cdot)]} \quad (\text{I.3.8})$$

with the action and Jacobian

$$\mathcal{S}[x(\cdot)] = \int_{t_0}^t \frac{[\dot{x}_\tau - F(x_\tau, \tau)]^2}{4D(x_\tau, \tau)} - J(x_\tau, \tau) d\tau, \quad (\text{I.3.9})$$

$$J(x, t) = \frac{1}{2}F'(x, t) + \frac{1}{4}D''(x, t). \quad (\text{I.3.10})$$

Note that we used Stratonovich convention and are therefore not bothered with modified calculus.

Suppose we are interested in an integral observable $\Omega = \Omega[x(\cdot)]$,

$$\Omega[x(\cdot)] := \int_{t_0}^t \omega(x_\tau, \dot{x}_\tau, \tau) d\tau, \quad (\text{I.3.11})$$

where $\omega(x, \dot{x}, \tau)$ is the kernel function that defines $\Omega[x(\cdot)]$. To incorporate the constraint into the WPI, we use the Fourier representation of the δ -function,

$$\delta(\Omega - \Omega[x(\cdot)]) = \frac{1}{2\pi} \int e^{ik(\Omega - \Omega[x(\cdot)])} dk. \quad (\text{I.3.12})$$

Including $\delta(\Omega - \Omega[x(\cdot)])$ and the initial distribution via $\Lambda(x_0) := -\ln p_0(x_0)$ into the new action $\tilde{\mathcal{S}}[x(\cdot); k]$, and performing the integral with respect to x_t , we get from (I.3.8) the PDF of the observable in terms of a constrained WPI,

$$p(\Omega) = \int dx_t \int dx_0 \int \frac{dk}{2\pi} \int_{(x_0, t_0)}^{(x_t, t)} \mathcal{D}x(\cdot) \tilde{P}[x(\cdot); k, \Omega] \quad (\text{I.3.13a})$$

$$\tilde{P}[x(\cdot); k, \Omega] = \exp \left[-\tilde{\mathcal{S}}[x(\cdot); k, \Omega] \right] \quad (\text{I.3.13b})$$

$$\tilde{\mathcal{S}}[x(\cdot); k, \Omega] = \Lambda(x_0) + \int_{t_0}^t s(x_\tau, \dot{x}_\tau, \tau; k) d\tau - ik\Omega \quad (\text{I.3.13c})$$

$$s(x_\tau, \dot{x}_\tau, \tau; k) = \frac{[\dot{x}_\tau - F(x_\tau, \tau)]^2}{4D(x_\tau, \tau)} - J(x_\tau, \tau) + ik\omega(x_\tau, \dot{x}_\tau, \tau) \quad (\text{I.3.13d})$$

In the spirit of our pedagogical example, the claim is that by applying a GA to the constrained WPI in the first line, we yield an approximation for $p(\Omega)$. We state that this approximation is asymptotically correct for rare Ω . This statement is plausible since by choosing rare values for Ω , the realisations $x(\cdot)$ giving rise to that value are rare by itself and dominate the integrand $P[x(\cdot); \Omega]$. In other words, by putting in place an exceptionally hard constraint, the variation of $x(\cdot)$ gets substantially narrow, and the path integral (I.3.13) is dominated by the mode of $P[x(\cdot); \Omega]$ and its immediate vicinity, analogous to the pedagogical example discussed in the previous section.

However, as in the example of the Γ -function, this argumentation is of rather qualitative nature. The GA of the Γ -function can be put quite straight forwardly into a systematic shape, for the GA of the WPI, however, the situation is intricate. In essence, our asymptotic method is equivalent to the weak noise limit, in which the GA gets asymptotically exact in the limit of $D(x, t) \rightarrow 0$. We could therefore rewrite the diffusion coefficient $D(x, t) \mapsto \frac{1}{d_0} \tilde{D}(x, t)$ such that $\tilde{D}(x, t)$ is dimensionless, and put in I.3.13b the weak noise parameter d_0 as a prefactor of the action $\tilde{\mathcal{S}}$.¹² In the weak

¹²The terms Λ , J , ω and Ω obtain a prefactor $1/d_0$. By substituting $q := k/d_0$ and taking the stationary distribution as initial distribution, only the Jacobian J is left with the prefactor. But since in the weak noise limit the realisations $x(\cdot)$ loose their

noise limit, $d_0 \rightarrow \infty$, the integrand of the WPI becomes a singularly narrow peak, just as choosing a practically impossible value for Ω . The GA of the WPI (I.3.13) therefore becomes also exact in the weak noise limit. This formal correspondence can be used to give the asymptotic method a systematic order of approximation. In section I.3.4, the weak noise parameter will be the inverse temperature $\beta = 1/T$.

I.3.3 Euler-Lagrange equations

In the previous section we have formulated in (I.3.13b) the constrained path-probability $P[x(\cdot); \Omega]$. We argued that the GA consists in substituting the integral of $P[x(\cdot), \Omega]$ with the value of the path-probability at its mode $\bar{x}(\cdot)$. The mode of $P[x(\cdot); \Omega]$ is given by the minimising trajectory $\bar{x}(\cdot)$ and parameter \bar{k} of the action $\tilde{\mathcal{S}}[x(\cdot); k]$ under the constraint $\Omega = \Omega[\bar{x}(\cdot)]$; a variational problem with constraint, where k is the Lagrange parameter.

To obtain $\bar{x}(\cdot)$ and \bar{k} , we need to solve the associated Euler-Lagrange equation (ELE)

$$0 = \frac{\partial s(x, \dot{x}, \tau)}{\partial x} \Big|_{x=x(\tau)} - \frac{d}{d\tau} \frac{\partial s(x, \dot{x}, \tau)}{\partial \dot{x}} \Big|_{x=x(\tau)} \quad (\text{I.3.14})$$

with boundary conditions

$$\frac{\partial \Lambda(x_0)}{\partial x_0} = \frac{\partial s(x, \dot{x}, \tau)}{\partial \dot{x}} \Big|_{x=x_0}, \quad 0 = \frac{\partial s(x, \dot{x}, \tau)}{\partial \dot{x}} \Big|_{x=x_t}. \quad (\text{I.3.15})$$

The solution of the ELE will depend on the Lagrange parameter k and has to be adjusted such that the constraint

$$\Omega[\bar{x}(\cdot)] = \int_{t_0}^t \omega(\bar{x}_\tau, \dot{\bar{x}}_\tau, \tau) d\tau \quad (\text{I.3.16})$$

is satisfied. Due to the analogy to optimisation problems, the minimising trajectory $\bar{x}(\cdot)$ is also called *optimal path*.

stochasticity, \mathcal{S} is not a stochastic integral anymore, and J does not contribute to the 0-th order GA.

Taking the function $s(x, \dot{x}, \tau)$ from (I.3.13d) and carrying out the differentiations yields the ELE

$$\ddot{x} = \frac{\dot{x} - F}{2D} (D'(\dot{x} + F) + 2\dot{D}) + FF' + \dot{F} + 2DJ'' + 2Dik(\partial_x - d_t \partial_{\dot{x}})w, \quad (\text{I.3.17a})$$

$$0 = \frac{\dot{x}_0 - F_0}{2D_0} + ik\partial_{\dot{x}}w_0 - A'_0, \quad (\text{I.3.17b})$$

$$0 = \frac{\dot{x}_t - F_t}{2D_t} + ik\partial_{\dot{x}}w_t, \quad (\text{I.3.17c})$$

where we dropped the arguments of x_τ , $F(x_\tau, \tau)$, $D(x_\tau, \tau)$, $w(x_\tau, \dot{x}_\tau, \tau)$ and derivatives, and indices denote evaluation at time τ , t_0 and t respectively. The 0-th order result of the GA is accordingly

$$p(\Omega) \sim e^{-\mathcal{S}[\bar{x}(\cdot), \bar{\kappa}]} . \quad (\text{I.3.18})$$

The pre-exponential factor can also be obtained, as will be demonstrated in the next chapter for additive noise. For multiplicative noise, the equations for the pre-exponential factor gets acutely involved, we therefore refrain from reporting preliminary results in that general case.

I.3.4 The pre-exponential factor

The determination of the pre-exponential factor for the asymptotic approximation was achieved in [1], which is the first publication included in this thesis. The second publication [2] of this thesis follows directly after [1] and is devoted to a particular application. In the provided reprints of the publications the force $F(x, t)$ will arise from a time dependent potential, $F(x, t) = -\partial_x V(x, t)$, the diffusion coefficient is simply proportional to temperature, $D = 2/\beta$, and the processes are taken to start from equilibrium, $p_0(x_0) = \exp[-\beta V(x_0, t_0)]/Z_0$. The observable of interest is work W , it therefore is $w(x, t) = \dot{V}(x, t)$, cf. (I.2.17). The application of the method will be demonstrated for physically relevant choices of $V(x, t)$, in particular, [2] addresses single molecule spectroscopy.

Asymptotics of work distributions: The pre-exponential factor^{*}

D. Nickelsen and A. Engel

Universität Oldenburg, Institut für Physik, 26111 Oldenburg, Germany

Received: date / Revised version: date

Abstract. We determine the complete asymptotic behaviour of the work distribution in driven stochastic systems described by Langevin equations. Special emphasis is put on the calculation of the pre-exponential factor which makes the result free of adjustable parameters. The method is applied to various examples and excellent agreement with numerical simulations is demonstrated. For the special case of parabolic potentials with time-dependent frequencies, we derive a universal functional form for the asymptotic work distribution.

PACS. 0 5.70.Ln, 05.40.-a, 05.20.-y

1 Introduction

With the discovery of work [1] and fluctuation [2,3] theorems in stochastic thermodynamics (for recent reviews see [4,5]), the traditional emphasis of statistical mechanics on averages was extended to include also large deviation properties. Indeed, averages like the one appearing in the Jarzynski equality

$$e^{-\beta F} = \langle e^{-\beta W} \rangle \quad (1.1)$$

are dominated by unlikely realization of the random variable (here the work W), and detailed information about the tail of the corresponding probability distribution is necessary to obtain an accurate result (see e.g. [6]). By definition, rare realizations are difficult to get, and consequently, numerically and even more experimentally generated histograms seldom reach far enough into the asymptotic regime. It is therefore desirable to have some additional and independent information about the asymptotic behaviour of the relevant probability distributions.

In the present paper we use the so-called method of optimal fluctuation to determine the asymptotics of work distributions in driven Langevin system. Special emphasis is put on the calculation of the pre-exponential factor that makes any fitting between histogram and asymptotics superfluous. By considering various examples, we show that the results for averages like (1.1) improve significantly if the pre-exponential factor is included. We use a novel method [7] to determine this pre-factor which builds on the spectral ζ -function of Sturm-Liouville operators. The method is very efficient and straightforward in its numerical implementation. It also allows to handle the case of zero modes which is relevant in the present situation. For

harmonic potentials with time-dependent frequency, we are able to derive the general form of the asymptotics of the work distribution analytically.

The paper is organized as follows. Section 2 gives the basic equations and fixes the notation. In section 3 we recall the basic steps in the determination of functional determinants from spectral ζ -functions and adapt the procedure to the present situation. Section 4 discusses two examples, one that can be solved analytically and merely serves as a test of the method, and one for which the analysis has to be completed numerically. In section 5 we elucidate the particularly interesting case of a harmonic oscillator with time-dependent frequency. Here, substantial analytic progress is possible. Finally, section 6 contains some conclusions. Some more formal aspects of the analysis are relegated to the appendices A-C.

2 Basic equations

We consider a driven stochastic system in the time interval $0 \leq t \leq T$ described by an overdamped Langevin equation of the form

$$\dot{x} = -V'(x, t) + \sqrt{2/\beta} \xi(t) . \quad (2.1)$$

The degrees of freedom are denoted by x , the time-dependent potential V gives rise to a deterministic drift, and $\xi(t)$ is a Gaussian white noise source obeying $\langle \xi(t) \rangle \equiv 0$ and $\langle \xi(t)\xi(t') \rangle = \delta(t-t')$. Derivatives with respect to x are denoted by a prime, those with respect to t by a dot. The system is coupled to a heat bath with inverse temperature β . The initial state $x(t=0) =: x_0$ of the system is sampled from the equilibrium distribution at $t=0$

$$\rho_0(x_0) = \frac{1}{Z_0} \exp(-\beta V_0(x_0)) \quad (2.2)$$

^{*} Dedicated to Werner Ebeling on the occasion of his 75th birthday.

with $V_0(x) := V(x, t = 0)$ the initial potential and

$$Z_0 = \int dx \exp(-\beta V_0(x)) \quad (2.3)$$

the corresponding partition function.

During the process, the system is externally driven and the potential changes from $V_0(x)$ to $V_T(x) := V(x, t = T)$ according to a given protocol. The work performed by the external driving depends on the particular trajectory $x(\cdot)$ the system follows and is given by [8]

$$W[x(\cdot)] = \int_0^T dt \dot{V}(x(t), t). \quad (2.4)$$

Due to the random nature of $x(\cdot)$, also W is a random quantity. According to the general rule of transformation of probability, its pdf is given by

$$P(W) = \int \frac{dx_0}{Z_0} e^{-\beta V_0(x_0)} \int dx_T \times \int_{x(0)=x_0}^{x(T)=x_T} \mathcal{D}x(\cdot) p[x(\cdot)] \delta(W - W[x(\cdot)]). \quad (2.5)$$

The probability measure in trajectory space is [9]

$$p[x(\cdot)] = \mathcal{N} \exp\left(-\frac{\beta}{4} \int_0^T dt (\dot{x} + V'(x, t))^2\right), \quad (2.6)$$

where for mid-point discretization in the functional integral we have

$$\mathcal{N} = \exp\left(\frac{1}{2} \int_0^T dt V''(x(t), t)\right). \quad (2.7)$$

Using the Fourier representation of the δ -function in (2.5), we find

$$P(W) = \mathcal{N} \int \frac{dx_0}{Z_0} \int dx_T \times \int \frac{dq}{4\pi/\beta} \int_{x(0)=x_0}^{x(T)=x_T} \mathcal{D}x(\cdot) e^{-\beta S[x(\cdot), q]} \quad (2.8)$$

with the action

$$S[x(\cdot), q] = V_0(x_0) + \int_0^T dt \left[\frac{1}{4} (\dot{x} + V')^2 + \frac{iq}{2} \dot{V} \right] - \frac{iq}{2} W. \quad (2.9)$$

The asymptotic behaviour of $P(W)$ may now be determined by utilizing the contraction principle of large deviation theory [10]. Roughly speaking, this principle stipulates that the probability of an unlikely event is given by the probability of its most probable cause [11, 12]. In the present context this means that whereas *typical* values of W are brought about by a variety of different trajectories $x(\cdot)$, the *rare* values from the tails of $P(W)$ are predominantly realized by one particular path $\bar{x}(\cdot)$ maximizing

$P[x(\cdot)] := \rho_0(x_0) p[x(\cdot)]$ under the constraint $W = W[x(\cdot)]$. A convenient way to implement this idea in the present context, is to evaluate the integrals in (2.8) by the saddle-point method. This is formally equivalent to considering the weak noise limit $\beta \rightarrow \infty$.

Let us therefore study expression (2.8) in the vicinity of a particular trajectory $\bar{x}(\cdot)$ and a particular value \bar{q} of q . We put $x(t) = \bar{x}(t) + y(t)$ and $q = \bar{q} + r$ and expand up to second order in $y(\cdot)$ and r . After several partial integrations, we find

$$S[x(\cdot), q] = \bar{S} + S_{\text{lin}} + S_{\text{quad}} + \dots \quad (2.10)$$

where

$$\bar{S} = S[\bar{x}(\cdot), \bar{q}], \quad (2.11)$$

$$S_{\text{lin}} = \frac{1}{2} \left[(\bar{V}'_0 - \dot{\bar{x}}_0) y_0 + (\bar{V}'_T + \dot{\bar{x}}_T) y_T - \int_0^T dt (\ddot{\bar{x}} + \dot{\bar{V}}' - \bar{V}' \bar{V}'' - i\bar{q} \dot{\bar{V}}') y - ir \left(W - \int_0^T dt \dot{\bar{V}} \right) \right], \quad (2.12)$$

$$S_{\text{quad}} = \frac{1}{4} \left[(\bar{V}''_0 y_0 - \dot{y}_0) y_0 + (\bar{V}''_T y_T + \dot{y}_T) y_T + \int_0^T dt y \left(-\frac{d^2}{dt^2} + \bar{V}''^2 + \bar{V}' \bar{V}''' - (1 - i\bar{q}) \dot{\bar{V}}'' \right) y + 2ir \int_0^T dt \dot{\bar{V}}' y \right]. \quad (2.13)$$

Here, the notation $\bar{V} := V(\bar{x}(t), t)$ and similarly for the derivatives of V has been used.

The most probable trajectory $\bar{x}(\cdot)$ realizing a given value W of the work is specified by the requirement that S_{lin} has to vanish for any choice of $y(\cdot)$ and r . We hence get the Euler-Lagrange equation (ELE)

$$\ddot{\bar{x}} + (1 - i\bar{q}) \dot{\bar{V}}' - \bar{V}' \bar{V}'' = 0 \quad (2.14)$$

together with the boundary conditions

$$\dot{\bar{x}}_0 - \bar{V}'_0 = 0, \quad \dot{\bar{x}}_T + \bar{V}'_T = 0. \quad (2.15)$$

From the term proportional to r we find back the constraint

$$W = \int_0^T dt \dot{\bar{V}}. \quad (2.16)$$

Note that for given W the solution for $\bar{x}(\cdot)$ is usually unique and includes the optimal choice of its initial and final point.

Neglecting contributions stemming from S_{quad} , we arrive at the estimate

$$P(W) \sim \exp(-\beta \bar{S}) \quad (2.17)$$

giving the leading exponential term for the asymptotic behaviour of $P(W)$. It is solely determined by the optimal

trajectory itself: Using the properties (2.14), (2.15) and (2.16) of $\bar{x}(\cdot)$ in (2.9), one can show

$$\begin{aligned} \bar{S} = & -\frac{W}{2} + \frac{1}{2}(\bar{V}_T + \bar{V}_0) - \frac{1}{4}(\bar{x}_T \bar{V}'_T + \bar{x}_0 \bar{V}'_0) \\ & + \frac{1}{4} \int_0^T dt \bar{V}'(\bar{V}' - \bar{x} \bar{V}'') + \frac{1-i\bar{q}}{4} \int_0^T dt \bar{x} \dot{\bar{V}}'. \end{aligned} \quad (2.18)$$

In many cases an improved estimate including the pre-exponential factor is desirable. To obtain it, also the neighbourhood of the optimal trajectory has to be taken into account. This is possible by retaining S_{quad} in the exponent and by performing the Gaussian integrals over $y_0, y_T, y(\cdot)$ and r .

In order to calculate

$$I := \int dy_0 \int dy_T \int \frac{dr}{4\pi/\beta} \int_{y(0)=y_0}^{y(T)=y_T} \mathcal{D}y(\cdot) e^{-\beta S_{\text{quad}}[y(\cdot), r]}, \quad (2.19)$$

we determine the eigenvalues λ_n and normalized eigenfunctions $\varphi_n(t)$ of the operator A defined by (cf. (2.13))

$$A := -\frac{d^2}{dt^2} + (\bar{V}'')^2 + \bar{V}' \bar{V}''' - (1-i\bar{q}) \dot{\bar{V}}'' \quad (2.20)$$

together with the Robin-type boundary conditions

$$\bar{V}_0'' \varphi_n(0) - \dot{\varphi}_n(0) = 0, \quad \bar{V}_T'' \varphi_n(T) + \dot{\varphi}_n(T) = 0. \quad (2.21)$$

Next we expand

$$y(t) = \sum_n c_n \varphi_n(t) \quad (2.22)$$

and replace the integrations over y_0, y_T and $y(\cdot)$ by integrations over the expansion parameters c_n according to

$$\begin{aligned} I = & \mathcal{J} \prod_n \frac{dc_n}{\sqrt{4\pi/\beta}} \\ & \times \int \frac{dr}{4\pi/\beta} \exp\left(-\frac{\beta}{4} \sum_n \lambda_n c_n^2 - \frac{i\beta r}{2} \sum_n c_n d_n\right). \end{aligned} \quad (2.23)$$

Here, we have introduced the notation

$$d_n := \int_0^T dt \varphi_n(t) \dot{\bar{V}}'(t), \quad (2.24)$$

and \mathcal{J} is a factor stemming from the Jacobian of the transformation of integration variables. With this transformation being linear, the Jacobian is a constant; with transformations between the eigenfunction systems of different operators being orthogonal, this constant cannot depend on the special form of V . In appendix A we show by comparison with an exactly solvable case that

$$\mathcal{J} = \sqrt{\frac{8\pi}{\beta}}. \quad (2.25)$$

Assuming that all eigenvalues are strictly positive, as necessary for $\bar{x}(\cdot)$ being a minimum of $S[x(\cdot)]$, the c_n integrals may be performed and we find

$$I = \sqrt{\frac{8\pi}{\beta}} \frac{1}{\sqrt{\prod_n \lambda_n}} \int \frac{dr}{4\pi/\beta} \exp\left(-\frac{\beta r^2}{4} \sum_n \frac{d_n^2}{\lambda_n}\right). \quad (2.26)$$

Integrating finally over r , we are left with

$$I = \frac{\sqrt{2}}{\sqrt{\prod_n \lambda_n}} \frac{1}{\sqrt{\sum_n \frac{d_n^2}{\lambda_n}}}. \quad (2.27)$$

Using

$$\prod_n \lambda_n = \det A \quad \text{and} \quad \sum_n \frac{d_n^2}{\lambda_n} = \langle \dot{\bar{V}}' | A^{-1} | \dot{\bar{V}}' \rangle, \quad (2.28)$$

we finally get

$$P(W) = \frac{\mathcal{N}\sqrt{2}}{Z_0} \frac{e^{-\beta \bar{S}}}{\sqrt{\det A \langle \dot{\bar{V}}' | A^{-1} | \dot{\bar{V}}' \rangle}} (1 + \mathcal{O}(1/\beta)). \quad (2.29)$$

This is the main result of this section. The same expression was obtained in [13] from a discretization of the functional integral.

3 Calculating determinants from spectral ζ -functions

The determination of the extremal action \bar{S} occurring in (2.29) requires the solution of the ELE (2.14). Although this can be done analytically only in a few exceptional cases, its numerical solution poses in general no difficulty. Similarly, the calculation of $\langle \dot{\bar{V}}' | A^{-1} | \dot{\bar{V}}' \rangle$ is rather straightforward. One solves the ordinary differential equation

$$A \psi(t) = \dot{\bar{V}}'(t) \quad (3.1)$$

with boundary conditions (2.21) and uses

$$\langle \dot{\bar{V}}' | A^{-1} | \dot{\bar{V}}' \rangle = \int_0^T dt \psi(t) \dot{\bar{V}}'(t). \quad (3.2)$$

The determination of $\det A$ is somewhat more involved. We will use a method introduced recently [7], see also [14], building on the spectral ζ -function of Sturm-Liouville operators. The essence of the method is contained in the relation

$$\frac{\det A}{\det A_{\text{ref}}} = \frac{F(0)}{F_{\text{ref}}(0)}, \quad (3.3)$$

where the eigenvalues λ_n of A are given by the zeros of $F(\lambda)$, and similarly $F_{\text{ref}}(\lambda) = 0$ determines the eigenvalues of the reference operator A_{ref} . Moreover, one has to ensure $F(\lambda)/F_{\text{ref}}(\lambda) \rightarrow 1$ for $|\lambda| \rightarrow \infty$. For operators of the type considered here,

$$A = -\frac{d^2}{dt^2} + g(t), \quad (3.4)$$

with homogeneous Robin boundary conditions

$$a \varphi(t=0) + b \dot{\varphi}(t=0) = 0, \quad (3.5)$$

$$c \varphi(t=T) + d \dot{\varphi}(t=T) = 0, \quad (3.6)$$

a convenient choice for $F(\lambda)$ is [7]

$$F(\lambda) = c\chi_\lambda(T) + d\dot{\chi}_\lambda(T), \quad (3.7)$$

where $\chi_\lambda(t)$ is the solution of the initial value problem

$$A\chi_\lambda(t) = \lambda\chi_\lambda(t), \quad \chi_\lambda(0) = -b, \quad \dot{\chi}_\lambda(0) = a. \quad (3.8)$$

Note that $\chi_\lambda(t)$ is defined for general λ . The initial condition in (3.8) is chosen such that $\chi_\lambda(t)$ satisfies the boundary condition (3.5) at $t = 0$ for all values of λ . Only if λ coincides with one of the eigenvalues of A , $\lambda = \lambda_n$, the boundary condition at $t = T$ is satisfied as well. In this case χ_λ is proportional to the eigenfunction φ_n corresponding to λ_n . The roots of the equation $F(\lambda) = 0$ are therefore indeed the eigenvalues of A .

In appendix B we show that for the reference operator

$$A_{\text{ref}} = -\frac{d^2}{dt^2} \quad (3.9)$$

with boundary conditions (3.5), (3.6) one finds

$$\frac{\det A_{\text{ref}}}{F_{\text{ref}}(0)} = -\frac{2}{bd}. \quad (3.10)$$

Hence, combining (3.3) and (3.10), the determination of $\det A$ boils down to the solution of the initial value problem (3.8). Numerically, this is again straightforward.

4 Examples

4.1 The sliding parabola

The simplest example for the class of problems considered is provided by a Brownian particle dragged by a harmonic potential moving with constant speed [15,16,17,18]

$$V(x, t) = \frac{(x - t)^2}{2}. \quad (4.1)$$

In this case, the full distribution $P(W)$ is known analytically [15,17]:

$$P(W) = \sqrt{\frac{\beta}{2\pi\sigma_W^2}} \exp\left(-\beta \frac{(W - \sigma_W^2/2)^2}{2\sigma_W^2}\right) \quad (4.2)$$

where

$$\sigma_W^2 = 2(T - 1 + e^{-T}). \quad (4.3)$$

This example hence merely serves as a test of our method. To apply (2.29), we first note that

$$\mathcal{N} = e^{T/2} \quad \text{and} \quad Z_0 = \sqrt{\frac{2\pi}{\beta}}. \quad (4.4)$$

Moreover, the ELE (2.14) is linear and can be solved analytically:

$$\bar{x}(t; W) = \frac{1}{2}(2t + e^{-t} - e^{t-T}) - W \frac{(2 - e^{-t} - e^{t-T})}{2(T + e^{-T} - 1)}.$$

Using this result in (2.18), we find

$$\bar{S} = \frac{(W - (T + e^{-T} - 1))^2}{4(T + e^{-T} - 1)}. \quad (4.5)$$

The operator A defined in (2.20) is, for the potential (4.1), given by

$$A = -\frac{d^2}{dt^2} + 1 \quad (4.6)$$

with boundary conditions

$$\varphi_n(0) - \dot{\varphi}_n(0) = 0, \quad \varphi_n(T) + \dot{\varphi}_n(T) = 0. \quad (4.7)$$

In order to determine $F(0)$, we have to solve the initial value problem

$$-\ddot{\chi}_0 + \chi_0(t) = 0, \quad \chi_0(0) = 1, \quad \dot{\chi}_0(0) = 1. \quad (4.8)$$

The solution is $\chi_0(t) = e^t$ implying (cf. (3.7)) $F(0) = 2e^T$. Using (3.3) and (3.10) we hence find

$$\det A = 4e^T. \quad (4.9)$$

Finally, $\dot{V}' = -1$, and in order to calculate $\langle \dot{V}' | A^{-1} | \dot{V}' \rangle$, we have to solve

$$\begin{aligned} \ddot{\psi}(t) - \psi(t) &= 1, \\ \psi(0) - \dot{\psi}(0) &= 0, \quad \psi(T) + \dot{\psi}(T) = 0 \end{aligned} \quad (4.10)$$

which gives

$$\psi(t) = \frac{1}{2}(e^{t-T} + e^{-t} - 2). \quad (4.11)$$

Plugging this into (3.2) yields

$$\langle \dot{V}' | A^{-1} | \dot{V}' \rangle = T + e^{-T} - 1. \quad (4.12)$$

Combining (2.29), (4.4), (4.5), (4.9), and (4.12), we find back (4.2). Since $P(W)$ is Gaussian, the quadratic expansion around the saddle-point already reproduces the complete distribution, i.e. there are no higher order terms in (2.29).

4.2 The evolving double-well

As a more involved example, we discuss the time-dependent potential proposed in [19]

$$V(x, t) = \alpha_1 x^4 + \alpha_2(1 - rt)x^2. \quad (4.13)$$

For $t < 1/r$, the potential has a single minimum, for $t > 1/r$, it evolves into a double-well. We consider the time interval $0 < t < T = 2/r$ which places the transition

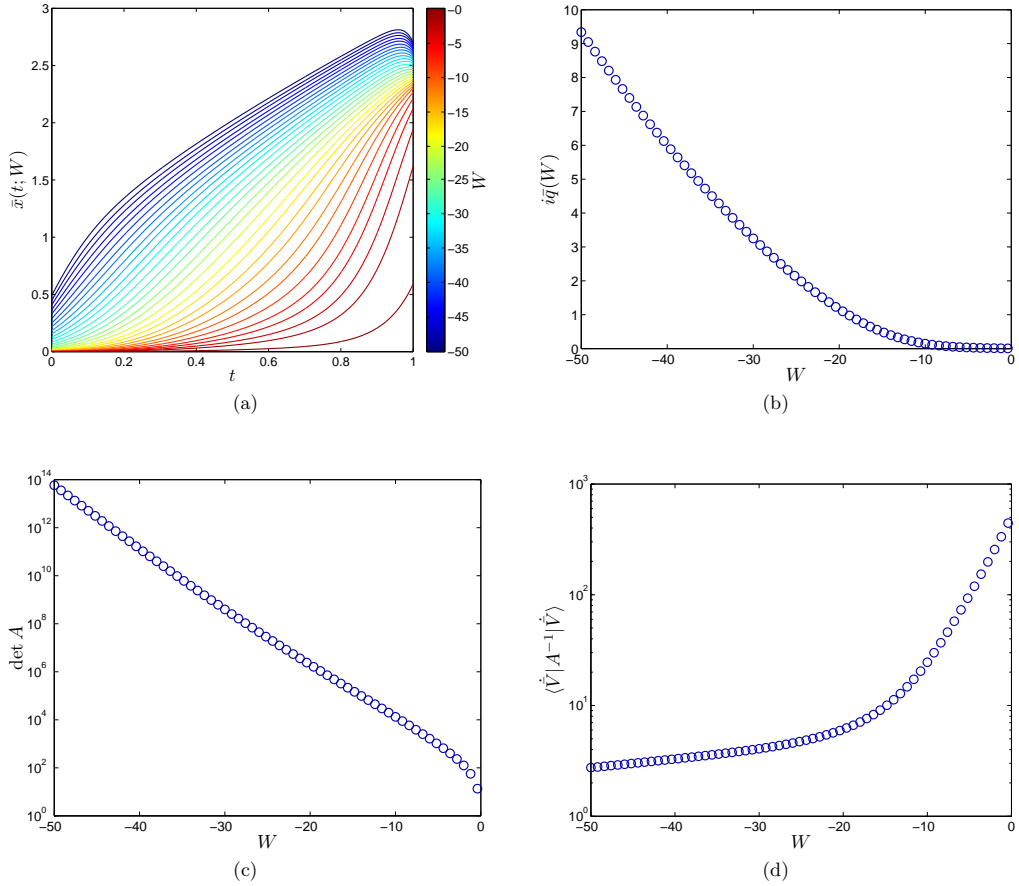


Fig. 4.1: Numerical determination of the asymptotic work distribution for the evolving double well (4.13) with $\alpha_1 = 1/2$, $\alpha_2 = 6$, $T = 1$ and $\beta = 1$: (a) optimal trajectories $\bar{x}(t; W)$, colours code values of the work W , (b) Lagrange parameter $i\bar{q}$, (c) determinant $\det A$ of the fluctuation operator A , and (d) quadratic form $\langle \dot{V}' | A^{-1} | \dot{V}' \rangle$, all as function of W .

at $t = T/2$. In contrast to the previous example, neither the work distribution, nor its asymptotics can be determined using solely analytical techniques. We will therefore generate the work distribution from simulations and solve the equations fixing the asymptotics numerically.

To begin with, we have from (2.3) and (2.7)

$$Z_0 = \int dx \exp[-\beta(\alpha_1 x^4 + \alpha_2 x^2)] \quad (4.14)$$

$$\mathcal{N} = \exp[(6\alpha_2 x^2 + \alpha_2)T - \frac{1}{2}\alpha_2 r T^2]. \quad (4.15)$$

The ELE (2.14) reads

$$\ddot{x} = 48\alpha_1^2 \bar{x}^5 + 32\alpha_1\alpha_2(1 - rt)\bar{x}^3 + [4\alpha_2^2(1 - rt)^2 + 2\alpha_2 r(1 - i\bar{q})]\bar{x}, \quad (4.16)$$

and its boundary conditions (2.15) are of the form

$$\begin{aligned} \dot{x}_0 &= 4\alpha_1 \bar{x}_0^3 + 2\alpha_2 \bar{x}_0, \\ \dot{x}_T &= -4\alpha_1 \bar{x}_T^3 - 2\alpha_2(1 - rT)\bar{x}_T. \end{aligned} \quad (4.17)$$

The constraint (2.4) is

$$W = \alpha_2 r \int_0^T dt \bar{x}(t; \bar{q})^2. \quad (4.18)$$

These equations can be solved numerically using a standard relaxation algorithm. The resulting optimal trajectories $\bar{x}(t; W)$ and the corresponding Lagrange parameters $i\bar{q}(W)$ are shown in Fig. 4.1a and Fig. 4.1b, respectively. Due to the mirror symmetry of the potential, there are for each value of W two optimal trajectories $\pm \bar{x}(t; W)$, from which we only display the positive one. The operator A

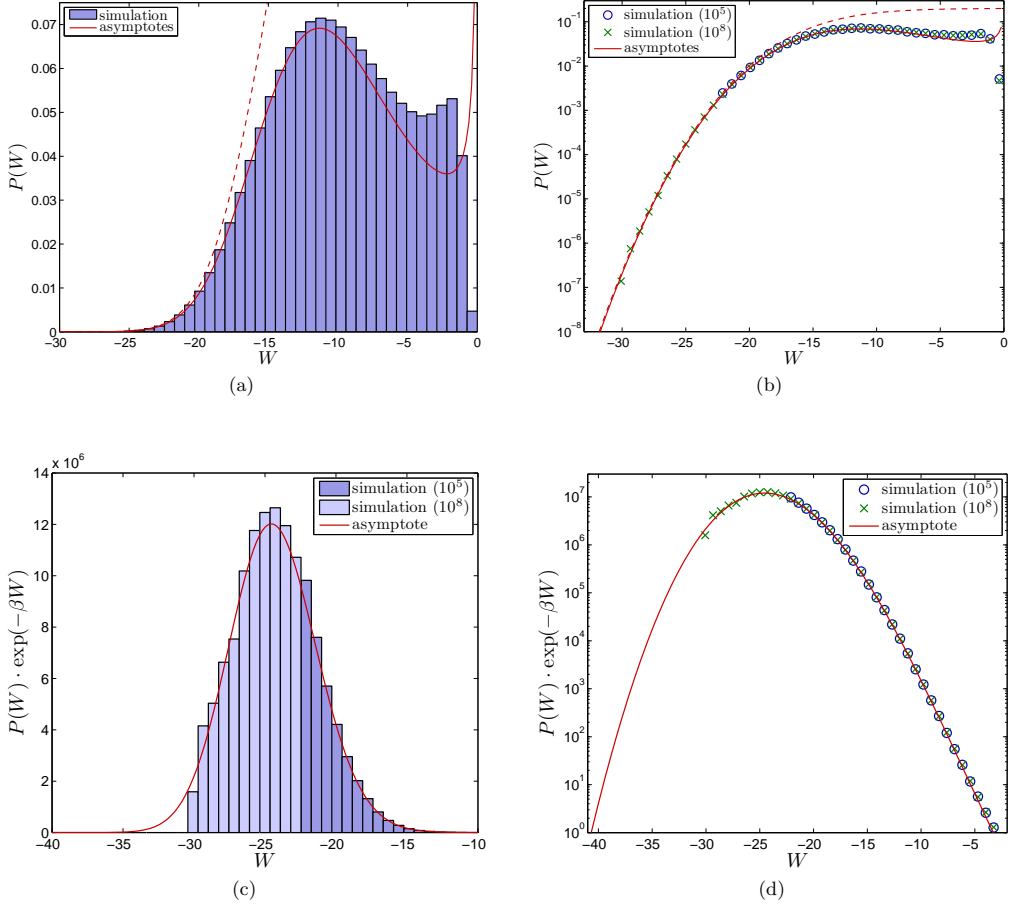


Fig. 4.2: Work distribution for the evolving double-well (4.13) for $\alpha_1 = 1/2$, $\alpha_2 = 6$, $T = 1$ and $\beta = 1$. The histogram and the symbols show results from simulation of the Langevin dynamics (2.1), the lines give the asymptotic forms (5.30) (full) with and (2.17) (dashed) without the pre-exponential factor. Subfigures (a) and (b) show a linear and logarithmic plot respectively of the work distribution itself, subfigures (c) and (d) display the distribution weighted with the factor $e^{-\beta W}$ as appearing, e.g., in the Jarzynski equality (1.1). In (b) and (d) circles and crosses represent histograms based on 10^5 and 10^8 work values respectively, in (c) results from 10^8 trajectories are shown in light blue.

from (2.20) acquires the form

$$A = -\frac{d^2}{dt^2} + 240\alpha_1^2\bar{x}^4 + 96\alpha_1\alpha_2(1-rt)\bar{x}^2 + 2\alpha_2r(1-i\bar{q}) + 4\alpha_2^2(1-rt)^2 \quad (4.19)$$

with the boundary conditions (2.21)

$$\begin{aligned} [12\alpha_1\bar{x}_0^2 + 2\alpha_2]\varphi_n(0) - \dot{\varphi}_n(0) &= 0, \\ [12\alpha_1\bar{x}_T^2 + 2\alpha_2(1-rt)]\varphi_n(T) + \dot{\varphi}_n(T) &= 0. \end{aligned} \quad (4.20)$$

To obtain $\det A$ from (3.3), we determine according to (3.7)

$$F(0) = [12\alpha_1\bar{x}_T^2 + 2\alpha_2(1-rt)]\chi_0(T) + \dot{\chi}_0(T) \quad (4.21)$$

by solving numerically the initial value problem (3.8)

$$\begin{aligned} \ddot{\chi}_0(t) &= [240\alpha_1^2\bar{x}^4 + 96\alpha_1\alpha_2(1-rt)\bar{x}^2 \\ &\quad + 2\alpha_2r(1-i\bar{q}) + 4\alpha_2^2(1-rt)^2]\chi_0(t) = 0, \\ \dot{\chi}_0(0) &= 1, \quad \dot{\chi}_0(T) = 12\alpha_1\bar{x}_T^2 + 2\alpha_2. \end{aligned} \quad (4.22)$$

Note that this has to be done for each value of W separately by using the appropriate results for $\bar{x}(t; W)$ and $\bar{q}(W)$. The result for $\det A$ as a function of W is depicted in Fig. 4.1c.

The last ingredient for the pre-exponential factor is $\langle \dot{V}' | A^{-1} | \dot{V} \rangle$ from (3.2). To determine it, we need to solve

the boundary value problem (3.1), (2.21)

$$\begin{aligned} \ddot{\psi}(t) - [240\alpha_1^2\bar{x}^4 + 96\alpha_1\alpha_2(1-rt)\bar{x}^2 \\ + 2\alpha_2r(1-i\bar{q}) + 4\alpha_2^2(1-rt)^2]\psi(t) + 2\alpha_2r\bar{x} \\ \dot{\psi}(0) = (12\alpha_1\bar{x}_0^2 + 2\alpha_2)\psi(0) \\ \dot{\psi}(0) = -[12\alpha_1\bar{x}_T^2 + 2\alpha_2(1-rT)]\psi(T) \end{aligned} \quad (4.23)$$

for each $\bar{x}(t; W)$ and $\bar{q}(W)$ and use the result in (3.2)

$$\langle \dot{V}' | A^{-1} | \dot{V} \rangle = -2\alpha_2r \int_0^T dt \bar{x}(t) \psi(t). \quad (4.24)$$

The values for $\langle \dot{V}' | A^{-1} | \dot{V} \rangle$ obtained in this way are shown in Fig. 4.1d.

Plugging the numerical results for \mathcal{N} , Z_0 , \bar{x} , $i\bar{q}$, $\det A$ and $\langle \dot{V}' | A^{-1} | \dot{V} \rangle$ into (2.29) and adding an additional factor 2 to account for the two equivalent solutions $\pm\bar{x}(t; W)$ for each value of W , we obtain the final result for the asymptotic form of the work distribution.

To investigate the accuracy of this result, we employed the Heun scheme to simulate the Langevin equation (2.1). In Fig. 4.2a we show the resulting histogram of 10^8 work values and the asymptotic behaviour determined above. The dashed lines represent the incomplete asymptotic form (2.17) without pre-exponential factor, whereas the full line shows the complete asymptotics. In the former case an overall constant factor has to be adjusted, in the latter no free parameters remain. If the region of work values $-30 < W < -20$ accessible from the simulation using 10^8 trajectories is utilized for the fit in the incomplete asymptotics, the two asymptotic expressions almost coincide in the tail of the distribution. Away from the asymptotic regime, however, they differ markedly from each other. If, therefore, less data would be available, the fitted incomplete asymptotics could badly fail to reproduce the true asymptotic behaviour, see also Fig. 5.1b. The parameter-free complete asymptotics is clearly advantageous.

Furthermore, there is a broad range of excellent agreement between histogram and complete asymptotics. This becomes in particular apparent when examining the weighted work distributions $P(W) \exp(-\beta W)$ shown in Fig. 4.2c and Fig. 4.2d. The average $\langle \exp(-\beta W) \rangle$ appearing in the Jarzynski equality (1.1) could already be accurately determined without the histogram at all by using nothing more than the complete asymptotics of $P(W)$.

5 The breathing parabola

A particularly interesting class of examples is provided by harmonic oscillators with time dependent frequency [20, 21]

$$V(x, t) = \frac{k(t)}{2} x^2. \quad (5.1)$$

Except for some special choices of $k(t)$, the full pdf of work is not known analytically. For our purpose the case

of a monotonously decreasing function $k(t)$ is most appropriate. Then $W \leq 0$ and we aim at determining the asymptotic form of $P(W)$ for $W \rightarrow -\infty$.

The ELE (2.14) is given by

$$\ddot{x} + ((1-i\bar{q})\dot{k} - k^2)\bar{x} = 0 \quad (5.2)$$

whereas the boundary conditions (2.15) acquire the form

$$\dot{x}_0 = k_0 x_0 \quad \text{and} \quad \dot{x}_T = -k_T x_T. \quad (5.3)$$

These equations constitute themselves a Sturm-Liouville eigenvalue problem. Consequently, there are *infinitely many* values $\bar{q}^{(0)}, \bar{q}^{(1)}, \dots$ for \bar{q} . Due to the mirror symmetry of the potential, each value $\bar{q}^{(n)}$ again admits two non-trivial solutions $\pm\bar{x}^{(n)}(\cdot)$.

The somewhat unusual feature of this situation is that the different solutions $\bar{q}^{(n)}$ are not related to the value W of the constraint. Also, the functional form of $\bar{x}^{(n)}(\cdot)$ is independent of W . The connection with the work value W under consideration is brought about exclusively by the prefactor of $\bar{x}^{(n)}(\cdot)$ which in view of (2.4) and (5.1) must be $\sqrt{|W|}$.

For the saddle-point approximation in (2.8) this means that for any value of W there are infinitely many stationary points of $P[x(\cdot)]$. Moreover, from (2.20) and (2.21) we find

$$A = -\frac{d^2}{dt^2} - (1-i\bar{q})\dot{k} + k^2, \quad (5.4)$$

$$k_0 x_0 - \dot{x}_0 = 0, \quad k_T x_T + \dot{x}_T = 0. \quad (5.5)$$

Comparing this with (5.2), (5.3) it is seen that the fluctuations around the optimal path $\bar{x}(\cdot)$ are governed by the same operator as the optimal path itself, as usual for a quadratic action. Together with the homogeneous boundary conditions (2.15), this implies that every saddle-point $\{\bar{q}^{(n)}, \pm\bar{x}^{(n)}(\cdot)\}$ has a *zero mode*, namely the optimal path $\bar{x}^{(n)}(\cdot)$ itself. From Courant's nodal theorem we know that $\bar{x}^{(n)}(\cdot)$ has n nodes. But if the Hessian of the saddle-point $\{\bar{q}^{(n)}, \pm\bar{x}^{(n)}(\cdot)\}$ has the eigenfunction $\bar{x}^{(n)}(\cdot)$ with zero eigenvalue and n nodes, it consequently must have $(n-1)$ eigenfunctions with *negative* eigenvalues. Therefore, only the solutions $\{\bar{q}^{(0)}, \pm\bar{x}^{(0)}(\cdot)\}$ of the ELE correspond to *maxima* of $P[x(\cdot)]$, all other solutions are saddle-points with unstable directions. These solutions are irrelevant for the asymptotics of $P(W)$, and it is therefore sufficient to determine the solutions to (5.2), (5.3) with the smallest value $\bar{q}^{(0)}$ of \bar{q} . To lighten the notation, we will denote the corresponding solutions in the following simply by $\{\bar{q}, \pm\bar{x}(\cdot)\}$.

The general expression (2.18) for \bar{S} greatly simplifies for a parabolic potential. First $xV' = 2V$, and the second and the third term in (2.18) cancel. Similarly, $xV'' = V'$ and the forth term vanishes. Finally, $x\dot{V}' = 2\dot{V}$ and the last term becomes proportional to W . We hence find the compact expression

$$\bar{S} = \frac{i\bar{q}}{2} |W|. \quad (5.6)$$

A complication also arises in the determination of the pre-exponential factor. Here we cannot use (2.29) because the zero-mode makes $\det A = 0$ and hence A^{-1} becomes singular. Nevertheless, we may proceed as in section 2 up to eq. (2.23) which now reads

$$I = \sqrt{\frac{8\pi}{\beta}} \int \prod_n \frac{dc_n}{\sqrt{4\pi/\beta}} \times \int \frac{dr}{4\pi/\beta} \exp\left(-\frac{\beta}{4} \sum_{n \geq 1} \lambda_n c_n^2 - \frac{i\beta r}{2} \sum_n c_n d_n\right). \quad (5.7)$$

Integrating over c_n with $n \geq 1$ yields

$$I = \sqrt{\frac{8\pi}{\beta}} \frac{1}{\sqrt{\det A'}} \int \frac{dc_0}{\sqrt{4\pi/\beta}} \times \int \frac{dr}{4\pi/\beta} \exp\left(-\frac{\beta r^2}{4} \sum_{n \geq 1} \frac{d_n^2}{\lambda_n} - \frac{i\beta r}{2} c_0 d_0\right), \quad (5.8)$$

where we have used the usual notation

$$\det A' := \prod_{n \geq 1} \lambda_n \quad (5.9)$$

for a determinant omitting the zero mode. The remaining integrals over r and c_0 are Gaussian and give

$$I = \frac{\sqrt{2}}{\sqrt{d_0^2 \det A'}}, \quad (5.10)$$

so that we end up with

$$P(W) = 2 \frac{\mathcal{N}\sqrt{2}}{Z_0} \frac{e^{-\beta \bar{S}}}{\sqrt{d_0^2 \det A'}} (1 + \mathcal{O}(1/\beta)), \quad (5.11)$$

where the leading factor of 2 again accounts for the two equipollent saddle-points $\{\bar{q}, \pm \bar{x}(\cdot)\}$. Comparing this result with (2.29), we realize that in the presence of a zero-mode we have to replace $\det A$ ($\dot{V}'|A^{-1}|\dot{V}'$) by $\det A'$ (d_0^2). In view of (2.28), this is quite intuitive: With λ_0 tending to zero, $\langle \dot{V}'|A^{-1}|\dot{V}' \rangle$ becomes more, and more dominated by d_0^2/λ_0 and cancelling λ_0 between $\det A$ and $\langle \dot{V}'|A^{-1}|\dot{V}' \rangle$ leaves us with (5.11).

We may finally express d_0 and $\det A'$ in terms of \bar{x} . The former is calculated from its definition (2.24) and $\varphi_0 = \bar{x}/\|\bar{x}\|$:

$$d_0 = \int_0^T dt \varphi_0 \dot{V}' = \int_0^T dt \frac{\bar{x}}{\|\bar{x}\|} \dot{k}\bar{x} = \frac{2W}{\|\bar{x}\|}. \quad (5.12)$$

The determination of $\det A'$ may be accomplished by implementing a slight variation of the method described in section 3 [7]. As shown in appendix C, eq. (3.3) has to be replaced by

$$\frac{\det A'}{\det A_{\text{ref}}} = \frac{\tilde{F}(0)}{F_{\text{ref}}(0)} \quad (5.13)$$

where

$$\tilde{F}(0) = \frac{d \|\chi_0\|^2}{\chi_0(T)}. \quad (5.14)$$

Using $d = 1$ and $\chi_0 = \bar{x}/\bar{x}(0)$, we find from (3.10)

$$\det A' = 2 \frac{\|\bar{x}\|^2}{\bar{x}_0 \bar{x}_T}. \quad (5.15)$$

Therefore, (5.11) may be written as

$$P(W) = \frac{\mathcal{N}}{Z_0} \frac{\sqrt{\bar{x}_0 \bar{x}_T}}{|W|} e^{-\beta \frac{\bar{S}}{2} |W|} (1 + \mathcal{O}(1/\beta)), \quad (5.16)$$

where

$$\mathcal{N} = \exp\left(\frac{1}{2} \int_0^T dt k(t)\right) \quad (5.17)$$

and

$$Z_0 = \sqrt{\frac{2\pi}{\beta k_0}} \quad (5.18)$$

are easily calculated.

We hence find for parabolas with time dependent frequency the universal asymptotic form

$$P(W) \sim C_1 \sqrt{\frac{\beta}{|W|}} e^{-\beta C_2 |W|} \quad (5.19)$$

with only the constants C_1 and C_2 depending on the special choice for $k(t)$. Note also that in this case the solution of the ELE is sufficient to get the full asymptotics including the prefactor.

As a simple example we first discuss the case

$$k(t) = \begin{cases} k_0 & \text{for } 0 \leq t \leq \tau \\ k_T & \text{for } \tau < t \leq T \end{cases}. \quad (5.20)$$

Here, $P(W)$ may again be calculated exactly. The particle gains energy only at $t = \tau$, where its position is still distributed according to $\rho_0(x)$. With $\Delta = k_0 - k_T > 0$, we hence find

$$P(W) = \int dx_\tau \rho_0(x_\tau) \delta(W + \frac{\Delta}{2} x_\tau^2) = \sqrt{\frac{\beta k_0}{\pi \Delta |W|}} \exp\left(-\beta \frac{k_0}{\Delta} |W|\right). \quad (5.21)$$

The ELE (5.2) is of the form

$$\ddot{x} - (1 - i\bar{q})\Delta\delta(t - \tau)\bar{x} - k^2\bar{x} = 0 \quad (5.22)$$

and has the solution

$$\bar{x}(t) = \begin{cases} \sqrt{\frac{2|W|}{\Delta}} e^{k_0(t-\tau)} & \text{for } 0 \leq t \leq \tau \\ \sqrt{\frac{2|W|}{\Delta}} e^{-k_T(t-\tau)} & \text{for } \tau \leq t \leq T \end{cases} \quad (5.23)$$

where

$$(1 - i\bar{q}) = -\frac{k_0 + k_T}{\Delta}. \quad (5.24)$$

Using this result in (5.16) and (5.6), we find back (5.21).

A somewhat more general example is given by

$$k(t) = \frac{1}{1+t}. \quad (5.25)$$

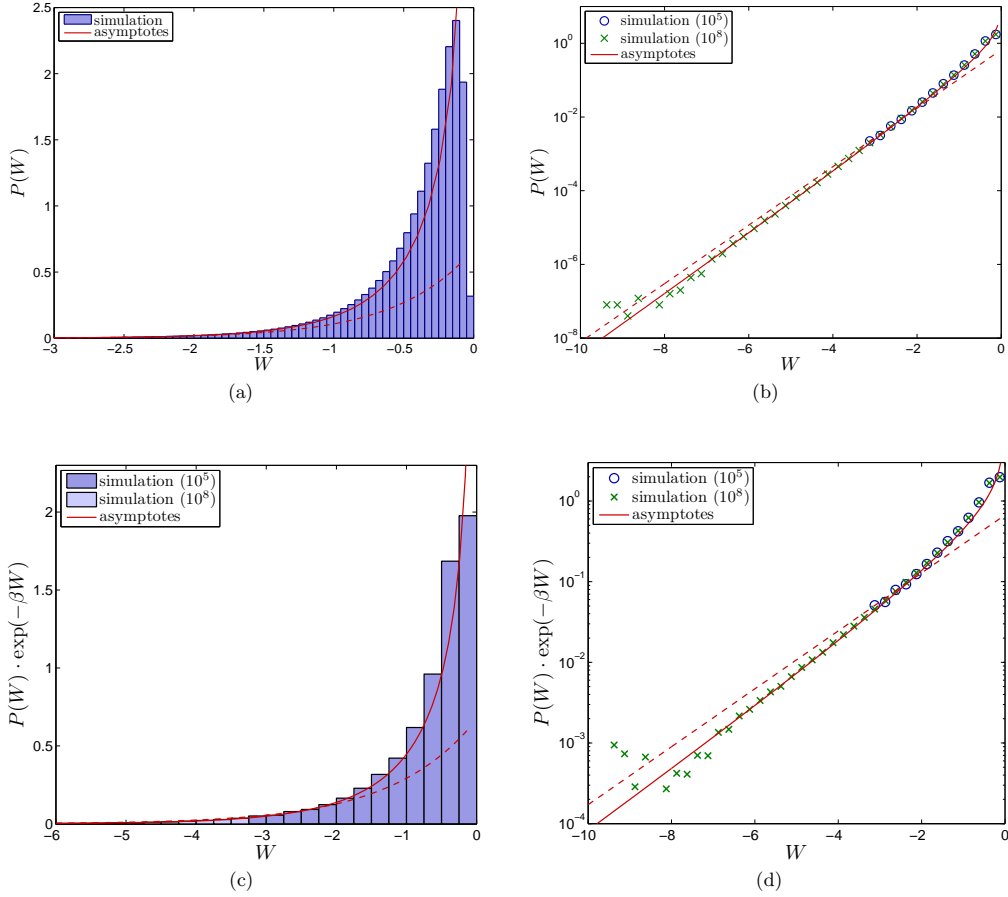


Fig. 5.1: Work distribution for a breathing parabola (5.1) with protocol (5.25) for $T = 2$ and $\beta = 1$. The histogram and the symbols show results from simulation of the Langevin dynamics (2.1), the lines give the asymptotic forms (5.30) (full) with and (2.17) (dashed) without the pre-exponential factor. Subfigures (a) and (b) show a linear and logarithmic plot respectively of the work distribution itself, subfigures (c) and (d) display the distribution weighted with the factor $e^{-\beta W}$ as appearing, e.g., in the Jarzynski equality (1.1). Circles and squares represent histograms based on 10^5 and 10^8 work values respectively, in (c) results from 10^8 trajectories are shown in light blue.

Here $P(W)$ is not known exactly, nevertheless, some analytical progress can be made in the determination of its asymptotics. To begin with, we have

$$\mathcal{N} = \sqrt{1+T} \quad \text{and} \quad Z_0 = \sqrt{\frac{2\pi}{\beta}}. \quad (5.26)$$

The ELE (5.2) can be solved analytically with the result

$$\bar{x}(t) = \pm \frac{\sqrt{|W|}}{\sqrt{g(\mu)}} \sqrt{1+t} \times \left(2\mu \cos(\mu \ln(1+t)) + \sin(\mu \ln(1+t)) \right). \quad (5.27)$$

Here, with $\nu = 2\mu \ln(1+T)$,

$$g(\mu) = \frac{1}{2} \left[\left(\mu - \frac{1}{4\mu} \right) \sin \nu - \cos \nu + 1 + \nu \left(\mu + \frac{1}{4\mu} \right) \right] > 0, \quad (5.28)$$

and $\mu = \sqrt{i\bar{q} - 9/4}$ is the smallest root of

$$(4\mu^2 - 3) \sin \frac{\nu}{2} - 8\mu \cos \frac{\nu}{2} = 0. \quad (5.29)$$

This equation has to be solved numerically. The solution for μ yields the value of $i\bar{q}$, determines the prefactor of \bar{x} in (5.27), and therefore fixes the complete asymptotics via (5.16).

For the special case $T = 2$ we find $\mu \cong 1.184$ implying $i\bar{q} \cong 3.654$ which results into

$$P(W) \sim 1.021 \sqrt{\frac{\beta}{|W|}} e^{-1.827 \beta |W|}. \quad (5.30)$$

In Fig. 5.1 we compare this asymptotics with results from numerical simulations of the Langevin equation. Here the incomplete asymptotics represented by the dashed line was fitted to the numerical results from 10^5 realizations. It is clearly seen in the logarithmic plots (b) and (d) that this procedure does not yield reliable results for the far tail of the distributions. The full asymptotics including the pre-exponential factor is again clearly superior and describes the true distribution up to rather large values of W .

6 Conclusion

In the present paper, we have shown how the complete asymptotic behaviour of work distributions in driven Langevin systems may be determined. The calculation of the pre-exponential factor was accomplished by a method building on the spectral ζ -function of the operator describing the quadratic fluctuations around the optimal trajectory. We have shown that the inclusion of the pre-exponential factor improves the asymptotics significantly and simplifies its application due to the absence of free parameters. For the examples considered, our results for the asymptotics match the outcome of extensive simulations perfectly and reach far into the region of work values accessible to simulations or experiments with moderate sample sizes.

For the class of harmonic systems with time-dependent frequency, we established the universal form

$$P(W) \sim C_1 \sqrt{\frac{\beta}{|W|}} e^{-\beta C_2 |W|} \quad (6.1)$$

of the asymptotic work distribution with only the two constants C_1 and C_2 depending on the detailed time-dependence of the frequency. We note that this form is at variance with the findings of Speck and Seifert [22] who claim that the work distribution for Langevin systems with slow but finite driving must always be Gaussian. Our general result (6.1) shows that while being presumably correct for the central part of the distribution, their statement does not hold for the asymptotics. We also note that the same asymptotic behaviour was found recently for a two-dimensional Langevin system with linear non-potential forces [23].

In view of the complex general expression (2.18) for the exponent in the asymptotics, in which all terms depend in a rather implicit way on the work value W , a further identification of universality classes for asymptotic work distributions remains an open challenge.

We would like to thank Daniel Grieser for clarifying remarks on the determinant of Sturm-Liouville operators and Markus Niemann for helpful discussions.

A Calculation of \mathcal{J}

Consider as special case of (2.1) the Langevin equation

$$\dot{x} = -cx + \sqrt{2/\beta} \xi(t) \quad (A.1)$$

with some real constant c . According to (2.6) and (2.7) the propagator of the corresponding Fokker-Planck equation is given by

$$p(x_T, T | x_0, 0) = e^{cT/2} \int_{x(0)=x_0}^{x(T)=x_T} \mathcal{D}x(\cdot) \exp \left(-\frac{\beta}{4} \int_0^T dt (\dot{x} + cx)^2 \right). \quad (A.2)$$

From the normalization condition $\int dx_T p(x_T, T | x_0, 0) = 1$, we have

$$1 = e^{cT/2} \sqrt{\frac{\beta(a+c)}{4\pi}} \int dx_0 \exp \left(-\frac{\beta(a+c)}{4} x_0^2 \right) \times \int_{x(0)=x_0}^{x(T)=x_T} dx_T \int \mathcal{D}x(\cdot) \exp \left(-\frac{\beta}{4} \int_0^T dt (\dot{x} + cx)^2 \right),$$

where $a > -c$ denotes some other real constant. By partial integration we find

$$\begin{aligned} 1 &= e^{cT/2} \sqrt{\frac{\beta(a+c)}{4\pi}} \int dx_0 \int dx_T \\ &\times \int_{x(0)=x_0}^{x(T)=x_T} \mathcal{D}x(\cdot) \exp \left(-\frac{\beta}{4} \left[(ax_0 - \dot{x}_0)x_0 + (cx_T + \dot{x}_T)x_T \right. \right. \\ &\quad \left. \left. + \int_0^T dt x \left(-\frac{d^2}{dt^2} + c^2 \right) x \right] \right) \\ &= e^{cT/2} \sqrt{\frac{\beta(a+c)}{4\pi}} \mathcal{J} \frac{1}{\sqrt{\det A}}, \end{aligned} \quad (A.3)$$

where the operator A is defined by

$$\begin{aligned} A\varphi &= -\ddot{\varphi} + c^2\varphi, \\ a\varphi(0) - \dot{\varphi}(0) &= 0, \quad c\varphi(T) + \dot{\varphi}(T) = 0. \end{aligned} \quad (A.4)$$

With the methods described in section 3 we easily find

$$\det A = 2(a+c) e^{cT}, \quad (A.5)$$

and comparison with (A.3) yields

$$\mathcal{J} = \sqrt{\frac{8\pi}{\beta}}. \quad (A.6)$$

Note that this value does not depend on a and c and is therefore valid for all situations considered in the present paper.

B Calculation of $\det A_{\text{ref}}$ and $F_{\text{ref}}(0)$

In this appendix we calculate the determinant of the operator

$$A_{\text{ref}} = -\frac{d^2}{dt^2} \quad (\text{B.1})$$

with boundary conditions

$$a \varphi(t=0) + b \dot{\varphi}(t=0) = 0 \quad (\text{B.2})$$

$$c \varphi(t=T) + d \dot{\varphi}(t=T) = 0. \quad (\text{B.3})$$

The main point for introducing this reference operator is that the ratio of determinants of two Sturm-Liouville operators has much nicer analytic properties than each determinant individually [14]. Intuitively, this is related to the fact that in the naive interpretation of the determinant as product of all eigenvalues each determinant separately is clearly infinite, whereas their ratio may remain bounded. Our derivation closely follows [14], where the corresponding analysis for Dirichlet boundary conditions was given.

We start with

$$\det A_{\text{ref}} = e^{-\zeta'_{\text{ref}}(0)}, \quad (\text{B.4})$$

where

$$\zeta_{\text{ref}}(s) := \sum_{n=1}^{\infty} \lambda_{\text{ref},n}^{-s} \quad (\text{B.5})$$

is the spectral ζ -function of the operator A_{ref} with $\lambda_{\text{ref},n}$ denoting its eigenvalues [7]. Let $\chi_{\lambda}(t)$ be the solution of

$$-\ddot{\chi}_{\lambda}(t) = \lambda \chi_{\lambda}(t), \quad \chi_{\lambda}(0) = -b, \quad \dot{\chi}_{\lambda}(0) = a. \quad (\text{B.6})$$

Then

$$F_{\text{ref}}(\lambda) := c\chi_{\lambda}(T) + d\dot{\chi}_{\lambda}(T) \quad (\text{B.7})$$

has zeros at all eigenvalues $\lambda = \lambda_{\text{ref},n}$ of A_{ref} . Correspondingly, $d \ln F_{\text{ref}}(\lambda)/d\lambda$ has poles at these eigenvalues with residues given by their multiplicities. We may hence write

$$\zeta_{\text{ref}}(s) = \frac{1}{2\pi i} \int_{\mathfrak{c}} d\lambda \lambda^{-s} \frac{d}{d\lambda} \ln F_{\text{ref}}(\lambda), \quad (\text{B.8})$$

where the contour \mathfrak{c} starts at $\lambda = \infty + i\epsilon$, goes down parallel to the real axis, makes a half-circle around the lowest eigenvalue $\lambda_{\text{ref},1} > 0$ and continues parallel to the real axis to $\lambda = \infty - i\epsilon$.

For the simple case of A_{ref} we may solve (B.6) and determine $F_{\text{ref}}(\lambda)$ explicitly:

$$F_{\text{ref}}(\lambda) = (ad - bc) \cos \sqrt{\lambda} T + (ca + bd\lambda) \frac{\sin \sqrt{\lambda} T}{\sqrt{\lambda}}. \quad (\text{B.9})$$

From this result we find

$$\frac{d}{d\lambda} \ln F_{\text{ref}}(\lambda) \sim \sqrt{\lambda} \quad (\text{B.10})$$

for large $|\lambda|$. Provided $s > 1/2$, we may hence deform \mathfrak{c} to the contour starting at $\lambda = -\infty + i\epsilon$, going up to a half-circle around $\lambda = 0$ and running back to $-\infty - i\epsilon$. Taking into account that the integrand has a branch cut

along the negative real axis and substituting $\lambda = -x \pm i\epsilon$, we find (for $s > 1/2$)

$$\zeta_{\text{ref}}(s) = \frac{\sin \pi s}{\pi} \int_0^{\infty} dx x^{-s} \frac{d}{dx} \ln F_{\text{ref}}(-x) \quad (\text{B.11})$$

$$= \frac{\sin \pi s}{\pi} \int_0^{\infty} dx x^{-s} \frac{d}{dx} \ln \left[(ad - bc) \cosh(\sqrt{x} T) + (ca - bdx) \frac{\sinh \sqrt{x} T}{\sqrt{x}} \right]. \quad (\text{B.12})$$

In order to use this expression in (B.4) it has to be analytically continued to $s = 0$. No problems arise at the lower limit of integration, $x = 0$. Using the representation

$$\begin{aligned} \frac{d}{dx} \ln F_{\text{ref}}(-x) &= \frac{T}{2\sqrt{x}} + \frac{1}{2x} \\ &+ \frac{d}{dx} \ln \left[\frac{ad - bc}{2\sqrt{x}} (1 + e^{-2\sqrt{x} T}) \right. \\ &\quad \left. + \frac{ca/x - bd}{2} (1 - e^{-2\sqrt{x} T}) \right], \end{aligned} \quad (\text{B.13})$$

we see, however, that the first two terms entail divergences at large x for $s \rightarrow 0$. Splitting the integral in (B.12) at $x = 1$, these dangerous terms may be integrated explicitly and the continuation to $s = 0$ presents no further problems.

At the end we find

$$\zeta'_{\text{ref}}(s=0) = -\ln \left(\frac{2}{bd} (cb - ad - caT) \right) \quad (\text{B.14})$$

implying

$$\det A_{\text{ref}} = \frac{2}{bd} (cb - ad - caT). \quad (\text{B.15})$$

To use this result in (3.3), we have finally to determine $F_{\text{ref}}(0)$. To this end, we need the solution $\chi_0(t)$ of

$$A_{\text{ref}} \chi_0 = -\ddot{\chi}_0 = 0, \quad \chi_0(0) = -b, \quad \dot{\chi}_0(0) = a \quad (\text{B.16})$$

which is given by

$$\chi_0(t) = at - b. \quad (\text{B.17})$$

Then

$$F_{\text{ref}}(0) = c\chi_0(T) + d\dot{\chi}_0(T) = acT - cb + da \quad (\text{B.18})$$

which, of course, also follows from (B.9) for $\lambda \rightarrow 0$. Combining (B.15) and (B.18) we arrive at (3.10).

C Calculation of $\det A'$

In this appendix we sketch the calculation of the determinant of a Sturm-Liouville operator omitting its zero mode for the case of Robin boundary conditions, where we closely follow [7]. The main idea is to replace $F(\lambda)$ as

defined in (3.7) by a function that is zero only at the *non-zero* eigenvalues of A and behaves asymptotically in the same way as $F(\lambda)$. Then all calculations may be done as before, and we end up with a relation similar to (3.3).

To get an idea how the replacement of $F(\lambda)$ may look like, it is instructive to consider the scalar product between the zero-mode χ_0 of A and a general solution χ_λ of (3.8). Note that then χ_0 fulfils *both* the boundary conditions at $t = 0$ and $t = T$ whereas χ_λ fulfils for general λ only the one at $t = 0$ as specified in (3.8). We find by partial integration

$$\begin{aligned}\lambda\langle\chi_0|\chi_\lambda\rangle &= \langle\chi_0|A\chi_\lambda\rangle \\ &= -\chi_0\dot{\chi}_\lambda|_0^T + \dot{\chi}_0\chi_\lambda|_0^T + \langle A\chi_0|\chi_\lambda\rangle \\ &= -\frac{\chi_0(T)}{d}(c\chi_\lambda(T) + d\dot{\chi}_\lambda(T))\end{aligned}\quad (\text{C.1})$$

implying

$$F(\lambda) = c\chi_\lambda(T) + d\dot{\chi}_\lambda(T) = -\frac{d}{\chi_0(T)}\lambda\langle\chi_0|\chi_\lambda\rangle. \quad (\text{C.2})$$

Hence

$$\tilde{F}(\lambda) = \frac{\lambda-1}{\lambda}F(\lambda) = (1-\lambda)\frac{d\langle\chi_0|\chi_\lambda\rangle}{\chi_0(T)}, \quad (\text{C.3})$$

vanishes at all eigenvalues $\lambda_n > 0$ (since F does), remains non-zero for $\lambda = \lambda_0 = 0$ (cf. C.2) and behaves asymptotically for large λ exactly as F . Similarly to the case without zero modes, one hence finds

$$\frac{\det A'}{\det A_{\text{ref}}} = \frac{\tilde{F}(0)}{F_{\text{ref}}(0)} \quad (\text{C.4})$$

which coincides with (5.13).

References

1. C. Jarzynski, Phys. Rev. Lett. **78**, (1997) 2690
2. D. J. Evans, E. G. D. Cohen, and G. P. Morriss, Phys. Rev. Lett. **71**, (1993) 2401
3. G. Gallavotti and E. G. D. Cohen, Phys. Rev. Lett. **74**, (1995) 2694
4. U. Seifert, Eur. Phys. J. **B64**, (2008) 423
5. M. Esposito and C. Van den Broeck, Phys. Rev. Lett. **104**, (2010) 090601, Phys. Rev. **E82**, (2010) 011143 and 011144
6. D. Collin, F. Ritort, C. Jarzynski, S. B. Smith, I. Tinoco and C. Bustamante, Nature **437**, (2005) 231
7. K. Kirsten and A. J. McKane, Ann. Phys. (N.Y.) **308**, (2003) 502
8. K. Sekimoto Prog. Theor. Phys. Supp. **130**, (1998) 17
9. M. Chaichian and A. Demichev, *Path integrals in Physics* (IOP Publishing, London, 2001)
10. H. Touchette, Phys. Rep. **478**, (2009) 1
11. I. M. Lifshitz, Sov. Phys. Usp. **7**, (1965) 549
12. B. I. Halperin and M. Lax, Phys. Rev. **148**, (1966) 722
13. A. Engel, Phys. Rev. **E80**, (2009) 021120
14. K. Kirsten and P. Loya, Am. J. Phys. **76**, (2008) 60
15. O. Mazonka, C. Jarzynski, [arXiv:cond-mat/9912121](#)
16. G. M. Wang, E. M. Seveck, E. Mittag, D. J. Searles, and D. J. Evans, Phys. Rev. Lett. **89**, (2002) 050601
17. R. van Zon and E. G. D. Cohen, Phys. Rev. **E67**, (2003) 046102, Phys. Rev. **E69**, (2004) 056121
18. E. G. D. Cohen, J. Stat. Mech., (2008) P07014
19. S. X. Sun, J. Chem. Phys. **118**, (2003) 5769
20. C. Jarzynski, Phys. Rev. **E56**, (1997) 5018
21. D. M. Carberry, J. C. Reid, G. M. Wang, E. M. Seveck, D. J. Searles, and D. J. Evans, Phys. Rev. Lett. **92**, (2004) 140601
22. T. Speck and U. Seifert, Phys. Rev. **E70**, (2004) 066112
23. C. Kwon, J. D. Noh, and H. Park, [arXiv:1102.2973](#)

Asymptotic work distributions in driven bistable systems

D. Nickelsen¹, A. Engel¹

¹ Universität Oldenburg, Institut für Physik, 26111 Oldenburg, Germany

E-mail: daniel.nickelsen@uni-oldenburg.de,
andreas.engel@uni-oldenburg.de

Abstract. The asymptotic tails of the probability distributions of thermodynamic quantities convey important information about the physics of nanoscopic systems driven out of equilibrium. We apply a recently proposed method to analytically determine the asymptotics of work distributions in Langevin systems to an one-dimensional model of single-molecule force spectroscopy. The results are in excellent agreement with numerical simulations, even in the centre of the distributions. We compare our findings with a recent proposal for an universal form of the asymptotics of work distributions in single-molecule experiments.

PACS numbers: 05.70.Ln, 02.50.-r, 05.40.-a, 05.20.-y

1. Introduction

Traditionally, statistical mechanics is concerned with *averages*; the probability distributions for thermodynamic quantities of macroscopic systems are so exceedingly sharp that only their most probable values matter. These in turn are practically identical with the averages. Only near instabilities, deviations from averages become important. In static cases these fluctuations are well described by the second moments of the respective distributions; if the dynamics is of importance as well, they are characterized by the correlation functions.

When investigating nanoscopic systems from the point of view of thermodynamics, the situation changes. Fluctuations are now strong and ubiquitous, and correspondingly, the probability distributions of relevant quantities are broad and poorly characterized by their leading moments alone. Whereas this seems rather obvious, it came as a real surprise that work [1] and fluctuation [2, 3] theorems which form the cornerstones of the emerging field of *stochastic thermodynamics* [4, 5, 6, 7, 8] are relations that probe the *very far tails* of the respective probability distributions. Very unlikely events now carry significant information about the physics of the system under consideration. On the one hand, interest in mathematical investigations like large deviation theory (see [9] and references therein) is renewed, on the other hand, techniques are in demand that allow to determine the *asymptotics* of probability distributions. Since rare events are hard to get in experiments and numerical simulations, approximate analytical procedures have to be developed.

In the present paper we apply a recently proposed method for the analytical determination of the asymptotics of work distributions in driven Langevin systems [10] to a simple model for single-molecule force spectroscopy. In these experiments (for a recent review see [11]) the free-energy difference ΔF between the folded and the unfolded state of a biomolecule is determined from the distribution of work W obtained in isothermal unfolding and refolding processes. If only one transition is monitored [13], the Jarzynski equation [1]

$$\langle e^{-\beta W} \rangle = e^{-\beta \Delta F} \quad (1)$$

is employed, where β denotes the inverse of the temperature. If histograms of work for both the forward and the reverse process are compiled [14], it may be advantageous to use the Crooks fluctuation theorem [15]

$$\frac{P(W)}{P_r(-W)} = e^{\beta(W - \Delta F)}. \quad (2)$$

Here, the free-energy difference ΔF is identified from the intersection of the probability density functions $P(W)$ of the forward and $P_r(-W)$ of the reverse process. Note that in both cases an accurate estimate for ΔF requires reliable information about the tails of the work probability distributions.

The paper is organized as follows. In section 2 we introduce the notation and review the general method [10]. Section 3 contains the application to an one-dimensional stochastic process with a time-dependent double-well potential and the comparison with numerical simulations of the system. In section 4 we discuss our results and in particular compare them with a recent proposal for the general shape of the tail of the work distribution in single-molecule experiments [19].

2. General Theory

To pave the way for the analysis and to fix the notation we summarize in the present section in a very condensed way the main steps of our approach to determine the asymptotic tail of work distributions in driven Langevin systems. For more details the reader is referred to [10].

We investigate a system described by an one-dimensional, overdamped Langevin equation which in dimensionless units has the form

$$\dot{x} = -V'(x, t) + \sqrt{2/\beta} \xi(t) . \quad (3)$$

Here x denotes the degree of freedom, V is a time-dependent potential modelling the external driving, and $\xi(t)$ is Gaussian white noise with $\langle \xi(t) \rangle \equiv 0$ and $\langle \xi(t) \xi(t') \rangle = \delta(t - t')$. We denote derivatives with respect to x by a prime, and those with respect to t by a dot. The initial state $x(t = 0) =: x_0$ of the process is sampled from the equilibrium distribution at $t = 0$ with inverse temperature β ,

$$\rho_0(x_0) = \frac{1}{Z_0} \exp[-\beta V_0(x_0)] . \quad (4)$$

Accordingly, $V_0(x) := V(x, t = 0)$ is the initial potential and

$$Z_0 = \int dx \exp[-\beta V_0(x)] \quad (5)$$

the corresponding partition function.

The work performed on the system for a particular trajectory $x(\cdot)$ is given by [16]

$$W[x(\cdot)] = \int_0^T dt \dot{V}(x(t), t) . \quad (6)$$

Due to the randomness inherent in $x(\cdot)$, the work W is itself a random quantity and its pdf can be written as

$$P(W) = \int \frac{dx_0}{Z_0} \exp[-\beta V_0(x_0)] \int dx_T \int_{x(0)=x_0}^{x(T)=x_T} \mathcal{D}x(\cdot) p[x(\cdot)] \delta(W - W[x(\cdot)]) . \quad (7)$$

For mid-point discretization we have [17]

$$p[x(\cdot)] = \mathcal{N}[x(\cdot)] \exp \left[-\frac{\beta}{4} \int_0^T dt (\dot{x} + V'(x, t))^2 \right] \quad (8)$$

with the normalization factor

$$\mathcal{N}[x(\cdot)] = \exp \left[\frac{1}{2} \int_0^T dt V''(x(t), t) \right] . \quad (9)$$

Hence

$$P(W) = \int \frac{dx_0}{Z_0} \int dx_T \int \frac{dq}{4\pi/\beta} \int_{x(0)=x_0}^{x(T)=x_T} \mathcal{D}x(\cdot) \mathcal{N}[x(\cdot)] \exp \{-\beta S[x(\cdot), q]\} \quad (10)$$

with the action

$$S[x(\cdot), q] = V_0(x_0) + \int_0^T dt \left[\frac{1}{4}(\dot{x} + V')^2 + \frac{iq}{2}\dot{V} \right] - \frac{iq}{2}W. \quad (11)$$

We are interested in the asymptotic behaviour of $P(W)$. Rare values of W are brought about by unlikely trajectories $x(\cdot)$. In the spirit of the contraction principle of large deviation theory [9], we expect that in the asymptotic tails of $P(W)$ there is *one* trajectory for each value of W that dominates $P(W)$. To find it, we have to maximize $P[x(\cdot)] := \rho_0(x_0)p[x(\cdot)]$ under the constraint $W = W[x(\cdot)]$. This can be done by using a saddle-point approximation of the integrals in (10). The result is

$$P(W) = \frac{\mathcal{N}\sqrt{2}}{Z_0} \frac{\exp[-\beta\bar{S}]}{\sqrt{\bar{R} \det A}} (1 + O(1/\beta)). \quad (12)$$

To use this expression in explicit examples, we first have to determine the most probable trajectory $\bar{x}(\cdot)$ satisfying the Euler-Lagrange equation (ELE)

$$\ddot{\bar{x}} + (1 - iq)\dot{\bar{V}}' - \bar{V}'\bar{V}'' = 0 \quad (13)$$

where $\bar{V}(t) := V(\bar{x}(t), t)$ and similarly for derivatives of V . The ELE is completed by the boundary conditions

$$\dot{\bar{x}}_0 - \bar{V}'_0 = 0, \quad \dot{\bar{x}}_T + \bar{V}'_T = 0 \quad (14)$$

and by the corresponding value \bar{q} of the Lagrange parameter q ensuring $W[\bar{x}(\cdot)] = W$. Using $\bar{x}(\cdot)$ and \bar{q} , we calculate $\bar{S} := S[\bar{x}(\cdot), \bar{q}]$ and $\bar{\mathcal{N}} := \mathcal{N}[\bar{x}(\cdot)]$. Then all terms in (12) depending *solely* on the optimal trajectory are determined.

The denominator $\sqrt{\bar{R} \det A}$ in (12) comprises the contribution from the *neighbourhood* of the optimal path and stems from the integral over the Gaussian fluctuations around $\bar{x}(\cdot)$ and \bar{q} . Here,

$$A := -\frac{d^2}{dt^2} + (\bar{V}'')^2 + \bar{V}'\bar{V}''' - (1 - iq)\dot{\bar{V}}'' \quad (15)$$

denotes the operator of quadratic fluctuations which acts on functions $\varphi(t)$ on the interval $0 < t < T$ obeying the boundary conditions

$$\begin{aligned} \bar{V}_0''\varphi(0) - \dot{\varphi}(0) &= 0, \\ \bar{V}_T''\varphi(T) + \dot{\varphi}(T) &= 0. \end{aligned} \quad (16)$$

A simple prescription to calculate $\det A$ is as follows [18]. Solve the initial value problem

$$\begin{aligned} A\chi(t) &= 0, \\ \chi(0) &= 1, \quad \dot{\chi}(0) = \bar{V}_0'' \end{aligned} \quad (17)$$

then

$$\det A = 2(\bar{V}_T''\chi(T) + \dot{\chi}(T)). \quad (18)$$

The factor \bar{R} in (12) accounts for the influence of the constraint (6) on the fluctuations around $\bar{x}(\cdot)$. Since also the trajectories from the neighbourhood of $\bar{x}(\cdot)$ have to yield the very same value of W , fluctuations violating this constraint are suppressed. This gives rise to a correction to the fluctuation determinant of the form

$$\bar{R} = \int_0^T dt \dot{\bar{V}}'(t) A^{-1} \dot{\bar{V}}'(t), \quad (19)$$

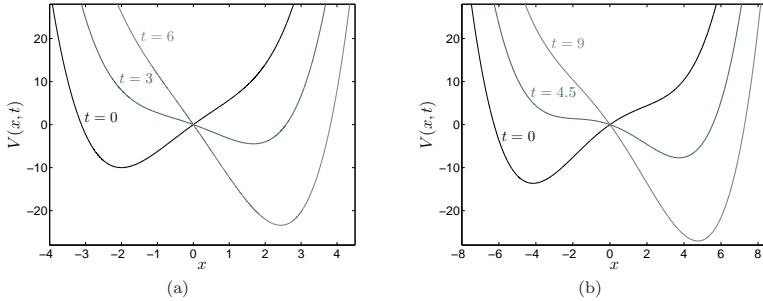


Figure 1: Evolution of the potential $V(x, t)$ (22) in the time-interval $0 < t < T$ for two exemplary parameter sets. Shown is $V(x, t)$ for $t = 0$, $t = T/2$ and $t = T$ respectively. (a) $a = 0.25$, $b = 0.5$, $c = 2$, $r = 3$, $T = 6$ and (b) $a = 0.025$, $b = 0.5$, $c = 3$, $r = 1$, $T = 9$.

where A^{-1} denotes the inverse operator of A . To explicitly determine \bar{R} , it is convenient to solve the ordinary differential equation

$$A \psi(t) = \dot{V}'(\bar{x}(t), t) \quad (20)$$

with boundary conditions (16) and to use

$$\bar{R} = \int_0^T dt \psi(t) \dot{V}'(t) . \quad (21)$$

3. The driven double-well

The unfolding and refolding of single molecules can be modeled by a time-dependent double-well potential of the form

$$V(x, t) = ax^4 - bx^2 + r(c - t)x , \quad (22)$$

where x denotes the extension of the molecule in the direction of the force [13, 14, 19]. The parameters a and b characterize depth and separation of the two minima of V , c fixes the moment at which V is symmetric, $V(x) = V(-x)$, and r denotes the transition rate. Choosing $T > c$ for the final time, the two minima will interchange global stability during the process. We have used two exemplary sets of parameters for which the time evolution of $V(x, t)$ is sketched in figure 1. The main differences between the two sets are that in (b) the minima are further apart and the transition rate r is smaller.

We now apply the analytic method to obtain the asymptotics (12) of the work distribution of the dynamics defined by the potential $V(x, t)$ (22). To clarify the procedure, we compile the necessary equations. We have from (5) and (9)

$$Z_0 = \int dx \exp [-\beta(ax^4 - bx^2 + rcx)] \quad (23)$$

$$\mathcal{N}[x(\cdot)] = \exp \left[6a \int_0^T dt x^2(t) - bT \right] . \quad (24)$$

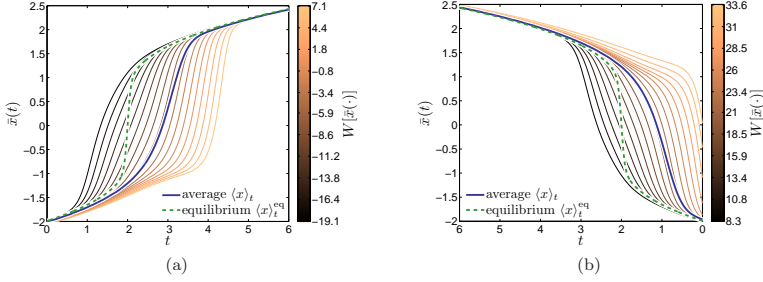


Figure 2: Trajectories for the potential shown in figure 1a for (a) the forward and (b) the reverse process. Shown are optimal trajectories $\bar{x}(\cdot)$ for exemplary work values W . For a comparison is plotted on top (thick lines), the average trajectory of the simulation (full blue line), and the average $\langle x \rangle_t^{\text{eq}}$ from the equilibrium distribution corresponding to the instantaneous values of the parameters (dashed line).

The ELE (13) reads

$$\ddot{x} = 48a^2\bar{x}^5 - 32a\bar{x}^3b + r(c-t)[12a\bar{x}^2 - 2b] + 4b^2\bar{x} + r(1 - i\bar{q}) , \quad (25)$$

and its boundary conditions (14) are of the form

$$\begin{aligned} 0 &= \dot{x}_0 - 4a\bar{x}_0^3 + 2b\bar{x}_0 - rc , \\ 0 &= \dot{x}_T + 4a\bar{x}_T^3 - 2b\bar{x}_T + r(c - T) . \end{aligned} \quad (26)$$

The constraint (6) is

$$W = -r \int_0^T dt \, \bar{x}(t; \bar{q}) . \quad (27)$$

Using a standard relaxation algorithm, the numerical solution of equations (25) - (27) for desired work values W yields optimal trajectories $\bar{x}(t)$ depicted exemplarily in figure 2.

The operator A from (15) acquires the form

$$A = -\frac{d^2}{dt^2} + 240a^2\bar{x}^4 - 96ab\bar{x}^2 + 24ar(c-t)\bar{x} + 4b^2 \quad (28)$$

with the boundary conditions (16)

$$\begin{aligned} 0 &= [12a\bar{x}_0^2 - 2b]\varphi(0) - \dot{\varphi}(0) , \\ 0 &= [12a\bar{x}_T^2 - 2b]\varphi(T) + \dot{\varphi}(T) . \end{aligned} \quad (29)$$

To obtain $\det A$ according to (18), we determine

$$\det A = [24a\bar{x}_T^2 - 4b]\chi(T) + 2\dot{\chi}(T) \quad (30)$$

by solving numerically the initial value problem (17)

$$\begin{aligned} \ddot{\chi}(t) &= [240a^2\bar{x}^4 - 96ab\bar{x}^2 + 24ar(c-t)\bar{x} + 4b^2]\chi(t) = 0 , \\ \dot{\chi}(0) &= 1 , \quad \dot{\chi}(0) = 12a\bar{x}_0^2 - 2b . \end{aligned} \quad (31)$$

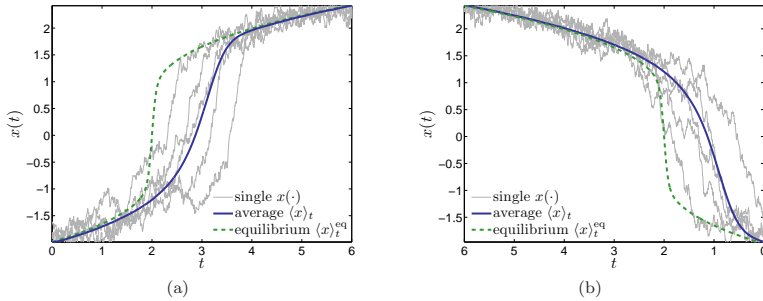


Figure 3: Trajectories for the potential shown in figure 1a for (a) the forward and (b) the reverse process. Shown is, exemplified by single realizations $x(\cdot)$, the range of trajectories attainable from the simulation (full grey lines), the average trajectory of the simulation (full blue line), and the average $\langle x \rangle_t^{\text{eq}}$ from the equilibrium distribution corresponding to the instantaneous values of the parameters (dashed line).

This has to be done for each value of W separately by using the appropriate results for $\bar{x}(t; W)$ and $\bar{q}(W)$.

The last ingredient for the pre-exponential factor is \bar{R} from (21). To determine it, we need to solve the boundary value problem (20), (16)

$$\begin{aligned} \ddot{\psi}(t) &= [240a^2\bar{x}^4 - 96ab\bar{x}^2 \\ &\quad + 24ar(c-t)\bar{x} + 4b^2]\psi(t) + r, \\ 0 &= [12a\bar{x}_0^2 - 2b]\psi(0) - \dot{\psi}(0), \\ 0 &= [12a\bar{x}_T^2 - 2b]\psi(T) + \dot{\psi}(T) \end{aligned} \quad (32)$$

for each $\bar{x}(t; W)$ and $\bar{q}(W)$ and use the result in (21)

$$\bar{R} = -r \int_0^T dt \psi(t). \quad (33)$$

Plugging the numerical results for Z_0 , \bar{N} , \bar{S} , $\det A$ and \bar{R} into (12), we obtain the final result for the asymptotic form of the work distribution. We carried out this program for the two processes characterized by the parameter sets given in the caption of figure 1, including for both cases the *reversed* processes defined by the substitution $t \rightarrow (T - t)$. From simulations of the Langevin equation (3), we also obtained from (6) the corresponding histograms of work distributions. The values of β and T are chosen such that most of the trajectories reach the right minimum of V at the end of the forward process, i.e. the molecules are stretched until virtually all of them unfold (cf. figure 3). The results for the asymptotics are shown in figure 4, together with the outcome of our numerical simulations.

In a recent paper [19], Palassini and Ritort propose an universal form for the tails of work distributions for single molecule stretching experiments given by

$$P(W) \sim n \frac{\Omega^{\alpha-1}}{|W - W_c|^\alpha} \exp \left[-\frac{|W - W_c|^\delta}{\Omega^\delta} \right]. \quad (34)$$

Table 1: Fit results for (34) for the two examples (a) and (b) shown in figure 1 for the forward (fw) and reverse (rv) process. N denotes the number of realizations used in the simulation, the other parameters are from the proposal (34).

Set	N	n	Ω	α	W_c	δ	λ
(a) fw	10^4	4.27E-4	9.31	-26.4	11.5	3.35	4.22
(a) rv	10^4	1.16E-5	8.64	-31.2	38.2	3.26	2.26
(b) fw	10^5	4.97	8.61	-3.01	19.9	2.47	1.45
(b) rv	10^5	1740	26.1	26.5	61.2	3.33	0.607

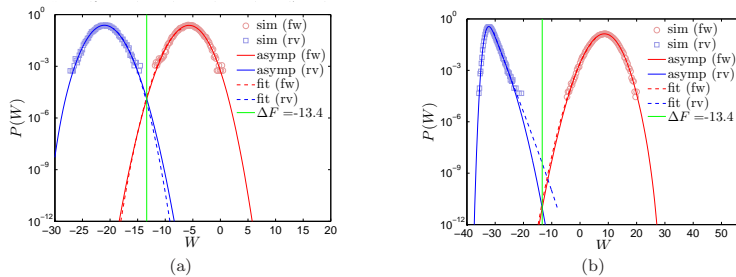


Figure 4: Work distributions $P(W)$ (forward process) and $P_r(-W)$ (reverse process) for the two potentials (a) and (b) shown in figure 1. Corresponding results obtained from numerical simulations are shown by open circles (forward process) and open squares (reverse process). Full lines depict the asymptotics according to (12), dashed lines are fits of (34). The value of the free-energy difference ΔF obtained from numerical integration of the partition functions Z_0, Z_T (23) is indicated by the vertical line.

Here, W_c is a characteristic work value, $\Omega > 0$ measures the tail width, and n, α and δ are further constants. The Jarzynski equation (1) stipulates $\delta > 1$. Based on (34), Palassini and Ritort present in [19] three slightly different analytical methods to improve the estimation of free-energy differences ΔF from the Jarzynski equation (1). To decide which approach to use, they distinguish three regimes defined by the parameter combination

$$\lambda := (\delta/\Omega)^{\delta/(\delta-1)} \ln N. \quad (35)$$

The three regimes are then identified by $\lambda > 1$, $\lambda \ll 1$ and $\lambda \lesssim 1$ respectively. They test their method with experimental data from DNA stretching experiments. For more details regarding the improved estimation of ΔF and the experiments see [19].

We fitted the empirical asymptotic form (34) to the tails of the work distributions obtained in our simulations by standard least-square fits, starting with a Gaussian distribution specified by $W_c = \langle W \rangle$, $\Omega^2 = 2 \langle (W - W_c)^2 \rangle$, $\alpha = 0$, $\delta = 2$ and $n = 1/\sqrt{\pi}$. A subtle point in the procedure is to find the optimal interval of work values for the fit. The resulting parameter values are listed in table 1, the corresponding fits are included into figure 4.

4. Discussion

As shown in Figure 4 for both parameter sets (a) and (b), we achieve an excellent agreement between simulation and asymptotics, not only asymptotically for the tails, but also for the centre of the work distributions. The good reproduction of the centre of the distribution is presumably due to the fact that also the probabilities of *typical* work values are dominated by single trajectories and their neighbourhood. Note also the perfect match between the free-energy difference ΔF and the intersection of our asymptotics $P(W)$ and $P_r(-W)$, which demonstrates that the Crooks relation (2) holds in its exact form for our asymptotics, as has been shown in [10].

In addition, figure 2 illustrates the optimal trajectories $\bar{x}(\cdot)$ which dominate the asymptotics of the work distributions (12). In comparison with the trajectories obtained from our simulations shown in figure 3, the trajectories $\bar{x}(\cdot)$ contributing to the tails of the work distribution are of much broader variety. Interestingly, the probability of small work values is dominated by $\bar{x}(\cdot)$ that run into the evolving right minimum even before the minimum is shaped.

For the parameter set (a), the fit of (34) compares well with the analytic asymptotics. In this case a combination of a histogram from experimental values and (34) would therefore result in reliable estimates for the free-energy difference ΔF . For the parameter set (b) only the forward process is well described by the fit, for the reverse one the tail of the distribution is markedly overestimated. This shifts the intersection point between $P(W)$ and $P_r(-W)$ away from the correct value of ΔF as can be seen in figure 4b. Also, some fit parameters for this case listed in table 1 clearly deviate from the other cases. To investigate that mismatch more closely, we also fitted (34) to the analytic asymptotics (not shown). This results into similar conspicuous fit parameters, but the fitting curve now is almost congruent with the analytic asymptotics. From that we conclude that the empirical asymptotics (34) is also valid in this case, but the number of work values obtained from the simulation is not enough to reliably fit (34). Note that rather than taking the intersection point between $P(W)$ and $P_r(-W)$, Palassini and Ritort use in [19] much more sophisticated methods to obtain estimates of ΔF , based on their empirical asymptotics (34). Our investigation aims only at validating (34).

In addition to the two parameter sets displayed in figure (1), we also investigated several other realizations of the potential (22) (not shown). Mostly, we found that fits of (34) to histograms of 10^4 to 10^5 work values extrapolate reliably to the asymptotic tail of the distribution. But as exemplified by the case shown in figure 4b, there is no guaranty that a number of 10^5 work values is sufficient.

5. Conclusions

The asymptotics of work distributions for driven Langevin systems can be determined by the method proposed in [10]. We employed this method to determine the asymptotics of a system defined by the potential (22) modelling the stretching of single molecules. The unfolding of the molecules corresponds to the forward process, the refolding to the reverse process. We obtained histograms of work by simulating the Langevin equation (3). The form of the work distributions are found to be near-Gaussian, similar to distributions measured in a DNA stretching experiment [19]. We observe excellent agreement between asymptotics and work distribution, not only for the asymptotic regime but also for the whole range of work values.

One aim of single molecule experiments is to obtain the free-energy difference between the folded and unfolded state of the molecule. If both the work distribution for the forward and reverse process is available, the Crooks relation (2) can be used to determine the free-energy difference. It is shown in [10] that the asymptotics (12) generally satisfies the Crooks relation exactly, which we demonstrated for two representative examples of the potential (22).

Finally, we tested the universal form (34) of the tails of work distributions proposed by M. Palassini and F. Ritort against our results for the asymptotics (12). For a broad range of parameters used for the model potential (22), we found a good agreement between (34) and our asymptotics. Only if the work distribution differs markedly from a Gaussian form, a reliable fit of (34) is likely to require more data points than usually acquired in single-molecule experiments. This might lead to a significant difference between the exact and estimated free-energy difference as illustrated by our examples.

Acknowledgements

We would like to thank Felix Ritort for interesting discussions and the organizers of the 2011 Nordita workshop "Foundations and Applications of Non-equilibrium Statistical Mechanics" where part of this work was done, for providing a stimulating atmosphere, and the ESF for financially supporting the workshop. D.N. acknowledges financial support from the Deutsche Forschungsgemeinschaft under grant EN 278/7.

References

- [1] Jarzynski C 1997 *Phys. Rev. Lett.* **78** 2690
- [2] Evans D J, Cohen E G D and Morriss G P 1993 *Phys. Rev. Lett.* **71** 2401
- [3] Gallavotti G and Cohen E G D 1995 *Phys. Rev. Lett.* **74** 2694
- [4] Jarzynski C 2011 *Ann. Rev. Condens. Matter Phys.* **2** 329
- [5] Seifert U 2008 *Eur. Phys. J.* **B64** 423
- [6] Esposito M and Van den Broeck C 2010 *Phys. Rev. Lett.* **104** 090601 *Phys. Rev. E* **82** 011143 and 011144
- [7] Sekimoto K 2010 *Stochastic Energetics* (Springer, Berlin)
- [8] Seifert U 2012 [arXiv:1205.4176](https://arxiv.org/abs/1205.4176)
- [9] Touchette H 2009 *Phys. Rep.* **478** 1
- [10] Nickelsen D and Engel A 2011 *Eur. Phys. J. B* **82** 207
- [11] Alemany A, Ribezzi M and Ritort F 2011 *AIP Proceedings conference* **1332** 96
- [12] Pohorille A, Jarzynski C, and Chipot C 2010 *J. Phys. Chem.* **114** 10235
- [13] Liphardt J, Dumont S, Smith S B, I. Tinoco Jr. I and C. Bustamante C 2002 *Science* **296** 1832
- [14] Collin D, Ritort F, Jarzynski C, Smith S B, Tinoco I and Bustamante C 2005 *Nature* **437** 231
- [15] Crooks G E 2000 *Phys. Rev. E* **61** 2361
- [16] Sekimoto K 1998 *Prog. Theor. Phys. Supp.* **130** 17
- [17] Chaichian M and A. Demichev A 2001 *Path integrals in Physics* (IOP Publishing, London)
- [18] Kirsten K and McKane A J 2003 *Ann. Phys. (N.Y.)* **308** 502
- [19] Palassini M and Ritort F 2011 *Phys. Rev. Lett.* **107** 060601

I.4 Conclusions

In the first of the two parts of this thesis, we have introduced the mathematical description of Markov processes, and discussed its relevance for stochastic thermodynamics, being the thermodynamics of nanoscopic systems in non-equilibrium.

We focused on continuous Markov processes, for which three equivalent descriptions were introduced, stochastic differential equations, the Fokker-Planck equation and Wiener path integrals. The embedding into discontinuous Markov process was carried out via the Kramers-Moyal expansion, with coefficients being directly related to the moments of the jump density which fixes the discontinuous component of the Markov process. Estimating the first two Kramers-Moyal coefficients from realisations of a Markov process yields a Fokker-Planck equation which approximately describes the Markov process, provided that the discontinuous component of the Markov process is negligible.

As a paradigm for thermodynamic interpretation of continuous Markov processes, we introduced the Langevin equation as a stochastic differential equation that models Brownian particles suspended in a fluid which experience molecular friction and thermal collisions while dragged through the fluid by an external force. The Brownian particles constitute a canonical ensemble, coupled to a heat bath at constant temperature being realised by the fluid. By examining the energy balance, we identified the work done by the external force and the heat dissipated into the fluid on the level of single trajectories of Brownian particles, including the first law relating work, heat and the internal energy difference between initial and final position of the particle.

Besides the first law, we also formulated the second law on the level of individual trajectories in terms of the total entropy production of particle and fluid. The total entropy production is the sum of the entropy difference between initial and final position of the particle plus the entropy produced in the fluid. Formulated as Wiener path integrals, the value of total entropy production proved to be a direct measure of irreversibility, in the sense that with increasing entropy production, the likelihood of concurrent trajectories that consume that entropy decreases exponentially

with that entropy production.

This relation between entropy production and irreversibility was shown to be quantitatively captured by fluctuation theorems which involve the exponential average of thermodynamic variables. Due to their relation to irreversibility, observing a convergence of the exponential average to the theoretical value implies that the ensemble of trajectories used for the exponential average include realisations that correspond to a time-reversal of the underlying dynamics. In other words, fluctuation theorems can be used to assess whether the stochastic dynamics of a system generates a subset of realisations that are typical for the reverse of that dynamics.

The connection to macroscopic thermodynamics was established by noting that using fluctuation theorems to estimate the lower bound of entropy production reproduces the second law.

Fluctuation theorems relate thermodynamic non-equilibrium quantities with equilibrium state variables. The prominent application of fluctuation theorems is therefore the recovery of free energy profiles from non-equilibrium measurements. The occurrence of reversed realisations in the non-equilibrium dynamics are crucial for the performance of these applications. If the non-equilibrium dynamics is known explicitly, we demonstrated that a asymptotic method is capable of assessing the reversed realisations in order to quantify the probability of these rare realisations and improve the recovery of free energy profiles.

As a special case of non-equilibrium states, we introduced non-equilibrium steady states which are possible for multidimensional dynamics or multiple heat baths. A non-equilibrium steady state is maintained by a non-conservative force which gives rise to an extra entropy production, which we introduced as the housekeeping entropy production. The housekeeping entropy production, the total entropy production and the difference between these two obey a fluctuation theorem, which in turn imply three faces of the second law. The irreversibility related to the housekeeping entropy accounts for the reversal of a current of particles or heat generated by non-conservative forces or multiple heat baths, respectively.

II Universal features of turbulent flows

Turbulent flows are omnipresent, ranging from the atmospheric boundary layer on large scales to applications like turbulent drag optimisation or turbulent mixing on small scales. The characterisation of intermittent velocity fluctuations is central in the majority of situations involving turbulent flows. Examples include predictions of extreme weather conditions, wind loads on buildings, air-planes, wind energy converters, site assessment for wind energy, turbulent mixing and combustion.

The introductory first chapter gives an account on basic aspects of fluid mechanics. In the second chapter, the idealised concept of fully developed turbulence is introduced, including established theories of fully developed turbulence which statistically approach the mentioned intermittent velocity fluctuations. The introduced approaches to turbulence can be recast as Markov processes, which is demonstrated in the third chapter. Section four and five exploit the consequences of fluctuation theorems and the asymptotic analysis developed in the first part. Finally, chapter six closes this part by classifying the discussed approaches to turbulence by their Markov representation and suggesting possible interpretations of the implications.

II.1 General theory

In this chapter we give a brief account on how the concepts of turbulence generation and energy transfer arise from fundamental considerations. The ruling equation for a viscid turbulent flow is the Navier-Stokes equation (NSE).

We briefly demonstrate in the first section II.1.1 how the NSE arises from Newton's equation of motion by discussing the forces that act on an infinitesimal fluid volume. Using the NSE, we show that an expression for the rate of energy dissipation in a turbulent flow can be derived. The second section II.1.2 explicates the generation of the highly irregular motion in a turbulent flow due to energy injection into the fluid, and addresses the applicability of statistical physics due to emerging degrees of freedom for increasing energy injection. In section II.1.3 we identify the mechanisms of energy transfer from large to small structures in a turbulent flow.

II.1.1 The Navier-Stokes equation (NSE)

The material of this section is adapted from the book by Landau and Lifshitz on fluid mechanics [10] and the book by Frisch on turbulence [108].

The motion of a fluid at position \mathbf{x} and time t is completely determined by the knowledge of fluid velocity $\mathbf{v}(\mathbf{x}, t)$, the fluid density $\varrho(\mathbf{x}, t)$ ¹³ and the pressure $p(\mathbf{x}, t)$. With the three components of velocity \mathbf{v} , the pressure p and the density ϱ , we have five quantities which have to be fixed by five equations to describe the motion of the fluid.

The first equation is the well known continuity equation

$$\frac{\partial \varrho(\mathbf{x}, t)}{\partial t} + \nabla \cdot (\varrho(\mathbf{x}, t) \mathbf{v}(\mathbf{x}, t)) = 0 \quad (\text{II.1.1})$$

as the consequence of conservation of mass.

The quantities fixed by the continuity equation are fluid velocity and density, the pressure field $p(\mathbf{x})$ does not enter. To formulate an equation including also $p(\mathbf{x})$, we make use of the fact that pressure gives rise to a force acting on a fluid volume, which allows us to set up Newton's equation of

¹³Quantities in this part of the thesis will be measured per unit mass.

II Universal features of turbulent flows

motion for a certain fluid volume. In differential form, this equation reads

$$\frac{\partial \mathbf{v}(\mathbf{x}, t)}{\partial t} + (\mathbf{v}(\mathbf{x}, t) \cdot \nabla) \mathbf{v}(\mathbf{x}, t) = -\frac{\nabla p(\mathbf{x})}{\varrho(\mathbf{x}, t)} \quad (\text{II.1.2})$$

and is known as the *Euler equation* ([10] p.4,14). The l.h.s. is the total time-derivative of $\mathbf{v}(\mathbf{x}, t)$, the r.h.s. is the acting force due to $p(\mathbf{x})$. The Euler equation includes three equations for each component of \mathbf{v} .

In the derivation of the Euler equation we did not include dissipation and transfer of energy. Therefore, the fluid motion takes place adiabatic, a requirement that constitutes the remaining fifth equation to fix all five quantities \mathbf{v} , ϱ and p .

Finally, the equations need to be supplemented with boundary conditions such as vanishing tangential velocity at confining walls.

The Euler equation describes inviscid fluids, that is, no molecular friction is taken into consideration. Accordingly, the kinetic energy of the fluid is conserved, and all processes in the fluid take place reversibly.

In a viscous fluid, molecular friction entails a dissipation of kinetic energy in form of heat, thus an irreversible process is added to the otherwise reversible processes of an inviscid fluid.

We now explicate the effect of taking viscosity into account. In a viscous fluid it can be shown that two more forces contribute to the equation of motion ([10] p.53f), namely

$$\mathbf{f}_1(\mathbf{x}, t) = \eta_1 \left(\Delta \mathbf{v}(\mathbf{x}, t) + \frac{1}{3} \nabla (\nabla \cdot \mathbf{v}(\mathbf{x}, t)) \right) \quad (\text{II.1.3a})$$

$$\mathbf{f}_2(\mathbf{x}, t) = \eta_2 \nabla (\nabla \cdot \mathbf{v}(\mathbf{x}, t)) \quad (\text{II.1.3b})$$

These forces simplify considerably for an incompressible fluid since then the velocity field $\mathbf{v}(\mathbf{x}, t)$ is divergence free. When dealing with liquid fluids, incompressibility can generally be assumed. Also a gaseous fluid can be assumed to be incompressible, as long as flow velocities stay well below the speed of sound.

Setting therefore $\nabla \cdot \mathbf{v}(\mathbf{x}, t) \equiv 0$ in (II.1.3) and including $\mathbf{f}_1(\mathbf{x}, t)$ into the Euler equation (II.1.2), we arrive at the so-called *Navier-Stokes equation* (NSE)

$$\frac{\partial \mathbf{v}(\mathbf{x}, t)}{\partial t} + (\mathbf{v}(\mathbf{x}, t) \cdot \nabla) \mathbf{v}(\mathbf{x}, t) = -\frac{1}{\varrho} \nabla p(\mathbf{x}) + \nu \Delta \mathbf{v}(\mathbf{x}, t) , \quad (\text{II.1.4})$$

governing the dynamics of a viscous, incompressible fluid. Here we defined the *kinematic* viscosity $\nu := \eta_1/\varrho$ (η_1 is called *dynamic* viscosity).

The convection term $(\mathbf{v} \cdot \nabla)\mathbf{v}$ couples the vector components of the NSE, as it couples the gradient of \mathbf{v} with all components of \mathbf{v} . It is due to this non-linear coupling of the vector components of (II.1.4) that makes an analytical solution of the NSE practically impossible. Furthermore, this non-linearity is responsible for a highly irregular and chaotic motion of the fluid, the very phenomenon which we call *turbulence*. On the other hand, we have the frictional force $\nu \Delta \mathbf{v}(\mathbf{x}, t)$ which damps this irregular motion and causes eventually a decay of turbulence. The higher the viscosity ν , the stronger the smoothing effect of friction. The interplay between the effects of the convection term and the frictional term governs the phenomenology of decaying turbulence.

To explore the effects of the frictional term, we examine the energy dissipation it provokes. To this end, we consider the total kinetic energy content of an incompressible fluid,

$$E_{\text{kin}} = \frac{\varrho}{2} \int v(\mathbf{x}, t)^2 \, d^3x . \quad (\text{II.1.5})$$

The time derivative of E_{kin} will include a term corresponding to energy flux, and another term accounting for dissipation of energy. To identify these contributions, we differentiate the integrand of E_{kin} , make use of the NSE (II.1.4) and obtain after some manipulations ([10] p.58f)

$$\frac{\partial}{\partial t} \frac{\varrho v(\mathbf{x}, t)^2}{2} = -\nabla \left[\varrho \mathbf{v}(\mathbf{x}, t) E(\mathbf{x}, t) - \mathbf{j}(\mathbf{x}, t) \right] - \varepsilon(\mathbf{x}, t) \quad (\text{II.1.6})$$

with the terms

$$E(\mathbf{x}, t) = \frac{\mathbf{v}(\mathbf{x}, t)^2}{2} + \frac{p(\mathbf{x})}{\varrho} , \quad (\text{II.1.7a})$$

$$j_k(\mathbf{x}, t) = \nu \sum_i v_i \left(\frac{\partial v_i(\mathbf{x}, t)}{\partial x_k} + \frac{\partial v_k(\mathbf{x}, t)}{\partial x_i} \right) , \quad (\text{II.1.7b})$$

$$\varepsilon(\mathbf{x}, t) = \frac{\nu}{2} \sum_{ik} \left(\frac{\partial v_i(\mathbf{x}, t)}{\partial x_k} + \frac{\partial v_k(\mathbf{x}, t)}{\partial x_i} \right)^2 . \quad (\text{II.1.7c})$$

The term $E(\mathbf{x}, t)$ is the local energy content which, multiplied with $\rho \mathbf{v}(\mathbf{x}, t)$ in (II.1.6), is the flux of energy due to motion of the fluid. As indicated by the dependence on viscosity ν , the terms $\mathbf{j}(\mathbf{x}, t)$ and $\varepsilon(\mathbf{x}, t)$ result from molecular friction. To tell the difference between $\mathbf{j}(\mathbf{x}, t)$ and $\varepsilon(\mathbf{x}, t)$, consider the integration of (II.1.6) over a certain volume. Applying Gauss's theorem, we see that the first term in (II.1.6) turns into a surface integral, accounting for the flux into and out of the volume, whereas the positive term $\varepsilon(\mathbf{x}, t)$ appears to represent a sink of energy in that volume. We therefore attribute $\varepsilon(\mathbf{x}, t)$ to energy dissipation due to molecular friction.

II.1.2 Turbulence generation and decay

Energy dissipation due to molecular friction is responsible for the decay of turbulence, as discussed in the previous chapter. In this chapter, we take into account the generation of turbulence, and relate it to the dissipation of kinetic energy.

Basically, turbulence is generated by imposing a certain initial condition on $\mathbf{v}(\mathbf{x}, t)$ which entails the highly irregular motion of a turbulent flow. Due to the frictional term in the NSE, the irregular motion will be smoothed out until the flow becomes laminar.

Practically, turbulence is forced by blocking a laminar flow with an obstacle, the wake of the obstacle is then a turbulent flow. This kind of turbulence generation is characterised by the incoming velocity v_{ch} of the laminar flow and a typical length scale ℓ_{ch} of the obstacle. Examples for ℓ_{ch} of obstacles are the diameter of a cylinder or the mesh size of a grid. A similar kind of turbulence generation are *free jets*, in which a flow is accelerated by directing it through a narrow nozzle, after which it hits a resting fluid. In this case, v_{ch} is typically taken to be the flow velocity at the nozzle and ℓ_{ch} the diameter of the nozzle.

In all cases, a stirring force is acting on the fluid implying an injection of turbulent energy into the fluid. The product of v_{ch} and ℓ_{ch} characterise the magnitude of this energy injection.

The form of the NSE (II.1.4) introduced in the previous chapter does not account for energy injection. We therefore augment the NSE with a

stirring force $\mathbf{f}(\mathbf{x}, t)$ and obtain the *forced* NSE

$$\frac{\partial \mathbf{v}(\mathbf{x}, t)}{\partial t} + (\mathbf{v}(\mathbf{x}, t) \cdot \nabla) \mathbf{v}(\mathbf{x}, t) = \nu \Delta \mathbf{v}(\mathbf{x}, t) - \frac{1}{\varrho} \nabla p(\mathbf{x}) + \mathbf{f}(\mathbf{x}, t) . \quad (\text{II.1.8})$$

The force $\mathbf{f}(\mathbf{x}, t)$ is usually assumed to be a random force with homogeneous, isotropic and stationary statistical properties. We do not need any more specifics on $\mathbf{f}(\mathbf{x}, t)$ as we are only interested in the mean energy injection caused by $\mathbf{f}(\mathbf{x}, t)$ ([108] p.77).

It is instructive to recast the forced NSE in dimensionless form, which we achieve by multiplying (II.1.8) with $\ell_{\text{ch}}/v_{\text{ch}}^2$ and obtain¹⁴

$$\frac{\partial \tilde{\mathbf{v}}(\tilde{\mathbf{x}}, \tilde{t})}{\partial \tilde{t}} + (\tilde{\mathbf{v}}(\tilde{\mathbf{x}}, \tilde{t}) \cdot \nabla) \tilde{\mathbf{v}}(\tilde{\mathbf{x}}, \tilde{t}) = \frac{1}{\text{Re}_{\text{ch}}} \Delta \tilde{\mathbf{v}}(\tilde{\mathbf{x}}, \tilde{t}) - \nabla \tilde{p}(\tilde{\mathbf{x}}) + \tilde{\mathbf{f}}(\tilde{\mathbf{x}}, \tilde{t}) \quad (\text{II.1.9})$$

where ∇ and Δ apply to $\tilde{\mathbf{x}}$, and we have defined the dimensionless number

$$\text{Re}_{\text{ch}} = \frac{v_{\text{ch}} \ell_{\text{ch}}}{\nu} \quad (\text{II.1.10})$$

which is known as *Reynolds number*.

Taking the viscosity as characteristic for the magnitude of energy dissipation, we may say that the Reynolds number relates the magnitude of energy injection with the magnitude of energy dissipation. It is furthermore evident from the dimensionless NSE (II.1.9) that Re_{ch} determines the impact of dissipation on the dynamics; for $\text{Re}_{\text{ch}} \rightarrow 0$ we get the forced version of the Euler equation (II.1.2). We will denote Re_{ch} also by Re .

The Reynolds number also has practical implications: If we aim at investigating the properties or effects of a turbulent flow on a too large scale to be done in a laboratory, we can instead set up a smaller version of the situation and rescale the results of the experiment according to the ratio of Reynolds numbers. The underlying concept is referred to as similarity principle ([10] p.67ff, [108] p.2).

There is no theorem that guarantees the existence and uniqueness of a solution of the NSE ([108] p.38). But a *stationary* solution of the NSE

¹⁴in terms of dimensionless quantities $\tilde{\mathbf{v}} = \mathbf{v}/v_{\text{ch}}$, $\tilde{\mathbf{x}} = \mathbf{x}/\ell_{\text{ch}}$, $\tilde{t} = t \cdot v_{\text{ch}}/\ell_{\text{ch}}$, $\tilde{p} = p \cdot \varrho/v_{\text{ch}}^2$,
 $\tilde{\mathbf{f}} = \mathbf{f} \cdot \ell_{\text{ch}}/v_{\text{ch}}^2$

in principle does exist for any reasonable flow situation ([10] p.114,131f). The stationary solution, however, will only be observable in reality if the solution is stable. A linear stability analysis shows that below a critical Reynolds number Re_{cr} , which is found to be of order 100, the stationary solution is insusceptible to small perturbations. This is reasonable, since small Reynolds numbers imply that molecular friction is predominant in the dynamics of the flow, and hence small perturbations are absorbed sufficiently fast. For $\text{Re}_{\text{ch}} \gtrsim \text{Re}_{\text{cr}}$, however, the flow becomes unstable when subjected to arbitrary small perturbations; ruling out the realisation of a stationary flow. The transition to an unstable flow for increasing Reynolds number can therefore be attributed to a magnitude of energy injection that is sufficiently larger than the magnitude of energy dissipation.

In the course of the stability analysis it turns out that with $\text{Re}_{\text{ch}} > \text{Re}_{\text{cr}}$, periodic modulations superimpose with the stationary solution of the flow. The frequencies and amplitude of the modulations are fixed by the perturbations, but the attendant phases enter the solution as additional degrees of freedoms which have to be fixed by extra initial conditions. Raising Re_{ch} well beyond Re_{cr} , more frequencies of broader range prevail in the flow involving an increasing number of degrees of freedoms.¹⁵ In addition to that, the flow becomes chaotic and therefore depends highly sensitively on the initial conditions.

The generation of additional degrees of freedom for Reynolds numbers $\text{Re}_{\text{ch}} > \text{Re}_{\text{cr}}$ in the flow allows for a close analogy to statistical physics: On the microscopic level, a macroscopic system has an immense number of degrees of freedom. If we were to predict the behaviour of the macroscopic object, it would be hopeless to do so by solving the equations of motion for each individual molecule. Instead it is feasible to consider the statistics of the degrees of freedom and extract integral values to describe the macroscopic system. The same applies for a flow at high Reynolds numbers. The attempt to solve the NSE would involve the knowledge of an immeasurable number of initial conditions, in extreme, the knowledge of position and velocity of all fluid molecules. But as the motion of flow is highly irregular and chaotic¹⁶, after a finite time any reference to the

¹⁵A dimensional analysis shows that the number of degrees of freedom in a turbulence flow scales with $(\text{Re}_{\text{ch}}/\text{Re}_{\text{cr}})^{9/4}$ ([10] p.139)

¹⁶it is indeed possible to recast the NSE as a dynamical system featuring high sensitivity to initial conditions

initial conditions would be lost. This renewal property provokes a random behaviour of flow properties which enables us to treat the flow velocity by statistical means, which will be the strategy in the following chapters.

II.1.3 Energy budget

We have argued that the Reynolds number relates energy injection with energy dissipation. It also seems likely that the immediate effect of energy injection is large scale motion, whereas molecular friction acts only on small scale motion. Taking ℓ_{ch} as the scale of the large scale motion, it stands to reason that the Reynolds number also relates the respective scales on which energy injection and molecular friction are acting, being in accord with the increasing range of frequencies prevailing in the flow for increasing Reynolds numbers as discussed in the previous section.

The impact of Re on the frequencies in the flow conveys an intuitive picture of energy injection and dissipation in the flow ([10] p. 134): Energy injection acts on small wavenumbers, heat dissipation takes place at large wavenumber. If we denote by k_{ch} the order of magnitude of wavenumbers influenced by energy injection and by k_{ν} the wavenumbers where energy is dissipated, we can expect that for sufficient high Reynolds numbers a range of wavenumbers $k_{\text{ch}} \ll k \ll k_{\nu}$ emerges in which neither energy injection nor dissipation has an influence. Consequently, in this range pure energy transfer from small to large wavenumbers must prevail.

The absence of forcing and dissipation reduces the forced NSE (II.1.8) to the Euler equation (II.1.2) in which we only have inertia terms, which is why the range of wavenumbers $k_{\text{ch}} \ll k \ll k_{\nu}$ is referred to as the *inertial range* ([108] p. 86). The transfer of energy to higher wavenumbers in the inertial range is known as *energy cascade*.

To further formalise the picture of subsequent injection, transfer and dissipation of energy, we define the mean energy injection rate

$$\mathcal{W}(t) = \varrho \int \mathbf{f}(\mathbf{x}, t) \cdot \mathbf{v}(\mathbf{x}, t) \, \text{d}^3x, \quad (\text{II.1.11})$$

and the mean energy dissipation rate as

$$\mathcal{E}(t) = \varrho \int \varepsilon(\mathbf{x}, t) \, \text{d}^3x \quad (\text{II.1.12})$$

with $\varepsilon(\mathbf{x}, t)$ given by (II.1.7c), as suggested by Frisch ([108] p. 18ff, 76ff). We then restrict our considerations to wavenumbers $k \leq K$ which we denote symbolically by an index K . For the energy transfer rate through wavenumber K we write $\Pi_K(t)$, we will come back to the explicit form of $\Pi_K(t)$ in a simplified setting in the next chapter.

Based on the forced NSE (II.1.8) and conservation laws for energy, momentum and helicity, and with E_{kin} given by (II.1.5), it is possible to formulate a cumulative energy flux equation in the form ([108] p. 25)

$$\partial_t E_{\text{kin},K}(t) = \mathcal{W}_K(t) - \mathcal{E}_K(t) - \Pi_K(t) . \quad (\text{II.1.13})$$

The statement of the equation is as follows: In the range of wavenumbers $k \leq K$, the kinetic energy carried by fluid elements is increased by injection of energy and decreased by dissipation and by transfer of energy to wavenumbers $k > K$.

We now successively simplify the cumulative energy flux equation by reasonable assumption. First, we restrict the energy injection \mathcal{W}_K to be time-independent. Consequently, after a sufficient amount of time, the flux of energy through wavenumbers will reach a steady state. In the steady state, the kinetic energy content of the flow will be constant for all K and the cumulative energy flux equation becomes

$$\mathcal{W}_K = \Pi_K + \mathcal{E}_K . \quad (\text{II.1.14})$$

Extending the wavenumber K to infinity, no transfer of energy to higher wavenumbers $k > K$ is possible, and we find

$$\mathcal{W}_\infty = \mathcal{E}_\infty =: \bar{\varepsilon} , \quad (\text{II.1.15})$$

where we defined the mean energy dissipation rate $\bar{\varepsilon}$, which due to energy conservation must equal the mean energy injection rate \mathcal{W}_∞ .

For wavenumbers in the inertial range, $k_{\text{ch}} \ll k \ll k_\nu$, we have $\mathcal{E}_k \approx 0$ and $\mathcal{W}_k = \mathcal{W}_\infty = \bar{\varepsilon}$, such that we find for the energy transfer rate

$$\Pi_k = \bar{\varepsilon} , \quad \text{for } k_{\text{ch}} \ll k \ll k_\nu . \quad (\text{II.1.16})$$

This equivalence between average energy transfer and energy dissipation will be useful in the next chapter. However, it should be kept in mind that Π_k and $\bar{\varepsilon}$ are quantities average over the fluid volume of consideration, the *local* versions $\Pi_k(\mathbf{x}, t)$ and $\varepsilon(\mathbf{x}, t)$ have to be distinguished.

II.2 Fully developed turbulence

So far, we kept our description on a rather general level. Imposing certain restrictions, an idealised picture of turbulence generation and decay emerges, which is referred to as fully developed turbulence, for which universal features of a statistical description may be expected. It are these universal features this chapter is devoted to.

We will begin in the first section with defining the assumptions that lead to fully developed turbulence, together with the conception of a statistical ensemble building the basis to address the phenomenology of fully developed turbulence by statistical means. In section II.2.2 we come back to the energy flux through wavenumbers discussed in the previous section. The last two sections will give an account on attempts to capture the universal features of fully developed turbulence that have been brought forward in the last 70 years.

II.2.1 Homogeneity, Isotropy, Stationarity

Shortly after the generation of turbulence, that is in closed distance to the obstacle, the flow field resembles the symmetries of the obstacle. As the turbulent flow develops further downstream, in a comoving frame the statistics of $\mathbf{v}(\mathbf{x}, t)$ restores the symmetries of the free NSE. These symmetries are homogeneity and isotropy. The freely decaying turbulence of such a homogeneous and isotropic flow far from boundaries is termed *fully developed turbulence*.

In addition to homogeneity and isotropy, we also assume that the generation and decay of turbulence has reached a steady state, as discussed in the context of the cumulative energy flux equation (II.1.13). The additional assumption of stationarity is crucial in constructing the statistical ensemble.

Statistical ensemble An intuitive understanding of fully developed turbulence is conveyed by an idealised experiment: Consider a closed sphere containing a fluid which we violently shake to stir that fluid. After we let the fluid rest shortly for a fixed time, we instantly measure the flow velocity far enough from the wall to preclude boundary effects, and thus yield the velocity field $\mathbf{v}(\mathbf{x})$. We repeat the experiment sufficiently often

to obtain a good statistics of the random field $\mathbf{v}(\mathbf{x})$ in the freely decaying turbulence, each sample at the same stage of the decay. Due to the symmetry of the set-up, the statistics of $\mathbf{v}(\mathbf{x})$ will be equal at each position \mathbf{x} and for each component of \mathbf{v} , it is hence sufficient to measure the magnitude of the velocity along an arbitrary symmetry axis to obtain $v(x)$. This is precisely what is meant by a homogeneous and isotropic flow field. We now transport this picture to the experimental realisations of turbulence generation explained in the previous chapter. The shaking of the sphere is realised by directing the laminar flow at an obstacle. The few seconds rest of the stirred fluid before the measurement is taken corresponds to let the flow evolve downstream and then measure the streamwise flow velocity $v(t)$ as it passes a measuring probe at fixed position. To convert the velocity signal $v(t)$ into a velocity field $v(x)$, we must avail ourselves of an approximation in which we use $x = \langle v(t) \rangle (t_f - t)$ with t_f being the length of the time signal¹⁷. The assumption underlying this approximation is that the time scale at which the “real” flow field $\mathbf{v}(\mathbf{x})$ evolves is sufficiently smaller than the timescale at which the flow field proceeds downstream. In other words, the changes in the flow field are so slow that it practically passes the measuring probe as an entity. This assumption is known as the *Taylor hypothesis of frozen turbulence* after G. Taylor [109] and has been well tested experimentally ([108] p. 58f). The Taylor hypothesis is assumed to hold true for $\langle (v - \langle v \rangle)^2 \rangle < 0.1 \langle v \rangle^2$.

Finally, the repetition of shaking and measuring to obtain an ensemble of flow field realisations $\{v(x)\}$ is simply achieved by recording one sufficient long velocity signal $v(t)$, rewrite it as a single velocity field $v(x)$ and then chop it into segments of a certain length L . In that sense, this experimental realisation continuously generates a turbulence flow, which we group into spheres of size L that proceed downstream. In the comoving frame and at sufficient distance to the position of turbulence generation, each sphere contains a sample of freely decaying, homogeneous and isotropic turbulence. By fixing the position at which we probe the flow velocity and by ensuring that the experiment is in a steady state, we always catch the same stage of decay of the generated turbulence.

¹⁷The coordinate systems points downstream. Accordingly, the “end” of the flow sample passes the probe first.

The above procedure is established practice to obtain $\{v(x)\}$ from a turbulent flow by experimental means. The remaining issue that needs clarification lies in choosing an appropriate value for the chopping length L . In the idealised experiment the largest coherent structure in each individual realisation $v(x)$ is of the order of magnitude of the diameter of the sphere. As a measure for the size of the largest coherent structures in the flow, we make use of the normalised autocorrelation function $R(r) = \langle v(x)v(x+r) \rangle / \langle v(x)^2 \rangle$ and choose for L the correlation length

$$L = \int_0^{\infty} R(r) \, dr \quad (\text{II.2.1})$$

which is known as the *integral length scale* [108–110]. Indeed, experiments show that L is in good agreement with the characteristic length ℓ_{ch} of the external forcing, being the counterpart of the sphere's diameter in the idealised experiment.

The notion of length scales leads us to revisit the picture of the energy cascade, which we discussed in terms of wavenumbers k in the previous chapter. The different values of the wavenumbers k are linked to eddies of various sizes $r \sim 1/k$, and the corresponding amplitudes account for the persistence of the respective eddies in the flow.

The energy cascade can then be perceived as follows: The external force acting on the flow results into coherent structures of dimension $L \sim 1/k_{\text{ch}}$ which may be taken as eddies of diameter L . Due to the inertia terms in the NSE (II.1.4), non-linear interaction causes the break-up of these eddies. As long as molecular friction is negligible, the ensemble of the resulting smaller eddies carry the same amount of energy as the ensemble of larger eddies they arose from. In the inertial range, this break-up of eddies repeats itself and thus transfers energy towards smaller scales. At some threshold $r = \lambda$, the molecular friction is no longer negligible, and for scales $r < \lambda$ dissipative effects emerge in addition to the non-linear interaction. While the break-up of eddies continues, molecular friction strengthens until eventually the input of energy from larger scales equals the dissipation of energy at a scale $r = \eta \sim 1/k_\nu$ ([108] p. 91f). For scales $r < \eta$ practically no eddies remain.

This phenomenological picture of cascading eddies is known as *Richardson*

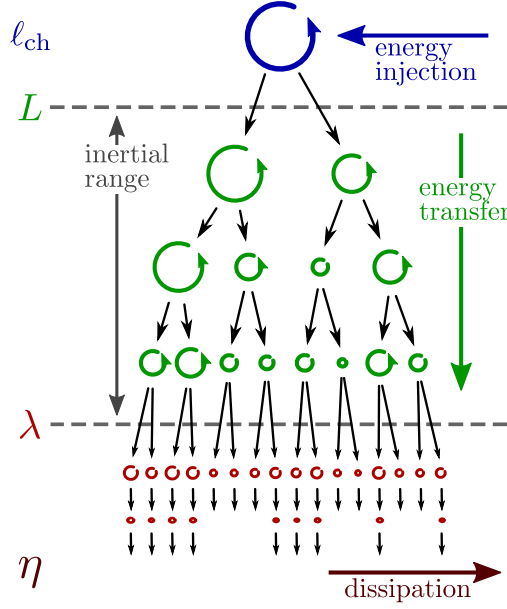


Figure II.1: Illustration of the Richardson cascade. Energy is injected by creation of eddies of size ℓ_{ch} , by repeated break-up of eddies this energy is transported in the inertial range, until it is eventually dissipated in the dissipative range. The integral length scale L and the Taylor microscale define the range of scale for which effects of energy injection and energy dissipation are negligible. The cascade ceases at the Kolmogorov dissipation scale η .

cascade [111, 112, 108]. However, we should keep in mind that the picture of eddies has its origin in the Fourier decomposition of the flow field and therefore is a merely conceptual picture.

The threshold λ is referred to as *Taylor microscale*, and the scale η is known as the *Kolmogorov dissipation scale*. The inertial range then is $L > r > \lambda$,¹⁸ and $\lambda \geq r \geq \eta$ is known as the *dissipative range*. See figure II.1 for an illustration of the Richardson cascade.

To define the Kolmogorov dissipation scale η , we redefine the *internal*

¹⁸By separation of turbulence generation and turbulence decay in experimental realisations, we can mitigate $k \gg k_{\text{ch}}$

Reynolds number as function of the scale r ,

$$\text{Re}_r := \frac{r v_r}{\nu} , \quad (\text{II.2.2})$$

where v_r denotes the typical velocity within eddies of size r . The *integral* scale Reynolds number $\text{Re}_L = Lv_L/\nu$ with $v_L = \langle v(t) \rangle$ is then of the same order of magnitude as the Reynolds number $\text{Re}_{\text{ch}} = \ell_{\text{ch}} v_{\text{ch}}/\nu$ defined in terms of characteristic quantities of the external forcing in (II.1.10). The scale where the dissipation of energy is in balance with input of energy from higher scales has an internal Reynolds number of one, we therefore define ν via $\text{Re}_\eta = \eta v_\eta/\nu = 1$ ([10] p. 134).

The Taylor microscale λ , which separates the inertial range $L > r > \lambda$ from the dissipative range $\lambda \geq r \geq \eta$, is defined by expanding the normalised autocorrelation function for small r [109],

$$R(r) = R(0) + \frac{r^2}{2} \frac{\partial^2 R(r)}{\partial r^2} \Big|_{r=0} + \dots , \quad (\text{II.2.3})$$

where the first order term vanishes because $R(r)$ is even, and then set λ such that $R(\lambda) = 1/2$,

$$\frac{1}{\lambda^2} := - \frac{\partial^2 R(r)}{\partial r^2} \Big|_{r=0} . \quad (\text{II.2.4})$$

The definition of the scales L and λ fixing the inertial range allows to formulate the inertial range condition in terms of the scale dependent Reynolds number Re_r as

$$\text{Re}_{\text{ch}} \gg \text{Re}_L > \text{Re}_r > \text{Re}_\lambda \gg 1 , \quad (\text{II.2.5})$$

where Re_r is defined in (II.2.2).

Before we proceed with the explicit statistical analysis of $\{v(x)\}$, we corroborate the assumption of homogeneity, isotropy and stationarity by the symmetries of free NSE without an external force term¹⁹ (II.1.4). We

¹⁹If the forcing respects these symmetries, then of course also the forced NSE (II.1.4) exhibits the symmetries.

express the symmetries in terms of invariances with respect to

$$\text{space-translations} \quad \mathbf{x} \quad \mapsto \mathbf{x} + \mathbf{x}', \quad (\text{II.2.6a})$$

$$\text{time-translations} \quad t \quad \mapsto t + t', \quad (\text{II.2.6b})$$

$$\text{rotations} \quad (\mathbf{x}, \mathbf{v}) \quad \mapsto (\mathbf{A}\mathbf{x}, \mathbf{A}\mathbf{v}), \quad (\text{II.2.6c})$$

$$\text{Galilean transformation} \quad (t, \mathbf{x}, \mathbf{v}) \mapsto (t, \mathbf{x} + \mathbf{v}'t, \mathbf{v} + \mathbf{v}'), \quad (\text{II.2.6d})$$

$$\text{scaling (for } \text{Re}_{\text{ch}} \rightarrow \infty) \quad (t, \mathbf{x}, \mathbf{v}) \mapsto (c^{1-h}t, c\mathbf{x}, c^h\mathbf{v}), \quad (\text{II.2.6e})$$

where \mathbf{A} is a rotation matrix, h a positive and c an arbitrary real number ([108] p. 17).

In general, a forcing of the flow breaks some or all of these symmetries. But due to the chaotic nature of the turbulent flow, the forcing loses quickly its influence and the above symmetries are restored as the flow proceeds downstream. In fact, the flow continues to be forced by integral scale motion of the fluid, but this internal forcing adopts the symmetries of the unforced NSE. In that sense, at the instance of turbulence generation, the integral scale Reynolds number equals the characteristic Reynolds number, $\text{Re}_L = \text{Re}_{\text{ch}}$, and decreases downstream due to turbulence decay. Hence, at sufficient distance to the turbulence generation and far from boundaries, it is justified to assume homogeneity and isotropy for the statistics of $\{\mathbf{v}(\mathbf{x})\}$, as long as Re_{ch} is large enough to guarantee a distinct regime to turbulence generation in which $\text{Re}_L \gg 1$.

Velocity increments With the above discussion we have established the conceptual basis for the statistical analysis of $\{v(x)\}$. In most of the cases, the statistical analysis is carried out either in terms of the spatial correlation tensor ([10] p. 140ff)

$$R_{ik}(\mathbf{r}; \mathbf{x}, t) = \langle v_i(\mathbf{x}, t) v_k(\mathbf{x} + \mathbf{r}, t) \rangle \quad (\text{II.2.7})$$

or by inspecting the moments of velocity increments projected on a unit vector \mathbf{e} ([108] p. 57ff)

$$S_u^n(\mathbf{r}; \mathbf{x}, \mathbf{e}, t) = \langle (\mathbf{e}\mathbf{v}(\mathbf{x} + \mathbf{r}, t) - \mathbf{e}\mathbf{v}(\mathbf{x}, t))^n \rangle, \quad (\text{II.2.8})$$

where the angular brackets denote an ensemble average over the samples $\{\mathbf{v}(\mathbf{x}, t)\}$.

We begin with a short discussion of the correlation tensor and demonstrate that both descriptions are in fact equivalent, and then focus on the analysis of velocity increments throughout the remaining part of this thesis.

The tensor $R_{ik}(\mathbf{r}; \mathbf{x}, t)$ can be diagonalised by choosing the coordinate system such that \mathbf{r} and the first component of \mathbf{x} point in the same direction. The diagonal entry R_{11} is then the *longitudinal* autocorrelation function in the direction of \mathbf{r} , and R_{22} and R_{33} are the *transversal* autocorrelation functions in the two perpendicular directions to \mathbf{r} . Owing to the assumed stationarity, homogeneity and isotropy of the statistics of the velocity field $\mathbf{v}(\mathbf{x}, t)$, we can restrict the arguments of $R_{ik}(\mathbf{r}; \mathbf{x}, t)$ to the absolute value of \mathbf{r} and drop the dependency on \mathbf{x} and t and simply write $R_{ik}(r)$.

Denoting the longitudinal component by $R_{\ell\ell}(r)$ and the two transversal components by $R_{tt}(r)$ and making use of the continuity equation, it can be shown that the longitudinal and transversal components are not independent but related by ([10] p. 142)

$$R_{tt}(r) = \frac{1}{2r} \frac{d(r^2 R_{\ell\ell}(r))}{dr} . \quad (\text{II.2.9})$$

It is therefore sufficient to analyse either the longitudinal or the transversal component. In view of the experimental procedure described above, the longitudinal component is the most common choice.

The same argumentation applies to the moments of the velocity increments, we therefore restrict ourselves to the longitudinal moments and write

$$S_u^n(r) = \langle (\mathbf{e}\mathbf{v}(\mathbf{x} + r\mathbf{e}, t) - \mathbf{e}\mathbf{v}(\mathbf{x}, t))^n \rangle . \quad (\text{II.2.10})$$

The underlying longitudinal velocity increments

$$u(r; \mathbf{x}, \mathbf{e}, t) := \mathbf{e} \cdot (\mathbf{v}(\mathbf{x} + r\mathbf{e}, t) - \mathbf{v}(\mathbf{x}, t)) \quad (\text{II.2.11})$$

of course still depend on \mathbf{x} , \mathbf{e} and t since stationarity, homogeneity and isotropy is only valid in the statistical sense, but for the sake of clarity we simply write $u(r) = u(r; \mathbf{x}, \mathbf{e}, t)$.

Denoting by $v_\ell(\mathbf{x}) = \mathbf{e}\mathbf{v}(\mathbf{x}, t)$ the longitudinal velocity component, we exemplify the equivalence of moments and correlation functions by means

of the structure function of second order

$$\begin{aligned}
 \frac{1}{2}S_u^2(r) &= \frac{1}{2} \left\langle (v_\ell(\mathbf{x} + r\mathbf{e}) - v_\ell(\mathbf{x}))^2 \right\rangle \\
 &= \frac{1}{2} \left\langle v_\ell(\mathbf{x} + r\mathbf{e})^2 - 2v_\ell(\mathbf{x} + r\mathbf{e})v_\ell(\mathbf{x}) + v_\ell(\mathbf{x})^2 \right\rangle \\
 &= \langle v_\ell^2 \rangle - \langle v_\ell(\mathbf{x} + r\mathbf{e})v_\ell(\mathbf{x}) \rangle \\
 &= \langle v_\ell^2 \rangle - R_{\ell\ell}(r) .
 \end{aligned} \tag{II.2.12}$$

The relation between moments and correlation functions of higher order can be derived along similar lines ([113] p. 20).

The n -th moment of velocity increments is usually referred to as the *structure functions of order n* ²⁰, indicating that the velocity increments address the spatial structure of the velocity field.

To obtain the structure functions from the ensemble $\{v(x)\}$, we simply apply the one-dimensional equivalent of (II.2.11),

$$u(r) = v(x+r) - v(x) , \tag{II.2.13}$$

to $\{v(x)\}$ for scales in the inertial range, $r = L..\lambda$, and end up with an ensemble $\{u(r)\}$. Evaluating the ensemble average in the one-dimensional version of (II.2.10) finally yields the structure functions,

$$S_u^n(r) = \langle (u(r))^n \rangle . \tag{II.2.14}$$

Note that by keeping $r > \lambda$, we can approximately assume that the samples $\{u(r)\}$ are sufficiently uncorrelated, as λ was defined in (II.2.4) as the distance in $v(x)$ for which correlations have considerably subsided. By taking only every second sample of $\{v(x)\}$ to obtain the ensemble $\{u(r)\}$, we would practically rule out any correlations, but it would also reduce the sample size by a factor two. In that sense, keeping $r > \lambda$ is a trade-off between uncorrelated samples and sample size.

II.2.2 Energy cascade

The energy cascade, that is the transfer of energy towards smaller scales due to repeated break-up of turbulent structures, is the central mechanism in fully developed turbulence. Having discussed the energy flux for

²⁰We will also say the n -th (order) structure function.

general turbulent flows in the first chapter, we will now address the energy cascade in terms of structure functions.

The four-fifths law Recall the cumulative energy flux equation in (II.1.13). In the subsequent discussion we found for a stationary energy flux a constant energy transfer rate $\Pi_k \equiv \bar{\varepsilon}$ in the inertial range, where $\bar{\varepsilon}$ is the mean energy dissipation rate. In the case of isotropic and homogeneous turbulence, it can be shown that Π_k can also be expressed in terms of the third order structure function ([108] p. 81),

$$\Pi_k = -\frac{1}{6\pi} \int_0^\infty \frac{\sin(kr)}{r} \left[(1 + r\partial_r)(3 + r\partial_r)(5 + r\partial_r) \right] \frac{S_u^3(r)}{r} dr . \quad (\text{II.2.15})$$

Hence, we expect a relation between $S_u^3(r)$ and $\bar{\varepsilon}$, which we are going to derive now.

To this end, we define the auxillary function

$$f(r) := \left[(1 + r\partial_r)(3 + r\partial_r)(5 + r\partial_r) \right] \frac{S_u^3(r)}{6\pi r} \quad (\text{II.2.16})$$

and use the dimensionless integration variable $z := kr$ to rewrite (II.2.15) as

$$\Pi_k = - \int_0^\infty \frac{\sin(z)}{z} f(z/k) dz . \quad (\text{II.2.17})$$

On the one hand, the amplitude of the oscillating function $\sin(z)/z$ rapidly decreases for increasing z , on the other hand, the argument $r = z/k$ of $f(z/k)$ changes only slowly for large k . In the limit of infinite Reynolds numbers, we can extent k to arbitrary large values without leaving the inertial range. We therefore take $f(z/k)$ as constant for the z values that contribute to the integral and demand ([108] p. 84ff)

$$f(r) \approx -\frac{2}{\pi} \bar{\varepsilon} \quad (\text{II.2.18})$$

to satisfy $\Pi_K = \bar{\varepsilon}$. The above condition constitutes an ODE for $S_u^3(r)$ and its solution reads

$$S_u^3(r) = -\frac{4}{5}\bar{\varepsilon}r + c_1r^{-a_1} + r^{-a_2}[c_2\cos(a_3\ln r) + c_3\sin(a_3\ln r)], \quad (\text{II.2.19})$$

where $a_1 \approx 0.75$, $a_2 \approx 1.1$, $a_3 \approx 2.0$ and c_1, c_2, c_3 are integration constants. In the limit $r \rightarrow 0$, the energy transfer rate must vanish, we therefore set all integration constants to zero and are left with

$$S_u^3(r) = -\frac{4}{5}\bar{\varepsilon}r, \quad \text{for } \lambda < r < L. \quad (\text{II.2.20})$$

This relation is known as Kolmogorov's *four-fifths law* [114] and is one of the most important results for fully developed turbulence. For homogeneous and isotropic turbulence and in the limit of infinite Reynolds numbers, it is an exact²¹ implication of the NSE (II.1.8) without any further assumptions ([108] p. 76ff). For sufficient high Reynolds numbers, the four-fifths law still holds in the inertial range which is often used to identify the inertial range in experimental data.

The fact that (II.2.20) is an exact result of the NSE awards the four-fifths law a special role: Every model of fully developed turbulence must obey (II.2.20) in the limit $\text{Re}_{\text{ch}} \rightarrow \infty$, or violate the assumptions of homogeneity and isotropy.

In his original derivation Kolmogorov actually found [114]

$$S_u^3(r) + \frac{4}{5}\bar{\varepsilon}r = 6\nu\frac{\partial S_u^2(r)}{\partial r} \quad (\text{II.2.21})$$

which is known as Kàrmàn-Howarth-Kolmogorov equation, as Kolmogorov built on results by von Kàrmàn and Howarth ([10] p. 140). This equation also holds for $r < \lambda$. For r in the inertial range, the second term is negligibly small ([10] p. 145), and we reproduce the four-fifths law.

Solved for $\bar{\varepsilon}$, (II.2.21) is a scale-resolved balance equation for the total energy dissipation, in which the term with $S_u^3(r)/r$ accounts for local energy transfer and $1/r\partial_r S_u^2(r)$ for local energy dissipation. Augmented with a term accounting also for energy injection, it is possible to examine the main contributions to the energy cascade for all scales r , see for instance the comprehensive article [115]. For completeness, we mention that

²¹The approximation of the integral (II.2.15) becomes exact for $k \rightarrow \infty$

(II.2.21) can be generalised to anisotropic turbulence ([108] p. 77).

The proportionality between $S_u^3(r)$ and $\bar{\varepsilon}$ has another implication: The signature of energy dissipation in the dissipative range is a negative skewness of the velocity increments. This connection might at first seem surprising, but it can qualitatively explained as follows. A negative skewness implies that the relative flow velocities at positions $x + r$ and x point more frequently in the opposed direction than in the same direction. This unbalance is assumed to be a signature of deforming turbulent structures; due to molecular friction, deformation goes with irreversible heat dissipation at small scales, slowing down the fluid motion. It is this irreversibility that makes the odds of observing the reversal of a compressing deformation smaller than the compression itself, which causes ultimately the excess of negative velocity increments in the statistics of $\{\mathbf{v}\}$. In the literature, the keyword that goes with this picture is *vortex stretching* (see, e.g., [108] p. 156 or [116] chapter 3.2).

To verify the four-fifths law by experimental means, we need to determine also $\bar{\varepsilon}$ from experimental data. Combining (II.1.7c) with (II.1.12) and (II.1.15), we find as an exact result of the NSE

$$\bar{\varepsilon} = \varrho \int \frac{\nu}{2} \sum_{ik} \left(\frac{\partial v_i(\mathbf{x})}{\partial x_k} + \frac{\partial v_k(\mathbf{x})}{\partial x_i} \right)^2 d^3x. \quad (\text{II.2.22})$$

Owing to homogeneity and isotropy this formula simplifies to the one-dimensional surrogate ([10] p. 142f)

$$\bar{\varepsilon} = \varrho \nu \int \sum_i \left(\frac{\partial v_i(\mathbf{x})}{\partial x_\ell} \right)^2 d^3x \approx 15\nu \left\langle \left(\frac{\partial v(x)}{\partial x} \right)^2 \right\rangle, \quad (\text{II.2.23})$$

where the last expression corresponds to an one-dimensional cut through the three-dimensional flow field ([113] p. 22). We mention that the reliability of the one-dimensional surrogate is under scrutiny [117].

Inverse energy cascade The energy dissipation rate $\varepsilon(\mathbf{x})$ has to be distinguished from the fluctuating rate of energy transfer throughout the cascade. Whereas $\varepsilon(\mathbf{x})$, as defined in (II.1.7c), is always positive, negative fluctuations of the energy transfer rate are known to be possible [118, 115].

On average, of course, we retain a positive energy transfer that must equal the energy dissipation. A negative energy transfer rate corresponds to an inverse energy cascade, that is to say, turbulent structures combine to larger structures and hence transfer energy to larger scales.

In two dimensional turbulence [119], the inverse energy cascade is known to be the dominant mechanism of energy transfer²² which is attributed to the natural alignment of eddies in the same plane, as vortices of equal orientation will coalesce [120, 121]; however, the precise mechanism responsible for the inverse energy cascade is subject to current research [122–124]. Under flow conditions that are reminiscent of two-dimensional turbulence, an inverse energy cascade is also observed in three-dimensional turbulence [125, 126] and is of great importance for geophysical fluid dynamics [123]. Recent results demonstrate that even full three-dimensional, homogeneous and isotropic turbulence always features a subset of non-linear evolution responsible for an inverse energy cascade [127, 128].

II.2.3 Scaling laws

We now turn to the universal features of turbulence, which manifest in scaling laws of the structure functions. The theory of fully developed turbulence has benefited a lot from dimensional analysis initiated by the work of Kolmogorov [129, 130, 114] and Obhukov [131, 132] in 1941. At this point, we will give a short survey of resulting scaling relations which will lead us to scaling laws proposed by Kolmogorov and others.

Dimensional analysis Starting point of the dimensional analysis is to deduce from the phenomenological picture of the Richardson cascade the physical quantities that affect the statistics of velocity increments $u(r)$ in the inertial range. We can rule out viscosity ν , and characteristic length scales and velocities associated with turbulence generation, as per definition effects of energy injection and dissipation are negligible in the inertial range. The only relevant energetic quantity in the inertial range is the energy transfer rate, which on average equals the mean energy dissipation

²²in addition to transfer of energy from forced scales to large scales comes a vorticity cascade from forced scales to small scales.

rate $\bar{\varepsilon}$. Hence, we are left with $\bar{\varepsilon}$, r and u as the relevant quantities in the inertial range. As u itself is zero on average, we inspect the second moment of u and find that, to respect the dimensions of the involved quantities, it can only be expressed in terms of $\bar{\varepsilon}$ and r by

$$\langle u^2 \rangle \sim \bar{\varepsilon}^{2/3} r^{2/3} . \quad (\text{II.2.24})$$

The above relation is known as Kolmogorov's *two-thirds law* [129].

Using (II.2.12), we can extract the r -dependency of the autocorrelation function, $R(r) \sim \text{const} - r^{2/3}$, from which we obtain by means of the Fourier transformation for the energy spectrum

$$E(k) = \frac{1}{2\pi} \int e^{ikr} R(r) \, dr \sim \bar{\varepsilon}^{2/3} k^{-5/3} \frac{1}{2\pi} \int e^{iy} \, dy \sim \bar{\varepsilon}^{2/3} k^{-5/3} , \quad (\text{II.2.25})$$

a prediction which proved to be particular well verified in experiments. In addition, Kolmogorov postulated that the constant of proportionality in (II.2.24) is universal and in his third paper from 1941 determined it to be $3/2$ using experimental measurements [114]. The constant of proportionality is now known as *Kolmogorov constant* C_2 and experimental results show that $C_2 \approx 1.9 \pm 0.2$ [133–135].²³

Applying the same dimensional arguments to the mean energy dissipation rate we find

$$\bar{\varepsilon} \sim \frac{u^3}{r} = \frac{u^2}{\tau} \quad (\text{II.2.26})$$

which is in agreement with the four-fifths law. The second relation follows by defining the *turn-over time* $\tau := r/u(r)$ which is the characteristic time scale within eddies of size r , suggesting that $\bar{\varepsilon}$ is the fraction of the kinetic energy u^2 available for energy transfer on scale r .

Finally, from analogous argumentation and combinations of above findings, we find for the Kolmogorov dissipation scale ([108] p. 91, [10] p. 138)

$$\eta \sim \left(\frac{\nu^3}{\bar{\varepsilon}} \right)^{1/4} , \quad (\text{II.2.27})$$

²³The Kolmogorov constant is often also defined as the constant of proportionality in the five-thirds law and then takes the value 0.53 ± 0.01 [136].

and that the relative size of the inertial range scales with the square root of the Reynolds number,

$$\text{Re}_{\text{ch}} \sim \left(\frac{L}{\lambda}\right)^2 \quad \text{or} \quad \text{Re}_{\text{ch}} \sim \left(\frac{L}{\eta}\right)^{4/3}. \quad (\text{II.2.28})$$

Kolmogorov scaling Observing a turbulent flow conveys an impression of *self-similarity*, that is to say, structures observed on a large scale L recur on smaller scales r in a similar fashion. Kolmogorov was led by the perception of cascading eddies proposed by Richardson [111], to consider, in the statistical sense, self-similarity for turbulent structures like eddies [129]. As the structure functions $S_u^n(r)$ are a statistical measure for structures in the flow, it stands to reason to postulate in the limit of infinite Reynolds numbers a *scaling law* of the form

$$S_u^n(r) = \left(\frac{r}{L}\right)^{\zeta_n} S_u^n(L) \propto r^{\zeta_n} \quad (\text{II.2.29})$$

with *scaling exponent* ζ_n to hold for all $r < L$. In words, the n -th moment of velocity increments on scale L has only to be multiplied with the scaling factor $(r/L)^{\zeta_n}$ to obtain the n -th moment on scale r .

In the simplest case, the scaling exponents account for the spatial dimensionality of the structures to be rescaled: The length of a line on scale L is simply multiplied with r/L to be reproduced on the smaller scale r , a surface needs to be multiplied with $(r/L)^2$, a volume with $(r/L)^3$. To obtain ζ_n for the structure functions in (II.2.29), we take from (II.2.26) the scaling of velocity increments as $u \sim (\bar{\varepsilon}r)^{1/3}$. Consequently, the scaling law (II.2.29) becomes

$$S_u^n(r) \sim \langle (\bar{\varepsilon}r)^{n/3} \rangle = \bar{\varepsilon}^{\zeta_n} r^{\zeta_n}, \quad \zeta_n = \frac{n}{3} \quad (\text{K41}) \quad (\text{II.2.30})$$

in accordance with Kolmogorov's works from the year 1941 ([108] p. 89ff); we will therefore refer to this scaling as *K41 scaling*.²⁴ Note that being a result of the dimensional analysis above, the K41 scaling $S_u^n(r) \propto r^{n/3}$ reproduces the two-thirds law (II.2.24) and the four-fifths law (II.2.26). Since the scaling $u \sim (\bar{\varepsilon}r)^{1/3}$ coincides with the scale-invariance property

²⁴Kolmogorov discussed in [114] only the structure functions of second and third order but seemed to be aware of the possible extension to arbitrary orders ([108] p. 97).

of the NSE (II.2.6e) for choosing $h = 1/3$, the scaling (II.2.30) should hold universally in the limit of infinite Reynolds numbers. Kolmogorov claimed furthermore that in this limit also the constant of proportionality in his two-thirds and four-fifths law are universal. Concerning this claim, Landau objected that $\varepsilon(\mathbf{x})$ is a strongly fluctuating quantity with considerable effects in the inertial range, the use of its average $\bar{\varepsilon}$ in (II.2.30) and the claim of its universality is therefore not justified ([10] p. 143, [108] p. 93ff, [115]). However, as already mentioned above, the constants of proportionality appear indeed to be universal [136, 115].

It took 21 years until Kolmogorov resumed the question of an universal scaling law and incorporated fluctuations of $\varepsilon(\mathbf{x})$ into the scaling ansatz (II.2.29) [112]. He based his derivation on the suggestion by Obukhov [137] to use a local average of the energy dissipation rate,

$$\varepsilon_r(\mathbf{x}) := \frac{3}{4\pi r^3} \int_{|\mathbf{x}-\mathbf{x}'| \leq r} \varepsilon(\mathbf{x}') \, d^3x', \quad (\text{II.2.31})$$

instead of the overall mean $\bar{\varepsilon}$. The idea is again that the local energy dissipation $\varepsilon_r(\mathbf{x})$ on scale r also fixes the energy transfer rate on that scale. To include the fluctuations of $\varepsilon_r(\mathbf{x})$ into the analysis, Obukhov argued further that $\varepsilon_r(\mathbf{x})$ should follow a log-normal distribution due to the following phenomenological picture ([108] p. 171ff, [113] p. 24ff):

In view of the Richardson cascade, the energy transfer towards smaller scales is realised by the break-up of eddies. Let us single out one of the smaller eddies on scale r . Its energy is a fraction h_1 of the energy of the larger eddy it emerged from. This larger eddy itself received a fraction h_2 of energy from an even larger eddy, and so on. We can therefore trace back that the energy of our small eddy on scale r has derived from the energy ε_0 of a mother eddy. Thus, the energy that is to be dumped on scale r can be written as $\varepsilon_r(\mathbf{x}) = \varepsilon_L(\mathbf{x}) \prod_j h_j$. Considering the logarithm of the dissipation rate, $\ln \varepsilon_r(\mathbf{x}) = \ln \varepsilon_L(\mathbf{x}) + \sum_j \ln h_j$, and owing to the central limit theorem, the random variable $\ln \varepsilon_r(\mathbf{x})$ should be approximately normal distributed, if the number of cascade steps is large enough. Obukhov therefore claimed that $\varepsilon_r(\mathbf{x})$ is distributed according to the log-normal

distribution

$$p(\varepsilon_r) = \frac{1}{\sqrt{2\pi\sigma_r^2\varepsilon_r^2}} \exp \left[-\frac{(\ln(\varepsilon_r/\bar{\varepsilon}) + \sigma_r^2/2)^2}{2\sigma_r^2} \right] \quad (\text{II.2.32})$$

such that the mean of ε_r is $\bar{\varepsilon}$. The remaining freedom in this model is the standard deviation σ_r , for which Kolmogorov and Obukhov assumed

$$\sigma_r^2(\mathbf{x}) = A(\mathbf{x}) + \mu \ln(L/r) , \quad (\text{II.2.33})$$

accounting for the increasing variance of energy transfer fluctuations towards the end of the cascade. The increase of energy transfer fluctuations can indeed be observed in experiments [115]. Furthermore, the logarithm in (II.2.33) ensures that the moments of $p(\varepsilon_r)$ obey a scaling law,

$$\begin{aligned} \langle \varepsilon_r(\mathbf{x})^n \rangle &= \left(\frac{r}{L} \right)^{\frac{\mu n}{2}(1-n)} e^{\frac{A(\mathbf{x})}{2}n(n-1) + n\bar{\varepsilon}} \\ &\propto r^{\frac{\mu n}{2}(1-n)} . \end{aligned} \quad (\text{II.2.34})$$

The constant μ is called *intermittency factor*, for reasons we will come to shortly, and is, due to the scale-invariance (II.2.6e), assumed to be universal. The universality of μ has indeed been proved well by experiments and it is found to be $\mu \approx 0.26$ [138]. The function $A(\mathbf{x})$ was meant to weaken the previous claim of universal constants of proportionality in the K41 theory, but has no influence on the scaling exponents.

Replacing the mean value $\bar{\varepsilon}$ by ε_r to take into account the scale-dependent fluctuations of the energy transfer and making use of the scaling (II.2.34) of the moments of ε_r , we arrive at the *K62 scaling*

$$S_u^n(r) \sim \langle (\varepsilon_r r)^{n/3} \rangle \sim r^{\zeta_n} , \quad \zeta_n = \frac{n}{3} + \frac{\mu}{18}(3n - n^2) \quad (\text{K62}) . \quad (\text{II.2.35})$$

The K62 model is also often referred to as the *log-normal model*.

Compared to the K41 scaling (II.2.30), the K62 scaling exponents are most notably not linear but have a term quadratic in n . The quadratic term provokes that ζ_n becomes a decreasing function in n for $n > (6 + 3\mu)/(2\mu) \approx 11$ and eventually turns negative. This behaviour

of ζ_n is commonly considered as unphysical due to two reasons. First, it can be shown that a decreasing ζ_n can not be reconciled with the incompressibility assumption in the derivation of the NSE, and second, the form of ζ_n violates the so-called Novikov inequality [139] valid for fully developed turbulence in the limit $\text{Re} \rightarrow \infty$ ([108] p. 172f). By substituting $n = 3$, we see that the K62 scaling respects the four-fifths law (II.2.20), whereas the two-thirds law (II.2.24) receives a minor correction, $S_u^2(r) \sim r^{2/3-\mu/9}$ where $\mu/9 \approx 0.03$. This correction applies analogously to the five-thirds law (II.2.25).

We mention that scaling exponents that depart from the K41 scaling are also called *anomalous* scaling exponents, and the deviation $\mu/9 \approx 0.03$ is often referred to as the anomaly parameter.

The K41 scaling only holds for the structure function of second and third order ([108] p. 91), whereas the K62 scaling agrees well with experimental results up to order of about eight ([108] p. 132). The incorporation of violent small-scale fluctuations of energy transfer hence improved the probabilistic description of extreme velocity fluctuations considerably. Note that in the case of K62 scaling, the limit $\text{Re} \rightarrow \infty$ is essential for the central limit theorem to be applicable, since we see from (II.2.28) that large Reynolds numbers imply a large inertial range, which in turn ensures a large number of steps in the cascade of eddies.

II.2.4 Small-scale intermittency

The K62 scaling belongs to the class of random cascade models. These models share the idea of Kolmogorov and Obhukov that due to repeated break-up of coarse structures into finer structures, fluctuations of the energy transfer at large scales entail rampant fluctuations of energy transfer and dissipation at small scales ([108] p. 165ff). These strong energetic fluctuations at small scales cause similar strong velocity fluctuations at small scales, a phenomenon known in turbulence research as *small-scale intermittency*. Random cascade models are just one of many attempts to incorporate small-scale intermittency into the description of small-scale turbulence.

Small-scale intermittency is widely considered to be one of the most challenging and intriguing phenomena in turbulence [140]. Small-scale intermittency is particularly pronounced in atmospheric turbulence [141–143],

and is also of importance in technical application, examples include turbulent mixing and combustion [144, 145], but also for loads on wind energy converters [146–150] and other constructions exposed to extreme weather conditions.

The term intermittency refers to short bursts of high activity in an otherwise moderately fluctuating signal. There are many ways to formally define intermittency. One is to take the fluctuations of a signal $f(t)$ and inspect the kurtosis of these fluctuations. A signature of intermittency is that the kurtosis exceeds considerably a value of three, which is the kurtosis of a Gaussian distribution. Or more specific, to accommodate in particular that intermittent bursts are short, after cutting out frequencies higher than a certain cut-off frequency, the kurtosis of the resulting signal should grow unbounded with this cut-off frequency ([108] p. 120). Regarding velocity fluctuations in a turbulent signal $v(t)$, it is common to change to the spatial domain by use of the Taylor hypothesis and inspect the distribution of velocity increments u on various scales r . The signature of small-scale intermittency are then *heavy tails* of the distribution $p(u, r)$, i.e. towards small scales the frequency of large velocity increments exceed any Gaussian prediction. According to the above discussion of the strong fluctuations of energy dissipation, there is no doubt that $p(u, r)$ will develop heavy tails when the scale r tends to zero. On the other hand, the frictional forces at very small scales will eventually damp down all intermittent fluctuations. The more intriguing question therefore is, how far does the intermittent behaviour extend into the inertial range. See figure II.2 for a typical signature of small-scale intermittency in $p(u, r)$.

The reason to use the rather qualitative criterion of heavy tails is that it accounts for all high order structure functions $S_u^n(r)$, which in turn are characterised by scaling laws (II.2.29) and in particular by the presumably universal scaling exponents ζ_n . Hence, a physical model for small-scale turbulence which predicts ζ_n that are consistent with all available theoretical and experimental results would be a great step towards understanding the mechanism responsible for small-scale intermittency in any turbulent flow. The K41 scaling, for instance, predicts a Gaussian form of $p(u, r)$ in the inertial range which clearly conflicts with the features of intermittency. Corrections to the K41 scaling law are therefore called *intermittency corrections*, of which the K62 scaling is just one example. Other approa-

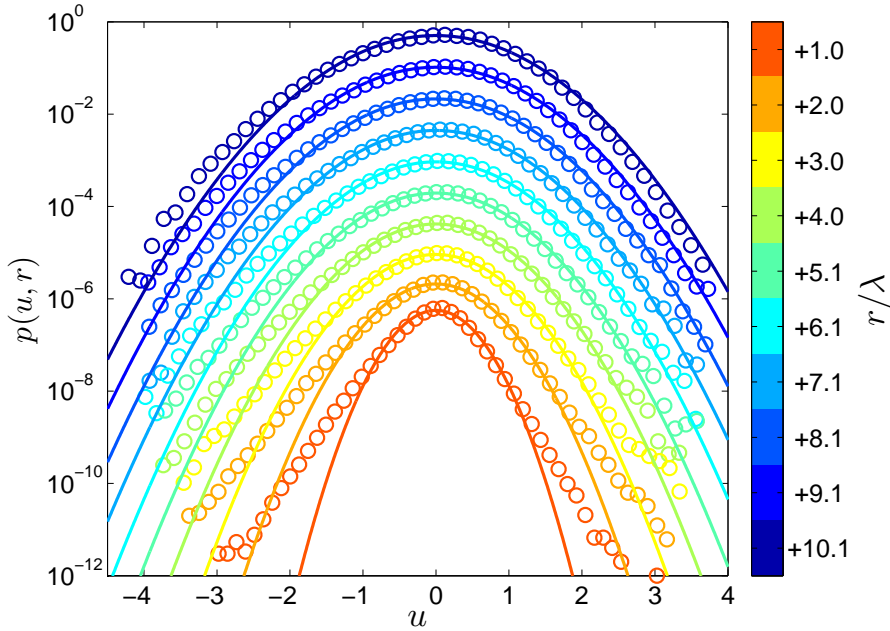


Figure II.2: Small-scale intermittency. The symbols are histograms for velocity increments $u(r)$ computed from the data used in [110] for various scales r covering the whole inertial range. Gaussian fits are included to emphasise the heavy tails towards smaller scales. Note also the negative skewness apparent on all scales. The PDFs $p(u, r)$ are shifted vertically for the sake of clarity.

ches apart from K62 include the β -model, multifractal models, non-linear scaling exponents, and, going beyond the scaling approach, extended self-similarity, random cascade models and Burger's turbulence. In this section, we will briefly introduce these approaches.

We note that, however, our discussion is by no means complete. For a broader overview we recommend chapter 8 and 9 of the book by Frisch [108], which includes a discussion of the mentioned fractal models and random cascade models, large deviation theory, shell models, dynamical systems, field theoretic approaches, functional and diagrammatic approaches, the closure problem of the averaged NSE, multiscale methods and renormalisation groups. In addition, the overview article by Sreenivasan and Antonia [140] primarily addresses scaling phenomenology, multifrac-

tality and kinematics of small-scale structures, and the review by Biferale [151] is devoted to shell models.

Modifications of scaling laws The β -model takes into account that turbulent structures can not be as space-filling as the structures they evolved from [152], that is, the ensemble of non space-filling structures does not occupy the full space with dimension $d = 3$, but instead a subspace of fractal dimension $d = d_{\text{fr}} < 3$. The consequence is that the scaling of extensive quantities (such as energy) is corrected by the volume-fraction $(r/L)^{3-d_{\text{fr}}}$. In terms of the scale-invariance (II.2.6e), we then have $h = 1/3 - (d_{\text{fr}} - 3)/3$ which results into the linear scaling

$$\zeta_n = \frac{n}{3} + (3 - d_{\text{fr}})\left(1 - \frac{n}{3}\right) \quad (\beta\text{-model}) , \quad (\text{II.2.36})$$

consistent with experimental results up to an order of about six ([108] p. 135ff).

The notion of fractals in the β -model has initiated *multifractal models* in which the cascade of eddies takes place in fractal subspaces of \mathbb{R}^3 with fractal dimensions $d_{\text{fr}} < 3$ [153–159], see also p. 143ff in [108]. The multifractality is then expressed by a continuous superposition of scaling laws, each of which featuring a scaling exponent $h_{\text{min}} < h < h_{\text{max}}$ and valid in a subspace of fractal dimension $d_{\text{fr}}(h)$. In contrast to pure scaling in the form (II.2.29), the multifractal model puts forward a *spectrum* of scaling laws. In the limit $r \rightarrow 0$, however, the method of steepest decent relates scaling exponent ζ_n and fractal dimension d_{fr} via a Legendre transformation, where a special choice of $d_{\text{fr}}(h)$ reproduces the K62 model. Therefore, the K62 model is also referred to as a multifractal model. In that sense, the β -model generalises the K41 model and the multifractal model the K62 model by inclusion of non space-filling turbulent structures at small scales.

As an illustrative example for fractal subspaces, *vortex filaments* may be named [118, 160], see also p. 184ff in [108]. Vortex filaments are basically long and thin swirls, their diameter is of the order of the Kolmogorov dissipation scale η and their extension can reach the integral length scale L . As filaments, their fractal dimension is close to one.

The role that vortex filaments play for the statistics of velocity increments, in particular for small-scale intermittency, is an objective of current research [161–163]. In the course of these efforts, She and Leveque proposed in

[164] a phenomenological characterisation of the energy dissipation field, itemised into an hierarchy of fluctuating structures ranging from the mean dissipation rate $\bar{\varepsilon}$ on the largest scale to the intermittent impact of vortex filaments on the smallest scale. Upon coarse-graining the dissipative scales to inertial range scales, they predict the universal scaling law,

$$\zeta_n = \left(1 - \frac{C_0}{3}\right) \frac{n}{3} + C_0 \left(1 - \beta^{\frac{n}{3}}\right). \quad (\text{II.2.37})$$

Here, $C_0 = 3 - d_{\text{fr}}$ is the codimension of the dominant intermittent structures, and the intermittency parameter β accounts for intermittency strength as it varies from one to zero. She and Leveque determined from their theory that $\beta = 2/3$. Note that K41 scaling is recovered if we set $\beta = 1$ and codimension $C_0 = 0$. Taking $d_{\text{fr}} = 1$ for vortex filaments and $\beta = 2/3$, the SL scaling exponents become

$$\zeta_n = \frac{n}{9} + 2 \left(1 - (2/3)^{\frac{n}{3}}\right) \quad (\text{SL}), \quad (\text{II.2.38})$$

which She and Leveque claim to hold universally. Indeed, the agreement with experimental data is excellent, which is remarkable considering the phenomenological nature of this proposal and that it goes without any adjustable parameters. The phenomenological model giving rise to (II.2.38) can also be formulated as a random cascade model with Poissonian distributed multipliers and is therefore also called log-Poisson model [165, 166].

Another approach to model small-scale intermittency was proposed by L'vov and Procaccia [167, 168], in which they address the n -point correlation function

$$R_n(r_1, r_2, \dots, r_n) = \langle u(r_1)u(r_2) \cdots u(r_n) \rangle \quad (\text{II.2.39})$$

where all $L > r_i > \lambda$. For the special case that all $r_1 = r_2 = \dots = r_n \equiv r$, the n -point correlation function becomes the n -th order structure function $S_u^n(r) = \langle u(r)^n \rangle$.

Two hypotheses of Kolmogorov type form the basis of the analysis of $R_n(r_1, \dots, r_n)$. The first hypothesis states that the correlation functions are homogeneous functions with scaling exponents ζ_n ,

$$R_n(cr_1, cr_2, \dots, cr_n) = c^{\zeta_n} R_n(r_1, r_2, \dots, r_n), \quad (\text{II.2.40})$$

which is the analogue of proposing scaling laws for structure functions. The second hypothesis addresses universality, in the sense that velocity increments in the inertial range are not correlated with the velocity increments on the scale of turbulence generation. A precise formulation of this hypothesis is given by the discussion of equation (3) in [167].

The proposal of L'vov and Procaccia involves multipoint correlation functions that are intermediate between the extremes $R_n(r_1, \dots, r_n)$ and $S_u^n(r)$. More precisely, they consider the case in which the scales (r_1, r_2, \dots, r_n) can be grouped into p small scales $(r_1, \dots, r_p) \sim r_0$ and $n-p$ larger scales $L > (r_{p+1}, \dots, r_n) \gg r_0$ and then propose that the full correlation function factorises into the intermediate p -point correlation function

$$R_p(r_1, \dots, r_p) = \langle u(r_1) \cdots u(r_p) \rangle \quad (\text{II.2.41})$$

with scaling exponent ζ_p and a homogeneous function $\Psi_{n,p}(r_{p+1}, \dots, r_n)$ with scaling exponent $\zeta_n - \zeta_p$,

$$R_n(r_1, r_2, \dots, r_n) = R_p(r_1, r_2, \dots, r_p) \Psi_{n,p}(r_{p+1}, r_{p+2}, \dots, r_n) . \quad (\text{II.2.42})$$

where the function $\Psi_{n,p}(r_{p+1}, \dots, r_n)$ derives from the underlying equations of motions, in this case the NSE or adequate models of turbulence. In the limit that $r_1 \simeq r_2 \simeq \dots \simeq r_p$, the intermediate correlation function becomes the structure function $S_u^p(r)$. Instead of two groups of scales, an arbitrary number of groups can be constructed, where each group is associated with an intermediate correlation function, only the group of the largest scales enters in terms of a homogeneous function Ψ . The relations that govern this kind of coalescence of scales into groups are known as *fusion rules* from which various scaling relations can be determined. A simple example of such a scaling relation has been verified experimentally [169, 170] and reads

$$R_{pq}(r_1, r_2) = \langle u(r_1)^p u(r_2)^q \rangle \sim \frac{S_p(r_1)}{S_p(r_2)} S_{p+q}(r_2) \quad (\text{II.2.43})$$

where $L > r_2 > r_1 > \lambda$.

In [171], L'vov and Procaccia use fusion rules in a diagrammatic perturbation theory that builds on the NSE in the limit of infinite Reynolds numbers. They use as a small parameter the anomaly parameter

$\delta_2 := \zeta_2 - 2/3 \approx 0.03$, and find in second order of δ_2 ,

$$\zeta_n = \frac{n}{3} - \frac{n(n-3)}{2} (\delta_2 + 2\delta_2^2(n-2)b) \quad (\text{LP}) \quad (\text{II.2.44})$$

with parameter $b \approx -1$.²⁵ Choosing $\delta_2 = 0$, we obtain the K41 scaling as it should be. The first order correction in δ_2 recovers the K62 scaling, and the second order introduces to ζ_n a cubic term in n . The main advantage over K62 is that ζ_n does not become negative for large n . Compared to the K62 scaling exponents, the agreement between the LP ζ_n above and experimental results improves for $n \geq 8$.

Extended self-similarity There is no doubt that Kolmogorov's four-fifths law must hold within the bounds of the assumption made in the derivation, as it has been derived from the full three dimensional NSE. Still, experimental data often satisfies the four-fifths law rather approximately. Deviation from the four-fifths law can accordingly only be attributed to non-compliance of the assumptions made in the derivation and experimental imperfections ([108], p. 129ff), including i) remaining inhomogeneities and anisotropy, ii) not negligible molecular friction (i.e. no clear-cut crossover from inertial to dissipative range), iii) uncertainties in the determination of $\bar{\varepsilon}$, iv) unjustified use of the Taylor hypothesis.

The fit of scaling exponents in the inertial range suffers from the same impairments as the verification of the four-fifths law. In addition to that, the structure functions of order six and higher exhibit undulations, of which the origin remains rather unclear. An improvement in the determination of the scaling exponents from experimental data can be achieved by a method known as *extended self-similarity* (ESS) by Benzi et al. [173]. In this method, instead of the structure functions itself, the ratio to the third structure function, $S_u^n(r)/S_u^3(r)$, are used to fit the scaling exponents.²⁶ The crucial assumption is that the above mentioned impairments affect all moments in a similar manner. The ESS method accounts for these

²⁵Renner and Peinke found that $b = -3/4$ is consistent with the scaling exponents implied by Yakhot's model which we introduce below. [172]

²⁶Instead of $S_u^3(r)$ any other structure function could be used here. But the fact that $S_u^3(r) \sim r$ makes $S_u^3(r)$ a reasonable choice.

imperfections as it introduces a correction to pure scaling in the form

$$S_u^n(r) \propto [S_u^3(r)]^{\zeta_n}. \quad (\text{ESS}) \quad (\text{II.2.45})$$

For the case of perfect measurements of ideally developed turbulence in the limit $\text{Re}_{\text{ch}} \rightarrow \infty$, we would recover the pure scaling behaviour discussed in the previous section. In that sense, ESS allows a determination of the scaling exponents ζ_n minus the effects induced by the mentioned impairments. In their investigations, Benzi et al. even presented convincing experimental evidence that the validity of ESS extends considerably far into the dissipative range.

Random cascade models The two main assumptions in setting up the K62 model were (i) the log-normal distribution for the local averaged energy dissipation ε_r and (ii) a standard deviation σ_r of the log-normal distribution that scales with $\ln r$. The log-normal distribution resulted naturally from the perception of a multiplicative cascade of eddies, whereas $\sigma_r \sim \ln(L/r)$ was a mere pragmatic assumption to retain the scaling law for the structure functions. This has led Castaing and co-workers to explore the r -dependency of σ_r experimentally [116], and they found that ε_r is indeed log-normal distributed, but that a scaling law for the variance of the log-normal distribution,

$$\sigma_r^2 = c_\sigma \left(\frac{r}{L} \right)^{-\beta}, \quad (\text{II.2.46})$$

is in better agreement with their measurements than the logarithmic dependency used in the K62 model. In addition, they were able to show that this power law results from applying an extremum principle to the probability of ε_r . The parameter β is found to be dependent on Re and not universal; for the measurements discussed in [116], $\beta \approx 0.3$.

The moments of ε_r become

$$\langle \varepsilon_r^n \rangle = \exp \left[c_\sigma \frac{n(n-1)}{2} \left(\frac{r}{L} \right)^{-\beta} + n\bar{\varepsilon} \right] \quad (\text{II.2.47})$$

and the K62 scaling (II.2.35) changes into

$$S_u^n(r) \sim \langle (\varepsilon_r r)^{\frac{n}{3}} \rangle \sim r^{\frac{n}{3}} e^{\frac{c_\sigma n(n-3)}{18} \left(\frac{r}{L} \right)^{-\beta}}. \quad (\text{II.2.48})$$

The authors of [116] also explored the consequence for the PDF of velocity increments, $p(u, r)$, on the basis of two assumptions. Their first assumption is that for a fixed value of ε , the velocity increments are normal distributed,

$$p(u|\varepsilon) = \frac{1}{\sqrt{2\pi}\sigma_\varepsilon} \exp \left[-\frac{u^2}{2\sigma_\varepsilon^2} \right]. \quad (\text{II.2.49})$$

Motivated by the scaling relation $\sigma \sim (\varepsilon r)^{1/3}$ and the log-normal model, the second assumption is that the standard deviation σ_ε is log-normal distributed

$$p(\sigma_\varepsilon, r) = \frac{1}{2\pi\Lambda_r^2} \exp \left[-\frac{(\ln(\sigma_\varepsilon/\sigma_0))^2}{2\Lambda_r^2} \right], \quad (\text{II.2.50})$$

where the variance Λ_r^2 is typically of the form (II.2.46). Both assumptions are well corroborated by their measurements.

Combining (II.2.49) and (II.2.50) yields the distribution

$$p(u, r) = \frac{1}{2\pi\Lambda_r} \int_0^\infty \exp \left[-\frac{u^2}{2\sigma_\varepsilon^2} \right] \exp \left[-\frac{(\ln(\sigma_\varepsilon/\sigma_0))^2}{2\Lambda_r^2} \right] \frac{d\sigma_\varepsilon}{\sigma_\varepsilon^2} \quad (\text{II.2.51})$$

which is a superposition of normal distributions and involves the free parameters σ_0 and Λ_r .

The normal distribution in (II.2.52) causes $p(u, r)$ to be even in u which contradicts the four-fifths law (II.2.20). To overcome this shortcoming, the normal distribution is augmented with a phenomenologically motivated skewness correction, and (II.2.52) becomes

$$p(u, r) = \frac{1}{2\pi\Lambda_r} \int_0^\infty \exp \left[-\frac{u^2}{2\sigma_\varepsilon^2} \left(1 + a_s \frac{u/\sigma_\varepsilon}{\sqrt{1+u^2/\sigma_\varepsilon^2}} \right) \right] \times \exp \left[-\frac{(\ln(\sigma_\varepsilon/\sigma_0))^2}{2\Lambda_r^2} \right] \frac{d\sigma_\varepsilon}{\sigma_\varepsilon^2} \quad (\text{II.2.52})$$

with the skewness parameter $a_s \approx -0.18$ claimed to be universal.

The parameter Λ_r accounts for the fluctuations of energy transfer on scale r and is therefore a quantity of interest in itself. Accordingly, the important result of [116] is not so much the explicit form of $p(u, r)$ in (II.2.52),

but rather to obtain A_r by fitting (II.2.52) to experimentally determined $p(u, r)$. As already mentioned, they found that A_r is well described by the power law in (II.2.46), for which $p(u, r)$ from (II.2.52) is in excellent agreement with measurements.

In the sequel of this article by Castaing and co-workers, their model has been cast in a more general formalism. Models using this formalism are known as *random cascade models* or *processes* ([108] p. 165) and have been widely used [165, 174–176, 138, 177–180]. In random cascade models, multipliers $h < 1$ are used to express the statistics of velocity increments on scales $r < L$ as $u = hu_L$. The multipliers are assumed to be a random variable and follow a scale dependent PDF $G_{rL}(\ln h)$, also referred to as a propagator. The propagator $G_{rL}(\ln h)$ then defines the PDF of velocity increments via a superposition of scaled PDFs $p_L(u/h)$ on the integral scale L [175],

$$p(u, r) = \int G_{rL}(\ln h) p_L\left(\frac{u}{h}\right) \frac{d \ln h}{h} . \quad (\text{RCM}) . \quad (\text{II.2.53})$$

The above prescription of how random multipliers determine the distribution of velocity increments at scales $r < L$ is the essence of random cascade models. The *randomness* enters through the random variable h , and the association with a *cascade* originates from writing the propagator as a convolution [175]

$$G_{rL}(\ln h) = \int G_{rr_1}(\ln h_1) G_{r_1L}(\ln h - \ln h_1) d \ln h_1 \quad (\text{II.2.54})$$

with the intermediate scale $L > r_1 > r$ and multiplier h_1 to express the statistics of velocity increments on scale r_1 as $u_1 = h_1 u_L$. Instead of only one intermediate scale r_1 , it is of course possible to set up $G_{rL}(\ln h)$ as a convolution of a series of intermediate scales $L > r_1 > r_2 > \dots > r$, and the connection to a cascade becomes obvious.

In view of (II.2.53), various special cases are included in the formalism of random cascade models.

(i) For the simplest choice, $G_{rL}(\ln h) = \delta(\ln h - \ln h_{rL})$, and assuming a normal distribution for $p_L(u)$, the PDF $p(u, r)$ will be Gaussian for all scales r which is the signature of the K41 model. In other words, for multipliers that are not random, the K41 model is recovered.

(ii) By taking for $G_{rL}(\ln h)$ a log-normal distribution with a variance $\Lambda_r \sim \ln(r/L)$, the PDF $p(u, r)$ develops the non-Gaussian tails known from small-scale intermittency. The structure functions exhibit a scaling law with scaling exponents of K62 form (II.2.35). This not surprising, as in the similar fashioned derivation of the K62 scaling we used the log-normal distribution (II.2.32) with variance (II.2.33).

(iii) Sticking to the log-normal distribution but taking a variance that is not proportional to $\ln(L/r)$, we abandon a scaling law and the r -dependence of the variance determines the function of r that supersedes the r in r^{ζ_n} . The PDF $p(u, r)$ will take the form (II.2.52) and the link to the afore introduced model by Castaing is established.

(iv) In [165, 166] it has been shown that by using for $G_{rL}(\ln h)$ a log-Poisson distribution instead of the log-normal distribution, the statistics of velocity increments exhibit the SL scaling law (II.2.38) proposed by She and Leveque. The expectation of the log-Poisson distribution is related to the logarithm of the local energy transfer. The connection between log-Poisson statistics of energy transfer and the scaling exponents proposed by She and Leveque is intriguing, since Poisson distributions are the natural distributions in the context of rare events [165]. Consider, for instance, the binomial distribution which gives the probability of success for n independent trials, where each trial has probability p_s for success and probability $1 - p_s$ for failure. For finite p_s but $n \rightarrow \infty$, the binomial distribution approaches the normal distribution. Whereas $p_s \rightarrow 0$ (indicating rare events) and $n \rightarrow \infty$ such that np_s stays finite is the limit of the Poisson distribution. In that sense, the log-Poisson model accounts for rare realisations of the cascade process, whereas the log-normal model concerns typical realisations. The experimentally demonstrated supremacy of the scaling exponents arising from the log-Poisson model over the exponents from the log-normal model also for high orders of structure functions hence suggests that the cascade process is dictated by rare events.

(v) In general, cascade models are closely related to the notion of fractals. Therefore, random cascade models are often combined with multifractal models and vice versa [153, 154, 158].

Burger's turbulence and Galilean invariance Polyakov and Yakhot were able to derive a partial differential equation for the distribution of

velocity increments, $p(u, r)$, in a field theoretic approach to turbulence [181, 182]. They explicitly take into account the effect of the large scale parameters $v_{\text{rms}}^2 = \langle (v - \langle v \rangle)^2 \rangle$ and ℓ_{ch} . In the limit of small scales $r \ll \ell_{\text{ch}}$ and increments $u \ll v_{\text{ch}}$, they recover a scaling law.

Starting point of their considerations is the Burgers' equation, an one-dimensional NSE without the pressure term,

$$\dot{v}(x, t) + v(x, t) v'(x, t) = \nu v''(x, t) . \quad (\text{II.2.55})$$

The Burger's equation is a fundamental partial differential equation in mathematics and well studied and therefore often serves as a basis of models for turbulence.

To introduce the external force responsible for turbulence generation, the Burgers' equation is typically augmented with a white noise random force

$$\begin{aligned} \dot{v}(x, t) + v(x, t) v'(x, t) &= \nu v''(x, t) + f(x, t) \\ \langle f(x, t) f(x', t') \rangle &= \kappa(x - x') \delta(t - t') , \end{aligned} \quad (\text{II.2.56})$$

where the spatial correlation function $\kappa(x - x')$ depends on the details of turbulence generation and is generally assumed to act only on large scales. Polyakov used in [181] the notion of a generating functional $\mathcal{Z}[\omega(\cdot)]$ where $\omega(x, t)$ is conjugate to velocity $v(x, t)$. By substituting the above forced Burgers' equation and applying field theoretic techniques (operator product expansion), he derives a partial differential equation for $\mathcal{Z}[\omega(\cdot)]$ for a steady energy flux and in the limit $\text{Re} \rightarrow \infty$. His result also explicitly includes large scale properties in form of the root-mean-square fluctuations of velocity, v_{rms} , which allows to incorporate different flow conditions and leads to intermittency corrections to K41 scaling. But this comes at the price of the breakdown of the Galilean invariance (II.2.6d) for the equations for $\mathcal{Z}[\omega(\cdot)]$, all other symmetries of the NSE (II.2.6) are respected.

Permitting the breakdown of Galilean symmetry is the marking distinction of this approach compared to other field-theoretical attempts to account for intermittency corrections of scaling exponents. Preserving the Galilean invariance and recovering the K41 model is particular delicate in functional approaches to a field-theoretic description of turbulence ([108] p. 215).

However, the model by Polyakov does not account for the influence of pressure. Resuming the work by Polyakov, Yakhot was able to include the

influence of pressure to the model by making use of the three-dimensional Gaussian forced NSE [182]. He further derived from the augmented equations for $\mathcal{Z}[\omega(\cdot)]$ the following partial differential equation for the PDF of velocity increments

$$-\frac{\partial(u\partial_r p(u, r))}{\partial u} + B \frac{\partial p(u, r)}{\partial r} = -\frac{A}{r} \frac{\partial(u p(u, r))}{\partial u} + \frac{v_{\text{rms}}}{\ell_{\text{ch}}} \frac{\partial^2(u p(u, r))}{\partial u^2} . \quad (\text{II.2.57})$$

Note that the flow parameters v_{rms} and ℓ_{ch} explicitly enter the equation. To explore the consequence of his theory for scaling laws, Yakhot derived from the above equation the corresponding equation for the structure functions,

$$\frac{\partial S_u^n(r)}{\partial r} = \frac{An}{n+B} \frac{S_u^n(r)}{r} + \frac{v_{\text{rms}}}{\ell_{\text{ch}}} \frac{n(n-1)}{n+B} S_u^{n-1}(r) , \quad (\text{II.2.58})$$

and substituted $S_u^n(r) = c_n r^{\zeta_n}$ to get

$$\zeta_n = \frac{An}{B+n} + \frac{r}{\ell_{\text{ch}}} \frac{v_{\text{rms}}}{c_n/c_{n-1}} \frac{n(n-1)}{B+n} r^{\zeta_{n-1}-\zeta_n} \quad (\text{YAK}) . \quad (\text{II.2.59})$$

The last term with prefactor r/ℓ_{ch} takes effects of energy injection explicitly into account. To resort to scales r where energy injection has no effect, that is assuming $r \ll \ell_{\text{ch}}$, Yakhot obtained

$$\zeta_n = \frac{An}{B+n} , \quad r \ll \ell_{\text{ch}} . \quad (\text{II.2.60})$$

In this limit the four-fifths law must hold and it follows for $n = 3$,

$$A = \frac{B+3}{3} . \quad (\text{II.2.61})$$

Demanding that the moment equation (II.2.58) implies $S_u^3(\ell_{\text{ch}}) \equiv 0$ and using $c_2 = C_2 \bar{\varepsilon}^{2/3}$ with Kolmogorov constant $C_2 \approx 2$ predicts a value of $B \approx 20$. In the limit $B \rightarrow \infty$, the K41 scaling is recovered, and maximum intermittency is obtained for $B = 0$.

With the numerical value $B \approx 20$ and A given by (II.2.61), the scaling

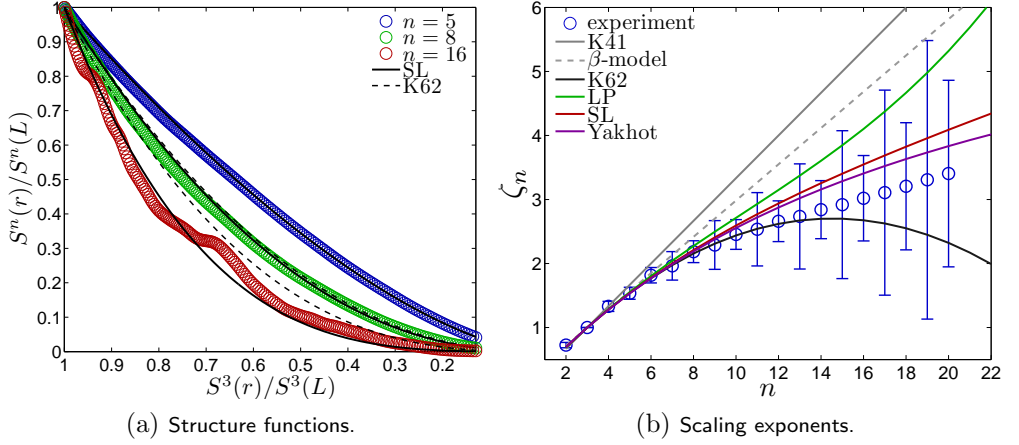


Figure II.3: Comparison of various theoretical predictions of scaling exponents with an experimental result using ESS. The experimental data consists of about 10^7 realisations $u(r)$ and is the same as used in [110] and figure II.2. The scaling exponents were obtained from fitting the structure functions shown in (a) to the ESS formula (II.2.45), the error bars are the standard deviations of the ζ_n determined from 10^3 blocks of 10^4 realisations $u(r)$. The scaling laws for the K62 model, (II.2.35), and suggested by She and Leveque (SL), (II.2.38), are included in (a). The resulting scaling exponents are shown in (b), which also includes the scaling exponents for the K41 model from (II.2.30), the β -model from (II.2.36), the scaling exponents derived by L'vov and Procaccia in (II.2.44) and the scaling exponents in (II.2.60) implied by Yakhots model. For the β -model the fractal dimension $d_{\text{fr}} = 2.85$ is used, for the K62 model the intermittency factor $\mu = 0.23$ and for the LP scaling exponents the parameter $b = -0.75$ as suggested in [172]. The K41 scaling, the SL scaling and the scaling suggested by Yakhot are parameter-free.

exponents (II.2.60) resulting from Yakhot's model for the scaling in the inertial range agree remarkably well with experimental data. See figure II.3 for a comparison of the scaling laws discussed in this section together with an experimental result using ESS.

In [183], Yakhot was able to extend his model such that also transversal velocity increments are taken into account, and he generalised the formulation to two-dimensional turbulence. In the extended form, the formalism of Yakhot's model can be used to demonstrate that ESS is a consequence of the NSE [184], and to predict that for large n the scaling exponents

ζ_n are asymptotically a linear function of n [185] as is the case for fractal models of turbulence and the SL scaling exponents (II.2.38). Indeed, in [186], the connection between Yakhot's model and multifractal models of turbulence is demonstrated.

In [172], Renner and Peinke pointed out that expansion of the scaling exponent (II.2.60) reproduces the scaling exponents (II.2.44) determined by L'vov and Procaccia, where the small parameter of the expansion was chosen to be $\delta_2 = \zeta_2 - 2/3$ as in (II.2.44) but with ζ_2 taken from (II.2.60),

$$\zeta_n = \frac{n}{3} \frac{2 + 3\delta}{2 + 3(n-2)\delta} = \frac{n}{3} - \frac{n(n-3)}{2} (\delta_2 + 2\delta_2^2(n-2)b) \quad (\text{II.2.62})$$

with $b = -3/4$ in agreement with $b \approx -1$ as predicted by L'vov and Procaccia.

II.3 Markov analysis

Having introduced the relevant results of fully developed turbulence for what follows in the remaining part of the thesis, let us take one step back and relate this part with the first part of the thesis.

We started the first part with Newton's equation of motion for Brownian particles and ended up with an intimate relation between entropy and irreversibility at the nanoscale. This part, we also started with Newton's equation of motion, but for fluid volumes. We worked us through various assumptions and concepts to arrive at a statistical description of velocity fluctuations in fully developed turbulence. Overall, the analysis for both cases involved exploring the balance between external energy injection and internal heat dissipation. The microscopic mechanism for heat dissipation traces back to non-zero viscosity both for Brownian particles and for decaying turbulence. By including the dynamics of Brownian particles on a time scale smaller than the Markov-Einstein time scale t_{ME} into an ideal heat bath, and likewise, by limiting ourselves in the case of decaying turbulence to the inertial range where dissipative effects are negligible, we coarse grained in both cases the microscopic dynamics to obtain a mesoscopic description of the physics.

In this part we attempt to push this analogy further and explore the implications of describing the statistics of velocity increments $u(r)$ as realisations of a MP.

II.3.1 Interpretation as stochastic process

As for the scaling law in the previous section, we can again say that the following approach uses the phenomenology of the Richardson cascade. The idea is that the eddy which evolved from a larger eddy bears no reference to that larger eddy after sufficient time. The concept of self-similarity conveys the same picture, as each eddy, regardless on its stage in the cascade, initiates its own cascade. In other words, by observing a cascade, it is not possible to decide whether it is the whole cascade or only a part of a larger cascade.

This perception – an eddy determines the next smaller eddy directly and the subsequent eddies only indirectly – suggests that the cascade of eddies is a MP. In terms of velocity increments u on scales r we can state the

II Universal features of turbulent flows

Markov assumption as follows: During the cascade process, an eddy of size L breaks into an eddy of size $g_1 L$ with fraction $0 < g_1 < 1$. The break-up of the smaller eddy results into an eddy of size $g_1 g_2 L$ where g_2 is independent from g_1 . Repeating this operation, we write the scale as $r = g_1 g_2 \dots g_{s(r)} L$, where $s(r)$ specifies the number of stages the cascade has to go through until it arrives at the scale r . Expressed on a logarithmic scale, we get $\ln r = \ln L + \ln g_1 + \ln g_2 + \dots + \ln g_{s(r)}$, or by assuming for the sake of clarity that all fractions are equal, $g_i \equiv g_0$,

$$\ln(L/r) = s(r) \ln(1/g_0) > 0 . \quad (\text{II.3.1})$$

Solving for the cascade stage yields

$$s(r) = \frac{\ln(r/L)}{\ln g_0} . \quad (\text{II.3.2})$$

We apply the same argument to the velocity increments as they evolve down the cascade, that is $u_r = h_1 h_2 \dots h_{s(r)} u_L$, and obtain

$$\ln(u_L/u_r) = s(r) \ln(1/h_0) , \quad (\text{II.3.3})$$

where $h_i \equiv h_0$ determines the fraction of velocity that an eddy receives from the eddy it evolved from. Solving for $w_r := \ln(u_r/u_L)$ yields

$$w_r = s(r) \ln h_0 \quad (\text{II.3.4})$$

which relates the logarithmic velocity increment w_r to the cascade stage $s(r)$ on scale r . Note that $\ln u_r \sim \ln r$ from (II.3.4) and (II.3.2) is in agreement with the scaling-invariance (II.2.6e). By considering $w(r) = \ln(u(r)/u_L)$ as a function of r and differentiating (II.3.4) with respect to r , we finally arrive at the ODE

$$\begin{aligned} -\frac{\partial_r u(r)}{u(r)} &= -\partial_r s(r) \ln h_0 = -\frac{\ln h_0}{\ln g_0} \frac{1}{r} , \quad a := \frac{\ln h_0}{\ln g_0} \\ \Rightarrow \quad \partial_r u(r) &= a \frac{u(r)}{r} , \quad u(L) = u_L . \end{aligned} \quad (\text{II.3.5})$$

The solution of this initial value problem is a scaling law

$$u(r) = u_L (r/L)^a . \quad (\text{II.3.6})$$

In these considerations, we only considered the velocity increments at single cascade stages and ignored the dynamics between these stages. In principle, the dynamics between the stages is deterministic and dominated by the non-linear terms of the NSE, but of course we can not take this dynamics explicitly into account. Instead, we make use of the chaotic property of a turbulent flow which implies that the outcome of each turbulent structure evolving to the next stage of the cascade exhibits a certain randomness. In the spirit of the log-normal model, we add the random variable $Z(s(r))$ with amplitude w_0 to the logarithmic velocity increments in (II.3.4),

$$w(r) = s(r) \ln h_0 + w_0 Z(s(r)) . \quad (\text{II.3.7})$$

We define $Z(s(r))$ as the outcome of the cumulated randomness in the cascade up to stage s , where random variables q_i account for the (logarithmic) velocity fluctuations at each stage. As in the log-normal model, we refer to the central limit theorem and infer that the cumulative random variable $Z(s(r))$ is normal distributed. The statistical properties of $Z(s(r))$ can readily be determined to be

$$\langle Z(s(r)) \rangle = \sum_{i=1}^{s(r)} \langle q_i \rangle = 0 , \quad (\text{II.3.8a})$$

$$\langle Z(s(r))^2 \rangle = \sum_{i,j=1}^{s(r)} \langle q_i q_j \rangle = \sum_{i,j=1}^{s(r)} \delta_{ij} = s(r) . \quad (\text{II.3.8b})$$

Here, we assumed in the first line that the fluctuations q_i are zero on average, and in the second line we used the Markov assumption that there are no correlations between the stages of the cascade.

To proceed, we write (II.3.8) as the continuous approximation

$$Z(s(r)) = \int_0^{s(r)} q(x) \, dx \quad (\text{II.3.9})$$

and require $\langle q(x)q(x') \rangle = \delta(x - x')$ to retain $\langle Z(s(r))^2 \rangle = s(r)$ as in (II.3.8b). The differentiation of (II.3.7) with respect to r now yields

$$\begin{aligned} -\frac{\partial_r u(r)}{u(r)} &= -\frac{a}{r} - \frac{w_0}{r \ln g_0} q(s(r)) , \quad b := -\frac{w_0^2}{2 \ln g_0} > 0 \\ \Rightarrow -\partial_r u(r) &= -a \frac{u(r)}{r} + \sqrt{2b \frac{u(r)^2}{r}} \xi(r) , \quad u(L) = u_L , \end{aligned} \quad (\text{II.3.10})$$

where the minus sign before ∂_r accounts for $dr < 0$ and we defined the new random variable $\xi(r) := q(s(r))/\sqrt{-r \ln g_0}$ such that the stochastic integral of $\xi(r)$ has the usual properties as in (A.1.11), which will allow us in the next section to identify drift and diffusion for an equivalent formulation with the corresponding FPE (cf. the transformation rule for the independent variable in (A.2.8)).

We stress, however, that the continuous approximation (II.3.9) involving $\xi(r)$ implies an infinitely divisible cascade process [166], otherwise $\xi(r)$ is not δ -correlated. Only for differences in scales that exceed the typical scale-interval covered by one cascade step, $\ln(r/r') > \ln(1/g_0)$, we can assume that the correlation $\langle \xi(r)\xi(r') \rangle \rightarrow 0$ vanishes. Solving (II.3.10) yet for arbitrary scales hence implies infinite many cascade stages, an assumption that is justified in the limit $\text{Re} \rightarrow \infty$.

From the mathematics presented in I.1.1 it is clear that (II.3.10) is a stochastic differential equation (SDE), and as such needs completion by specifying the rule of discretisation. In the derivation of (II.3.10) we clearly distinguished the deterministic and stochastic origin. Following van Kampen (cf. p. 15), we therefore identify $\sqrt{bu^2/r}\xi(r)$ as external noise for which the mid-point rule should be taken [19, 5, 4], which comes with the convenience that we do not have to bother with modified calculus.²⁷

We observe that on the logarithmic scale $s(r)$ the stochastic process defined by (II.3.10) is in fact nothing else then geometric Brownian motion (GBM) discussed as example in I.1 and A.1. We will discuss the solutions

²⁷In principle, any other discretisation is possible, but then we have to make sure to modify the rules of calculus accordingly. In the case of the pre-point rule, for instance, we would need to replace ordinary calculus by Itô calculus and use the Itô lemma for the variable transformation $s(r)$. The resulting SDE would then have to be interpreted in Itô, and manipulations of the SDE have to comply with Itô calculus. Furthermore, the coefficients of the SDE would loose their physical meaning.

of the above SDE in the following section.

The phenomenology of the calculation presented in this section is the essence of random cascade model [187, 188, 153], see also p. 165ff in [108]. The connection of random cascade models to a SDE has been first discussed by She in [166] for the log-Poisson model (II.2.38) and picked up by others [189, 190, 179, 178, 191]. We will come back to the relation between random cascade models and SDEs in more detail in the next section.

We explicate the analogy to Brownian motion:

The exact process of collisions between Brownian particles and the fluid molecules is coarse grained by considering only the random outcome of the collisions. The energy injection by the random force is provided by an ideal heat bath which models the kicks received by the Brownian particle from the fluid molecules. The interpretation of the ideal heat bath is the essential ingredient in the thermodynamic interpretation of the MP accomplished in chapter I.2.

In the case of a turbulent cascade, the velocity fluctuations throughout the cascade is a result of the energy injection on large scales and the subsequent transfer of energy to smaller scales due to the non-linear interaction of fluid elements. In the SDE (II.3.10), the energy injection is realised by randomising u_L , and the stochastic term $b\sqrt{u^2/r}\xi(r)$ accounts for the fluctuations in velocity that result from the transfer of energy to scale r . The energy dissipation at small scales does not enter this model which hinders a thermodynamic interpretation. But the exclusion of dissipation effects in the Markovian description of the cascade suggests that the Markov condition can only be met at scales where dissipative effects are negligible. Indeed, in chapter II.3.3 we will see that the Markov assumption holds for $r > r_{\text{ME}} \approx \lambda$, where r_{ME} is the spatial analog of the Markov-Einstein time scale t_{ME} discussed after (I.1.78).

The SDE (II.3.10) further constitutes a prescription to artificially generate realisations $u(\cdot)$. In the limit $\text{Re} \rightarrow \infty$, in which $\lambda \rightarrow 0$, we could compose a flow field $v(x)$ by connecting the realisations $u(\cdot)$ in series. We hence obtain an ideal flow field $v(x)$ that respects the characteristics of the cascade process introduced above, ideal in the sense that $\text{Re} \rightarrow \infty$.

We mention that it should be kept in mind that a realisation $u(\cdot)$ is not one specific cascade of one eddy. Instead, a large ensemble of realisation

$u(\cdot)$ reflects the statistics caused by the cascade. Considering $u(r)$, we just probe the spatial structures of the flow field being composed of cascades, without being able to pick out a certain cascade.

II.3.2 Drift and diffusion

We have seen in the previous section that a log-normal random cascade model can be represented by a SDE. Formulating the process as a SDE implies the definition of drift and diffusion coefficients $D^{(1)}(u, r)$ and $D^{(2)}(u, r)$. In this section, we will explore the representation of the approaches to turbulence, which we introduced in II.2, in terms of $D^{(1,2)}(u, r)$.

Kolmogorov scaling For the cascade model (II.3.4) without stochasticity, we already found the scaling (II.3.6) implying the following scaling law for the structure functions

$$S_u^n(r) = \langle u_L^n \rangle \left(\frac{r}{L} \right)^{\zeta_n}, \quad \zeta_n = n \frac{\ln h_0}{\ln g_0}. \quad (\text{II.3.11})$$

It is apparent that $g_0 = h_0^3$ recovers the K41 scaling (II.2.30). If we want to formulate this model in terms of a stochastic process, we can set

$$D^{(1)}(u, r) = -\frac{1}{3} \frac{u}{r}, \quad D^{(2)}(u, r) \equiv 0 \quad (\text{K41}), \quad (\text{II.3.12})$$

where the only randomness arises from drawing the initial value u_L from a distribution $p_L(u)$.

By including stochasticity in the cascade model, we found the Stratonovich SDE (II.3.10). Integration of this SDE yields (see appendix A.1, applying ordinary calculus)

$$\frac{u(r)}{u_L} = \left(\frac{r}{L} \right)^a \exp \left[\sqrt{2b \ln(L/r)} Z(r) \right], \quad (\text{II.3.13})$$

where $Z(r)$ is a Gaussian random variable with zero mean and variance one. Hence, $u(r)/u_L$ is a log-normal distributed random variable with mean $a \ln(r/L)$ and variance $2b \ln(L/r)$.

The equivalent FPE that governs the PDF $p(u, r)$ reads according to

(I.1.18) and (I.1.19)

$$\begin{aligned}
 -\partial_r p(u, r) &= \left[-\partial_u D^{(1)}(u, r) + \partial_u^2 D^{(2)}(u, r) \right] p(u, r), \quad p(u, L) = p_L(u), \\
 D^{(1)}(u, r) &= -(a-b) \frac{u}{r}, \quad D^{(2)}(u, r) = b \frac{u^2}{r}
 \end{aligned} \tag{II.3.14a}$$

with initial distribution $p_L(u)$, and the minus sign before ∂_r again accounts for $dr < 0$. Using the substitutions $s = \ln(L/r)$ and $w = \ln(u/u_L)$, the solution of the FPE can be determined to be

$$p(u, r) = \frac{1}{u \sqrt{4\pi b \ln \frac{L}{r}}} \int p_L(u_L) \exp \left[-\frac{\left(\ln \frac{u}{u_L} - a \ln \frac{r}{L} \right)^2}{4b \ln \frac{L}{r}} \right] du_L \tag{II.3.15}$$

which is a log-normal distribution for $u/u_L > 0$ with mean $a \ln(r/L)$ and variance $2b \ln(L/r)$ in agreement with the solution of the SDE above.

From the FPE (II.3.14a) above and the moment equation (I.1.30), we can conveniently obtain the scaling of the structure functions for the stochastic cascade,

$$\begin{aligned}
 -r \partial_r S_u^n(r) &= \left[-(a-b)n + bn(n-1) \right] S_u^n(r) \\
 \Rightarrow \frac{S_u^n(r)}{S_u^n(L)} &= \left(\frac{r}{L} \right)^{an - bn^2} = \left(\frac{r}{L} \right)^{(a-3b)n - bn(n-3)}.
 \end{aligned} \tag{II.3.16}$$

In comparison with the moments in (II.2.34) for the K62 model, we indeed find that the phenomenological introduced SDE (II.3.10) is equivalent to the K62 model.

We recover the K62 scaling for $b = \mu/18$ and $a = (2+\mu)/6 \approx 1/3 + 0.04$. The solution for $p(u, r)$ above is therefore the PDF for velocity increments u in an ideal K62 process. See figure II.4 for a plot of $p(u, r)$ for various scales r and intermittency factors μ .

The resulting drift and diffusion for the K62 process read

$$D^{(1)}(u, r) = -\frac{3+\mu}{9} \frac{u}{r}, \quad D^{(2)}(u, r) = \frac{\mu}{18} \frac{u^2}{r} \quad (\text{K62}). \tag{II.3.17}$$

The equivalence between the K62 model and the FPE with $D^{(1,2)}(u, r)$ as above have been first found by Friedrich and Peinke [192, 193].

II Universal features of turbulent flows

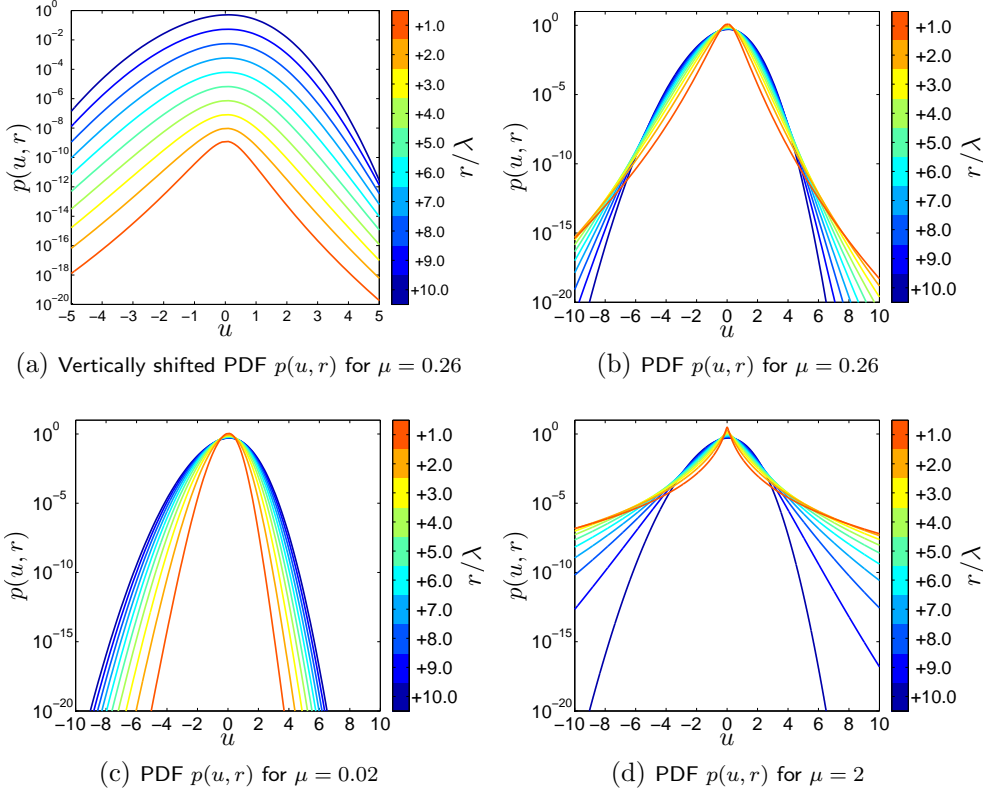


Figure II.4: Analytic solutions $p(u, r)$ of the FPE for the K62 process for various scales r and intermittency factors μ . The analytic solution is given by (II.3.15), for the initial distribution $p_L(u_L)$ a skew-normal distribution was taken that was fitted to experimental data from [110].

In the picture of the multiplicative cascade, the K62 model implies a scaling $g_0 = h_0^{3-d_{\text{fr}}}$ with fractal dimension $d_{\text{fr}} = 3 - 1/a = 3\mu/(2 + \mu) \approx 0.35$ and an amplitude of velocity fluctuations of $w_0^2 = \mu/9 \ln(1/g_0)$.

The equivalence between the K62 scaling on a logarithmic scaling, i.e. the velocity increment as a function of the cascade stage, and the geometric Brownian motion, i.e. the Black-Scholes model for stock prices [194, 195], establishes a curious connection between the classical models of turbulent flows and stock markets.

Multifractal model We have shown that the Kolmogorov model K62 is equivalent to a FPE, if we use a drift coefficient linear in u and a diffusion coefficient quadratic in u , as specified in (II.3.17). We now aim at exploring the general connection between drift and diffusion coefficients $D^{(1,2)}(u, r)$ and scaling exponents ζ_n .

To this end, we assume a general power series for $D^{(1,2)}(u, r)$,

$$D^{(1)}(u, r) = - \sum_{k=0}^{\infty} d_k^{(1)}(r) u^k, \quad D^{(2)}(u, r) = \sum_{k=0}^{\infty} d_k^{(2)}(r) u^k. \quad (\text{II.3.18})$$

Substitution of (II.3.18) into the moment equation (I.1.30) yields

$$\begin{aligned} -\partial_r S_u^n(r) &= \sum_{k=0}^{\infty} \left[-n d_k^{(1)}(r) S_u^{n+k-1}(r) + n(n-1) d_k^{(2)}(r) S_u^{n+k-2}(r) \right] \\ &= \sum_{k=0}^{\infty} \left[-n d_{k-1}^{(1)}(r) + n(n-1) d_k^{(2)}(r) \right] S_u^{n+k-2}(r), \end{aligned} \quad (\text{II.3.19})$$

where we have set $d_{-1}^{(1)}(r) \equiv 0$.

By defining the matrix

$$\mathbf{A} = \begin{pmatrix} a_{02} & a_{03} & a_{04} & a_{05} & \dots \\ a_{11} & a_{12} & a_{13} & a_{14} & \ddots \\ a_{20} & a_{21} & a_{22} & a_{23} & \ddots \\ 0 & a_{30} & a_{31} & a_{32} & \ddots \\ 0 & 0 & \ddots & \ddots & \ddots \end{pmatrix} \quad (\text{II.3.20})$$

with diagonals

$$\begin{aligned} a_{nk}(r) &= n d_{k-1}^{(1)}(r) - n(n-1) d_k^{(2)}(r) \\ &= (d_{k-1}^{(1)}(r) + d_k^{(2)}(r)) n - d_k^{(2)}(r) n^2, \end{aligned} \quad (\text{II.3.21})$$

we can rewrite (II.3.19) as a linear system of ordinary differential equations

$$\partial_r S_u^n(r) = A_j^n(r) S_u^j(r). \quad (\text{II.3.22})$$

II Universal features of turbulent flows

For the case that $d^{(1)}(r)$ and $d^{(2)}(r)$ depend reciprocally on r , we can rewrite (II.3.22),

$$r \partial_r S_u^n(r) = A_j^n S_u^j(r) , \quad (\text{II.3.23})$$

with now constant $d^{(1)}$, $d^{(2)}$, a_{nk} and A_j^n .

Substitution of the scaling ansatz $S_u^n(r) = r^h$ in (II.3.23) results into the condition $\det(A_j^n - h \delta_j^n) = 0$ in order to obtain non-trivial solutions for $S_u^n(r)$. The general form of this solution yields the sought connection between a scaling law and drift and diffusion coefficients,

$$\begin{aligned} S_u^n(r) &= \sum_i v_i^n r^{h_i} \\ &= v_1^n r^{h_1} + v_2^n r^{h_2} + v_3^n r^{h_3} + \dots \stackrel{!}{=} c_n r^{\zeta_n} , \end{aligned} \quad (\text{II.3.24})$$

with h_i being the i -th eigenvalue to the i -th eigenvector \mathbf{v}_i of matrix \mathbf{A} . The task might be to find for given ζ_n a matrix \mathbf{A} of form (II.3.20) that has eigenvalues h_i und eigenvectors \mathbf{v}_i such that (II.3.24) is satisfied. The entries a_{nk} of that matrix \mathbf{A} then define $d_k^{(1)}$, $d_k^{(2)}$ and thus $rD^{(1)}$, $rD^{(2)}$ using (II.3.18). But as we are equating a power series in r on the l.h.s. with *one* power of r on the r.h.s. of (II.3.24), we are forced to set $v_i^n = c_n \delta_{h_i \zeta_i}$ such that \mathbf{A} is diagonal. The entries of the diagonal are then the desired scaling exponents, that is, $a_{n2} = \zeta_n$. Using (II.3.21) and (II.3.18), we get

$$\zeta_n = a_{n2} = (d_1^{(1)} + d_2^{(2)})n - d_2^{(2)}n^2 , \quad d_{k \neq 1}^{(1)} = d_{k \neq 2}^{(2)} = 0 , \quad (\text{II.3.25a})$$

$$\Rightarrow D^{(1)}(u, r) = -d_1^{(1)} \frac{u}{r} , \quad D^{(2)}(u, r) = d_2^{(2)} \frac{u^2}{r} . \quad (\text{II.3.25b})$$

The form of $D^{(1,2)}(u, r)$ above is the most general form that allows a scaling law. Hence, by comparing the $D^{(1,2)}(u, r)$ above with the K62 form of $D^{(1,2)}(u, r)$ in (II.3.17), we see that the K62 scaling is already the most general scaling law covered by a FPE. This limitation of a FPE to K62 scaling has also been found along other lines by Hosokawa [196].

Writing the scaling exponents in (II.3.24) as $h_i = \frac{1}{3} - (1 - \frac{1}{3}d_{\text{fr}}(i))$ with fractal dimension $d_{\text{fr}}(i)$, we may interpret the sum in (II.3.24) as the superposition of scaling laws in subspaces of fractal dimension $d_{\text{fr}}(i)$, very much like the multifractal model we mentioned in (II.2.3) (cf. discussion

of equation (8.40) in [108]). For a full correspondence to the multifractal model, however, a continuous superposition of powers in the form

$$D^{(1,2)}(u, r) = \frac{1}{r} \int_{k_{\min}}^{k_{\max}} d^{(1,2)}(k) u^k dk \quad (\text{II.3.26})$$

seems promising, which we leave for further studies.

Scaling beyond K62 In the previous paragraph, we found that the restriction to a FPE to describe the stochastic process in $u(r)$ also limits the resulting scaling law of $S_u^n(r)$ to the form of K41 or K62. In particular, this restriction rules out the promising SL scaling law (II.2.38). By extending our analysis to discontinuous MPs, however, we will now demonstrate that the SL scaling does have a representation as a MP.

In chapter I.1.4 we learnt that a MP is in general a jump process with a continuous component. The continuous component can be fixed by a drift coefficient $A(u, r)$ and a diffusion coefficient $B(u, r)$, whereas the occurrence of jumps of width w is given by a jump density $\theta(w|u, r)$ with moments $\Psi^{(k)}(u, r)$. Realistic MPs always have a discontinuous component, but in many applications this component is small such that $D^{(1)} = A + \Psi^{(1)} \simeq A$ and $D^{(2)} = B + \Psi^{(2)}/2 \simeq B$, and the FPE with $D^{(1,2)}$ is a reasonable approximation of the process.

To bridge to scaling laws of structure functions $S_u^n(r)$, recall that for the choice $A(u, r) = a(r)u$, $B(u, r) = b(r)u^2$ and $\Psi^{(k)}(u, r) = d^{(k)}(r)u^k$, the moments follow from the Kramers-Moyal expansion (KME) as

$$S_u^n(r) = S_u^n(L) \exp \left[- \int_L^r na(r) + n(n-1)b(r) + \sum_{k=1}^n \binom{n}{k} d^{(k)}(r) dr \right]. \quad (\text{II.3.27})$$

(The minus in the exponent is due to $dr < 0$, see (I.1.76) and (I.1.82).) Let us temporarily restrict ourselves to a pure jump process, i.e. $a(r) \equiv 0$ and $b(r) \equiv 0$. For the special case $d^{(k)}(r) = d^{(k)}/r$ with constant $d^{(k)}$, we obtain the scaling law

$$S_u^n(r) = S_u^n(L) r^{-\sum_{k=1}^n \binom{n}{k} d^{(k)}}. \quad (\text{II.3.28})$$

II Universal features of turbulent flows

Hence, to obtain a scaling law with exponents ζ_n , we require that the $d^{(k)}$ satisfy

$$\sum_{k=1}^n \binom{n}{k} d^{(k)} \stackrel{!}{=} -\zeta_n . \quad (\text{II.3.29})$$

In some sense, the $d^{(k)}$ are the coefficients of a binomial expansion of $-\zeta_n$. For the SL scaling, it is indeed possible to solve (II.3.29) for the $d^{(k)}$, if we also take an appropriate drift term into account,

$$A(u, r) = -\frac{1}{3} \left(1 - \frac{C_0}{3}\right) \frac{u}{r} , \quad B(u, r) \equiv 0 , \quad (\text{II.3.30a})$$

$$\Psi^{(k)}(u, r) = C_0 \left(\beta^{1/3} - 1\right)^k \frac{u^k}{r} \quad (\text{SL}) . \quad (\text{II.3.30b})$$

The corresponding KMCs are $D^{(1)}(u, r) = A(u, r) + \Psi^{(1)}(u, r)$ and $D^{(k)}(u, r) = \Psi^{(k)}(u, r)/k!$ for $k \geq 2$.²⁸

As expected, the K41 process in (II.3.12) is recovered if we set the intermittency parameter to $\beta = 1$, which corresponds to zero intermittency, and insert the codimension $C_0 = 0$.

Due to $\beta^{1/3} - 1 \approx -0.13$, the odd moments $\Psi^{(k)}(u, r)$ turn out to be negative which incorporates a negative skewness of $\theta(w|u, r)$ for positive u . From the k -dependence we see also that the moments $\Psi^{(k)}(u, r)$ decrease with increasing k only if $|u| < |1/(\beta^{1/3} - 1)|$, implying that intensive intermittent bursts are to be expected if $|u|$ is already quite large. The KMCs, however, are still decreasing rather fast for increasing k and reasonable values for u , suggesting that an approximation of the jump process as a continuous process is reasonable.

However, it is desirable to set up the master equation of the form (I.1.67) or (I.1.70) that governs the dynamics of u . To do so, we need to solve the moment problem

$$\int w^k \theta(w|u, r) \, dw = \frac{C_0}{r} (bu)^k , \quad b := \beta^{1/3} - 1 \quad (\text{II.3.31})$$

in order to get hold of the jump density $\theta(w|u, r)$. This is a challenging problem. Exponential distributions seem to be a promising candidate, alt-

²⁸The KME with this KMCs should be solvable.

though a (compound) Poisson distribution would be the more natural choice (cf. [5] p. 237ff). Also promising is to formulate the characteristic function of $\theta(w|u, r)$ in terms of its moments $\Psi^{(k)}(u, r)$. At this point, however, further analysis has to be left for future study.

We note that similar considerations were pursued by Hosokawa in which he considered the moments of $\ln \varepsilon_r$ instead of $u(r)$ [196].

Random cascade models Regarding scaling laws, only the two Kolmogorov scalings can be reproduced by a FPE. We will now discuss the representation of turbulence models that do not rest on scaling laws of the form r^{ζ_n} . We begin with random cascade models.

In random cascade models, the PDF of velocity increments, $p(u, r)$, is obtained by propagating the PDF at integral scale, $p_L(u_L)$, to smaller scales making use of random multipliers h , see (II.2.53).

Amblard and Brossier discuss in [177] the connection of random cascade models to stochastic processes. They considered the Itô SDE

$$-\partial_r u(r) = -a(r)u(r) + \sqrt{2b(r)}u(r)\xi(r), \quad u(L) = u_L \quad (\text{II.3.32})$$

with positive coefficients $a(r)$ and $b(r)$. The general solution reads (see appendix A.1)

$$u(r) = \Phi_{rL} u_L \quad (\text{II.3.33})$$

$$\Phi_{rL} = \exp \left[\int_L^r a(r') + b(r') \, dr' + \int_L^r \sqrt{2b(r')} \xi(r') \, dr' \right], \quad (\text{II.3.34})$$

where $\ln \Phi_{rL}$ is a normal distributed random variable with mean μ_Φ and variance σ_Φ^2 given by

$$\mu_\Phi(r, L) = \int_L^r a(r') + b(r') \, dr', \quad (\text{II.3.35a})$$

$$\sigma_\Phi^2(r, L) = -2 \int_L^r b(r') \, dr'. \quad (\text{II.3.35b})$$

The form of the solution (II.3.33) is the same construction that led to the propagator formulation (II.2.53) in random cascade models: The statistics

of velocity increments on scale r is expressed by the statistics of a random multiplier Φ_{rL} . This equivalence becomes explicit by writing down the PDF for $u(r)$,

$$p(u, r) = \frac{1}{\sqrt{4\pi\sigma_\Phi(r, L)}} \int_0^\infty \exp \left[- \frac{(\ln h - \mu_\Phi(r, L))^2}{2\sigma_\Phi^2(r, L)} \right] p_L\left(\frac{u}{h}\right) \frac{d \ln h}{h}, \quad (\text{II.3.36})$$

where we defined $h := u/u_L$, and $p_L(u_L)$ is the PDF of the velocity increments on integral scale L . Clearly, the propagator G_{rL} from (II.2.53) reads in this case

$$G_{rL}(\ln h) = \frac{1}{\sqrt{4\pi\sigma_\Phi(r, L)}} \exp \left[- \frac{(\ln h - \mu_\Phi(r, L))^2}{2\sigma_\Phi^2(r, L)} \right]. \quad (\text{II.3.37})$$

This propagator is equivalent to Green's function of the FPE

$$\begin{aligned} -\partial_r p(u, r) &= \left[-\partial_u D^{(1)}(u, r) + \partial_u^2 D^{(2)}(u, r) \right] p(u, r), \quad p(u, L) = p_L(u) \\ D^{(1)}(u, r) &= -a(r)u, \quad D^{(2)}(u, r) = b(r)u^2 \quad (\text{RCM}). \end{aligned} \quad (\text{II.3.38})$$

According to (A.2.3), the FPE corresponds to the SDE (II.3.32). From the FPE also follows by use of the moment equation (I.1.30) an ODE for the structure function,

$$-\partial_r S_u^n(r) = \left[-na(r) + n(n-1)b(r) \right] S_u^n(r), \quad (\text{II.3.39})$$

where substitution of the scaling ansatz $S_u^n(r) = S_u^n(L) r^{\zeta_n(r)}$ yields

$$\zeta_n(r) = \frac{1}{\ln r} \int_L^r n \left(a(r') - (n-1)b(r') \right) dr'. \quad (\text{II.3.40})$$

Note that solving the moment equation (II.3.39) results into

$$S_u^n(r) = S_u^n(L) \exp \left[n\mu_\Phi(r, L) + \frac{1}{2}n^2\sigma_\Phi^2(r, L) \right] \quad (\text{II.3.41})$$

in agreement with the moments of the log-normal distribution in (II.3.36). On the basis of the drift and diffusion coefficients $D^{(1,2)}(u, r)$ from (II.3.38)

and the resulting scaling exponents $\zeta_n(r)$ in (II.3.40), we can discuss the same special cases as we did in view of the propagator formulation (II.2.53) for random cascade processes.

(i) In accordance with (II.3.12), setting $a(r) = 1/(3r)$ and $b(r) \equiv 0$ recovers the K41 scaling exponents (II.2.30). We also see from (II.3.35b) that in this case the multiplier Φ_{rL} in (II.3.33) is not a random variable.

(ii) Only if $a(r)$ and $b(r)$ depend reciprocally on r , the scaling exponents become constant and take the K62 form (II.2.35) which is in compliance with our discussion of (II.3.25b). In this case Φ_{rL} is a log-normal distributed random variable with variance $A_r \sim \ln(L/r)$.

(iii) By leaving the K62 form of $D^{(1,2)}(u, r)$ but keeping the same scale dependency, say $a(r) = a_0 \partial_r \ln f(r)$ and $b(r) = b_0 \partial_r \ln f(r)$, we obtain a modified scaling law of the form $S_u^n(r) \propto f(r)^{\zeta_n}$ with now $\zeta_n = a_0 n - b_0 n(n-1)$. The random cascade process defined by such a choice of $D^{(1,2)}(u, r)$ was experimentally examined by Arneodo [189], which he termed *continuous self-similar* cascade. Note that in this case we can always transform to the new scale $s = \ln f(r)$ such that drift and diffusion become scale-independent. The MP is then stationary in s . Note also that for the special case $f(r) = S_u^3(r)$, we recover the ESS scaling (II.2.45). In that sense, ESS corresponds to a special random cascade model.

(iv) For arbitrary $a(r)$ and $b(r)$, we still have a log-normal random cascade model where $a(r)$ and $b(r)$ determine the mean and variance of the associated log-normal distribution for the multipliers Φ_{rL} according to (II.3.35). In view of the introductory derivation of the K62 model in terms of a random cascade model, we see that this restriction is due to the fact that a FPE is only equivalent to a SDE with *Gaussian* white noise $\xi(r)$ ([20] chapter 3.3). A SDE with *Poissonian* white noise, for instance, would lead to the log-Poisson model by She and Leveque, for which a master equation is needed to describe how $p(u, r)$ evolves in scale. Note that the white noise property of $\xi(r)$ is equivalent to $\langle \xi(r)\xi(s) \rangle = \delta(r-s)$, that is the Markov assumption of the cascade.

As a last remark regarding random cascade models, we mention that drift and diffusion of the form (II.3.38) exclude a skewness in the solution $p(u, r|u_L, L)$ of the corresponding FPE. A skewness in $p(u, r)$ can only enter through a skewness in the initial PDF $p_L(u)$. This is a known shortcoming of standard random cascade models of the form (II.3.36) [178].

Yakhot's model Recall Yakhot's model of turbulence which we introduced in section II.2.4 p. 143. In this model two parameters, B and A , enter, together with two characteristics of the specific turbulent flow under consideration, the root-mean-square fluctuations v_{rms} and the characteristic length scale of turbulence generation ℓ_{ch} . The result of Yakhot's efforts is the partial differential equation for $p(u, r)$ in II.2.57.

Davoudi und Tabar [197, 198] showed that solutions of the PDE (II.2.57) satisfy the Kramers-Moyal expansion (KME)²⁹

$$-\partial_r p(u, r) = \sum_{k=1}^{\infty} (-1)^k \partial_u^k [D^{(k)}(u, r) p(u, r)] , \quad (\text{II.3.42a})$$

$$D^{(k)}(u, r) = \frac{\alpha_k}{r} u^k - \beta_k u^{k-1} , \quad (\text{II.3.42b})$$

$$\alpha_k = (-1)^k A \frac{\Gamma(B+1)}{\Gamma(B+k+1)} = \frac{A(-1)^k}{(B+1)(B+2)\cdots(B+k)} , \quad (\text{II.3.42c})$$

$$\beta_k = (-1)^k \frac{v_{\text{rms}}}{\ell_{\text{ch}}} \frac{\Gamma(B+2)}{\Gamma(B+k+1)} = \frac{v_{\text{rms}}}{\ell_{\text{ch}}} \frac{(-1)^k}{(B+2)(B+3)\cdots(B+k)} , \quad (\text{II.3.42d})$$

where $\Gamma(x)$ is the gamma function and we set $\beta_1 := 0$.

For a further discussion we substitute $A = (B+3)/3$ from (II.2.61) and rewrite the coefficient β_2 to get for the Kramers-Moyal coefficients (KMCs) the suggestive form

$$D^{(k)}(u, r) = \frac{\alpha_k - \tilde{\beta}_k(u, r)}{r} u^k , \quad (\text{II.3.43})$$

$$\alpha_k = \frac{(-1)^k (B+3)}{3(B+1)\cdots(B+k)} , \quad \tilde{\beta}_k(u, r) = \frac{r/u}{\ell_{\text{ch}}/v_{\text{rms}}} \frac{(-1)^k}{(B+2)\cdots(B+k)} ,$$

where $\tilde{\beta}_2(u, r)$ now is dimensionless. Four special cases are apparent.

(i) It is clear that due to $\Gamma(B+k+1)$ in the denominator of (II.3.42c) and (II.3.42d), the coefficients α_k and β_k will rapidly decrease with increasing k . It is hence a reasonable approximation to truncate the KME after the second term and obtain a FPE with drift and diffusion given by

$$D^{(1)}(u, r) = \frac{\alpha_1}{r} u , \quad D^{(2)}(u, r) = \frac{\alpha_2 - \tilde{\beta}_2(u, r)}{r} u^2 , \quad (\text{YAK}) \quad (\text{II.3.44})$$

$$\alpha_1 = -\frac{B+3}{3(B+1)} , \quad \alpha_2 = \frac{B+3}{3(B+1)(B+2)} , \quad \tilde{\beta}_2(u, r) = \frac{r/u}{\ell_{\text{ch}}/v_{\text{rms}}} \frac{1}{B+2} .$$

²⁹In [198] the term $\beta_k u^{k-1}$ enters $D^{(k)}(u, r)$ with the opposite sign than in (II.3.42b) which is not correct.

This approximation is in opposition to a “blind” application of Pawula’s theorem, as we not use $D^{(4)}(u, r) \approx 0$ to argue that all coefficients $D^{(\geq 3)}(u, r)$ are negligible. If $D^{(4)}(u, r)$ is not exactly zero, the higher coefficients might as well diverge despite $D^{(4)}(u, r) \approx 0$, but here we know that $\alpha_k \rightarrow 0$ and $\beta_k \rightarrow 0$ for $k \rightarrow \infty$ without using Pawula’s theorem. However, it is difficult to say whether the influence of the entirety of $D^{(\geq 3)}(u, r)$, despite the negligibility of the individual terms for $k \rightarrow \infty$, remains significant for the dynamics.

(ii) For $r/u \ll \ell_{\text{ch}}/v_{\text{rms}}$, expressing that typical time scales of the internal dynamics of turbulent structures are small compared to the characteristic time scale associated with turbulence generation, we may neglect $\tilde{\beta}_2(u, r)$ in the KME and arrive at

$$-r \partial_r p(u, r) = \sum_{k=1}^{\infty} (-1)^k \partial_u^k [\alpha_k u^k p(u, r)] . \quad (\text{II.3.45})$$

The moments equation of this KME is of the same form as (I.1.81), for which we found the solution (I.1.82) implying a scaling law with exponents

$$\zeta_n = \frac{n}{3} \frac{B + 3}{B + n} \quad (\text{II.3.46})$$

in agreement with (II.2.60).

(iii) Neglecting also $\tilde{\beta}_2(u, r)$ in the FPE, that is in the limit $\tilde{\beta}_2(u, r) \rightarrow 0$ for all u and r , drift and diffusion coefficients of the FPE (II.3.44) take the K62 form in (II.3.17). Therefore, instead of resorting to inertial range scales $L > r > \lambda$, the K62 scaling is included into Yakhot’s model in the limit of a clear-cut time scale separation between internal dynamics of turbulent structures and turbulence generation.³⁰

(iv) In the limit $B \rightarrow \infty$, all $D^{(k)}(u, r)$ vanish for $k \geq 2$ and we recover the K41 form of $D^{(1)}(u, r)$ in (II.3.12) which excludes any intermittency corrections from the model. This role of B is in accord with the discussion of scaling exponents after (II.2.59), but here we do not need to resort to comparing scaling laws.

In total, Yakhot’s model constitutes a generalisation of K62 in two aspects.

³⁰This is of course hard to achieve, since even for $L/\langle u_L \rangle \ll \ell_{\text{ch}}/v_{\text{rms}}$ we can not rule out fluctuations of u_L that bring L/u_L close to $\ell_{\text{ch}}/v_{\text{rms}}$, which, to lower extent, also applies for time scales r/u at smaller scales.

First, by including all $D^{(k)}(u, r)$ instead of only $D^{(1,2)}(u, r)$, the scaling exponents (II.3.46) also account for a jump process underlying the continuous K62 process. And second, direct effects of turbulence generation on the dynamics in the inertial range are accounted for by the coefficient $\tilde{\beta}_k(u, r)$ in (II.3.43) and imply a departure from a scaling law.

Note, however, that for certain values of u and r all even $D^{(k)}(u, r)$ become negative, which is contradictory to the general form of $D^{(k)}(x, t)$ given in (I.1.78). In terms of the dimensionless turn-over time $\tau_r := |(r/u)/(\ell_{\text{ch}}/v_{\text{rms}})|$ and the critical value $\tau_{\text{cr}} = 3(B+1)/(B+3) = 1/\zeta_1$, the $D^{(k)}(u, r)$ become negative for $\tau_r < \tau_{\text{cr}}$.

In the Markov formalism, Yakhot's model is hence only valid as long as the normalised time scale of eddy dynamics is larger than the critical value τ_{cr} . Instead of the inertial range condition $\text{Re}_L > \text{Re}_r > \text{Re}_\lambda$ from (II.2.5), the Markov representation of Yakhot's model suggests that the K62 scaling law can be expected if

$$1 \gg \tau_r > \tau_{\text{cr}} \approx 0.37 . \quad (\text{II.3.47})$$

This condition is hardly fulfilled and gets more likely to be violated for large fluctuations of u which are described by high order structure functions. This observation might explain the failure of the K62 scaling at high order.

It is further reasonable to assume that the restriction $\tau_r > \tau_{\text{cr}}$ amounts to the principle of time scale separation underlying the Markov assumption. Accepting $\text{Re}_r > \text{Re}_\lambda$ as the analog of $\tau_r > \tau_{\text{cr}}$ then implies that the Markov assumption is linked to $r > \lambda$, a guess which will be confirmed in the next section.

In closing this chapter, we mention that it should also be interesting to tackle the moment problem for Yakhots scaling exponents (II.3.46),

$$\int w^k \theta(w|u, r) \, dw = \frac{B! (B+3)}{3r} \frac{(-u)^k}{(B+k)!} , \quad (\text{II.3.48})$$

which would yield the jump density $\theta(w|u, r)$ and thus a master equation governing the evolution of $p(u, r)$.

II.3.3 Experimental investigations

In the hitherto discussion on MPs representing the eddy cascade in fully developed turbulence, we demonstrated how many major achievements in turbulence research find their counterpart in the theory of MPs. The point of origin was to assume that once an eddy has evolved into smaller eddies, these smaller eddies start their own cascade without reference to the eddy they came from, which we interpreted as being equivalent to the memoryless property of a MP. The equivalence of the Markov description to established theories of turbulence legitimates this interpretation, however, experimental evidence that the Markov assumption holds is called for. In this section we will give a survey of experimental investigations regarding the Markov assumption and also the applicability of a FPE.

At the beginning of the first part, we formally defined the Markov condition in (I.1.2) which states that in a time-ordered series of events, the current event is only influenced by the most recent one. A direct consequence of the Markov condition is the Chapman-Kolmogorov relation (CKR) (I.1.64) which typifies the kind of Markov chain we associate with the eddy cascade. Building on the CKR, we found that continuous MPs are fixed by SDEs and the corresponding FPEs, and discontinuous MPs can be described by a KME. Hence, if the CKR holds, all results of the first part hold.

The first work that pursued the Markov representation of the eddy cascade was in fact experimental. In [192, 193], Friedrich and Peinke demonstrated that the PDF of velocity increments, $p(u, r)$, indeed satisfies the CKR. They determined conditional probabilities $p(u_1, r_1 | u_2, r_2)$ from a free jet experiment and substituted these into the CKR for a number of triples $r_1 < r_2 < r_3$. In the spirit of a Markov chain, they used the experimentally determined $p(u_1, r_1 | u_2, r_2)$ to propagate $p_L(u_L)$ successively downwards in scale in comparison to the directly measured $p(u, r)$. Both investigations demonstrated the validity of the CKR for all accessible u and r which constitutes convincing evidence that the evolution of velocity increments u in scale r is a MP.

Friedrich and Peinke also addressed the question whether the MP is continuous or discontinuous by estimation of the first four KMCs $D^{(1-4)}(u, r)$ according to the procedure described in the context of the definition of $D^{(k)}$

in (I.1.78). They found that, within the error margin, $D^{(3,4)}(u, r)$ vanish for all accessible u and r , whereas $D^{(1,2)}(u, r)$ have well-defined limits. Referring to the theorem of Pawula as discussed after (I.1.79), they argued that the MP should be continuous, that is to say, the jump density (I.1.71) is a δ -function for which all moments (including $D^{(4)}$) vanish. This is a bold statement, since it is hardly possible to prove $D^{(4)}(u, r) \equiv 0$ for all u and r by experimental means, and $D^{(4)}(u, r) \approx 0$ does not imply that the FPE is a good approximation, as the KME is not a systematic expansion in the sense that a small $D^{(4)}$ implies smaller $D^{(\geq 4)}$. In other words, a jump density that has a vanishing fourth moment needs only to be vanishing in the part that contributes to the forth moment and might as well involve a significant probability for extreme jumps, a scenario not unthinkable in the context of turbulence.

However, such a scenario remains to be peculiar, and $D^{(4)}(u, r) \approx 0$ is a respectable indication that a FPE is a good approximation of the MP. Furthermore, the finding (II.3.42) by Davoudi and Tabar which implies that the higher $D^{(k)}(u, r)$ rapidly tend to zero, a finding that builds on the PDE (II.2.57) for $p(u, r)$ which Yakhot derived by using the full NSE, corroborates the assumption that $D^{(4)}(u, r) \approx 0$ indicates $D^{(\geq 3)}(u, r) \rightarrow 0$ for all u and r in the limit $k \rightarrow \infty$.

The pioneering work by Friedrich and Peinke, now primarily referred to as *Markov analysis*, entailed more activity than we can present here. However, we review a selection of developments, for further information we refer the reader to the review article by Friedrich et al. [26].

A major improvement of the analysis was achieved by Renner et al. in [110, 113]. The authors confirmed in a careful free jet experiment the validity of the Markov assumption³¹, but identified a scale below which the Markov assumption breaks down. In a sophisticated statistical procedure, the so-called Wilcoxon test (for details see appendix A in [110]), they pinpointed this scale to be about the Taylor length scale λ . The Wilcoxon test thus confirmed the Markov assumption for all scales $r \gtrsim \lambda$ (and $r < L$). As below the scale λ the dissipative range succeeds the inertial range, the

³¹The next chapter will analyse the data taken in this experiment and also give some characteristics of this data. Histograms of u approximating $p(u, r)$ were already presented in figure II.2, the scaling behaviour was analysed in figure II.3.

role of λ in the Markov analysis suggests that molecular friction causes the break-down of the Markov assumption. In analogy to Einsteins theory of Brownian motion, the exact scale above which the Markov assumption holds is termed *Markov-Einstein length scale* r_{ME} , the spatial analogue of the Markov-Einstein time scale t_{ME} discussed after (I.1.78). Various experimental investigations confirmed that $r_{\text{ME}} \simeq \lambda$ holds for different flow conditions and a wide range of Reynolds numbers [199, 191, 23].

Renner and co-workers also addressed the question whether a FPE is a suitable approximation of the MP. The estimated $D^{(4)}(u, r)$ is of similar shape as $D^{(2)}(u, r)$ but by three orders of magnitude smaller and within the error margin not distinguishable from being zero. Using the KME truncated after the fourth term with $D^{(2)}(u, r)$ and $D^{(4)}(u, r)$ estimated from their data, they further demonstrated that the influence of $D^{(4)}(u, r)$ on the eighth-order structure function $S_u^8(r)$ is negligible compared to the influence of $D^{(2)}(u, r)$. Truncating therefore the KME after the second term, they obtained the FPE³²

$$-\partial_r p(u, r|u_L, L) = [-\partial_u D^{(1)}(u, r) + \partial_u^2 D^{(2)}(u, r)]p(u, r|u_L, L) \quad (\text{II.3.49})$$

with the estimated drift and diffusion coefficients

$$D^{(1)}(u, r) = -a_0 r^{0.6} - a_1 r^{-0.67} u + a_2 u^2 - a_3 r^{0.3} u^3 \quad (\text{II.3.50a})$$

$$D^{(2)}(u, r) = b_0 r^{0.25} - b_1 r^{0.2} u + b_2 r^{-0.73} u^2 \quad (\text{II.3.50b})$$

$$a_0 = 0.0015, \quad a_1 = 0.61, \quad a_2 = 0.0096, \quad a_3 = 0.0023, \quad (\text{II.3.50c})$$

$$b_0 = 0.033, \quad b_1 = 0.009, \quad b_2 = 0.043. \quad (\text{II.3.50d})$$

Solving this FPE numerically, Renner et al. found for various scales that $p(u, r|u_L, L)$ fixed by the FPE above is in perfect agreement with the experimental result, confirming again the permissibility to approximate the MP with a FPE. Note that the estimation of $D^{(1,2)}(u, r)$ involves the conditional PDFs $p(u, r|u_L, L)$, in order to describe the measured $p(u, r)$ the FPE (II.3.49) needs to be complemented by the measured initial distribution $p_L(u)$.

The form of the drift $D^{(1)}(u, r)$ in (II.3.50a) is approximately the same as

³²Velocity increment u and scale r are given in units of $\sigma_\infty = 0.54 \text{ m/s}$ at infinite scales and the Taylor length scale $\lambda = 6.6 \text{ mm}$, respectively.

for the K62 model in (II.3.17), if we acknowledge that the term linear in u is significant larger than the other terms. The diffusion coefficient $D^{(2)}(u, r)$, however, is clearly not purely quadratic in u as the K62 counterpart in (II.3.17). The constant term is responsible for background fluctuations that persist $u = 0$ and ensures that $D^{(2)}(u, r) > 0$ for all u and r . The linear term, though small, proves to be crucial in order to account for the skewness in $p(u, r)$.

As pointed out by Renner et al. in [110], the corresponding SDE to the FPE (II.3.49) can also be formulated involving an additive and a multiplicative noise term

$$-\partial_r u(r) = D^{(1)}(u, r) + \xi_0(r) + u(r)\xi_2(r) , \quad (\text{II.3.51})$$

where $\xi_0(r)$ is determined by the constant term of $D^{(2)}(u, r)$ and $\xi_2(r)$ by the quadratic term of $D^{(2)}(u, r)$, and the linear term of $D^{(2)}(u, r)$ gives rise to a correlation between $\xi_0(r)$ and $\xi_2(r)$. It is this correlation between additive and multiplicative noise sources that is responsible for the skewness in a generalisation of random cascade models [178].

By the same authors, data from a cryogenic helium jet experiment [179] for Reynolds numbers ranging from $\text{Re}_{\text{ch}} \approx 10^4$ to $\text{Re}_{\text{ch}} \approx 10^6$ was used to characterise how the terms in $D^{(1,2)}$ depend on the Reynolds number. On the basis of ten sets of $\{v(x) \mid \text{Re}\}$, they determined drift and diffusion to be

$$D^{(1)}(u, r) = -a_1(r) u , \quad (\text{II.3.52a})$$

$$D^{(2)}(u, r) = b_0(r; \text{Re}) - b_1(r; \text{Re}) u + b_2(r; \text{Re}) u^2 , \quad (\text{II.3.52b})$$

$$a_1(r) = 0.67 + 0.2\sqrt{r/\lambda} , \quad (\text{II.3.52c})$$

$$b_0(r; \text{Re}) = 2.8\text{Re}^{-3/8} r/\lambda , \quad b_1(r; \text{Re}) = 0.68\text{Re}^{-3/8} r/\lambda . \quad (\text{II.3.52d})$$

Accordingly, the drift $D^{(1)}(u, r)$ proved to be independent from Re , whereas the diffusion is in all terms Reynolds dependent. Specifically, the constant and linear terms of $D^{(2)}(u, r)$ could explicitly be formulated as functions of Re , but the quadratic term evades such a simple dependency. In the limit of infinite Reynolds numbers, the quadratic term should acquire the asymptotic form $b_2(r; \infty) = a_1(r)/2 - 1/6$ in order to respect the four-fifths

law (II.2.20). Indeed, the estimated form of $b_2(r; \text{Re})$ exhibits a tendency towards $b_2(r; \infty)$ for increasing Re , but still remains distinct from $b_2(r; \infty)$ to a considerable extent.

Instead of velocity increments, Naert et al. used the one-dimensional surrogate (II.2.23) and (II.2.31) to compute the locally averaged energy dissipation rate ε_r from a set $\{v(x)\}$ measured in a free jet experiment [190]. Instead of the physical scale r , they used $l = \ln(L/r)$ which now varies from $l = 0$ to $l \simeq \ln(L/r_{\text{ME}})$.

To describe the evolution of the stochastic variable $x(l) := \ln \varepsilon(l)$ from large to small scales, they estimated drift and diffusion coefficients in x and l . It turned out that a drift $D^{(1)}(x, l)$ linear in x and a constant diffusion $D^{(2)}$, i.e. an Ornstein-Uhlenbeck process, is well suited to describe their data. The fourth order coefficient is found to be constant and $\sqrt{D^{(4)}} \approx 0.05 D^{(2)}$, indicating that also for $\ln \varepsilon(l)$ the underlying jump process is negligible. The Markov-Einstein length turned out to be $r_{\text{ME}} \simeq \eta$, which means, in the case of the stochastic variable $x(l)$, the Markov assumption appears to hold even in the dissipative range.

The solution $p(x, l)$ of the FPE of an Ornstein-Uhlenbeck process is Gaussian which confirms the widely used assumption that $\varepsilon(r)$ is log-normal distributed. The variance of $p(x, l)$ increases exponentially with l implying that in physical scale r the variance obeys a power law in agreement with the result (II.2.46) of Castaing and co-workers and in contradiction to K62.

However, in a subsequent investigation, Marcq and Naert examined the statistical properties of the noise by extracting $\xi(l)$ from the Ornstein-Uhlenbeck process and found that $\xi(l)$ is indeed uncorrelated for $r > r_{\text{ME}}$ but exhibits a considerable skewness [200]. They argue that this skewness is the consequence of neglecting the third order coefficient $D^{(3)}(ur)$. Ultimately, a non-Gaussian $\xi(l)$ indicates that the approximation of the MP by a FPE does not hold, whereas the δ -correlation of $\xi(l)$ above the elementary step-size r_{ME} proves the Markov assumption to be justified.

In the later article, Renner and Peinke also investigated ε_r , but coupled with the stochastic process for $u(r)$, that is to say, a two-dimensional coupled stochastic process in the variables $u(r)$ and $x(r) = \ln(\varepsilon_r/\bar{\varepsilon})$ [201]. Performing a two-dimensional Markov analysis, they found a diagonal dif-

fusion matrix and that the stochastic process in $u(r)$ is a scale-dependent Ornstein-Uhlenbeck process where the diffusion coefficient depends on x . The drift of the process in $x(r)$ is also linear in x and scale-dependent, but the diffusion coefficient is of rather complicated form and depends on r and both u and x . Hence, the stochastic processes for $u(r)$ and $x(r)$ couple only via their stochastic term, a finding that supports the perception that the randomness of u originates from fluctuations of energy dissipation. Indeed, if ε_r was not a stochastic variable, $u(r)$ would reduce to a Gaussian. Consequently, the intermittent fluctuations of $u(r)$ on small scales trace back to the stochastic and scarcely accessible nature of energy dissipation. Note that the considerable simplification of the stochastic process in u was achieved by extending the analysis to two dimensions, instead of mapping the high-dimensional problem of turbulence on the analysis of longitudinal velocity increments. A further simplification can be expected by also including transversal velocity increments into the stochastic analysis.

We discussed phenomenological achievements of the Markov analysis that were initiated by the work of Friedrich and Peinke. On the methodological side, significant progress has been made on the procedure to extract drift and diffusion coefficients from experimental data involving maximum-likelihood estimators [202–204], finite-size corrections in poor sampled statistics [205, 24, 25] and corrections in the presence of strong measurement noise [142, 206]. A comparison of different estimation procedures is provided in [207].

Finally, we mention that the Markov analysis is also applied to atmospheric turbulence [208] and wind farms [150, 209], and even found its way to fields of research that are not related to turbulence wherever complexity is involved, see page 106 of [210] for an overview.

II.4 Fluctuation theorems and irreversibility

In the first chapters of this part of the thesis, we have introduced various theories and models that address universal properties of velocity fluctuations in the idealised concept of fully developed turbulence. In the preceding chapter, we demonstrated that these 'traditional' approaches to turbulence all have a Markovian counterpart, implying drift and diffusion coefficients $D^{(1,2)}(u, r)$, and in principle also a jump density $\theta(w|u, r)$.

In chapter I.2 of the first part, we have in particular discussed the total entropy production (EP) S_{tot} of a thermodynamic MP as defined in (I.2.40) in terms of the potential φ defined in (I.1.39a). The potential is basically the integral of $D^{(1)}/D^{(2)}$ and implies by (I.1.39a) an instantaneous stationary distribution p^{st} . The entropy S_{tot} is directly related to the irreversibility of the process, as we learnt from (I.2.64), and as such obeys the fluctuation theorems (FTs) in (I.2.70) and (I.2.69). The FTs include the second law $S_{\text{tot}} > 0$ as shown in (I.2.71)

In view of this interpretation of MPs, the aim of this chapter is to explore the implications of the various Markov approaches to turbulence discussed in the previous chapter. In the following we will always use ordinary calculus, therefore, discretisations of stochastic integrals have to be made in mid-point, and equivalent SDEs need to be formulated in the Stratonovich convention, but we do not have to bother with modified calculus.

II.4.1 Experimentally estimated versus K62

The ultimate aim would be to find a universal FT for velocity increments, in which the EP $S_{\text{tot}}[u(\cdot)]$ qualifies the irreversibility of the energy cascade. This EP would at the same time allow to distinguish realisations $u(\cdot)$ of the direct energy cascade ($S_{\text{tot}}[u(\cdot)] > 0$), from the realisations of the inverse energy cascade ($S_{\text{tot}}[u(\cdot)] < 0$). We will see that this is a particularly difficult endeavour.

On the one hand, we can estimate $D^{(1,2)}(u, r)$ directly from experimental data and expect that the resulting $S_{\text{tot}}[u(\cdot)]$ defines a FT that holds for this very data. The convergence of the FT for the available amount of data, however, is only guaranteed for sufficient number of realisations $u(\cdot)$ with $S_{\text{tot}}[u(\cdot)] < 0$, a requirement that is typically not met in macroscopic systems such as turbulent flows, cf. the discussion of the scope

of stochastic thermodynamics after (I.2.71). Furthermore, with $D^{(1,2)}(u, r)$ being tailored to match the statistics of experimental data without any physical input, the entropy $S_{\text{tot}}[u(\cdot)]$ evades a direct physical interpretation.

On the other hand, getting hold of proper $D^{(1,2)}(u, r)$ from first principles involving physical quantities, such as the energy transfer rate ε_r , length scales L and ϱ or viscosity ν , is an unsolved problem.³³ In addition, the extreme sensitivity of the FT to the correct modelling of extreme events is delicate, but at the same time constitutes a valuable tool to benchmark possible $D^{(1,2)}$.

At this point, we present our third publication [3], in which we contrast the FT from experimentally estimated $D^{(1,2)}(u, r)$ (II.3.50) with the FT resulting from the K62 theory (II.3.17). By doing so, also the basic concepts of stochastic thermodynamics will be recapped. Note that the experimental data referred to in the publication is the data discussed in [110] which we already used in the previous chapters. Note also that the parameter $\nu = (6 + 4\mu)/\mu \approx 27$ introduced in the publication bears no reference to viscosity so far denoted by ν . In the remaining part of this thesis it will always be $\nu = (6 + 4\mu)/\mu$.

³³An exception are $D^{(1,2)}$ from Yakhot's model involving L and v_{rms} , but these $D^{(1,2)}$ are not without problems as we have discussed in II.4.2 p.166 .

Probing small-scale intermittency with a fluctuation theorem

Daniel Nickelsen* and Andreas Engel

Institut für Physik, Carl von Ossietzky Universität Oldenburg, 26111 Oldenburg, Germany

We characterize statistical properties of the flow field in developed turbulence using concepts from stochastic thermodynamics. On the basis of data from a free air-jet experiment, we demonstrate how the dynamic fluctuations induced by small-scale intermittency generate analogs of entropy-consuming trajectories with sufficient weight to make fluctuation theorems observable at the macroscopic scale. We propose an integral fluctuation theorem for the entropy production associated with the stochastic evolution of velocity increments along the eddy-hierarchy and demonstrate its extreme sensitivity to the accurate description of the tails of the velocity distributions.

PACS numbers: 47.27.-i, 05.10.Gg, 05.40.-a, 05.70.Ln

All processes in nature are bound to produce entropy. This central dogma of macroscopic thermodynamics got substantially qualified in the preceding decade by new insights into the properties of small, strongly fluctuating systems. If entropy *consuming* trajectories occur with appreciable probability, thermodynamic *inequalities* may be considerably tightened to assume the form of *equalities* [1, 2]. The emerging field of stochastic thermodynamics (for recent reviews see [3, 4]) focuses on the full probability distributions of thermodynamic variables like heat, work, and entropy and establishes thermodynamic relations for individual fluctuating histories of the systems under consideration. Most prominent among these relations are the so-called *fluctuation theorems* (FTs) quantifying the relative frequency of entropy-consuming as compared to entropy-producing trajectories. Applications of these developments concern free-energy estimates of biopolymers [5, 6], the efficiency of nano-machines [7, 8], and the thermodynamic cost of information processing [9, 10], to name a few.

On the experimental side, most investigations have been done with *nanoscopic* setups like in single-molecule manipulations [11–13], colloidal particle dynamics [14–16] or harmonic oscillators [16]. For these systems, typical free-energy differences are of order $k_B T$ and the ubiquity of *thermal* fluctuations ensures the broad distributions of work, heat, and entropy which are indispensable for the application of fluctuation theorems. Increasing the size of these systems to macroscopic orders, the importance of thermal fluctuations fades, entropy-consuming trajectories become exceedingly rare, and the fluctuation theorems degenerate to the inequalities known from traditional thermodynamics. Besides some investigations in granular media [17–19], rather few examples of *macroscopic* systems have been identified which are amenable to an analysis using FTs.

Turbulent flow of liquids and gases is a fascinating phenomenon with many different facets that has been captivating scientists for centuries. Despite its broad range of technical relevance including turbulent drag [20], turbulent mixing [21], atmospheric turbulence with implications for climatic models [22] and the prospects of wind

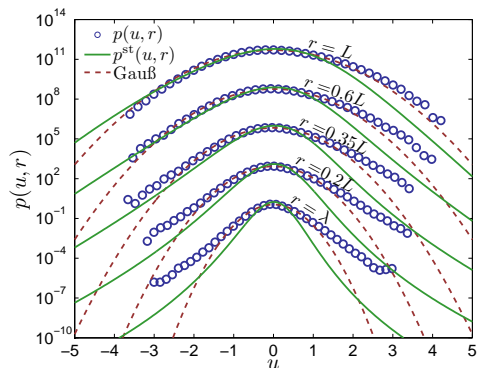


FIG. 1. Distribution $p(u, r)$ of velocity increments u at various scales r (circles) in the turbulent flow of a free jet experiment [25]. The velocity increments u are given in units of the standard deviation $\sigma_\infty = 0.54$ m/s at infinite scales. Also shown is the instantaneous stationary distribution $p^{\text{st}}(u, r)$ defined in (5) (full lines) and Gaussian fits to the experimental data (dashed lines). Both the deviation from the Gaussian approximation and from the stationary distribution increases when approaching smaller scales. For the sake of clarity, the distributions for various scales are vertically shifted by 10^3 .

energy [23, 24], several aspects of turbulent flows are still not fully understood. In particular, the intricate pattern of small-scale flow in developed turbulence with its intermittent change between laminar periods and violent bursts of activity have eluded a thorough theoretical understanding so far.

In the present letter, we show that the fluctuating flow field of developed turbulence represents a proper test system for stochastic thermodynamics. The *dynamic* fluctuations of turbulence show up at a macroscopic scale and, at the same time, are strong enough to generate “non-mainstream” trajectories with sufficient frequency to observe FTs in action. Using data from a free air jet experiment, we elucidate the nature of the entropy-consuming trajectories and demonstrate the convergence

of an integrated FT for data sets of rather small size. We further discuss how to use the FT for the statistical description of the flow field.

Applications of FTs to turbulent flow have been discussed before. On the experimental side, fluctuations of the heat flux [26], the injected power [27] and the pressure [28], as well as the motion of tracer particles [29] were studied. Numerical investigations concerned fluctuations of the injected power in the shell-model [30, 31] and properties of augmented Navier-Stokes equations in two dimensions [32]. All these investigations focused on variants of the *steady-state* FT [1, 33]. The FT we propose in this letter is qualitatively different. It is no steady-state FT but characterizes the *non-stationary* stochastic evolution of velocity increments along the eddy-hierarchy. It is somewhat similar in spirit to the detailed FT proposed in [34], which, however, describes the enstrophy cascade in two-dimensional turbulence.

In a standard setup, isotropic turbulence is generated by injecting energy into the flow by an external force field at a large, so-called integral scale L [35, 36]. By repeated break-up of eddies, a self-similar eddy hierarchy forms which is characteristic for developed turbulence [37]. On average, energy is transferred along the cascade to smaller and smaller scales until, due to molecular friction, it is dissipated in the viscous range. The Taylor scale λ marks the length scale above which the influence of dissipation is still negligible.

A suitable way to characterize the stationary, homogeneous, and isotropic flow field $\mathbf{v}(\mathbf{x}, t)$ in the *inertial range* between L and λ is via the probability density function $p(u, r)$ of longitudinal velocity increments [36]

$$u(r) := \mathbf{e} \cdot (\mathbf{v}(\mathbf{x} + \mathbf{e}r, t) - \mathbf{v}(\mathbf{x}, t)). \quad (1)$$

Here, r denotes the scale at which the velocity difference u is evaluated, \mathbf{e} is a unit vector and due to the average symmetries of the turbulent flow, the statistical properties of u only depend on r . Fig. 1 shows histograms of this distribution using data obtained in a turbulent air jet experiment [25]. In this setup, $L = 6.7$ cm, $\lambda = 6.6$ mm, and the nozzle-based Reynolds number is about $2.7 \cdot 10^4$. The flow velocity $v(t)$ is measured a distance of 125 nozzle diameters away from the nozzle and then converted to a flow field $v(\mathbf{x})$ by use of the Taylor hypothesis. Chopping $v(\mathbf{x})$ into non-overlapping intervals, $N = 5 \cdot 10^4$ trajectories $u(r)$ are obtained from which the shown histograms are compiled. As Fig. 1 clearly shows, $p(u, r)$ exhibits a Gaussian form for scales $r \approx L$ and develops pronounced non-Gaussian tails towards scales $r \approx \lambda$. This effect is commonly referred to as *small-scale intermittency*, as intermittent bursts in $\mathbf{v}(\mathbf{x})$ cause the boosted occurrence of large values of u on small scales [38].

An inventive approach to characterize the properties of the distribution $p(u, r)$ in the inertial range is to interpret $u(r)$ as realizations of a *Markov process* on the eddy hierarchy with the scale r playing the role of time [39]. The

evolution of $p(u, r)$ is then described by a Master equation with initial condition at $r = L$, for which a Kramers-Moyal expansion [40] may be performed. For a variety of experimental situations, the Markovian character of $u(r)$ was verified, and the coefficients $D^{(k)}$ of the corresponding Kramers-Moyal expansion were determined on the basis of experimental data [41–44]. Moreover, in the limit of large Reynolds number, it is possible to systematically derive the Master equation governing the evolution of $p(u, r)$ from the underlying Navier-Stokes equations of the fluid flow and to recursively calculate the coefficients $D^{(k)}$ [45, 46]. In either way, one finds that drift and diffusion coefficients, $D^{(1)}$ and $D^{(2)}$ respectively, have well-defined, non-zero limits, whereas all higher coefficients in the Kramers-Moyal expansion vanish asymptotically. We are thus left with a Fokker-Planck equation (FPE) of the form

$$-\partial_r p(u, r | u_L, L) = [-\partial_u D^{(1)}(u, r) + \partial_u^2 D^{(2)}(u, r)] p(u, r | u_L, L) \quad (2)$$

ruling the statistics of velocity increments on the eddy-hierarchy of developed turbulence. The minus sign on the l.h.s. of the FPE indicates that the evolution proceeds from large to small scales.

The drift and diffusion coefficients, $D^{(1)}$ and $D^{(2)}$, typically depend on r and u ; for the data shown in Fig. 1 one obtains, e.g., [25]

$$D^{(1)}(u, r) = -a_0 r^{0.6} - a_1 r^{-0.67} u + a_2 u^2 - a_3 r^{0.3} u^3 \quad (3)$$

$$D^{(2)}(u, r) = b_0 r^{0.25} - b_1 r^{0.2} u + b_2 r^{-0.73} u^2 \quad (4)$$

with

$$a_0 = 0.0015, \quad a_1 = 0.61, \quad a_2 = 0.0096, \quad a_3 = 0.0023, \\ b_0 = 0.033, \quad b_1 = 0.009, \quad b_2 = 0.043.$$

The stochastic dynamics defined by (2) therefore exhibits characteristics of a *driven non-equilibrium* system. This is apparent also from the difference between $p(u, r)$ and the *instantaneous* stationary distribution of the FPE (2) for fixed scale r given by

$$p^{\text{st}}(u, r) = \frac{e^{-\varphi(u, r)}}{Z(r)}, \quad Z(r) = \int e^{-\varphi(u, r)} du \quad (5)$$

with the stochastic potential

$$\varphi(u, r) = \ln D^{(2)}(u, r) - \int_{-\infty}^u \frac{D^{(1)}(u', r)}{D^{(2)}(u', r)} du'. \quad (6)$$

Examples of $p^{\text{st}}(u, r)$ have been included into Fig. 1.

In the spirit of stochastic thermodynamics [3], we now associate with every individual trajectory $u(r)$ a total

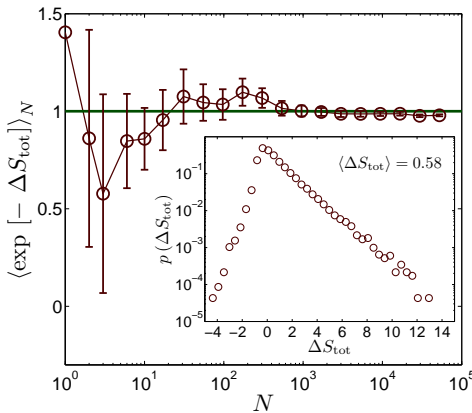


FIG. 2. Empirical average $\langle \exp[-\Delta S_{\text{tot}}] \rangle_N$ defined in (9) for the experimental data of Fig. 1 as a function of the sample size N . According to the fluctuation theorem (8), the average has to converge to the horizontal line. The inset depicts the corresponding distribution of the total entropy production ΔS_{tot} as defined by (7).

entropy production

$$\Delta S_{\text{tot}}[u(\cdot)] = - \int_L^\lambda \partial_r u(r) \partial_u \varphi(u(r), r) dr - \ln \frac{p(u_\lambda, \lambda)}{p(u_L, L)}. \quad (7)$$

In the usual thermodynamic setting, the first term on the r.h.s. of (7) would describe the heat exchange with the reservoir, whereas the second one gives the entropy change of the system itself. The total entropy production (7) fulfills the integral FT [47]

$$\langle e^{-\Delta S_{\text{tot}}} \rangle_{u(\cdot)} = 1, \quad (8)$$

where the average is over the different realizations of $u(r)$.

A reliable estimate of the exponential average in (8) on the basis of a finite sample set is possible only if trajectories with $\Delta S_{\text{tot}}[u(\cdot)] < 0$ occur with sufficient frequency. We have used subsets of size N of the realizations for $u(r)$ underlying Fig. 1 together with their entropy productions determined by (7) and calculated the empirical average

$$\langle e^{-\Delta S_{\text{tot}}} \rangle_N = \frac{1}{N} \sum_{i=1}^N e^{-\Delta S_{\text{tot}}^{(i)}} \quad (9)$$

corresponding to (8). The results shown in Fig. 2 demonstrate that convergence to the asymptotic value is rather fast. This is corroborated by the appreciable weight of

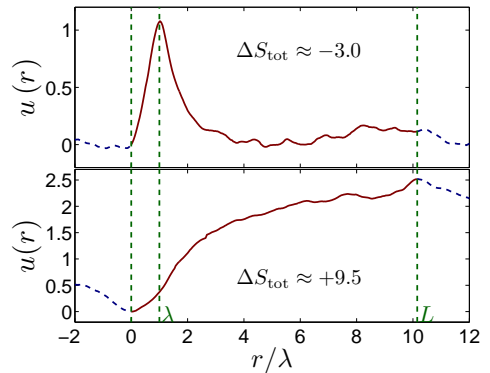


FIG. 3. Typical form of measured velocity increments $u(r)$ (full lines) realizing a very small (top) and a very large (bottom) entropy production ΔS_{tot} defined by (7). The dashed lines show the average part of $v(x)$ neighboring $u(\cdot)$. The Taylor scale λ and integral scale L are indicated by vertical lines.

trajectories with *negative* entropy production in the distribution $p(\Delta S_{\text{tot}})$ shown in the inset. The macroscopic fluctuating flow fields of developed turbulence therefore share important features with the thermodynamic variables of nanoscopic non-equilibrium systems under the influence of thermal noise. In particular, in both cases the respective probability distributions are sufficiently broad to allow an application of the concepts of stochastic thermodynamics.

The convergence of the empirical average (9) to the theoretical value 1 given by (8) also indicates that the drift and diffusion coefficients (3), (4), estimated on the basis of the experimental data, describe the stochastic properties of the process $u(r)$ rather well. Conversely, by monitoring (9) during the numerical estimation of $D^{(1)}$ and $D^{(2)}$, one has a simple, “on-the-fly” criterion to quantify the accuracy of this estimation with an emphasis on the precise modeling of entropy-consuming events. The method presently used for the verification of $D^{(1)}$ and $D^{(2)}$ involves the numerical solution of the FPE with the estimated drift and diffusion coefficients and a comparison with the underlying experimental trajectories [25], which is, of course, a much more cumbersome procedure.

It is interesting to elucidate some characteristics of the entropy-consuming trajectories. To contrast entropy-consumption with entropy production, we show in Fig. 3 the *average* of 50 extreme sequences $u(r)$ giving rise to very small and very large values of ΔS_{tot} respectively. These averages display the distinct features common to all individual trajectories of the corresponding class. As expected, trajectories giving large and small values of ΔS_{tot} look rather different from each other. Large en-

tropy production, as shown in the bottom panel of Fig. 3, is related to a continuous decrease of u for decreasing r . In contrast, *negative* values of ΔS_{tot} require violent fluctuations at *small* scales together with a smooth flow at large scales as shown in the top panel of Fig. 3. Therefore, the same class of fluctuations that causes small-scale intermittency in developed turbulence also ensures the good convergence of the integral FT (8).

This connection becomes also apparent when studying the deviations from dimensional scaling in developed turbulence. Consider the moments

$$S^n(r) = \int u^n p(u, r) du \quad (10)$$

of the distribution $p(u, r)$. The self-similar eddy-hierarchy suggests scaling laws for these moments of the form $S^n(r) \propto r^{\zeta_n}$ defining the scaling exponents ζ_n . A relation for these exponents, the so-called *K62 scaling*, was proposed in 1962 by Kolmogorov and Oboukhov on the basis of dimensional analysis and some simplifying assumptions about the stochastic energy transfer between scales [48, 49]:

$$\zeta_n = \frac{n}{3} - \mu \frac{n(n-3)}{18}. \quad (11)$$

The intermittency factor μ describes deviations from pure dimensional (K41 [50]) scaling. It is an experimental fit factor with typical values of about 0.25 [36]. For the data of Fig. 1 $\mu \approx 0.227$.

Choosing

$$D^{(1)}(u, r) = -\frac{3+\mu}{9r}u, \quad D^{(2)}(u, r) = \frac{\mu}{18r}u^2, \quad (12)$$

the stochastic dynamics (2) reproduces the K62 scaling (11) for the moments (10) for any initial distribution $p(u_L, L)$ [25, 42]. Note that this is already the most general case: In order to find a scaling law $S^n(r) \propto r^{\zeta_n}$ from the Fokker-Planck dynamics (2), one must have $D^{(1)} \sim u/r$ and $D^{(2)} \sim u^2/r$ [51].

These dependencies are, however, also special with respect to the FT (8). Given (12), we may transform to logarithmic “time” $\log L/r$ to end up with a FPE describing a *stationary* process without external driving. The FT then merely describes the *relaxation* process from an initial non-equilibrium distribution to the stationary state $p^{\text{st}} = \delta(u)$ where all $S^n(r) \rightarrow 0$ [39, 52]. Corrections to K62 scaling therefore correspond to a non-trivial “time” dependence of drift and diffusion coefficients in the FPE and hence express genuine non-equilibrium dynamics along the eddy-hierarchy.

To highlight the sensitivity of the FT to small-scale intermittency, we specify (8) to the drift and diffusion coefficients (12) of K62 scaling. Using (6) and (7), we find

$$\left\langle \frac{u_r'' p_r(u_r)}{u_L'' p_L(u_L)} \right\rangle = 1, \quad (13)$$

with $\nu = \frac{6+4\mu}{\mu} \approx 28$. This large value of ν is consistent with the qualitative picture discussed above: Trajectories corresponding to large values of ΔS_{tot} have $u_L > u_r$, whereas those with negative ΔS_{tot} feature $u_L < u_r$. Using data from numerical simulations of the Langevin equation corresponding to (12), we indeed find a smooth convergence of (13) for sample sizes of 10^4 or larger.

The crucial point, however, is that (13) fails dramatically for realistic turbulent flows. Using again the experimental data of Fig. 1, the average in (13) results into about 10^{70} instead of 1! The value 1 is only approached if small-scale fluctuations occur with the frequency characteristic for the K62 model. The much more frequent and stronger fluctuations of a *realistic* turbulent flow, however, cause the rapid divergence of (13), which we explain by the well known fact that K62 underestimates the frequency of large fluctuations on small scales (i.e., the scaling (11) is only good for $n \lesssim 10$ [36, 53]). Hence, the corresponding failure of K62 to accurately describe the *tails* of $p(u, r)$ is most strikingly demonstrated by the breakdown of (13).

In conclusion, we have shown that the violent small-scale fluctuations in turbulent flows make developed turbulence an interesting model system for stochastic thermodynamics. We have proposed an integral fluctuation theorem that characterizes the stochastic evolution of velocity increments along the eddy-hierarchy which is extremely sensitive to the precise modeling of small-scale intermittency. Moreover, it may be used as a simple “sum-rule” to quantify the accuracy of parameter estimation from experimental data drawn from turbulent flows. As also other models of developed turbulence like those yielding scaling laws different from K62 [54, 55], propagator methods [56], or field-theoretic approaches [45, 57] correspond to a Markovian dynamics of velocity increments on the eddy-hierarchy [46, 51, 58] it should be interesting to apply our analysis also to these approaches.

Acknowledgments. We thank C. Renner, R. Friedrich and J. Peinke for providing us with excellent data, and R. Friedrich, C. Honisch, O. Kamps, M. Niemann, J. Peinke and M. Wächter for fruitful discussions. DN acknowledges financial support from the Deutsche Forschungsgemeinschaft under grant EN 278/7 and from the Heinz-Neumüller foundation.

* d.nickelsen@uni-oldenburg.de

- [1] D. J. Evans, E. G. D. Cohen, and G. P. Morriss, Phys. Rev. Lett. **71**, 2401 (1993).
- [2] C. Jarzynski, Phys. Rev. Lett. **78**, 2690 (1997).
- [3] U. Seifert, Rep. Prog. Phys. **75**, 126001 (2012).
- [4] C. Jarzynski, Annu. Rev. Cond. Mat. **2**, 329 (2011).
- [5] A. Pohorille, C. Jarzynski, and C. Chipot, J. Phys. Chem. B **114**, 10235 (2010).

- [6] M. Palassini and F. Ritort, Phys. Rev. Lett. **107**, 060601 (2011).
- [7] U. Seifert, Phys. Rev. Lett. **106**, 020601 (2011).
- [8] C. Van den Broeck, N. Kumar, and K. Lindenberg, Phys. Rev. Lett. **108**, 210602 (2012).
- [9] S. Toyabe, T. Sagawa, M. Ueda, E. Muneyuki, and M. Sano, Nat. Phys. **6**, 988 (2010).
- [10] D. Mandal and C. Jarzynski, Proc. Natl. Acad. Sci. USA **109**, 11641 (2012).
- [11] D. Collin *et al.*, Nature **437**, 231 (2005).
- [12] I. Junier, A. Mossa, M. Manosas, and F. Ritort, Phys. Rev. Lett. **102**, 070602 (2009).
- [13] C. Jarzynski, Nat. Phys. **7**, 591 (2011).
- [14] G. M. Wang, E. M. Sevick, E. Mittag, D. J. Searles, and D. J. Evans, Phys. Rev. Lett. **89**, 050601 (2002).
- [15] J. Mehl, B. Lander, C. Bechinger, V. Blickle, and U. Seifert, Phys. Rev. Lett. **108**, 220601 (2012).
- [16] S. Ciliberto, S. Joubaud, and a. Petrosyan, Journal of Statistical Mechanics: Theory and Experiment **2010**, P12003.
- [17] K. Feitosa and N. Menon, Phys. Rev. Lett. **92**, 164301 (2004).
- [18] A. Naert, Europhys. Lett. **97**, 20010 (2012).
- [19] S.-H. Chong, M. Otsuki, and H. Hayakawa, Phys. Rev. E **81**, 041130 (2010).
- [20] J. Jimenez, Annu. Rev. Fluid Mech. **36**, 173 (2004).
- [21] P. E. Dimotakis, Annu. Rev. Fluid Mech. **37**, 329 (2005).
- [22] A. J. Arnfield, Int. J. Climatol. **23**, 1 (2003).
- [23] F. Böttcher, S. Barth, and J. Peinke, Stoch. Env. Res. Risk. A. **21**, 299 (2006).
- [24] P. Milan, M. Wächter, and J. Peinke, Phys. Rev. Lett. **110**, 138701 (2013).
- [25] C. Renner, J. Peinke, and R. Friedrich, J. Fluid Mech. **433**, 383 (2001).
- [26] X.-D. Shang, P. Tong, and K.-Q. Xia, Phys. Rev. E **72**, 015301 (2005).
- [27] E. Falcon, S. Aumaître, C. Falcón, C. Laroche, and S. Fauve, Phys. Rev. Lett. **100**, 064503 (2008).
- [28] S. Ciliberto *et al.*, Physica A **340**, 240 (2004).
- [29] M. M. Bandi, J. R. Cressman, and W. I. Goldburg, J. Stat. Phys. **130**, 27 (2007).
- [30] S. Aumatre, S. Fauve, S. McNamara, and P. Poggi, Eur. Phys. J. B **19**, 449 (2001).
- [31] T. Gilbert, Europhys. Lett. **67**, 172 (2004).
- [32] G. Gallavotti, L. Rondoni, and E. Segre, Physica D **187**, 338 (2004).
- [33] G. Gallavotti and E. G. D. Cohen, Phys. Rev. Lett. **74**, 2694 (1995).
- [34] M. Baiesi and C. Maes, Phys. Rev. E **72**, 056314 (2005).
- [35] L. D. Landau and E. M. Lifshitz, *Fluid Mechanics* (Butterworth-Heinemann, 1987).
- [36] U. Frisch, *Turbulence* (Cambridge University Press, 1995).
- [37] L. F. Richardson, *Weather prediction by numerical process* (Cambridge University Press, 1922).
- [38] K. R. Sreenivasan and R. A. Antonia, Annu. Rev. Fluid Mech. **29**, 435 (1997).
- [39] R. Friedrich and J. Peinke, Phys. Rev. Lett. **78**, 863 (1997).
- [40] H. Risken, *The Fokker-Planck equation: methods of solution and applications* (Springer, 1989).
- [41] P. Marcq and A. Naert, Physica D **124**, 368 (1998).
- [42] R. Friedrich, J. Peinke, M. Sahimi, and M. Reza Rahimi Tabar, Phys. Rep. **506**, 87 (2011).
- [43] C. Honisch and R. Friedrich, Phys. Rev. E **83**, 066701 (2011).
- [44] D. Kleinhans, Phys. Rev. E **85**, 026705 (2012).
- [45] V. Yakhot, Phys. Rev. E **57**, 1737 (1998).
- [46] J. Davoudi and M. R. Tabar, Phys. Rev. Lett. **82**, 1680 (1999).
- [47] U. Seifert, Phys. Rev. Lett. **95**, 040602 (2005).
- [48] A. N. Kolmogorov, J. Fluid Mech. **13**, 82 (1962).
- [49] A. M. Oboukhov, J. Fluid Mech. **13**, 77 (1962).
- [50] A. N. Kolmogorov, Dokl. Akad. Nauk. SSSR **30**, 299 (1941).
- [51] I. Hosokawa, Phys. Rev. E **65**, 027301 (2002).
- [52] M. Esposito and C. Van den Broeck, Phys. Rev. Lett. **104**, 090601 (2010).
- [53] F. Anselmet, Y. Gagne, E. J. Hopfinger, and R. A. Antonia, J. Fluid Mech. **140**, 63 (1984).
- [54] Z.-S. She and E. Leveque, Phys. Rev. Lett. **72**, 336 (1994).
- [55] V. S. Lvov and I. Procaccia, Phys. Rev. E **62**, 8037 (2000).
- [56] B. Castaing, Y. Gagne, and E. Hopfinger, Physica D **46**, 177 (1990).
- [57] V. Yakhot, J. Fluid Mech. **495**, 135 (2003).
- [58] P. Amblard and J. Brossier, Eur. Phys. J. B **12**, 579 (1999).

The K62 second law We add a discussion concerning the K62 iFT from equation (13),

$$\left\langle \frac{u_r^\nu p_r(u_r)}{u_L^\nu p_L(u_L)} \right\rangle = 1. \quad (\text{II.4.1})$$

Note that via $g = 2 - \nu$, the parameter $\nu \approx 27$ is directly related to the exponential growth rate g of geometric Brownian motion, where $g > 1$ signifies divergence and $g < 1$ signifies decay in the evolution of the stochastic variable, see the discussion after (A.1.14). As $\nu \geq 4$, we always have a negative growth rate $g \leq -2$ and therefore decaying turbulence, as it should be.

Analogous to recovering the second law from an iFT, cf. (I.2.71), we find from (II.4.1) by exponentiation and application of Jensen's inequality the second law like inequality

$$\left\langle \ln \frac{u_L}{u_r} \right\rangle \geq \frac{1}{\nu} \left\langle \ln \frac{p_r(u_r)}{p_L(u_L)} \right\rangle. \quad (\text{II.4.2})$$

We recognise on the r.h.s. the Shannon entropy $S(r) = -\langle \ln p_r(u) \rangle$, and, in view of the K62 random cascade model, cf. (II.3.3), we identify the l.h.s. as the sum of the averaged logarithm of the multipliers $h_i = u_i/u_{i+1}$, and write

$$\langle \ln H_r \rangle = \sum_{i=1}^{s(r)} \langle \ln h_i \rangle \leq \frac{1}{\nu} \Delta S. \quad (\text{II.4.3})$$

Here, $s(r)$ is the number of stages the cascade took until it reached a scale r , cf. (II.3.2), $H_r = h_1 h_2 \cdots h_{s(r)}$ is the overall multiplier such that $u_r = H_r u_L$, and $\Delta S(r) = S(r) - S(L)$ is the difference in Shannon entropy between final and initial stage of the cascade.

In section I.2.4, we discussed the condition $S_m \sim -\Delta S$ under which the validity of a FT can be expected to be observable in a system, where S_m was defined as the entropy transferred into a heat bath. Here, we have $S_m = -\ln H_r$, the formally introduced entropy S_m therefore accounts for the overall multiplier statistics.

The Shannon entropy $S(r)$ can be computed up to quadrature from the solution (II.3.15) of the K62 process (II.3.14a) and, as shown in figure

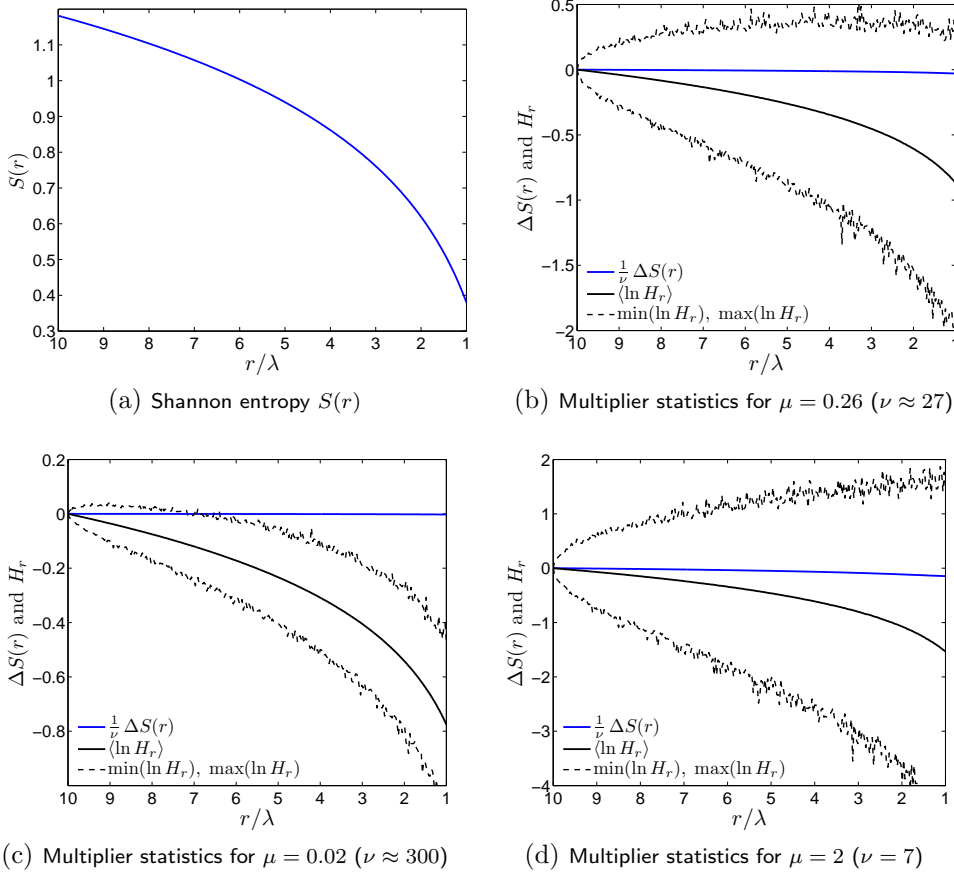


Figure II.5: Illustration of the second law for the K62 model for $L = 10$ and $\lambda = 1$. The Shannon entropy $S(r) = -\langle \ln p(u, r) \rangle_u$, shown in (a), determines via $\Delta S(r) = S(L) - S(r) < 0$ the upper bound for the average of the overall log-multiplier $\ln H_r = \ln u_L / u_r$ in the second law like inequality (II.4.3). The average log-multiplier $\langle \ln H_r \rangle$, and its minimum and maximum value is depicted in (b), (c) and (d) for various values of intermittency factor μ , together with the upper bound $\frac{1}{\nu} \Delta S(r) < 0$ for $\langle \ln H_r \rangle$. To determine $S(r)$, the analytic solutions for $p(u, r)$ from (II.3.15) was used, see also figure II.4. The multiplier statistics was obtained from generating 10^6 samples of $u(r)$ from the solution (II.3.13) of the corresponding SDE.

II.5a, is found to be positive for all scales and decreasing for increasing intervals $L - r$. Due to the latter property, the difference in Shannon entropy

is negative, and therefore also the upper bound for the sum of multipliers. Hence, the multiplier statistics must be such that strictly $\langle H_r \rangle < 1$, that is, multipliers $h_i < 1$ outbalance $h_i > 1$ on average and velocity increments $u(r)$ predominantly decrease in the cascade process. This is a reasonable statement for a second law - like inequality with regard to a turbulent cascade.

Single realisations of H_r , however, may still be positive, corresponding to instances where $h_i > 1$ outbalance $h_i < 1$ and velocity increments $u(r)$ predominantly increase in the cascade process. Taking the commonly accepted value of $\mu = 0.26$ for the intermittency factor, Figure II.5b shows the upper bound $\frac{1}{\nu}\Delta S$, together with the average multiplier $\langle \ln H_r \rangle$ and maximum and minimum values of $\ln H_r$, where the set of multipliers H_r was determined from generating 10^6 samples of $u(r)$ from the solution (II.3.13) of the K62 process (II.3.17). It is evident that the upper bound $\frac{1}{\nu}\Delta S$ only plays a minor role, compared to $\langle \ln H_r \rangle$ it can be taken as zero. For increasing intervals $L - r$, the average multiplier $\langle \ln H_r \rangle$ decreases, indicating that instances of increasing velocity increments over short ranges of scales are more likely than those over large ranges of scale, a result being in agreement with intuition. On the other hand, the maximal realisations $\ln H_r$ remain more or less constantly at a positive level, indicating that instances of increasing velocity increments over the complete range of scales remain possible. These instances, as discussed in [3], are both indispensable for the convergence of the FT and responsible for small-scale intermittency.

We included into figure II.5 the same analysis for two other values of the intermittency factor, $\mu = 0.02$ corresponding to vanishing intermittency, and $\mu = 2$ corresponding to extreme intermittency. For $\mu = 0.02$, practically no instances $\ln H_r > 0$ occur, in particular for large scale intervals $L - r$. For $\mu = 2$, despite decreasing $\langle \ln H_r \rangle$ for increasing $L - r$, the value of maximal multipliers H_r even increases for large scale intervals $L - r$.

The last point to make concerns the relation to an inverse energy cascade which was, due to its intricacy, not discussed in [3]. If we accept that in an inverse cascade velocity increments increase while evolving downwards in scale, we can argue that the realisations $u(\cdot)$ giving rise to extreme negative values of $S_{\text{tot}}[u(\cdot)]$, shown in figure 3 in [3], signify an inverse energy

cascade.³⁴ However, as mentioned in chapter II.3.1, it is disputable to interpret a single realisation $u(\cdot)$ as a single cascade. A realisation $u(\cdot)$ is merely a spatial snapshot of the outcome of a superordinate cascade process, and rather not the velocity of a certain eddy as it evolves down-scale.

II.4.2 Beyond K62 scaling

We now turn to discuss the expressions for entropy production arising from the various Markov representations of traditional approaches to turbulence discussed in the previous chapter. When appropriate, we also discuss the resulting integral fluctuation theorems and the implied second law. Starting point will always be the drift and diffusion coefficients.

Multifractal model We have seen in II.3.2 that by choosing

$$D^{(1)}(u, r) = - \sum_{k=0}^N \frac{d_k^{(1)}}{r} u^k, \quad D^{(2)}(u, r) = \sum_{k=0}^N \frac{d_k^{(2)}}{r} u^k, \quad (\text{II.4.4})$$

the structure functions obey a spectrum of scaling laws, which is the essence of the multifractal model discussed in II.2.3. For the discussion of FTs it is more convenient to consider instead of the $D^{(1)}(u, r)$ the coefficient

$$F(u, r) = D^{(1)}(u, r) - D^{(2)'}(u, r) = - \sum_{k=0}^N \frac{f_k}{r} u^k \quad (\text{II.4.5})$$

where $f_k = (d_k^{(1)} + k d_{k+1}^{(2)})/d_0^{(2)}$, and we will use $d_k = d_k^{(2)}/d_0^{(2)}$.

The EP $S_m[u(\cdot)]$ that is associated with the entropy transferred into a heat bath follows according to (I.2.41a) from the integral

$$S_m[u(\cdot)] = \int_L^r \partial_{r'} u(r') [-\partial_u \varphi(u(r'), r')] \, dr', \quad (\text{II.4.6a})$$

$$\partial_u \varphi(u, r) = - \frac{F(u, r)}{D(u, r)}. \quad (\text{II.4.6b})$$

³⁴Measurements show that the fluctuations of energy transfer are of the same order of magnitude as the average energy dissipation rate $\bar{\varepsilon}$ [115], being reminiscent of $\Delta\mathcal{F} \sim k_B T$, which is the condition in order to expect the convergence of FTs.

II Universal features of turbulent flows

For this class of MPs, the integral in the EP $S_m[u(\cdot)]$ can be explicitly calculated. To accomplish the integration, we consider the power series expansion

$$\partial_u \varphi(u, r) = \frac{f_0 + f_1 u + f_2 u^2 + \cdots + f_N u^N}{1 + d_1 u + d_2 u^2 + \cdots + d_N u^N} = \sum_{n=0}^{\infty} a_n u^n, \quad (\text{II.4.7})$$

where the coefficients a_n are to be determined. Indeed, successive differentiation of the above fraction and an observant eye leads to the finding that the a_n are the solution of the linear set of equation

$$D_n^j a^n = f_j \quad \Rightarrow \quad a^n = (D^{-1})_n^j f_j \quad (\text{II.4.8})$$

with the coefficient matrix and its inverse,

$$\mathbf{D} = \begin{pmatrix} 1 & 0 & 0 & \cdots \\ d_1 & 1 & 0 & \cdots \\ d_2 & d_1 & 1 & \cdots \\ \vdots & \ddots & \ddots & \ddots \end{pmatrix} \quad \text{and} \quad \mathbf{D}^{-1} = \begin{pmatrix} \bar{d}_0 & 0 & 0 & \cdots \\ \bar{d}_1 & \bar{d}_0 & 0 & \cdots \\ \bar{d}_2 & \bar{d}_1 & \bar{d}_0 & \cdots \\ \vdots & \ddots & \ddots & \ddots \end{pmatrix}. \quad (\text{II.4.9})$$

Owing to the diagonal structure of the matrix and the fact that the \bar{d}_k are the solution of the homogeneous equation, the entries of the inverse matrix can be determined from the recursion

$$\bar{d}_n = - \sum_{k=0}^{n-1} \frac{d_{n-k}}{\bar{d}_k}. \quad (\text{II.4.10})$$

For the coefficients of the power series follows finally

$$a_n = \sum_{k=0}^n \bar{d}_{n-k} f_k. \quad (\text{II.4.11})$$

Having this set, the EP becomes

$$\begin{aligned} S_m[u(\cdot)] &= \int_L^r \partial_{r'} u(r') [-\partial_u \varphi(u(r'), r')] \, dr' \\ &= \sum_{n=0}^{\infty} \frac{a_n}{n+1} \left(u_L^{n+1} - u_r^{n+1} \right). \end{aligned} \quad (\text{II.4.12})$$

The associated second law constitutes a constraint for the structure functions,

$$\sum_{n=1}^{\infty} \frac{a_{n-1}}{n} \left[S_u^n(L) - S_u^n(r) \right] \geq \left\langle \ln \frac{p_r(u_r)}{p_L(u_L)} \right\rangle = -\Delta S. \quad (\text{II.4.13})$$

At this point, however, an explicit form of f_k and d_k is needed, in order to compute the coefficients a_n .

As already mentioned, the full correspondence to the multifractal model is to be expected if the power series in (II.4.4) is written as an integral, cf. (II.3.26). In this case, the recursive equation for $\bar{d}(n)$ should turn into a differential equation, and the equation for the coefficient $a(n)$ becomes a convolution integral. However, we leave the continuous formulation for further study.

Random cascade models In the Markovian description, the class of log-normal random cascade models are defined by drift and diffusion of the form $D^{(1)}(u, r) = -\tilde{a}(r)u$ and $D^{(2)}(u, r) = b(r)u^2$. Again, we rewrite the drift $D^{(1)}$ as the coefficient $F = D^{(2)} - D^{(2)'}$, that is

$$F(u, r) = -a(r)u, \quad D(u, r) = b(r)u^2, \quad (\text{II.4.14})$$

where $a(r) = \tilde{a}(r) + 2b(r)$.

We define the scale function $\Lambda(r) := a(r)/b(r)$ and the log-multiplier $H(r) := \ln \frac{u(r)}{u_L} = \sum_{i=1}^{s(r)} \ln h_i$, cf. (II.4.3), such that we can write for S_m

$$\begin{aligned} S_m[u(\cdot)] &= - \int_L^r \frac{a(r')}{b(r')} \frac{\partial_{r'} u(r')}{u(r')} dr' \\ &= - \int_L^r \Lambda(r') \frac{dH(r')}{dr'} dr' \\ &= - \int_0^{H(r)} \Lambda(r(H')) dH'. \end{aligned} \quad (\text{II.4.15})$$

Here, $r(H)$ is the scale reached after the cascade has performed $s(r)$ cascade stages. The scale function $\Lambda(r)$ may be interpreted as the EP rate

along the scale-path $r(H)$ as a function of the log-multiplier H . By choosing $\Lambda(r)$ we can hence influence the form of the EP $S_m[u(\cdot)]$, which raises hope that a suitable $f(r)$, defining a meaningful EP $S_m[u(\cdot)]$ in the context of a turbulence cascades, also defines a meaningful MP in terms of the resulting $D^{(1,2)}(u, r)$. Attempts along such lines, however, remained unsatisfactory.

For K62 scaling it is $\Lambda(r) \equiv \nu$ and we retrieve the K62 FT (II.4.1). Due to cancellation, the form of the K62 FT is also obtained for an arbitrary choice of $a(r) = b(r)$, i.e. continuous self-similarity. Accordingly, the FT for scaling laws of the form $S_u^n(r) = [f(r)]^{\zeta_n}$ is insensitive to the function $f(r)$, including the ESS case $f(r) = S_u^3(r)$.

To inspect a FT that deviates from the K62 form, we employ the experimental results by Castaing and co-workers which we discussed in chapter II.2.4. Their object of investigation was the variance of energy transfer fluctuations, for which they found $\sigma_r \sim r^{-\delta}$ with $\delta \approx 0.3$, cf. (II.2.46). This variance also determines the variance of the propagator in the associated log-normal random cascade model, for which we found in (II.3.35b) that $b(r) \sim \partial_r \sigma_r \sim r^{-\beta-1}$. Accordingly, we keep the K41 coefficient $a(r)$ and modify the K62 coefficient $b(r)$,

$$\begin{aligned} a(r) &= \frac{3+2\mu}{9} \frac{1}{r}, \quad b(r) = \frac{\mu}{18} \frac{1}{r^{1+\delta}} \\ \Rightarrow \quad \Lambda(r) &= \nu r^\delta \end{aligned} \tag{II.4.16}$$

such that $\delta = 0$ recovers the K62 result. The explicit formula for the associated EP S_m reads

$$\begin{aligned} S_m[u(\cdot)] &= \int_{\Lambda_0}^{\Lambda(r)} \ln u(r(\Lambda')) \, d\Lambda' - \left[\Lambda' \ln u(r(\Lambda')) \right]_{\Lambda_0}^{\Lambda(r)} \\ &= \delta \int_L^r r'^{\delta-1} \ln u(r') \, dr' - \left[r'^\delta \ln u(r') \right]_L^r. \end{aligned} \tag{II.4.17}$$

To assess the validity of the resulting FT, we used the same data as in chapter II.4.1 to compute the ensemble $\{S_m[u(\cdot)]\}$ from the above formula and plugged the result into the FT

$$1 = \left\langle \frac{p_r(u_r)}{p_L(u_L)} e^{-S_m[u(\cdot)]} \right\rangle. \tag{II.4.18}$$

Unfortunately, for the predicted value of $\delta = 0.3$ the FT exhibits a similar divergence as for K62, and even a variation of δ did not improve the situation.

We offer an explanation for this failure of applying the FT for random cascade models to experimental data. Standard random cascade models, as considered by drift and diffusion coefficients above, do not account for the skewness of the PDFs $p(u, r)$ observed in experiments and demanded by the four-fifth law. A vanishing skewness of $p(u, r)$, however, implies a vanishing energy dissipation rate $\bar{\varepsilon}$ ruling out irreversible processes in the flow. But it is the very balance between irreversible process and their reversals the derivation of FTs rest on, suggesting that the skewness in a model of turbulence is crucial for the validity of the resulting FT for real data.

More promising might be the log-Poisson random cascade model by She and Leveque, for which we found a jump process underlying a Liouville process, cf. (II.3.30). The Liouville process is defined by the deterministic drift $D^{(1)}(u, r) = -1/9 u/r$, and the jump process is characterised by a transition probability $\chi(u^+|u, r)$ for a jump velocity increment from u to u^+ at scale r , for which we found the moments $\Psi^{(k)}(u, r) = C_0 (bu)^k/r$ with $b = \beta^{1/3} - 1$. The drift implies the scaling $u(r) = u_L(r/L)^{1/9}$.

In order to extract the pure jump process, it is convenient to consider the scaled velocity increments $\tilde{u}(r) := (\frac{L}{r})^{\frac{1}{9}} u(r)$ and scaled transition probability $\tilde{\chi}(\tilde{u}^+|\tilde{u}, r) := (\frac{L}{r})^{\frac{1}{9}} \chi((\frac{L}{r})^{\frac{1}{9}} \tilde{u}^+ | (\frac{L}{r})^{\frac{1}{9}} \tilde{u}, r)$.

From considerations similar to those in chapter (I.2.3), it follows that the EP $S_m[\tilde{u}(\cdot)]$ is determined by [29]

$$S_m[\tilde{u}(\cdot)] = \sum_{j=1}^n \ln \frac{\tilde{\chi}(\tilde{u}_j^+|\tilde{u}_j, r_j)}{\tilde{\chi}(\tilde{u}_j|\tilde{u}_j^+, r_j)}, \quad (\text{II.4.19})$$

where the sum is over all jumps. The associated FT remains unchanged,

$$1 = \left\langle \frac{\tilde{p}_r(\tilde{u}_r)}{\tilde{p}_L(\tilde{u}_L)} e^{S_m[\tilde{u}(\cdot)]} \right\rangle. \quad (\text{II.4.20})$$

A test of this FT with experimental data is still pending, since the explicit form of $\chi(u^+|u, r)$ remains to be determined from the moments $\Psi^{(k)}(u, r)$.

Yakhot's model Recall drift and diffusion coefficients from Yakhot's model (II.3.44)

$$D^{(1)}(u, r) = -\frac{a_1}{r} u, \quad D^{(2)}(u, r) = \frac{a_2}{r} u^2 - b_2 u \quad (\text{II.4.21})$$

$$a_1 = \frac{B+3}{3(B+1)}, \quad a_2 = \frac{B+3}{3(B+1)(B+2)}, \quad b_2 = \frac{v_{\text{rms}} \lambda}{\sigma_{\infty} L} \frac{1}{B+2},$$

where u , r and b_2 are dimensionless by using the same normalisation as in [3] reprinted in chapter II.4.1. We first simplify

$$\begin{aligned} \partial_u \varphi(u, r) &= \frac{(a_1 + 2a_2)u - b_2 r}{a_2 u^2 - b_2 u r} \\ &= \frac{1}{u} \frac{\nu u - \delta_1 r}{u - \delta_1 r}, \quad \delta_1 := \frac{b_2}{a_2} = \frac{3 v_{\text{rms}} \lambda}{\sigma_{\infty} L} \frac{B+1}{B+3} \end{aligned} \quad (\text{II.4.22})$$

with the K62 parameter $\nu = (2a_2 - a_1)/a_2 = B+4 \approx 24$. In the following we assume that $|u(r)| > \delta_1 r$ in order to ensure $D^{(2)}(u, r) > 0$, which is the known complication with Yakhot's model in the Markov representation (cf. the last paragraph in II.3.2).

We subtract the K62 contribution

$$\begin{aligned} u \cdot \partial_u \varphi(u, r) - \nu &= (\nu - 1) \frac{\delta_1 r / u}{1 - \delta_1 r / u} \\ &= \frac{\nu}{u} + \frac{\nu - 1}{u} \sum_{k=1}^{\infty} \left(\frac{\delta_1 r}{u} \right)^k \end{aligned} \quad (\text{II.4.23})$$

to get the two equivalent expressions

$$\partial_u \varphi(u, r) = \frac{\nu}{u} + \frac{\nu - 1}{u} \frac{\delta_1 r}{u - \delta_1 r} \quad (\text{II.4.24a})$$

$$= \frac{\nu}{u} + \frac{\nu - 1}{u} \sum_{k=1}^{\infty} \left(\frac{\delta_1 r}{u} \right)^k. \quad (\text{II.4.24b})$$

The first expression can be readily integrated to get

$$\varphi(u, r) = \nu \ln u + (\nu - 1) \ln \left(1 - \frac{\delta_1 r}{u} \right) \quad (\text{II.4.25})$$

which implies the non-normalised stationary distribution

$$p_{\text{nn}}^{\text{st}}(u, r) := \exp \left[-\varphi(u, r) \right] = u^{-\nu} \left(1 - \frac{\delta_1 r}{u} \right)^{1-\nu}. \quad (\text{II.4.26})$$

The K62 model is recovered in the limit $\delta_1 \rightarrow 0$. The term involving δ_1 can thus be viewed as the Yakhot extension of the K62 model. Note that $p_{\text{nn}}^{\text{st}}(u, r)$ in the above form is not normalisable.

The second expression for $\partial_u \varphi(u, r)$ in (II.4.24) is convenient to partially perform the integral in $S_{\text{m}}[u(\cdot)]$,

$$\begin{aligned} S_{\text{m}}[u(\cdot)] &= \int_L^r \partial_{r'} u(r') \left[-\partial_u \varphi(u(r'), r') \right] \text{d}r' \\ &= -\nu \int_L^r \frac{\partial_{r'} u(r')}{u(r')} \text{d}r' - (\nu-1) \int_L^r \sum_{k=1}^{\infty} \frac{\partial_{r'} u(r')}{u(r')^{k+1}} (\delta_1 r')^k \text{d}r' \\ &= -\nu \ln \frac{u(r)}{u(L)} + (\nu-1) \left[\sum_{k=1}^{\infty} \frac{1}{k} \left(\frac{\delta_1 r'}{u(r')} \right)^k \right]_L^r + R[u(\cdot)] \\ &= R[u(\cdot)] - \left[\nu \ln u(r') + (\nu-1) \ln \left(1 - \frac{\delta_1 r'}{u(r')} \right) \right]_L^r \\ &= R[u(\cdot)] - \Delta \varphi, \end{aligned} \quad (\text{II.4.27})$$

with the work-like functional

$$\begin{aligned} R[u(\cdot)] &= -(\nu-1) \int_L^r \frac{1}{r'} \sum_{k=1}^{\infty} \left(\frac{\delta_1 r'}{u(r')} \right)^k \text{d}r' \\ &= -(\nu-1) \int_L^r \frac{1}{r'} \frac{\delta_1 r' / u(r')}{1 - \delta_1 r' / u(r')} \text{d}r' \\ &= \delta_1 (\nu-1) \int_L^r \frac{1}{u(r') - \delta_1 r'} \text{d}r' \end{aligned} \quad (\text{II.4.28})$$

The resulting Yakhot FT then reads

$$1 = \left\langle \frac{p_r(u_r)/p_{\text{nn}}^{\text{st}}(u_r, r)}{p_L(u_L)/p_{\text{nn}}^{\text{st}}(u_L, L)} e^{-R[u(\cdot)]} \right\rangle \quad (\text{II.4.29})$$

$$= \left\langle \frac{u_r (u_r - \delta_1 r)^{\nu-1}}{u_L (u_L - \delta_1 L)^{\nu-1}} \frac{p_r(u_r)}{p_L(u_L)} e^{-R[u(\cdot)]} \right\rangle \quad (\text{II.4.30})$$

In the limit $\delta_1 \rightarrow 0$, we have $R[u(\cdot)] \equiv 0$ and recover the K62 FT. Note that by equating $\nu = B + 4$ with the K62 result $\nu = (6 + 4\mu)/\mu$, we obtain the reasonable prediction $\mu = 6/B \approx 0.3$ for $\delta_1 \rightarrow 0$.

For the data from [110] it is $\delta_1 \simeq 0.19$.³⁵ If we cut out all realisations violating $|u(r)| > \delta_1 r$, being about one half of all $\{u(\cdot)\}$, and substituting the remaining $u(\cdot)$ into the r.h.s. of the FT above, we get approximately zero instead of one. Being well below the theoretical value of one implies that negative EPs are too rare, indicating that Yakhot's model underestimates the intermittency of realisations $u(\cdot)$, it therefore stands to reason to expect that incorporating the underlying jump process would correct this discrepancy.

In contrast to random cascade models, the FT can be satisfied by modifying the K62 correction parameter. However, to satisfy the FT, we need a value of $\delta_1 = 6.48$, which is far too out compared to the predicted value $\delta_1 \simeq 0.19$, ruling out to consider corrections of the involved quantities. Also, $\delta_1 = 6.48$ substantially tightens the condition $|u(r)| > \delta_1 r$.

In any case, the inconsistency that $D^{(2)}(u, r) < 0$ for $|u(r)| < \delta_1 r$ remains. Motivated by the constant offset observed in practically all experimentally estimated $D^{(2)}(u, r)$, a modification of the diffusion coefficient in the form $D^{(2)}(u, r) = \delta_0 a_2 - \delta_1 a_2 u + a_2 u^2/r$ seems promising. The only consistent value for δ_0 that ensures $D^{(2)}(u, r) \geq 0$ turns out to be $\delta_0 = \delta_1^2/4$, since for $\delta_0 < \delta_1^2/4$ is $D^{(2)}(u, r) < 0$ still possible, and for $\delta_0 > \delta_1^2/4$ we encounter a complex valued EP $S_{\text{m}}[u(\cdot)]$. However, the resulting FT becomes singular for too large fluctuations of $u(r)$.

For completeness we report that the second law-like equation takes the

³⁵taking $v_{\text{rms}} = 0.3818 \text{ m/s}$, $\lambda = 6.6 \text{ mm}$, $L = 67 \text{ mm}$, $\sigma_{\infty} = 0.54 \text{ m/s}$ and $B = 20$ in
 $\delta_1 = \frac{3v_{\text{rms}}\lambda(B+1)}{L\sigma_{\infty}(B+3)}$

form

$$\left\langle R[u(\cdot)] \ln \frac{u_L (u_L - \delta L)^{\nu-1}}{u_r (u_r - \delta r)^{\nu-1}} \right\rangle \geq \left\langle \ln \frac{p_r(u_r)}{p_L(u_L)} \right\rangle = -\Delta S, \quad (\text{II.4.31})$$

but refrain from attempting an interpretation.

As a last comment, we mention that the above procedure used to obtain the form $S_m[u(\cdot)] = R[u(\cdot)] - \Delta\varphi$ as in (II.4.27) can be generalised to arbitrary polynomial forms of $F(u, r)$ and $D(u, r)$. This generalised procedure is similar to the manipulations of (II.4.7) for the multifractal model, only that the expansion is in $1/u$ instead of u , and the coefficients f_k and d_k may have arbitrary r -dependencies.

II.5 Asymptotic analysis

In this chapter we will apply the asymptotic analysis developed in chapter I.3 to the Markovian description of fully developed turbulence. This analysis will include the examination of realisations giving rise to extreme values of S_m , the asymptotic form of $p(u, r)$ and the resulting asymptotic scaling exponents ζ_n .

The results presented in this chapter are rather preliminary, in the sense that they were obtained only recently.

II.5.1 Realisations of extreme entropy

In the previous chapters we found that small-scale intermittency is formally related to negative EP $S_{\text{tot}}[u(\cdot)] < 0$. From the discussion of the second law-like inequality resulting from the K62 model, (II.4.3), followed that the EP $S_m[u(\cdot)]$ is equivalent to the log-multiplier of velocity increments of the turbulent cascade, and negative $S_m[u(\cdot)]$ imply positive multipliers which signify an inverse turbulent cascade. This interpretation of negative $S_m[u(\cdot)]$ is not as clear for more sophisticated models than K62, however, it is interesting to examine the most likely realisations that give rise to extreme values of $S_m[u(\cdot)]$. These realisations are nothing else than the solutions of the Euler-Lagrange equations (ELE) deriving from the path integral representation of the respective MP.

We can readily transfer the ELE obtained in chapter (I.3.17) to the case of velocity increments $u(r)$,

$$\ddot{u} = \frac{\dot{u} + F}{2D} (D'(\dot{u} - F) + 2\dot{D}) + FF' - \dot{F} + 2DJ'' + 2Dik(\partial_u - d_r \partial_{\dot{u}})w, \quad (\text{II.5.1a})$$

$$0 = \frac{\dot{u}_0 + F_L}{2D_L} - ik\partial_{\dot{u}}w_L + A'_L, \quad (\text{II.5.1b})$$

$$0 = \frac{\dot{u}_\lambda + F_\lambda}{2D_\lambda} - ik\partial_{\dot{u}}w_\lambda. \quad (\text{II.5.1c})$$

Here, in analogy to $x(t)$, primes denote partial derivatives with respect to u and dots with respect to r , and we dropped the arguments of u_r , $F(u_r, r)$, $D(u_r, r)$, $w(u_r, \dot{u}_r, r)$ and derivatives, and indices denote evaluation at scales r , L and λ respectively.

II Universal features of turbulent flows

Substitution of the constraint

$$S_m[u(\cdot)] = \int_L^\lambda w(u_r, \dot{u}_r, r) \, dr, \quad (\text{II.5.2a})$$

$$w(u, \dot{u}, r) = \dot{u} \frac{F(u, r)}{D(u, r)}, \quad (\text{II.5.2b})$$

and simplifications yield

$$\ddot{u} = \frac{1}{2} \frac{D}{D'} (\dot{u}^2 - F^2) + \dot{u} \frac{\dot{D}}{D} + F' F + 2D J' - (1 - 2ik) \frac{\dot{F} D - F \dot{D}}{D} \quad (\text{II.5.3a})$$

$$0 = \frac{\dot{u}_0 + F_L}{2D_L} - ik \frac{F_L}{D_L} + A'_L, \quad (\text{II.5.3b})$$

$$0 = \frac{\dot{u}_\lambda + F_\lambda}{2D_\lambda} - ik \frac{F_\lambda}{D_\lambda}. \quad (\text{II.5.3c})$$

Let us consider as an analytically solvable example the K62 coefficients from (II.3.17),

$$\begin{aligned} F(u, r) &= -a \frac{u}{r}, \quad D(u, r) = b \frac{u}{r^2}, \\ a &= \frac{3 + 2\mu}{9}, \quad b = \frac{\mu}{18}, \end{aligned} \quad (\text{II.5.4})$$

for which the ELE becomes

$$\ddot{u}(r) = \frac{\dot{u}(r)}{u(r)} - \frac{\dot{u}(r)}{r}, \quad (\text{II.5.5a})$$

$$0 = \dot{u}_L L + a(2ik - 1)u_L + 2bu_L^2 A'(u_L), \quad (\text{II.5.5b})$$

$$0 = \dot{u}_\lambda \lambda + a(2ik - 1)u_\lambda. \quad (\text{II.5.5c})$$

The solutions of this ELE are power laws,

$$\bar{u}(r; k) = u_M \left(\frac{r}{L} \right)^{a(1 - 2ik)}, \quad (\text{II.5.6})$$

where u_M denotes the mode of the initial PDF $p_L(u_L)$. To obtain the optimal fluctuations $\bar{u}(r; S_m)$ as a function of the EP S_m , we adjust k

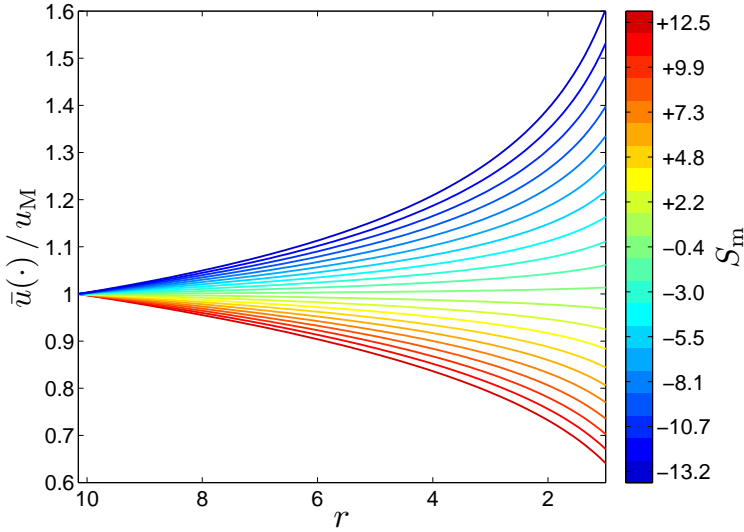


Figure II.6: Most likely realisations of the K62 process for various values of EP S_m . More specific, the shown trajectories are the solutions (II.5.8) of the ELE (II.5.5) subject to the constraint (II.5.2) for the stochastic process defined by (II.5.4).

such that $\bar{u}(r; k)$ satisfies the constraint

$$\begin{aligned} S_m(k) &= S_m[\bar{u}(r; k)] = -a\nu(1 - 2ik) \ln \frac{\lambda}{L} \\ \Rightarrow \quad ik(S_m) &= \frac{1}{2} + \frac{S_m}{2a\nu \ln(\lambda/L)} . \end{aligned} \quad (\text{II.5.7})$$

The optimal fluctuations hence read

$$\bar{u}(r; S_m) = u_M \left(\frac{r}{L} \right)^{\frac{S_m}{\nu \ln(L/\lambda)}} , \quad (\text{II.5.8})$$

in which the exponent is the EP S_m scaled with a measure for the length of the inertial range. The optimal fluctuations are depicted for various values of S_m in figure II.6.

A few special cases are apparent.

(i) For an initial PDF $p_L(u_L)$ with zero mean and zero skewness it is $u_M = 0$ and hence $\bar{u}(r; S_m) \equiv 0$. In other words, the most likely (and

average) realisation in a K62 process without initial skewness will always be identical zero, regardless the value of EP we impose. This uncoupling of $\bar{u}(r; S_m)$ and S_m for vanishing skewness hints that the formal EP S_m indeed has bearings with the energy production in the cascade.

(ii) The most likely realisation for $S_m = 0$ is $\bar{u}(r; S_m) \equiv u_M$, identical to the cases in which no turbulence generation takes place, i.e. $L = 0$, or in which the inertial range extends to zero scale or is of infinite length, i.e. $\lambda = 0$ or $L \rightarrow \infty$ respectively.

The connection to the log-multiplier $\ln H = \ln(u(r)/u_L)$, discussed in the context of the K62 second law (II.4.3), is established by writing

$$\ln \frac{\bar{u}(r; S_m)}{u_M} = \frac{S_m}{\nu \ln(L/\lambda)} \ln \frac{r}{L}, \quad (\text{II.5.9})$$

in which the sign of S_m obviously determines whether $H < 1$ or $H > 1$, signifying a direct or inverse cascade process.

Let us now see how the optimal fluctuations $\bar{u}(r; S_m)$ look like for the experimentally estimated drift and diffusion (II.3.50) from [110], used in [3] (chapter II.4).

Solving the resulting ELE analytically is hopeless and we refrain from writing down the explicit equations. Instead we employed the relaxation method **bvp4c** implemented in the numerical computing environment **MatLab**. The relaxation algorithm takes an initial guess for the solution and adapts this guess iteratively to satisfy the linear set of equations that arises from the boundary value problem to be solved. For small values of S_m we used the K62 solution (II.5.8) as the initial guess, for large values of S_m we used an already obtained solution for a similar value of S_m .

The solutions $\bar{u}(r; S_m)$ of the ELE for the experimentally estimated drift and diffusion using **bvp4c** are depicted in figure II.7. It is apparent that $\bar{u}(r; S_m)$ shows qualitatively the same behaviour as for the K62 case, which may not prove but indicate that the interpretation of S_m within the theoretical K62 model is also valid in realistic turbulent flows. Nevertheless, a striking difference is that for positive S_m the initial values of the optimal fluctuations clearly deviate from the mode of the initial distribution.

A peculiarity arises in solving the ELE numerically: The sign of $\bar{u}(r; S_m)$ is prone to the initial guess. By taking as an initial guess the K62 solution (II.5.8), we obtained the solutions shown in figure II.7. But by reversing

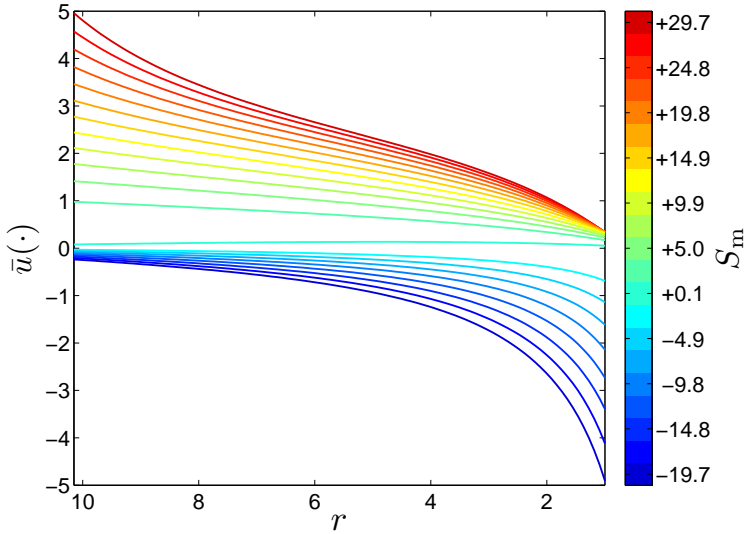


Figure II.7: Most likely realisations of the stochastic process defined by drift and diffusion estimated in [110] from experimental data for various values of EP S_m . The realisations are obtained from solving the ELE (II.5.3) with `bvp4c` in MatLab.

the sign of the initial guess, also the solutions $\bar{u}(r; S_m)$ reverse their sign, see for example figure II.8a. Hence, the numerical solution of the ELE appears to be bistable, and consequently, the path-probability $P[\bar{u}(r; S_m)]$ is bimodal. By comparing the values for the action $\mathcal{S}[\bar{u}(r; S_m)]$ for entirely positive and entirely negative solutions in figure II.8b, we find that in the case of negative S_m both solutions are balanced, whereas for positive S_m , the negative solutions tend to be more likely. The *average* realisations $u(\cdot)$ giving rise to extreme values of EP, as discussed in [3] (chapter II.4.1), hence have contributions from both the negative and the positive modes of $P[\bar{u}(r; S_m)]$.

The finding that for positive values of S_m the negative solutions are more likely is in accord with the four-fifths law, $\langle u(r)^3 \rangle = -\frac{4}{5}\bar{\varepsilon}r < 0$. The balance of probability of positive and negative solutions for negative values of S_m , suggesting a vanishing skewness in the realisations $\{u(r); S_m < 0\}$, remains curious. We should also keep in mind, that by comparing only the probabilities $P[\bar{u}(r; S_m)]$ evaluated at the *optimal* fluctuation $\bar{u}(\cdot)$, we obtain

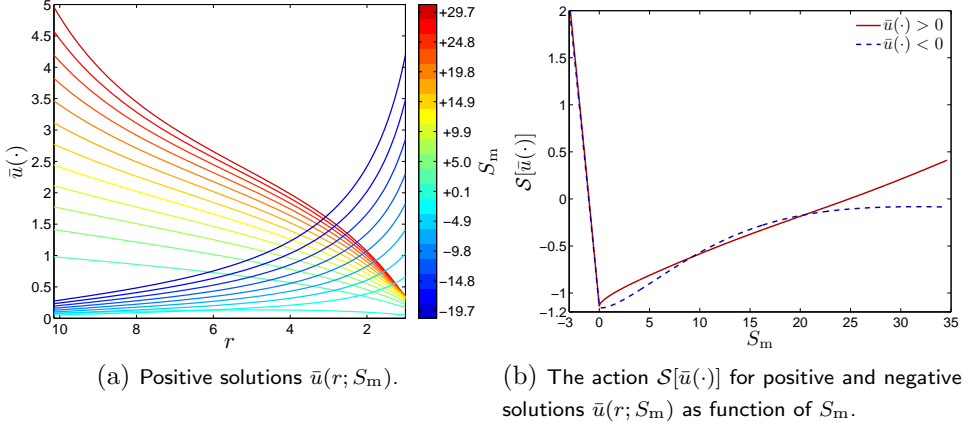


Figure II.8: The ELE (II.5.3) is numerically bistable. Depending on the initial guess, the solutions of the ELE using `bvp4c` are positive or negative, for positive and negative values of S_m separately. In (a) we show an example of only positive solutions, the negative solutions are barely distinguishable from the mirrored positive solutions. In (b) we assess the probability $P[\bar{u}(\cdot)] = \exp[-\mathcal{S}[\bar{u}(\cdot)]]$ of positive and negative solutions by means of the action $\mathcal{S}[\bar{u}(\cdot)]$.

no information about the fluctuations in the vicinity of $\bar{u}(\cdot)$. We therefore refrain from a further interpretation and leave it for future studies.

II.5.2 Asymptotic $p(u, r)$ and ζ_n

In the previous section, we used the ELE to calculate the most likely realisations giving rise to preset values of S_m . Instead of imposing the constraint with respect to S_m , we can also impose the boundary condition that $u(r)$ takes a certain value u^* at scale r^* with $L > r^* > \lambda$.

In this case, the ELE (II.5.1) reads

$$\ddot{u} = \frac{\dot{u} + F}{2D} (D'(\dot{u} - F) + 2\dot{D}) + FF' - \dot{F} + 2DJ'' , \quad (\text{II.5.10a})$$

$$0 = \frac{\dot{u}_0 + F_L}{2D_L} + A'_L , \quad (\text{II.5.10b})$$

$$u(r^*) = u^* . \quad (\text{II.5.10c})$$

Solving the above ELE for a certain value of u^* and r^* yields the asymptotics

$$p(u^*, r^*) \sim \exp \left[-\mathcal{S}[u(r; u^*, r^*)] \right]. \quad (\text{II.5.11})$$

Hence, by varying u^* and r^* we obtain an approximation of $p(u, r)$ which is asymptotically exact in the limit of $|u| \rightarrow \infty$, if we assume that infinite values for u are singularly rare.

Taking again the K62 model as an analytic accessible example, we obtain from (II.5.5) the ELE

$$\ddot{u}(r) = \frac{\dot{u}(r)}{u(r)} - \frac{\dot{u}(r)}{r}, \quad (\text{II.5.12a})$$

$$0 = \dot{u}_L L - a u_L + 2b u_L^2 \mathcal{A}'(u_L), \quad (\text{II.5.12b})$$

$$u(r^*) = u^*. \quad (\text{II.5.12c})$$

Note that the ODE remains the same since $F(u, r)/D(u, r)$ is not a function of scale r . The solutions are again power laws,

$$u(r) = u^* \left(\frac{r}{r^*} \right)^c, \quad (\text{II.5.13})$$

where the exponent c has to be determined from

$$0 = (a - c) p_L(u_L(c)) + 2b u_L(c) p'_L(u_L(c))$$

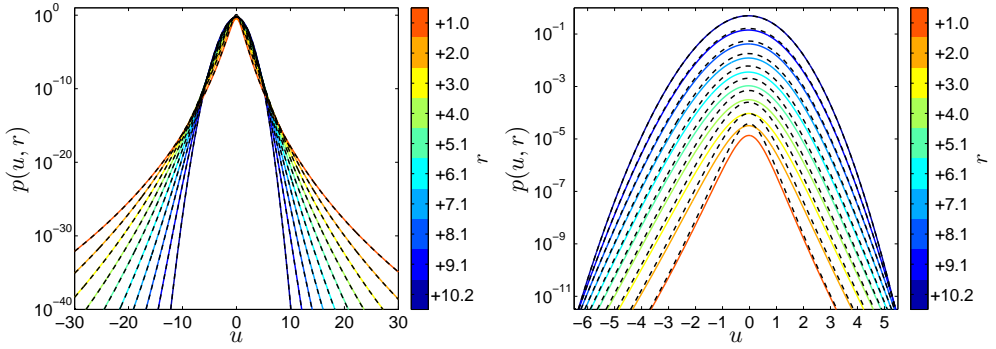
$$u_L(c) = u^* \left(\frac{L}{r^*} \right)^c.$$

Substitution of (II.5.13) into the action $S[u(\cdot)]$ yields the asymptotics

$$p(u, r) \sim \left(\frac{L}{r} \right)^{\frac{(c-a)^2}{4b} + \frac{b-a}{2}}, \quad (\text{II.5.14})$$

or, with $a = (3 + 2\mu)/9$ and $b = \mu/18$ substituted from (II.3.17),

$$p(u, r) \sim \left(\frac{L}{r} \right)^{\frac{(3c-1-2\mu/3)^2}{2\mu} - \frac{2+\mu}{12}}. \quad (\text{II.5.15})$$



(a) Asymptotic and analytic solution, zoomed out. (b) Asymptotic and analytic solution, zoomed in.

Figure II.9: Asymptotics of $p(u, r)$ for the K62 process defined by (II.5.4). The coloured lines are the asymptotic solutions given by (II.5.15) for $\mu = 0.25$, $L = 10.15$ and $\lambda = 1$ and various values of scale r . The dashed lines are the analytic solutions given in (II.3.15). The pre-exponential factor of the asymptotics is obtained from fits to the analytic solution in the far tails of $p(u, r)$.

In figure II.9, we compare the asymptotic solution with the exact solution from (II.3.15), in which we used $\mu = 0.25$, $L = 10.15$ and $\lambda = 1$, and we took $p_L(u_L)$ from fitting a skew-normal distribution to the experimentally determined result using again the data from [110] as in the previous section. The agreement between the measured and fitted $p_L(u_L)$ can be judged from II.11a for the largest scale $r = L$. From figure II.9 it is apparent that the asymptotics of $p(u, r)$ coincides with the analytical result for values of u that are barely accessible in a comparable experiment.³⁶

The asymptotics in (II.5.15) only includes the exponential factor, a constant pre-exponential factor has been obtained from fitting the asymptotic $p(u, r)$ to the analytical solution (II.3.15) for values of u that are sufficiently far in the tails to ensure the validity of the asymptotic assumption. For a more realistic process, where the analytic solution is not known, the determination of a constant pre-exponential factor requires an interval of u -values in which both the asymptotics is valid and the histogram determined from an experiment or simulation approximates $p(u, r)$ sufficiently well.

³⁶Such as the experiment in [110] with matching $L = 10.15$, $\lambda = 1$ and $p_L(u_L)$.

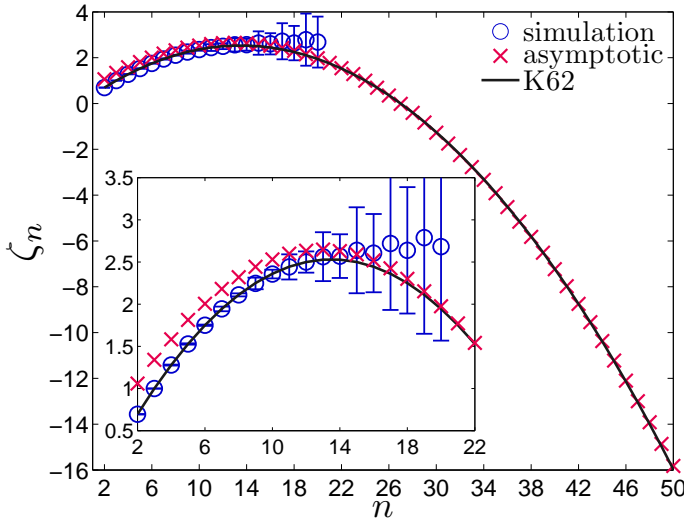


Figure II.10: Asymptotic scaling exponents for the K62 process for $\mu = 0.25$. The asymptotic solutions shown in figure II.9 imply structure functions $S_u^n(r)$, from which asymptotic scaling exponents have been derived, shown as red crosses. The scaling exponents determined from an ensemble of 10^7 realisations $u(r)$, generated from the analytical solution of the K62 SDE in (II.3.13), are included as blue circles, the exact scaling law (II.2.35) for the K62 model is added as a black line. The scaling exponents are obtained by fitting the ESS formula (II.2.45), the error bars are the standard deviations of the ζ_n determined from 10^3 blocks of 10^4 realisations $u(r)$.

The asymptotic $p(u, r)$ can be used to determine the scaling exponents ζ_n of the corresponding structure functions asymptotically. To this end, the structure functions are computed by

$$S_u^n(r) = \int u^n p(u, r) du, \quad (\text{II.5.16})$$

and, according to the ESS procedure explained after (II.2.45), ζ_n is obtained as the slope of a linear fit of $\ln S^n(r)$ as function of $\ln S^3(r)$.

In figure II.10, we demonstrate that by using the asymptotics of $p(u, r)$ from figure II.9, the scaling exponents resulting from the proposed procedure are excellent in a range of $n = 20$ to $n = 50$. For values $n < 20$, the

determination of the moments rests on the centre of $p(u, r)$ for which the asymptotic solution is not accurate, for $n > 50$ the range in u covered by the asymptotic solution is not sufficient³⁷.

Instead of using K62 as the analytical accessible example, it is interesting to see how the method performs for the experimental data from [110] as used in the previous section.

We take again the drift and diffusion coefficients $D^{(1,2)}(u, r)$ experimentally estimated in [110]. By substituting the numerical solutions of the ELE obtained by using `bvp4c` in `MatLab` into (II.5.11), we yield the asymptotics of $p(u, r)$ defined by the Markov process extracted from the experimental data. In figure II.11a, we compare the asymptotic $p(u, r)$ with the experimental result, for which we took for $p_L(u_L)$ again the skew-normal distribution fitted to the experimental data.

In determining a pre-exponential factor, we face the problem explicated above for the K62 example: The experimentally determined $p(u, r)$ does not reach sufficiently far into the tail of $p(u, r)$ where the asymptotic solution is valid. As a preliminary work-around, we determined the 10-th order structure function $S_u^{10}(r)$ from both the experimental data and the asymptotics, and adjusted the pre-exponential factor such that $S_u^{10}(r)$ is identical for both. The 10-th order structure function was chosen as it proved to be the largest order n for which $S_u^n(r)$ is reliable.

We stress that the estimation of $D^{(1,2)}(u, r)$ can only use the available experimental measurements covering the range of u -values as apparent from figure II.11a. Consequently, by taking these $D^{(1,2)}(u, r)$ to determine the asymptotic solution of the FPE, we extrapolate the measured $p(u, r)$ to higher values of $|u|$ under the assumption that the form of the FPE defined by $D^{(1,2)}(u, r)$ governs the evolution of $p(u, r)$; very much like assuming that a random variable is Gaussian distributed and predicting the probability of unobservable realisations by estimating mean and variance from the available data. It is therefore arguable to expect that by determining the asymptotic solution of the FPE, we also obtain the true asymptotic

³⁷The part of $p(u, r)$ being relevant for structure functions $S_u^n(r)$ beyond order $n = 50$ is so far in the tails, that the asymptotics of $p(u, r)$ exceeds the standard machine accuracy of `MatLab`. A limitation that can be overcome without much effort.

behaviour of the underlying experiment.

Nevertheless, for completeness, we show the resulting asymptotic scaling exponents in figure II.11b which are clearly unsatisfactory. We impute this unsatisfactory result to the uncertain determination of the pre-exponential factor.

Indeed, premature results give hope that an explicit determination of the pre-exponential factor as demonstrated in section I.3.4 improves the situation considerably for two reasons. First, we do not have to determine the pre-exponential factor from fits, and therefore do not rely on experimentally determined $p(u, r)$. And second, since we also achieve the u -dependency of the pre-exponential factor, the range of u values for which the asymptotics is valid should enlarge. Efforts to determine the pre-exponential factor have to be left for future studies.

In closing, we mention that instead of using the asymptotics of $p(u, r)$ to determine high order structure functions, the moment equation of the corresponding FPE can be used to set up an iteration procedure. The general form of drift and diffusion estimated in [110] from experimental data reads

$$D^{(1)}(u, r) = -a_0(r) - a_1(r)u + a_2(r)u^2 - a_3(r)u^3, \quad (\text{II.5.17a})$$

$$D^{(2)}(u, r) = b_0(r) - b_1(r)u + b_2(r)u^2. \quad (\text{II.5.17b})$$

Employing the moment equation (I.1.30) and solving for the highest order structure function yields

$$S_u^{n+4} = \frac{1}{a_3(r)} \left[(n+1)b_0(r)S_u^n(r) + (a_0 + (n+1)b_1(r))S_u^{n+1}(r) \right. \\ \left. + (a_1(r) + (n+1)b_2(r))S_u^{n+2}(r) + a_2(r)S_u^{n+3}(r) + \frac{1}{n+2}\partial_r S_u^{n+2}(r) \right]. \quad (\text{II.5.18})$$

The above formula yields the $(n+4)$ -th order structure function and needs as input the three next smaller structure functions.

One way to initialise the iteration is using $S_u^1(r) \equiv 1$ and taking $S_u^2(r) = c_2 r^{\zeta_2}$ and $S_u^3(r) = c_3 r^{\zeta_3}$ with $c_{2,3}$ and $\zeta_{2,3}$ fitted to the experimental data, arguing that a scaling law is a good approximation for the second and third order structure functions, and the derivative $\partial_r S_u^2$ can be calculated analytically. In this case, we have nested equations of depth

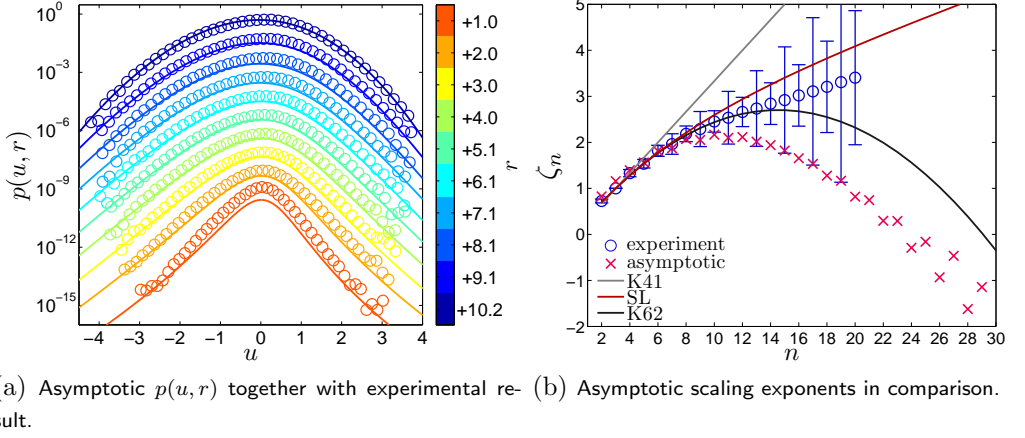


Figure II.11: Asymptotics of $p(u, r)$ for the Markov process defined by the experimentally estimated drift and diffusion (II.3.50). The coloured lines in (a) are the asymptotic solutions given by (II.5.11) for various values of scale r , which derive from the numeric solutions of the corresponding ELE (II.5.10) obtained with `bvp4c`. The coloured symbols are the corresponding histograms determined from the experimental data which was used in [110] to estimate the drift and diffusion coefficients used here. The asymptotic solutions imply structure functions $S_u^n(r)$, from which asymptotic scaling exponents have been derived, shown as red crosses in (b). In addition, scaling exponents determined from the exponential data and some theoretical predictions are included into (b), please refer to figure II.3. The pre-exponential factor of the asymptotics is obtained from fitting $S_u^{10}(r)$ to the experimental result.

$n - 4$ to determine the n -th order structure function. Another possibility is to take $S_u^1(r)$, $S_u^2(r)$ and $S_u^3(r)$ directly from measurements or simulations of the SDE, compute $\partial_r S_u^2$ numerically and iterate to higher order structure functions by means of numerical $S_u^n(r)$.

In any case, after very few steps, the iteration results into structure functions that depart drastically from the experimentally determined ones and become divergent. We hence face a highly sensitive dependency on the initial conditions as characteristic for chaotic systems. In addition, taking simpler forms of drift and diffusion reveals that dropping the odd term $b_1(r)u$ of the diffusion coefficient, responsible for the skewness of the dynamics and correlation between the additive and multiplicative noise (cf.

(II.3.51)), the iteration procedure improves in comparison with according simulation results.

We leave the implications of these observations for further studies.

II.6 Closing discussion

We close the part on turbulence with a summarising discussion.

II.6.1 Classification

The Markov representation is a unifying framework for a variety of established theories of turbulence, allowing a classification of these theories in terms of Markov processes.

The central turbulence theory is the K62 model. The K62 model may be viewed as the harmonic oscillator of the Markovian description of turbulence, in the sense that it is fully analytical solvable, captures the main features of turbulence, and from an alteration of the K62 process more realistic models of turbulence arise. Depending on the kind of alteration, the generalisations of the K62 model belong to different branches of turbulence research.

The **K62 model**, with scaling exponents $\zeta_n = n/3 - \mu/18n(n-3)$, is characterised by drift $D^{(1)}(u, r) \propto u/r$ and diffusion $D^{(2)}(u, r) \propto u^2/r$. The fluctuation theorem associated with K62 involves only boundary terms. Considering only the deterministic process defined by $D^{(1)}(u, r)$, we retrieve the trivial case of K41, $\zeta_n = n/3$. We now give an overview of the emerging models of turbulence by various alterations of K62.

(i) A linear drift $D^{(1)}(u, r) = a(r)u$ and quadratic diffusion $D^{(2)}(u, r) = b(r)u^2$ for arbitrary $a(r)$ and $b(r)$ represent **log-normal random cascade models**, that is to say, the random variable u is described by a log-normal distribution. The explicit form of $a(r)$ and $b(r)$ determines the variance $\sigma^2(r)$ of the log-normal distribution, the associated fluctuation theorem receives an integral contribution.

Only for $a(r) \propto 1/r$ and $b(r) \propto 1/r$, retrieving the K62 model, it is $\sigma^2(r) \sim \ln(r)$ and the moments of $u(r)$ exhibit a scaling law.

By altering $a(r)$ and $b(r)$ but keeping the r -dependency equal, that is $a(r)/b(r) = \text{const}$, we abandon a scaling law, but the boundary form of the K62 fluctuation theorem is retained. The random cascade process for $a(r)/b(r) = \text{const}$ has been termed **continuously self-similar**, and the stochastic processes becomes a stationary process.

For the special choice $a(r) \sim b(r) \sim \partial_r \ln S^m(r)$ the moments of $u(r)$ scale as $(S^m(r))^{\zeta_n}$, being the conjecture of **extended self-similarity**, where $m = 3$ is the most common choice.

A shortcoming of log-normal random cascade models is the vanishing **skewness** in the statistics of $u(r)$. In terms of Markov processes, a skewness can principally be added to the dynamics³⁸ by, e.g., introducing an additive noise term coupled to the existing multiplicative noise term in the stochastic differential equation, or by augmenting the Fokker-Planck equation with a suitable third Kramers-Moyal coefficient $D^{(3)}(u, r)$.

(ii) Instead of keeping the u dependency and altering the r dependency, we may also keep $D^{(1,2)}(u, r) \propto 1/r$ but allow an arbitrary combination of powers in u . For this choice of $D^{(1,2)}(u, r)$, the moments of $u(r)$ become a superposition of scaling laws with distinct linear exponents. Allocating the scaling laws with fractal subspaces of \mathbb{R}^3 , we obtain the essence of **multifractal models** of turbulence. The explicit correspondence to multifractal models, however, remains to be established. The associated fluctuation theorem is again of boundary form, involving the moments of $u(r)$.

(iii) Keeping the K62 drift but adding to the K62 diffusion a term linear in u , that is $D^{(2)}(u, r) \sim \beta u + bu^2/r$, we obtain the *continuous* approximation of **Yakhot's model** of turbulence.

The full equivalence to Yakhot's model is achieved by taking also the higher Kramers-Moyal coefficients into account, $D^{(k)}(u, r) \sim \beta_k u^{k-1} + b_k u^k/r$ for $k \geq 2$. The stochastic process is now a *discontinuous* process.

The coefficient β_k accounts for effects of energy injection. Neglecting that effect by setting $\beta_k = 0$, the Kramers-Moyal expansion implies **Yakhot's scaling law** $\zeta_n = n/3 (B + 3)/(B + n)$.

An expansion of Yakhot's scaling law to third order in the anomaly parameter $\delta_2 = \zeta_2 - 2/3$ recovers the scaling exponents suggested by **L'vov and Procaccia** being cubic in n . Cubic scaling exponents correspond to a Kramers-Moyal expansion truncated after the third term.

(iv) The K62 process is composed of a deterministic component and

³⁸Initialising the process with an asymmetric $p_L(u_L)$ introduces a decaying skewness to the process, even for a dynamics defined by $D^{(k)}(u, r)$ being invariant under $u \mapsto -u$.

a Gaussian process. Substituting the Gaussian process with a jump process, where the moments of the jump density are $\Psi^{(k)}(u, r) \propto (bu)^k/r$ with $b = (2/3)^{1/3} - 1$, defines a jump process being equivalent to the **log-Poisson random cascade model**. This model exhibits scaling laws with the scaling exponents $\zeta_n = n/9 + 2 - (2/3)^{n/3}$ derived by **She and Leveque**.

(v) Drift and diffusion coefficients can also be obtained directly from **experimental measurements**. Generally, $D^{(1)}(u, r)$ and $D^{(2)}(u, r)$ are of similar form as in the K62 process, but $D^{(2)}(u, r)$ involves two extra terms, being constant and linear in u , and each term in $D^{(1,2)}(u, r)$ is a different function of r . The stationary distribution at scale $r = L$ defined by $D^{(1,2)}(u, L)$ generally differs from the measured initial distribution $p_L(u)$ of the process. Accordingly, non-equilibrium is imposed by both, initialising the process off equilibrium, and driving the process.

II.6.2 Interpretation

The thermodynamic interpretation of Markov processes discussed in the first part provokes a similar fashioned interpretation of the Markov representation of fully developed turbulence.

Starting point is again the K62 process. Being a stationary process in logarithmic scale $\ln(L/r)$, the K62 process is a relaxation process from an initial distribution $p_L(u_L) \neq \delta(u_L)$. Consequently, non-equilibrium can only be imposed by initialising the process off equilibrium. In the limit $\ln(L/r) \rightarrow \infty$, all moments of $u(r)$ will be zero and we are left with a free laminar flow. The average tendency of the K62 process towards small scales is therefore a decrease of fluctuations.

The second law like inequality discussed in section II.4.1 confirms indeed that the average log-multiplier $\langle H_r \rangle = \langle \ln(u(r)/u_L) \rangle$ is bounded from above by the difference in Shannon entropy $\Delta S(r)$ between final and initial state of the turbulent cascade. The Shannon entropy difference $\Delta S(r)$ is found to be negative for all scales and monotonically decreasing with decreasing r , implying that strictly $\langle u(r) \rangle < \langle u_L \rangle$, in particular towards the end of the cascade. However, by assessing the multiplier statistics, we have

seen that instances with $H_r > 1$ remain possible throughout the inertial range, the maximum value of H_r being approximately constant.

The convergence of the K62 fluctuation theorem is dependent on realisations $u_r > u_L$, corresponding to spatial velocity fluctuations which, contrary to the average tendency, build up while evolving towards smaller scales. Since $S_m = \nu \ln(u_L/u_\lambda)$ (with $\nu = (6 + 4\mu)/\mu \approx 27$), these increasing spatial velocity fluctuations correspond formally to a consumption of entropy, $S_m < 0$, but with S_m bearing no reference to thermodynamic entropy production. Nevertheless, since $S_m < 0$ corresponds to velocity fluctuations $u(r)$ exceeding the typical fluctuations u_L they evolved from, it is tempting to think of some kind of reservoir that provides velocity fluctuations throughout the cascade, in accord with the construction of the K62 process as a random cascade process in section II.3.1. Accepting such a perception of a reservoir, the form of the diffusion coefficient, $D^{(2)} \sim u^2$, suggests that in a cascade process the turbulent energy $u(r)^2$ is the analog of the thermal energy $k_B T$ in a thermodynamic process. But this perception bears an inconsistency, since $u(r)^2$ depends on the realisation $u(r)$ itself and can therefore not be regarded as an equilibrium property of an ideal reservoir. It is safer to think of $D^{(2)} \sim u^2$ as the result of accumulated randomness towards the end of the cascade.

In any case, realisations $u(\cdot)$ with $u(r) > u_L$ are characterised by $S_m[u(\cdot)] < 0$. Such realisations might be the result of mingling cascades, where one cascade was initialised by such a large fluctuation that $u(r)$ is still larger than the large-scale fluctuation u_L of a second cascade. Another possibility is that one strong small-scale fluctuation arises from an aggregation of many small-scale structures, corresponding to an inverse cascade with multipliers larger than one. The fact that strong small-scale fluctuations are significantly more frequent than equally strong large-scale fluctuations, cf. figure II.2, indicates that an aggregation of small-scale structures is the predominant mechanism that causes $u(r) > u_L$, and we claim that $S_m[u(\cdot)] < 0$ is a signature of a concurrent inverse cascade in addition to the direct cascade.

In stochastic thermodynamics, $S_m[x(\cdot)] < 0$ accounts for collisions between fluid molecules and particles in which the particle is kicked primarily from one side, rectifying thermal noise into directed motion. The exact dynamics of such collisions is not resolved by the stochastic process, taking

place below the Markov-Einstein time scale t_{ME} . What is the analog mechanism in a turbulent cascade?

In constructing the K62 process as a random cascade process in section II.3.1, we coarse-grained the exact dynamics of the break-up of eddies as a Gaussian noise accounting only for the outcome of the break-up, in close analogy to consider the collision of a Brownian particle with fluid molecules only as a random change in particle velocity. Accordingly, we expect the mechanism that is responsible for $S_m[u(\cdot)] < 0$, implying $u(r) > u_L$, to take place during the break-up of eddies. The decrease of scale r after a break-up is given by $r_{\text{ME}} \approx \lambda$, with λ being the Taylor microscale indicating the scale below which molecular friction is prevailing. It is therefore tempting to speculate about a connection between $S_m[u(\cdot)] < 0$ and molecular friction, such as $S_m[u(\cdot)] < 0$ being the hallmark of velocity fluctuations which build up in the dissipative range, enter the inertial range from below and manifest themselves as intermittent fluctuations at small scales, $u(r) > u_L$. The underlying mechanism might be that the rate of energy dissipation is smaller than the rate of energy transfer into the dissipative range, provoking occasional aggregations of accumulated small turbulent structures to intermittent fluctuations, characterised by instances of *negative* energy transfer rates which ensures that on average we retain the balance between energy dissipation and energy transfer. For high Reynolds numbers, implying a smaller dissipative range, this mechanism would intensify. In the picture of multifractal models we may say that less space-filling turbulent structures towards the end of the cascade create a bottleneck of energy transfer. However, these considerations are clearly speculative, but might offer new perspectives worth pursuing.

The above considerations were mainly based on the K62 model. The Markov process defined by drift and diffusion estimated from experimental data exhibits qualitatively the same characteristics as the K62 process, in particular the correspondence between $S_m[u(\cdot)] < 0$ and realisations $u(r)$ which increase towards smaller scales, as discussed in sections II.4.1 and II.5.1. We therefore assume that the above considerations also apply qualitatively to real turbulent flows.

The failure of K62 in modelling the extreme value statistics of $u(r)$, demonstrated by the break-down of the K62 fluctuation theorem when applied to experimental data, however, suggests that the details of the K62

process need to be modified, cf. the discussion of modifications in the previous section. Such a modification may be to substitute the Gaussian noise with Poissonian noise, leading to the significantly more successful scaling exponents derived by She and Leveque. Another modification is to combine various cascade processes taking place in fractal subspaces as in multifractal models.

An important modification is the inclusion of a skewness, i.e. breaking the invariance with respect to $u \mapsto -u$. The K62 model and related random cascade models do not include a skewness in u : The trajectories $u(r)$ generated by solving the respective stochastic differential equations will hence be negative and positive to equal shares, provided the initial distribution $p_L(u_L)$ is symmetric. This symmetry corresponds to reversible processes in the turbulent cascade, as a balanced occurrence of positive and negative $u(r)$ imply that instances of positive energy transfer are as frequent as instances of negative energy transfer.

In contrast, the stochastic process defined by drift and diffusion obtained from experimental data does exhibit a skewness. Indeed, restricting the realisations $u(\cdot)$ to a positive production of associated entropy, $S_m[u(\cdot)] > 0$, the asymptotic analysis of section II.5.1 revealed a slight unbalance in favour of *negative*, decreasing $u(r)$, relating negative skewness with a decay of spatial velocity fluctuations, in compliance with the average tendency. Realisations $u(\cdot)$ giving rise to a consumption of entropy, $S_m[u(\cdot)] < 0$, on the other hand, exhibit an increase of fluctuations towards small scales, and a mere balance between negative and positive $u(r)$. The similar analysis of experimentally measured realisations $u(r)$ presented in [3] (section II.4.1) confirmed that decreasing $u(r)$ are characterised by $S_m + \Delta S > 0$ and increasing $u(r)$ by $S_m + \Delta S < 0$, where the Shannon entropy ΔS can be shown to have a negligible influence, as is the case for the K62 process.

In conclusion, a consumption of entropy S_m signifies fluctuations $u(r)$ that contribute to small-scale intermittency, bearing reference to instances of inverse cascades. The relation to transfer and dissipation of energy in the cascade and a negative skewness in the statistics of $u(r)$ is intriguing but remains unclear. If a model of turbulence accounts for the correct balance between direct and inverse cascades coexisting in a realistic turbulent flow, the fluctuation theorem resulting from the Markov representation of that

model will be satisfied for experimental data.

II.6.3 Possible future studies

The results presented in this thesis offer a couple of starting points for future studies.

We have demonstrated the equivalence of Markov processes to many established models of turbulence. Besides this theoretical legitimation of using Markov processes to approach turbulence, we have also given a survey of experimental evidence that the turbulent cascade is indeed Markovian. The natural next step is, instead of finding the Markovian counterpart of *existing* models of turbulence, to use the gathered knowledge on the Markov description of turbulence and construct a theoretical model on the very level of Markov processes. A starting point may be exact relations of velocity increments as the Kármán-Howarth-Kolmogorov relation (II.2.21), or to specify the Markov representation of multifractal models (II.3.26) to consider subspaces with inverse cascades, or to adapt other existing Markov representations in order to better reproduce experimental results.

The aim of such efforts, instead finding the amplitudes and exponents of scaling laws, would be to find a form of drift and diffusion coefficients, and even a jump density, to capture the universal features of fully developed turbulence. In doing so, the comparison with the presented forms of MPs in chapter II.3, the convenient experimental verification using fluctuation theorems demonstrated in chapter II.4 and the asymptotic analysis discussed in chapter (II.5) may be of assistance.

Apart from being a test equation for possible drift and diffusion coefficients (and even jump densities), the fluctuation theorem is for itself an intriguing object to focus on. The implications of scale reversal to the direction of the energy cascade, for instance, is an open question, which also leaves the interpretation of the associated entropy production to be of rather speculative nature.

Instead of scale reversal, other involutions are possible, such as a reversal of velocity direction, $u \mapsto -u$, bearing reference to time-reversal. This involution is of interest, as it reverses the skewness of velocity increments,

and along with the skewness also the energy transfer in the turbulent cascade. The entropy in the fluctuation theorem building on this involution therefore directly targets the irreversibility of energy transfer. Unfortunately, or interestingly, the linear term in the diffusion coefficient, which proved to be the important term of the skewness, provokes a divergent behaviour of the entropy, spoiling the convergence of its fluctuation theorem. The reason for this divergence could not be clarified satisfactorily. Other courses of action may be a fluctuation theorem in two dimensions. A promising starting point is the Markov analysis in $u(r)$ and $\varepsilon(r)$ by Renner et al., which we discussed at the end of section II.3.3. Or two sources of noise acting on different scales as in (II.3.51). Both could allow an analysis of non-equilibrium steady states in the very dynamics of $u(r)$ or $\varepsilon(r)$, involving the housekeeping entropy production to maintain the steady states and the non-negative excess entropy for transitions between steady states. These two entropy productions and the total entropy production obey each a separate fluctuation theorem, implying three faces of the second law, as discussed at the end of section I.2.3.

An intricate point in the Markov analysis of experimental data is the justification to truncate the Kramers-Moyal expansion after the second term and obtain a Fokker-Planck equation, as it relies on proving that exactly $D^{(4)}(u, r) \equiv 0$. In fact, due to experimental and statistical limitations, it is only possible to show $D^{(4)}(u, r) \approx 0$. Accordingly, instead of asking *how small* $D^{(4)}(u, r)$ is, the more appropriate question is to ask *how likely* is $D^{(4)}(u, r) \equiv 0$. A Bayesian analysis of the hypothesis “ $D^{(4)}(u, r) \equiv 0$ ” is promising to tackle that question.

The analysis of optimal fluctuations $u(r)$ giving rise to extreme entropy productions given in section II.5.2 raises the question how the skewness of $u(r)$ is respected in the Markov representation. The Euler-Lagrange equation for other Markov representations than the K62 process and the experimentally extracted Markov process should therefore be interesting. To allow a more profound analysis, the fluctuation determinant for multiplicative noise, determined for additive noise in [1], would account for the vicinity of the optimal fluctuations $u(r)$.

A computation of the fluctuation determinant for multiplicative noise

which determines the pre-exponential factor would also improve the asymptotics of $p(u, r)$, as discussed in section II.5.2, significantly.

Other open issues are to determine the jump density of the log-Poisson model, (II.3.30b), and to establish the explicit corresponds between multifractal models and the power series form of drift and diffusion coefficients, (II.3.26).

Conclusions

Markov processes are well suited to capture both, thermodynamic processes of nanoscopic systems under non-equilibrium conditions, and cascade processes in fully developed turbulence. In contrast to macroscopic systems which are dominated by the *average* tendency of their microscopic dynamics, the properties of nanoscopic systems are characterised by *rare* stochastic realisations of their dynamics.

In closing this thesis, we relate the main statements of stochastic thermodynamics with the main results discussed for fully developed turbulence.

A paradigm to study stochastic thermodynamics is the Brownian motion of tiny particles suspended in a fluid. But many other systems are well described in the framework of stochastic thermodynamics. Closely related to Brownian motion are processes in biological cells, in particular the functioning of molecular motors. Benefiting from the understanding of molecular motors, the engineering of nanoscopic devices is on the rise, revealing an intimate relation between information and entropy. Stochastic thermodynamics is well suited to define the various working principles of a nanoscopic device. Other examples for applications of stochastic thermodynamics are active particles, nanoscale measurements and many more. Regarding fully developed turbulence, a variety of established theories find a representation as a Markov process. A central role takes the K62 theory by Kolmogorov. Altering and augmenting the Markov representation of the K62 model leads to extended self-similarity, random cascade models, models resulting from field theoretic approaches and multifractal models. In addition, it is possible to capture the features of a turbulent flow by extracting a Markov process directly from experimental data.

The intuitive formulation of Brownian motion in terms of stochastic differential equations allows to study the effects of inhomogeneous media and temperature gradients.

II Universal features of turbulent flows

The unified representation of the various established theories of fully developed turbulence as Markov processes is convenient for a contrasting juxtaposition of these models. In addition, combining features of models and incorporating refinements to overcome inconsistencies become feasible tasks.

An advantage of stochastic thermodynamics is its applicability to single realisations of the system under consideration. Notions of heat and work allow a formulation of the first law on the level of individual trajectories. The second law, being an inequality for entropy production, are stated more precisely as fluctuation theorems, being equalities. Both the first law and the fluctuation theorems hold arbitrarily far from equilibrium. The Markov representation of models of turbulence address individual probes of the spatial structures of a turbulent flow, and, vice versa, allow to generate artificial data that carry the exact properties specified by the model under consideration. Formally, the Markov representation associates production of entropy to individual probes of spatial structures which in turn satisfy a fluctuation theorem. Validating the fluctuation theorem for extracted Markov processes from experimental data is an on-the-fly criterion for the quality of the extraction.

The entropy production of individual trajectories of nanoscopic systems is not restricted by the second law, only the average entropy production is bound to be positive. The rare individual trajectories that *consume* entropy are contrary to the average tendency of the dynamics and as such of particular interest. Molecular motors, for instance, are capable of rectifying thermal noise to perform useful work. Possible implications for nanoscopic devices are intriguing.

The average tendency of spatial velocity fluctuations in fully developed turbulence is to diminish towards small scales. This decrease of fluctuations is associated with a break-up of turbulent structures and a production of entropy. Despite the rather macroscopic dimensions of a turbulent flow, small-scale velocity fluctuations, exceeding in magnitude the large-scale fluctuations and associated with a consumption of entropy, are a predominant phenomenon in a turbulent flow, a phenomenon which is known as small-scale intermittency. The Markov representation suggests that these intermittent small-scale fluctuations result from an aggregation of turbu-

lent structures.

Fluctuation theorems are valid arbitrarily far from equilibrium, but nevertheless involve equilibrium state variables. This connection allows the recovery of equilibrium information from non-equilibrium measurements. A prominent application that exploits this property of fluctuation theorems is the determination of free-energy profiles from force-spectroscopy of single biomolecules.

Fluctuation theorems are prone to the balance between entropy producing and entropy consuming fluctuations. In fully developed turbulence, velocity fluctuations associated with entropy consumption are responsible for small-scale intermittency. Accordingly, fluctuation theorem arising from the Markov representation of a model of turbulence will only hold for experimental measurements if this model precisely assesses the occurrence of intermittent small-scale fluctuations. The K62 theory is an example where the fluctuation theorem fails an experimental test, whereas the fluctuation theorem for the Markov process extracted from experimental measurements holds for these measurements. The latter finding validates that continuous Markov processes are well suited to capture small-scale intermittency, calling for a meaningful Markov theory of fully developed turbulence.

A reliable recovery of equilibrium information from non-equilibrium measurements is dependent on capturing the statistics of entropy consuming events. Typically, these events are also the rare events of the non-equilibrium process, hampering the recovery of equilibrium information. The path integral formulation of continuous Markov process is suitable to develop an asymptotic method which allows to examine these rare events. The asymptotic method also quantifies the probability of the rare event, improving the recovery of equilibrium information from non-equilibrium measurements.

In the context of Markov representations of fully developed turbulence, the asymptotic method can be used to determine the probability of extreme intermittent small-scale fluctuations of velocity and asymptotically extrapolate the scaling exponents.

Overall, the Markov representation of cascade processes constitutes a

consistent approach to fully developed turbulence. The Markov processes representing the two Kolmogorov theories arise naturally from applying the Markov assumption to the cascade of turbulent structures. The results of the developing field of stochastic thermodynamics provide valuable tools for the analysis of the Markov representations. Accordingly, the Markov analysis of fully developed turbulence is a promising endeavour, from which new insights regarding the mechanism small-scale intermittency and the irreversibility of energy transfer can be expected, and therefore deserves further study.

References

- [1] NICKELSEN D AND ENGEL A. *Asymptotics of work distributions: the pre-exponential factor*. The European Physical Journal B, **82**(3-4), pp. 207–218 (2011).
- [2] NICKELSEN D AND ENGEL A. *Asymptotic work distributions in driven bistable systems*. Physica Scripta, **86**(5), p. 058503 (2012).
- [3] NICKELSEN D AND ENGEL A. *Probing Small-Scale Intermittency with a Fluctuation Theorem*. Physical Review Letters, **110**(21), p. 214501 (2013).
- [4] GARDINER C. *Stochastic Methods: A Handbook for the Natural and Social Sciences*. Springer Series in Synergetics (Springer, 2009), fourth edition.
- [5] VAN KAMPEN NG. *Stochastic Processes in Physics and Chemistry* (Elsevier, 2007), third edition.
- [6] CHAICHIAN M AND DEMICHEV A. *Path integrals in physics: Stochastic processes and quantum mechanics* (Institute of Physics Publishing, 2001).
- [7] LAU A AND LUBENSKY T. *State-dependent diffusion: Thermodynamic consistency and its path integral formulation*. Physical Review E, **76**(1), p. 11123 (2007).
- [8] LEMONS DS. *Paul Langevin’s 1908 paper “On the Theory of Brownian Motion” [“Sur la theorie du mouvement brownien,” C. R. Acad. Sci. (Paris) 146, 530–533 (1908)]*. American Journal of Physics, **65**(11), p. 1079 (1997).

- [9] EINSTEIN A. *Über die von der molekularkinetischen Theorie der Wärme geforderte Bewegung von in ruhenden Flüssigkeiten suspendierten Teilchen*. Annalen der Physik, **322**(8), pp. 549–560 (1905).
- [10] LANDAU LD AND LIFSHITZ EM. *Hydrodynamik*. Number 6 in Lehrbuch der Theoretischen Physik (Akademie-Verlag-Berlin, 1981).
- [11] MARCONI U, PUGLISI A, RONDINI L AND VULPIANI A. *Fluctuation–dissipation: Response theory in statistical physics*. Physics Reports, **461**(4-6), pp. 111–195 (2008).
- [12] TUPPER PF AND YANG X. *A paradox of state-dependent diffusion and how to resolve it*. Proceedings of the Royal Society A: Mathematical, Physical and Engineering Sciences, **468**(2148), pp. 3864–3881 (2012).
- [13] PESCE G, MCDANIEL A, HOTTOVY S, WEHR J AND VOLPE G. *Stratonovich-to-Itô transition in noisy systems with multiplicative feedback*. Nature communications, **4**, p. 2733 (2013).
- [14] YANG M AND RIPOLL M. *Brownian motion in inhomogeneous suspensions*. Physical Review E, **87**(6), p. 062110 (2013).
- [15] DURANG X, KWON C AND PARK H. *The overdamped limit for the Brownian motion in an inhomogeneous medium*. arXiv:1309.5750 (2013).
- [16] KUROIWA T AND MIYAZAKI K. *Brownian motion with multiplicative noises revisited*. Journal of Physics A: Mathematical and Theoretical, **47**(1), p. 012001 (2014).
- [17] FARAGO O AND GRØNBECH JENSEN N. *Langevin dynamics in inhomogeneous media: Re-examining the Itô-Stratonovich dilemma*. Physical Review E, **89**(1), p. 013301 (2014).
- [18] RUBIN KJ, PRUESSNER G AND PAVLIOTIS GA. *Mapping multiplicative to additive noise*. arXiv:1401.0695 (2014).
- [19] KAMPEN NG. *Itô versus Stratonovich*. Journal of Statistical Physics, **24**(1), pp. 175–187 (1981).

- [20] RISKEN H. *The Fokker-Planck equation: Methods of solution and applications* (Springer, 1989), second edition.
- [21] CHERNYAK VY, CHERTKOV M AND JARZYNSKI C. *Path-integral analysis of fluctuation theorems for general Langevin processes*. Journal of Statistical Mechanics: Theory and Experiment, **P08001** (2006).
- [22] GILLESPIE DT. *Exact stochastic simulation of coupled chemical reactions*. The Journal of Physical Chemistry, **81**(25), pp. 2340–2361 (1977).
- [23] STRESING R, KLEINHANS D, FRIEDRICH R AND PEINKE J. *Different methods to estimate the Einstein-Markov coherence length in turbulence*. Physical Review E, **83**(4) (2011).
- [24] HONISCH C AND FRIEDRICH R. *Estimation of Kramers-Moyal coefficients at low sampling rates*. Physical Review E, **83**(6), p. 066701 (2011).
- [25] HONISCH C, FRIEDRICH R, HÖRNER F AND DENZ C. *Extended Kramers-Moyal analysis applied to optical trapping*. Physical Review E, **86**(2), p. 026702 (2012).
- [26] FRIEDRICH R, PEINKE J, SAHIMI M AND REZA RAHIMI TABAR M. *Approaching complexity by stochastic methods: From biological systems to turbulence*. Physics Reports, **506**(5), pp. 87–162 (2011).
- [27] TANG K, AO P AND YUAN B. *Robust reconstruction of the Fokker-Planck equations from time series at different sampling rates*. Europhysics Letters, **102**(4), p. 40003 (2013).
- [28] PAWULA R. *Approximation of the Linear Boltzmann Equation by the Fokker-Planck Equation*. Physical Review, **162**, pp. 186–188 (1967).
- [29] SEIFERT U. *Stochastic thermodynamics, fluctuation theorems and molecular machines*. Reports on progress in physics., **75**(12), p. 126001 (2012).

- [30] SEIFERT U. *Stochastic thermodynamics: principles and perspectives*. The European Physical Journal B, **64**(3-4), pp. 423–431 (2008).
- [31] DUHR S AND BRAUN D. *Why molecules move along a temperature gradient*. Proceedings of the National Academy of Sciences of the United States of America, **103**(52), pp. 19678–82 (2006).
- [32] DUHR S AND BRAUN D. *Thermophoretic Depletion Follows Boltzmann Distribution*. Physical Review Letters, **96**(16), p. 168301 (2006).
- [33] WÜRGER A. *Thermophoresis in Colloidal Suspensions Driven by Marangoni Forces*. Physical Review Letters, **98**(13), p. 138301 (2007).
- [34] PIAZZA R AND PAROLA A. *Thermophoresis in colloidal suspensions*. Journal of Physics: Condensed Matter, **20**(15), p. 153102 (2008).
- [35] HOTTOVY S, VOLPE G AND WEHR J. *Thermophoresis of Brownian particles driven by coloured noise*. Europhysics Letters, **99**(6), p. 60002 (2012).
- [36] SEKIMOTO K. *Langevin equation and thermodynamics*. Progress of Theoretical Physics Supplement, **130**, pp. 17–27 (1998).
- [37] LÓPEZ C AND MARINI BETTOLO MARCONI U. *Multiple time-scale approach for a system of Brownian particles in a nonuniform temperature field*. Physical Review E, **75**(2), p. 021101 (2007).
- [38] BENJAMIN R AND KAWAI R. *Inertial effects in Büttiker-Landauer motor and refrigerator at the overdamped limit*. Physical Review E, **77**(5), p. 051132 (2008).
- [39] VAN DEN BROECK C AND ESPOSITO M. *Three faces of the second law. II. Fokker-Planck formulation*. Physical Review E, **82**(1) (2010).
- [40] SEIFERT U. *Entropy Production along a Stochastic Trajectory and an Integral Fluctuation Theorem*. Physical Review Letters, **95**(4), p. 040602 (2005).

- [41] ESPOSITO M AND VAN DEN BROECK C. *Three Detailed Fluctuation Theorems*. Physical Review Letters, **104**(9), p. 090601 (2010).
- [42] ESPOSITO M AND VAN DEN BROECK C. *Three faces of the second law. I. Master equation formulation*. Physical Review E, **82**(1), pp. 1–10 (2010).
- [43] OONO Y AND PANICONI M. *Steady State Thermodynamics*. Progress of Theoretical Physics Supplement, **130**, pp. 29–44 (1998).
- [44] HATANO T AND SASA SI. *Steady-State Thermodynamics of Langevin Systems*. Physical Review Letters, **86**(16), pp. 3463–3466 (2001).
- [45] SPECK T AND SEIFERT U. *Integral fluctuation theorem for the housekeeping heat*. Journal of Physics A: Mathematical and General, **38**(34), pp. L581–L588 (2005).
- [46] SPECK T AND SEIFERT U. *Restoring a fluctuation-dissipation theorem in a nonequilibrium steady state*. Europhysics Letters, **74**(3), pp. 391–396 (2006).
- [47] BOKSENBOJM E, MAES C, NETOČNÝ K AND PEŠEK J. *Heat capacity in nonequilibrium steady states*. Europhysics Letters, **96**(4), p. 40001 (2011).
- [48] ABREU D AND SEIFERT U. *Thermodynamics of Genuine Nonequilibrium States under Feedback Control*. Physical Review Letters, **108**(3), p. 30601 (2012).
- [49] LEE J AND PRESSÉ S. *A derivation of the master equation from path entropy maximization*. The Journal of chemical physics, **137**(7), p. 074103 (2012).
- [50] VERLEY G AND LACOSTE D. *Fluctuation theorems and inequalities generalizing the second law of thermodynamics out of equilibrium*. Physical Review E, **86**(5), p. 051127 (2012).
- [51] SPINNEY R AND FORD I. *Nonequilibrium Thermodynamics of Stochastic Systems with Odd and Even Variables*. Physical Review Letters, **108**(17), pp. 1–5 (2012).

- [52] HARRIS RJ AND SCHÜTZ GM. *Fluctuation theorems for stochastic dynamics*. Journal of Statistical Mechanics: Theory and Experiment, **P07020** (2007).
- [53] EVANS DJ, COHEN EGD AND MORRISS GP. *Probability of second law violations in shearing steady states*. Physical Review Letters, **71**(15), pp. 2401–2404 (1993).
- [54] EVANS D AND SEARLES D. *Equilibrium microstates which generate second law violating steady states*. Physical Review E, **50**(2), pp. 1645–1648 (1994).
- [55] GALLAVOTTI G AND COHEN EGD. *Dynamical Ensembles in Nonequilibrium Statistical Mechanics*. Physical Review Letters, **74**(14), pp. 2694–2697 (1995).
- [56] GALLAVOTTI G AND COHEN E. *Dynamical ensembles in stationary states*. Journal of Statistical Physics, **80**, pp. 931–970 (1995).
- [57] VAN DEN BROECK C. *The many faces of the second law* (2010).
- [58] JARZYNSKI C. *Equalities and Inequalities: Irreversibility and the Second Law of Thermodynamics at the Nanoscale* (2011).
- [59] JARZYNSKI C. *Nonequilibrium Equality for Free Energy Differences*. Physical Review Letters, **78**(14), pp. 2690–2693 (1997).
- [60] JARZYNSKI C. *Equilibrium free-energy differences from nonequilibrium measurements: A master-equation approach*. Physical Review E, **56**(5), pp. 5018–5035 (1997).
- [61] CROOKS GE. *Entropy production fluctuation theorem and the nonequilibrium work relation for free energy differences*. Physical Review E, **60**, pp. 2721–2726 (1999).
- [62] CROOKS G. *Path-ensemble averages in systems driven far from equilibrium*. Physical Review E, **61**(3), pp. 2361–2366 (2000).
- [63] HUMMER G AND SZABO A. *Free energy reconstruction from nonequilibrium single-molecule pulling experiments*. Proceedings of the

- National Academy of Sciences of the United States of America, **98**, pp. 3658–3661 (2001).
- [64] LIPHARDT J, ONOA B, SMITH SB, TINOCO I AND BUSTAMANTE C. *Reversible unfolding of single RNA molecules by mechanical force*. Science, **292**(5517), p. 733 (2001).
- [65] COLLIN D, RITORT F, JARZYNSKI C, SMITH SB, TINOCO I AND BUSTAMANTE C. *Verification of the Crooks fluctuation theorem and recovery of RNA folding free energies*. Nature Physics, **437**(7056), p. 231 (2005).
- [66] MOSSA A, MANOSAS M, FORNS N, HUGUET JM AND RITORT F. *Dynamic force spectroscopy of DNA hairpins: I. Force kinetics and free energy landscapes*. Journal of Statistical Mechanics: Theory and Experiment, **P02060** (2009).
- [67] DUDKO O, GRAHAM T AND BEST R. *Locating the Barrier for Folding of Single Molecules under an External Force*. Physical Review Letters, **107**(20), p. 208301 (2011).
- [68] ALEMANY A, MOSSA A, JUNIER I AND RITORT F. *Experimental free-energy measurements of kinetic molecular states using fluctuation theorems*. Nature Physics, **8**(9), pp. 688–694 (2012).
- [69] GEBHARDT JCM, BORNSCHLÖGL T AND RIEF M. *Full distance-resolved folding energy landscape of one single protein molecule*. Proceedings of the National Academy of Sciences of the United States of America, **107**(5), pp. 2013–8 (2010).
- [70] JARZYNSKI C. *Single-molecule experiments: Out of equilibrium*. Nature Physics, **7**(8), pp. 591–592 (2011).
- [71] CHUNG HS, MCHALE K, LOUIS JM AND EATON WA. *Single-Molecule Fluorescence Experiments Determine Protein Folding Transition Path Times*. Science, **335**(6071), pp. 981–984 (2012).
- [72] GORE J, RITORT F AND BUSTAMANTE C. *Bias and error in estimates of equilibrium free-energy differences from nonequilibrium*

- measurements*. Proceedings of the National Academy of Sciences of the United States of America, **100**(22), pp. 12564–9 (2003).
- [73] PALASSINI M AND RITORT F. *Improving Free-Energy Estimates from Unidirectional Work Measurements: Theory and Experiment*. Physical Review Letters, **107**(6), p. 060601 (2011).
 - [74] LECHNER W AND DELLAGO C. *On the efficiency of path sampling methods for the calculation of free energies from non-equilibrium simulations*. Journal of Statistical Mechanics: Theory and Experiment, **P04001** (2007).
 - [75] OBERHOFER H AND DELLAGO C. *Efficient extraction of free energy profiles from nonequilibrium experiments*. Journal of computational chemistry, **30**(11), pp. 1726–36 (2009).
 - [76] ZUCKERMAN D AND WOOLF T. *Efficient dynamic importance sampling of rare events in one dimension*. Physical Review E, **63**(1), p. 016702 (2000).
 - [77] ZUCKERMAN D AND WOOLF T. *Theory of a Systematic Computational Error in Free Energy Differences*. Physical Review Letters, **89**(18), p. 180602 (2002).
 - [78] ZUCKERMAN DM AND WOOLF TB. *Systematic Finite-Sampling Inaccuracy in Free Energy Differences and Other Nonlinear Quantities*. Journal of Statistical Physics, **114**(5/6), pp. 1303–1323 (2004).
 - [79] POHORILLE A, JARZYNSKI C AND CHIPOT C. *Good practices in free-energy calculations*. The journal of physical chemistry. B, **114**(32), pp. 10235–53 (2010).
 - [80] OBERHOFER H, DELLAGO C AND GEISLER PL. *Biased sampling of nonequilibrium trajectories: can fast switching simulations outperform conventional free energy calculation methods?* The journal of physical chemistry. B, **109**(14), pp. 6902–15 (2005).
 - [81] WILLIAMS SR. *Rare-event sampling for driven inertial systems via the nonequilibrium distribution function*. Physical Review E, **88**(4), p. 043301 (2013).

- [82] ENGEL A. *Asymptotics of work distributions in nonequilibrium systems*. Physical Review E, **80**(2), pp. 1–7 (2009).
- [83] WANG GM, SEVICK EM, MITTAG E, SEARLES DJ AND EVANS DJ. *Experimental Demonstration of Violations of the Second Law of Thermodynamics for Small Systems and Short Time Scales*. Physical Review Letters, **89**(5), p. 050601 (2002).
- [84] CARBERRY D, REID J, WANG G, SEVICK E, SEARLES D AND EVANS D. *Fluctuations and Irreversibility: An Experimental Demonstration of a Second-Law-Like Theorem Using a Colloidal Particle Held in an Optical Trap*. Physical Review Letters, **92**(14) (2004).
- [85] BLICKLE V, SPECK T, HELDEN L, SEIFERT U AND BECHINGER C. *Thermodynamics of a Colloidal Particle in a Time-Dependent Nonharmonic Potential*. Physical Review Letters, **96**(7), p. 070603 (2006).
- [86] ALTLAND A, DE MARTINO A, EGGER R AND NAROZHNY B. *Fluctuation Relations and Rare Realizations of Transport Observables*. Physical Review Letters, **105**(17), p. 170601 (2010).
- [87] SAIRA OP, YOON Y, TANTTU T, MÖTTÖNEN M, AVERIN DV AND PEKOLA JP. *Test of Jarzynski and Crooks fluctuation relations in an electronic system*. Physical Review Letters, **109**(18), pp. 1–13 (2012).
- [88] CILIBERTO S, IMPARATO A, NAERT A AND TANASE M. *Heat Flux and Entropy Produced by Thermal Fluctuations*. Physical Review Letters, **110**(18), p. 180601 (2013).
- [89] CAMPISI M, BLATTMANN R, KOHLER S, ZUECO D AND HÄNGGI P. *Employing circuit QED to measure non-equilibrium work fluctuations*. New Journal of Physics, **15**(10), p. 105028 (2013).
- [90] JARZYNSKI C. *Rare events and the convergence of exponentially averaged work values*. Physical Review E, **73**(4), p. 46105 (2006).

- [91] ESPOSITO M, KAWAI R, LINDENBERG K AND VAN DEN BROECK C. *Efficiency at Maximum Power of Low-Dissipation Carnot Engines*. Physical Review Letters, **105**(15), p. 150603 (2010).
- [92] BLICKLE V AND BECHINGER C. *Realization of a micrometre-sized stochastic heat engine*. Nature Physics, **7**(12), pp. 1–4 (2011).
- [93] SEIFERT U. *Efficiency of Autonomous Soft Nanomachines at Maximum Power*. Physical Review Letters, **106**(2), p. 020601 (2011).
- [94] ESPOSITO M, KUMAR N, LINDENBERG K, VAN DEN BROECK C AND BROECK CVD. *Stochastically driven single-level quantum dot: A nanoscale finite-time thermodynamic machine and its various operational modes*. Physical Review E, **85**(3), pp. 1–4 (2012).
- [95] VAN DEN BROECK C, KUMAR N AND LINDENBERG K. *Efficiency of Isothermal Molecular Machines at Maximum Power*. Physical Review Letters, **108**(21), p. 210602 (2012).
- [96] ZIMMERMANN E AND SEIFERT U. *Efficiencies of a molecular motor: a generic hybrid model applied to the F 1 -ATPase*. New Journal of Physics, **14**(10), p. 103023 (2012).
- [97] BARATO AC AND SEIFERT U. *An autonomous and reversible Maxwell’s demon*. Europhysics Letters, **101**(6), p. 60001 (2013).
- [98] HOPPENAU J, NIEMANN M AND ENGEL A. *Carnot process with a single particle*. Physical Review E, **87**(6), p. 062127 (2013).
- [99] TOYABE S, SAGAWA T, UEDA M, MUNHEYUKI E AND SANO M. *Experimental demonstration of information-to-energy conversion and validation of the generalized Jarzynski equality*. Nature Physics, **6**(12), pp. 988–992 (2010).
- [100] MANDAL D AND JARZYNSKI C. *Work and information processing in a solvable model of Maxwell’s demon*. Proceedings of the National Academy of Sciences of the United States of America, **109**(29), p. 6 (2012).

- [101] BÉRUT A, ARAKELYAN A, PETROSYAN A, CILIBERTO S, DIL-
LENSCHNEIDER R AND LUTZ E. *Experimental verification of Land-
auer's principle linking information and thermodynamics*. Nature
Physics, **483**(7388), pp. 187–189 (2012).
- [102] MANDAL D, QUAN HT AND JARZYNSKI C. *Maxwell's Refrigera-
tor: An Exactly Solvable Model*. Physical Review Letters, **111**(3), p.
030602 (2013).
- [103] BÉRUT A, PETROSYAN A AND CILIBERTO S. *Detailed Jarzynski
equality applied to a logically irreversible procedure*. Europhysics
Letters, **103**(6), p. 60002 (2013).
- [104] ANDRIEUX D AND GASPARD P. *Information erasure in copolymers*.
Europhysics Letters, **103**(3), p. 30004 (2013).
- [105] DEFFNER S AND JARZYNSKI C. *Information processing and the
second law of thermodynamics: an inclusive, Hamiltonian approach*.
Physical Review X, **3**(4), p. 14 (2013).
- [106] BARATO AC AND SEIFERT U. *Unifying Three Perspectives on In-
formation Processing in Stochastic Thermodynamics*. Physical Re-
view Letters, **112**(9), p. 090601 (2014).
- [107] HOPPENAU J AND ENGEL A. *On the energetics of information
exchange*. Europhysics Letters, **105**(5), p. 50002 (2014).
- [108] FRISCH U. *Turbulence* (Cambridge University Press, Cambridge,
1995).
- [109] TAYLOR GI. *Statistical theory of turbulence*. Proceedings of the
Royal Society of London, **151**(873), pp. 421–444 (1935).
- [110] RENNER C, PEINKE J AND FRIEDRICH R. *Experimental indicati-
ons for Markov properties of small-scale turbulence*. Journal of Fluid
Mechanics, **433**, pp. 383–409 (2001).
- [111] RICHARDSON LF. *Weather prediction by numerical process* (Cam-
bridge University Press, 1922).

- [112] KOLMOGOROV AN. *A refinement of previous hypotheses concerning the local structure of turbulence in a viscous incompressible fluid at high Reynolds number*. Journal of Fluid Mechanics, **13**(01), p. 82 (1962).
- [113] RENNER C. *Markowanalysen stochastisch fluktuierender Zeitserien*. Ph.D. thesis, Carl von Ossietzky Universität Oldenburg (2002).
- [114] KOLMOGOROV AN. *Dissipation of energy in locally isotropic turbulence*. Dokl. Akad. Nauk SSSR, **32**(1), pp. 16–18 (1941).
- [115] MOURI H, TAKAOKA M, HORI A AND KAWASHIMA Y. *On Landau’s prediction for large-scale fluctuation of turbulence energy dissipation*. Physics of Fluids, **18**(1), p. 015103 (2006).
- [116] CASTAING B, GAGNE Y AND HOPFINGER E. *Velocity probability density functions of high Reynolds number turbulence*. Physica D: Nonlinear Phenomena, **46**(2), pp. 177–200 (1990).
- [117] STOLOVITZKY G, MENEVEAU C AND SREENIVASAN K. *Comment on “Isotropic Turbulence: Important Differences between True Dissipation Rate and Its One-Dimensional Surrogate”*. Physical Review Letters, **80**(17), pp. 3883–3883 (1998).
- [118] KRAICHNAN RH. *On Kolmogorov’s inertial-range theories*. Journal of Fluid Mechanics, **62**(02), p. 305 (1974).
- [119] BOFFETTA G AND ECKE RE. *Two-Dimensional Turbulence*. Annual Review of Fluid Mechanics, **44**(1), pp. 427–451 (2012).
- [120] KRAICHNAN RH. *Inertial Ranges in Two-Dimensional Turbulence*. Physics of Fluids, **10**(7), p. 1417 (1967).
- [121] FRIEDRICH R, VOSS KUHLE M, KAMPS O AND WILCZEK M. *Two-point vorticity statistics in the inverse cascade of two-dimensional turbulence*. Physics of Fluids, **24**(12), p. 125101 (2012).
- [122] CHERTKOV M, CONNAUGHTON C, KOLOKOLOV I AND LEBEDEV V. *Dynamics of Energy Condensation in Two-Dimensional Turbulence*. Physical Review Letters, **99**(8), p. 084501 (2007).

- [123] XIAO Z, WAN M, CHEN S AND EYINK GL. *Physical mechanism of the inverse energy cascade of two-dimensional turbulence: a numerical investigation*. Journal of Fluid Mechanics, **619**, p. 1 (2008).
- [124] CENCINI M, MURATORE-GINANNESCHI P AND VULPIANI A. *Nonlinear Superposition of Direct and Inverse Cascades in Two-Dimensional Turbulence Forced at Large and Small Scales*. Physical Review Letters, **107**(17), pp. 1–5 (2011).
- [125] FRANCOIS N, XIA H, PUNZMANN H AND SHATS M. *Inverse Energy Cascade and Emergence of Large Coherent Vortices in Turbulence Driven by Faraday Waves*. Physical Review Letters, **110**(19), p. 194501 (2013).
- [126] MARINO R, MININNI PD, ROSENBERG D AND POUQUET A. *Inverse cascades in rotating stratified turbulence: Fast growth of large scales*. Europhysics Letters, **102**(4), p. 44006 (2013).
- [127] BIFERALE L, MUSACCHIO S AND TOSCHI F. *Inverse Energy Cascade in Three-Dimensional Isotropic Turbulence*. Physical Review Letters, **108**(16), pp. 1–5 (2012).
- [128] LÓPEZ-CABALLERO M AND BURGUETE J. *Inverse Cascades Sustained by the Transfer Rate of Angular Momentum in a 3D Turbulent Flow*. Physical Review Letters, **110**(12), p. 124501 (2013).
- [129] KOLMOGOROV AN. *The local structure of turbulence in incompressible viscous fluid for very large Reynolds numbers*. Dokl. Akad. Nauk SSSR, **30**(4), pp. 299–303 (1941).
- [130] KOLMOGOROV AN. *On the degeneration of isotropic turbulence in an incompressible viscous fluid*. Dokl. Akad. Nauk SSSR, **31**(6), pp. 538–541 (1941).
- [131] OBUKHOV AM. *On the distribution of energy in the spectrum of turbulent flow*. Dokl. Akad. Nauk SSSR, **32**(1), pp. 22–24 (1941).
- [132] OBUKHOV AM. *Spectral energy distribution in a turbulent flow*. Izv. Akad. Nauk SSSR Ser. Geogr. Geofiz., **5**(4-5), pp. 453–466 (1941).

- [133] HOSOKAWA I, OIDE S AND YAMAMOTO K. *Isotropic Turbulence: Important Differences between True Dissipation Rate and Its One-Dimensional Surrogate*. Physical Review letters, **77**(22), pp. 4548–4551 (1996).
- [134] ISHIHARA T, GOTOH T AND KANEDA Y. *Study of High-Reynolds Number Isotropic Turbulence by Direct Numerical Simulation*. Annual Review of Fluid Mechanics, **41**(1), pp. 165–180 (2009).
- [135] CHIEN CC, BLUM DB AND VOTH GA. *Effects of fluctuating energy input on the small scales in turbulence*. Journal of Fluid Mechanics, **737**(2), pp. 527–551 (2013).
- [136] SREENIVASAN KR. *On the universality of the Kolmogorov constant*. Physics of Fluids, **7**(11), p. 2778 (1995).
- [137] OBUKHOV AM. *Some specific features of atmospheric turbulence*. Journal of Fluid Mechanics, **13**(01), p. 77 (1962).
- [138] ARNEODO A, BAUDET C, BELIN F, BENZI R, CASTAING B, CHABAUD B, CHAVARRIA R, CILIBERTO S, CAMUSSI R, CHILLÀ F, DUBRULLE B, GAGNE Y, HEBRAL B, HERWEIJER J, MARCHAND M, MAURER J, MUZY JF, NAERT A, NOULLEZ A, PEINKE J, ROUX F, TABELING P, VAN DE WATER W AND WILLAIME H. *Structure functions in turbulence, in various flow configurations, at Reynolds number between 30 and 5000, using extended self-similarity*. Europhysics Letters, **34**(6), pp. 411–416 (1996).
- [139] NOVIKOV EA. *Intermittency and scale similarity in the structure of a turbulent flow*. Journal of Applied Mathematics and Mechanics, **35**(2), pp. 231–241 (1971).
- [140] SREENIVASAN KR AND ANTONIA RA. *The phenomenology of small-scale turbulence*. Annu. Rev. Fluid Mech., **29**(72), p. 435 (1997).
- [141] BÖTTCHER F, RENNER C, WALDL HP AND PEINKE J. *On the statistics of wind gusts*. Boundary-Layer Meteorology, **108**(1), pp. 163–173 (2003).

- [142] BÖTTCHER F, BARTH S AND PEINKE J. *Small and large scale fluctuations in atmospheric wind speeds*. Stochastic Environmental Research and Risk Assessment, **21**(3), pp. 299–308 (2006).
- [143] POUQUET A AND MARINO R. *Geophysical Turbulence and the Duality of the Energy Flow Across Scales*. Physical Review Letters, **111**(23), p. 234501 (2013).
- [144] WARHAFT Z. *Passive Scalars in Turbulent Flows*. Annual Review of Fluid Mechanics, **32**(1), pp. 203–240 (2000).
- [145] DIMOTAKIS PE. *Turbulent mixing*. Annual Review of Fluid Mechanics, **37**(1), pp. 329–356 (2005).
- [146] PEINKE J, BARTH S, BÖTTCHER F, HEINEMANN D AND LANGE B. *Turbulence, a challenging problem for wind energy*. Physica A: Statistical Mechanics and its Applications, **338**(1-2), pp. 187–193 (2004).
- [147] MÜCKE T, KLEINHANS D AND PEINKE J. *Atmospheric turbulence and its influence on the alternating loads on wind turbines*. Wind Energy, **14**(2), pp. 301–316 (2011).
- [148] WÄCHTER M, HEISS ELMANN H, HÖLLING M, MORALES A, MILAN P, MÜCKE T, PEINKE J, REINKE N AND RINN P. *The turbulent nature of the atmospheric boundary layer and its impact on the wind energy conversion process*. Journal of Turbulence, **13**, p. N26 (2012).
- [149] RINN P, HEISS ELMANN H, WÄCHTER M AND PEINKE J. *Stochastic method for in-situ damage analysis*. The European Physical Journal B, **86**(1), p. 3 (2012).
- [150] MILAN P, WÄCHTER M AND PEINKE J. *Turbulent Character of Wind Energy*. Physical Review Letters, **110**(13), p. 138701 (2013).
- [151] BIFERALE L. *Shell models of energy cascade in turbulence*. Annual Review of Fluid Mechanics, **35**(1), pp. 441–468 (2003).

- [152] FRISCH U, SULEM PL AND NELKIN M. *A simple dynamical model of intermittent fully developed turbulence*. Journal of Fluid Mechanics, **87**(04), p. 719 (1978).
- [153] MENEVEAU C AND SREENIVASAN K. *Simple multifractal cascade model for fully developed turbulence*. Physical Review Letters, **59**(13), pp. 1424–1427 (1987).
- [154] BENZI R, BIFERALE L, PALADIN G, VULPIANI A AND VERGASSOLA M. *Multifractality in the statistics of the velocity gradients in turbulence*. Physical Review Letters, **67**(17), pp. 2299–2302 (1991).
- [155] ARNEODO A, BACRY E AND MUZY J. *The thermodynamics of fractals revisited with wavelets*. Physica A: Statistical Mechanics and its Applications, **213**(1-2), pp. 232–275 (1995).
- [156] YAKHOT V AND SREENIVASAN K. *Towards a dynamical theory of multifractals in turbulence*. Physica A: Statistical Mechanics and its Applications, **343**, pp. 147–155 (2004).
- [157] AURELL E, FRISCH U, LUTSKO J AND VERGASSOLA M. *On the multifractal properties of the energy dissipation derived from turbulence data*. Journal of Fluid Mechanics, **238**(1), p. 467 (2006).
- [158] CHAKRABORTY S, SAHA A AND BHATTACHARJEE J. *Large deviation theory for coin tossing and turbulence*. Physical Review E, **80**(5), p. 56302 (2009).
- [159] ZYBIN KP AND SIROTA VA. *Vortex filament model and multifractal conjecture*. Physical Review E, **85**(5), p. 056317 (2012).
- [160] JIMENEZ J AND WRAY AA. *On the characteristics of vortex filaments in isotropic turbulence*. Journal of Fluid Mechanics, **373**, pp. 255–285 (1998).
- [161] PIROZZOLI S. *On the velocity and dissipation signature of vortex tubes in isotropic turbulence*. Physica D: Nonlinear Phenomena, **241**(3), pp. 202–207 (2012).

- [162] ZYBIN K, SIROTA V AND ILYIN A. *Small-scale vorticity filaments and structure functions of the developed turbulence*. Physica D: Non-linear Phenomena, **241**(3), pp. 269–275 (2012).
- [163] ZYBIN KP AND SIROTA VA. *On the multifractal structure of fully developed turbulence*. p. 12 (2013).
- [164] SHE ZS AND LEVEQUE E. *Universal scaling laws in fully developed turbulence*. Physical Review Letters, **72**(3), pp. 336–339 (1994).
- [165] DUBRULLE B. *Intermittency in fully developed turbulence: Log-Poisson statistics and generalized scale covariance*. Physical Review Letters, **73**(7), pp. 959–962 (1994).
- [166] SHE ZS AND WAYMIRE E. *Quantized Energy Cascade and Log-Poisson Statistics in Fully Developed Turbulence*. Physical Review Letters, **74**(2), pp. 262–265 (1995).
- [167] L’VOV V AND PROCACCIA I. *Fusion rules in turbulent systems with flux equilibrium*. Physical Review letters, **76**(16), pp. 2898–2901 (1996).
- [168] L’VOV V AND PROCACCIA I. *Towards a nonperturbative theory of hydrodynamic turbulence: Fusion rules, exact bridge relations, and anomalous viscous scaling functions*. Physical Review E, **54**(6), pp. 6268–6284 (1996).
- [169] FAIRHALL A, DHRUVA B, L’VOV V, PROCACCIA I AND SREENIVASAN K. *Fusion Rules in Navier-Stokes Turbulence: First Experimental Tests*. Physical Review Letters, **79**(17), pp. 3174–3177 (1997).
- [170] BENZI R, BIFERALE L AND TOSCHI F. *Multiscale Velocity Correlations in Turbulence*. Physical Review Letters, **80**(15), pp. 3244–3247 (1998).
- [171] L’VOV VS AND PROCACCIA I. *Analytic calculation of the anomalous exponents in turbulence: Using the fusion rules to flush out a small parameter*. Physical Review E, **62**(6), pp. 8037–8057 (2000).

- [172] RENNER C AND PEINKE J. *A Generalization of Scaling Models of Turbulence*. Journal of Statistical Physics, **146**(1), pp. 25–32 (2011).
- [173] BENZI R, TRIPICCIONE R, BAUDET C, MASSAIOLI F AND SUCCI S. *Extended self-similarity in turbulent flows*. Physical Review E, **48**(1), pp. R29–R32 (1993).
- [174] CASTAING B AND DUBRULLE B. *Fully Developed Turbulence: A Unifying Point of View*. Journal de Physique II, **5**(7), pp. 895–899 (1995).
- [175] CASTAING B. *The Temperature of Turbulent Flows*. Journal de Physique II, **6**(1), pp. 105–114 (1996).
- [176] CHILLA F, PEINKE J AND CASTAING B. *Multiplicative Process in Turbulent Velocity Statistics: A Simplified Analysis*. Journal de Physique II, **6**(4), pp. 455–460 (1996).
- [177] AMBLARD PO AND BROSSIER JM. *On the cascade in fully developed turbulence. The propagator approach versus the Markovian description*. The European Physical Journal B, **12**(4), pp. 579–582 (1999).
- [178] DUBRULLE B. *Affine turbulence*. The European Physical Journal B, **13**(1), pp. 1–4 (2000).
- [179] CHANAL O, CHABAUD B, CASTAING B AND HÉBRAL B. *Intermittency in a turbulent low temperature gaseous helium jet*. The European Physical Journal B, **17**(2), pp. 309–317 (2000).
- [180] CHEVILLARD L, CASTAING B AND LÉVÊQUE E. *On the rapid increase of intermittency in the near-dissipation range of fully developed turbulence*. The European Physical Journal B, **45**(4), pp. 561–567 (2005).
- [181] POLYAKOV A. *Turbulence without pressure*. Physical Review E, **52**(6), pp. 6183–6188 (1995).
- [182] YAKHOT V. *Probability density and scaling exponents of the moments of longitudinal velocity difference in strong turbulence*. Physical Review E, **57**(2), pp. 1737–1751 (1998).

- [183] YAKHOT V. *Mean-field approximation and a small parameter in turbulence theory*. Physical Review E, **63**(2), p. 026307 (2001).
- [184] YAKHOT V. *Mean-Field Approximation and Extended Self-Similarity in Turbulence*. Physical Review Letters, **87**(23), p. 234501 (2001).
- [185] YAKHOT V. *Pressure-velocity correlations and scaling exponents in turbulence*. Journal of Fluid Mechanics, **495**, pp. 135–143 (2003).
- [186] YAKHOT V. *Probability densities in strong turbulence*. Physica D: Nonlinear Phenomena, **215**(2), pp. 166–174 (2006).
- [187] MANDELBROT BB. *Intermittent turbulence in self-similar cascades: divergence of high moments and dimension of the carrier*. Journal of Fluid Mechanics, **62**(02), p. 331 (1974).
- [188] BENZI R, PALADIN G, PARISI G AND VULPIANI A. *On the multifractal nature of fully developed turbulence and chaotic systems*. Journal of Physics A: Mathematical and General, **17**(18), pp. 3521–3531 (1984).
- [189] ARNEODO A, MUZY JF AND ROUX SG. *Experimental Analysis of Self-Similarity and Random Cascade Processes: Application to Fully Developed Turbulence Data*. Journal de Physique II, **7**(2), pp. 363–370 (1997).
- [190] NAERT A, FRIEDRICH R AND PEINKE J. *Fokker-Planck equation for the energy cascade in turbulence*. Physical Review E, **56**(6), pp. 6719–6722 (1997).
- [191] SIEFERT M AND PEINKE J. *Complete multiplier statistics explained by stochastic cascade processes*. Physics Letters A, **371**(1-2), pp. 34–38 (2007).
- [192] FRIEDRICH R AND PEINKE J. *Description of a Turbulent Cascade by a Fokker-Planck Equation*. Physical Review Letters, **78**(5), pp. 863–866 (1997).

References

- [193] FRIEDRICH R AND PEINKE J. *Statistical properties of a turbulent cascade*. Physica D: Nonlinear Phenomena, **102**(1-2), pp. 147–155 (1997).
- [194] BLACK F AND SCHOLES M. *The pricing of options and corporate liabilities*. The journal of political economy, **81**(3), pp. 637–654 (1973).
- [195] PAUL W AND BASCHNAGEL J. *Stochastic Processes: From Physics to Finance* (Springer, 1999).
- [196] HOSOKAWA I. *Markov process built in scale-similar multifractal energy cascades in turbulence*. Physical Review. E, Statistical, nonlinear, and soft matter physics, **65**(2 Pt 2), p. 027301 (2002).
- [197] DAVOUDI J AND TABAR MR. *Theoretical Model for the Kramers-Moyal Description of Turbulence Cascades*. Physical Review Letters, **82**(8), pp. 1680–1683 (1999).
- [198] DAVOUDI J AND REZA RAHIMI TABAR M. *Multiscale correlation functions in strong turbulence*. Physical Review E, **61**(6 Pt A), pp. 6563–7 (2000).
- [199] LÜCK S, RENNER C, PEINKE J AND FRIEDRICH R. *The Markov-Einstein coherence length—a new meaning for the Taylor length in turbulence*. Physics Letters A, **359**(5), pp. 335–338 (2006).
- [200] MARCQ P AND NAERT A. *A langevin equation for the energy cascade in fully developed turbulence*. Physica D: Nonlinear Phenomena, **124**(4), pp. 368–381 (1998).
- [201] RENNER C, PEINKE J AND FRIEDRICH R. *On the interaction between velocity increment and energy dissipation in the turbulent cascade*. p. 18 (2002).
- [202] NAWROTH A, PEINKE J, KLEINHANS D AND FRIEDRICH R. *Improved estimation of Fokker-Planck equations through optimization*. Physical Review E, **76**(5), p. 56102 (2007).

- [203] KLEINHANS D AND FRIEDRICH R. *Maximum likelihood estimation of drift and diffusion functions*. Physics Letters A, **368**(3-4), pp. 194–198 (2007).
- [204] KLEINHANS D. *Estimation of drift and diffusion functions from time series data: A maximum likelihood framework*. Physical Review E, **85**(2), p. 026705 (2012).
- [205] RAGWITZ M AND KANTZ H. *Indispensable Finite Time Corrections for Fokker-Planck Equations from Time Series Data*. Physical Review Letters, **87**(25), p. 254501 (2001).
- [206] CARVALHO J, RAISCHEL F, HAASE M AND LIND P. *Evaluating strong measurement noise in data series with simulated annealing method*. Journal of Physics: Conference Series, **285**, p. 012007 (2011).
- [207] GOTTSCHALL J AND PEINKE J. *On the definition and handling of different drift and diffusion estimates*. New Journal of Physics, **10**(8), p. 83034 (2008).
- [208] LIND P, MORA A, GALLAS J AND HAASE M. *Reducing stochasticity in the North Atlantic Oscillation index with coupled Langevin equations*. Physical Review E, **72**(5), p. 056706 (2005).
- [209] RAISCHEL F, SCHOLZ T, LOPES VV AND LIND PG. *Uncovering wind turbine properties through two-dimensional stochastic modeling of wind dynamics*. Physical Review E, **88**(4), p. 042146 (2013).
- [210] FRIEDRICH J AND FRIEDRICH R. *Generalized vortex model for the inverse cascade of two-dimensional turbulence*. Physical Review E, **88**(5), p. 053017 (2013).
- [211] PETERS O AND KLEIN W. *Ergodicity Breaking in Geometric Brownian Motion*. Physical Review Letters, **110**(10), p. 100603 (2013).

References

A Technical details of continuous MPs

A.1 Itô calculus

The material presented in this chapter is adapted from part 4 of the book by Gardiner [4].

In this appendix, we provide a quick introduction to the calculus of stochastic differential equations (SDEs). The simplest form of a SDE is the Wiener process $W(t)$ which is a sequence of Gaussian random number with zero mean and variance t . As for infinitesimal t also the variance is infinitesimal small, the Wiener process is continuous but can be shown to be non-differentiable. On the other hand, integration of a random function $\xi(t)$ with zero mean and correlation function $\langle \xi(t - t') \rangle = \delta(t - t')$ reproduces the Wiener process $W(t)$. In that sense, the Gaussian white noise $\xi(t)$ is the non-existing derivative of $W(t)$,

$$dW(t) = W(t + dt) - W(t) = \xi(t)dt . \quad (\text{A.1.1})$$

Despite this pathology, $\xi(t)$ can be meaningfully combined with differential equations to form SDEs, constituting in many cases a simpler approach to stochastic processes than equivalent probabilistic descriptions. However, we have to keep in mind that $\xi(t)$ is only rigorously defined under an integral, very much like the δ -function.

The general form of a SDE is

$$\dot{x}(t) = f(x(t), t) + g(x(t), t) \xi(t) , \quad x(t = t_0) = x_0 . \quad (\text{A.1.2})$$

The solution of this SDE is the stochastic variable $x(t)$ which can in principle be obtained by integrating

$$x(t) = x_0 + \int_{t_0}^t f(x(\tau), \tau) d\tau + \int_{t_0}^t g(x(\tau), \tau) dW(\tau) . \quad (\text{A.1.3})$$

As the integrands are stochastic, the occurring *stochastic integrals* are not of Riemann type. For Riemann integrals, applying lower sum, upper sum, trapezoidal rule or other suitable discretisations, the value of the integral will always be the same in the continuous limit.

This is not the case for stochastic integrals, with the consequence that SDEs are only well defined if along with the SDE also the rule of discretisation is specified. The mathematically simplest rule is the *pre-point*

rule, where the integrand is evaluated at the beginning of each discretisation interval. The SDE is then called *Itô SDE*. The drawback with the Itô convention is that the rules of calculus need to be modified. Ordinary calculus can be used if the *mid-point* rule is used, for which the integrand is evaluated at the centre of each discretisation interval. In this case, the SDE is referred to as *Stratonovich SDE*.³⁹ The various discretisation rules will be formalised in appendix (A.3).

The modified calculus arising from the Itô interpretation of a SDE is called *Itô calculus*. Building on the Itô convention of stochastic integrals, it can be shown that $dW^2 = dt$ and $dW^{n+2} = 0$ for $n \geq 1$, which is the starting point of Itô calculus.

With regard to SDEs, the most important implication of Itô calculus is the *Itô lemma*. For a stochastic variable $x(t)$, the Itô lemma states that the total differential of a function $f(x(t), t)$ reads

$$df(x(t), t) = f'(x(t), t)dx + \frac{1}{2}f''(x(t), t)dW(t)^2 + \dot{f}(x(t), t)dt. \quad (\text{A.1.4})$$

Since $dW(t) = \sqrt{dt}$, the Itô lemma collects all terms of order dt .

We exemplify the use of Itô's lemma (A.1.4) by changing the variable $x(t)$ to $y(x(t))$ and get the formula

$$\begin{aligned} dy(x) &= y'(x)dx + \frac{1}{2}y''(x)dx^2 \\ &= y'(x)[f(x, t)dt + g(x, t)dW(t)] + \frac{1}{2}y''(x)g(x, t)^2dW(t)^2 \\ \Rightarrow \dot{y}(x(t)) &= y'(x)[f(x, t) + g(x, t)\xi(t)] + \frac{1}{2}y''(x)g(x, t)^2, \end{aligned} \quad (\text{A.1.5})$$

where we used Itô's lemma (A.1.4) in the first line and substituted $dx(t)$ from the general form of the SDE in (A.1.2) in the second line. This prescription is known as *Itô's formula* for change of variables and is often used to solve SDEs.

Let us consider *geometric Brownian motion* (GBM) with constant drift as an example. The SDE reads

$$\dot{x}(t) = a(t)x(t) + \sqrt{2b(t)}x(t)\xi(t), \quad \text{Itô}. \quad (\text{A.1.6})$$

³⁹More specific, the Stratonovich stochastic integral takes the average of beginning and end of the discretisation intervals, and is therefore only *related* to the mid-point rule ([4] p.96). In the limit of infinitesimal discretisation intervals, however, this distinction becomes irrelevant.

This SDE can be solved using the transformation $y(x) = \ln x$. We identify $f(x, t) = a(t)x$ and $g(x, t) = \sqrt{2b(t)}x$ and get for $y(t)$ the SDE

$$\begin{aligned} \dot{y}(x(t)) &= y'(x(t)) [a(t)x(t) + \sqrt{2b(t)}x(t)\xi(t)] + y''(x(t))b(t)x(t)^2 \\ &= a(t) + \sqrt{2b(t)}\xi(t) - b(t) \\ \Rightarrow \dot{y}(t) &= (a(t) - b(t)) + \sqrt{2b(t)}\xi(t) . \end{aligned} \quad (\text{A.1.7})$$

Note that by making use of Itô's formula, we now have the drift $a(t) - b(t)$ with the noise induced component $-\dot{b}(t)$.

The above SDE can readily be integrated,

$$y(t) = y(t_0) + A(t) - B(t) + \sqrt{2b(t)}Z(t) , \quad (\text{A.1.8})$$

where

$$A(t) = \int_{t_0}^t a(t') dt' , \quad (\text{A.1.9a})$$

$$B(t) = \int_{t_0}^t b(t') dt' , \quad (\text{A.1.9b})$$

$$(\text{A.1.9c})$$

and

$$Z(t) = \int_{t_0}^t \xi(t') dt' \quad (\text{A.1.10})$$

is a Gaussian random variable with zero mean and variance t , as we see from

$$\langle Z(t) \rangle = \int_{t_0}^t \langle \xi(t') \rangle dt' = 0 , \quad (\text{A.1.11a})$$

$$\begin{aligned} \langle Z(t)^2 \rangle &= \int_{t_0}^t \int_{t_0}^t \langle \xi(t') \xi(t'') \rangle dt' dt'' \\ &= \int_{t_0}^t \int_{t_0}^t \delta(t' - t'') dt' dt'' = \int_{t_0}^t dt' = t . \end{aligned} \quad (\text{A.1.11b})$$

Note that $\langle Z(dt)^2 \rangle = dt$ in retrospect confirms $dW(t)^2 = dt$ as used above. The random variable $y(t)$ is therefore also a Gaussian random variable with mean $A(t) - B(t)$ and variance $2B(t)$. Accordingly, $x(t)$ is a log-normal random variable

$$x(t) = x_0 \exp \left[A(t) - B(t) + \sqrt{2B(t)} Z(t) \right] . \quad (\text{A.1.12})$$

Its PDF reads

$$p(x, t) = \frac{1}{x \sqrt{4\pi B(t)}} \exp \left[- \frac{(\ln(x/x_0) - (A(t) - B(t)))^2}{4B(t)} \right] . \quad (\text{A.1.13})$$

The moments of a log-normal distribution all exist and read in this case

$$\langle x(t)^n \rangle = \langle x_0^n \rangle \exp \left[(A(t) - B(t)) n + B(t) n^2 \right] . \quad (\text{A.1.14})$$

In standard GBM, the coefficients $a(r)$ and $b(r)$ are constants, and $A(t) - B(t)$ becomes $(a - b)(t - t_0)$. The ratio $g := a/b$ is known as exponential growth constant⁴⁰, see [211] for a discussion. Taking an arbitrary initial distribution $p_0(x_0) \neq \delta(x_0)$, for $g > 1$, all moments of $x(t)$ diverge exponentially, and for $g < 1$, all moments decay exponentially. Hence, for $g < 1$, the stationary solution is $p^{\text{st}}(x) = \delta(x)$ for which all trajectories get stuck at $x = 0$.

Note that interpretation of the SDE (A.1.6) in Stratonovich convention would lead to the mean $A(t)$ instead of $A(t) - B(t)$, as then ordinary calculus applies and the last term in the first line of (A.1.7) does not contribute.

⁴⁰also, the exponential growth rate $g := (a/b)/(t - t_0)$

A.2 Transformation of time in a SDE

We want to transform time in the SDE

$$\dot{x}(t) = f(x, t) + g(x, t)\xi(t) . \quad (\text{A.2.1})$$

Integration from t to $t + \Delta t$, where Δt is a infinitesimal time-step, yields

$$\begin{aligned} x(t + \Delta t) &= x(t) + f_\alpha(x, t)\Delta t + \int_t^{t+\Delta t} g(x, t)\xi(t) dt \\ &= x(t) + f_\alpha(x, t)\Delta t + g_\alpha(x, t)Z(\Delta t) . \end{aligned} \quad (\text{A.2.2})$$

Here we have used the mean-value theorem for integration, where the index α indicates evaluation at time $t + \alpha\Delta t$ with $0 \leq \alpha \leq 1$, and we have used the Gaussian random variable $Z(\Delta t)$ defined in (A.1.10) with zero mean and variance Δt from (A.1.11).

In fact, the mean-value theorem is not defined for a stochastic integral. The consequence that we applied it anyway is that in the limit $\Delta t \rightarrow 0$ the value chosen for α does still matter. The choice of α is equivalent to the choice of discretisation of the SDE, i.e. $\alpha = 0$ for pre-point and $\alpha = 1/2$ for mid-point. Indeed, we show in appendix A.3 that the PDF $p(x, t)$ obeys the Fokker-Planck equation (FPE)

$$\dot{p}(x, t) = \left[-\partial_x (f(x, t) + \alpha g'(x, t)g(x, t)) + \frac{1}{2}\partial_x^2 g(x, t)^2 \right] p(x, t) , \quad (\text{A.2.3})$$

where the value of α still enters.

We return to the question of time transformation.

Suppose we want transform time from t to $s = a(t)$. For convenience, we denote $b(s) := a^{-1}(s)$. Using $ds = \dot{a}(t)dt$, that is $\partial_t = \dot{a}(b(s))\partial_s$, the SDE reads

$$\dot{a}(b(s))\dot{\tilde{x}}(s) = \tilde{f}(\tilde{x}, s) + \tilde{g}(\tilde{x}, s)\xi(b(s)) , \quad (\text{A.2.4})$$

where $\tilde{x}(s) := x(b(s))$, $\tilde{f}(\tilde{x}, s) := f(\tilde{x}, b(s))$ and $\tilde{g}(\tilde{x}, s) := g(\tilde{x}, b(s))$ are now evaluated for the new time s .

The noise $\xi(b(s))$ needs special attention if we require that the properties

of the stochastic integral $\tilde{Z}(\Delta s)$ of new noise $\tilde{\xi}(s)$ are of the form (A.1.11), that is in particular $\langle \tilde{Z}(\Delta s)^2 \rangle = \Delta s$. This requirement is met if we use

$$\tilde{\xi}(s) = \frac{\xi(b(s))}{\sqrt{\dot{a}(b(s))}} , \quad (\text{A.2.5})$$

since then we have consistently

$$\begin{aligned} ds &= (\tilde{\xi}(s)ds)^2 = \frac{[\xi(b(s))ds]^2}{\dot{a}(b(s))} \\ &= \frac{[\xi(t)\dot{a}(t)dt]^2}{\dot{a}(t)} = \dot{a}(t)[\xi(t)dt]^2 = \dot{a}(t)dt , \end{aligned} \quad (\text{A.2.6})$$

where we used $[\xi(t)dt]^2 = dt$.

With an equivalent but more tedious calculation we can also explicitly show that

$$\begin{aligned} \langle \tilde{Z}(\Delta s)^2 \rangle &= \int_s^{s+\Delta s} \int_s^{s+\Delta s} \langle \tilde{\xi}(s')\tilde{\xi}(s'') \rangle ds' ds'' \\ &= \int_s^{s+\Delta s} \int_s^{s+\Delta s} \frac{1}{\sqrt{\dot{a}(b(s'))\dot{a}(b(s''))}} \langle \xi(b(s'))\xi(b(s'')) \rangle ds' ds'' \\ &= \int_{b(s)}^{b(s+\Delta s)} \int_{b(s)}^{b(s+\Delta s)} \frac{\dot{a}(t')\dot{a}(t'')}{\sqrt{\dot{a}(t')\dot{a}(t'')}} \langle \xi(t')\xi(t'') \rangle dt' dt'' \\ &= \int_{b(s)}^{b(s+\Delta s)} \int_{b(s)}^{b(s+\Delta s)} \dot{a}(t') \delta(t' - t'') dt' dt'' \\ &= \int_{b(s)}^{b(s+\Delta s)} \dot{a}(t'') dt'' = a(b(s+\Delta s)) - a(b(s)) = \Delta s . \end{aligned} \quad (\text{A.2.7})$$

Note that instead of $[\xi(t)dt]^2 = dt$ in the derivation (A.2.6), we used here that $\langle \xi(t)\xi(t') \rangle = \delta(t - t')$.

Substitution of (A.2.5) into (A.2.1) yields the transformed SDE

$$\dot{\tilde{x}}(s) = \frac{\tilde{f}(\tilde{x}, s)}{\dot{a}(b(s))} + \frac{\tilde{g}(\tilde{x}, s)}{\sqrt{\dot{a}(b(s))}} \tilde{\xi}(s) . \quad (\text{A.2.8})$$

We reason from $\langle \tilde{Z}(\Delta s)^2 \rangle = \Delta s$ that also $\langle \tilde{\xi}(s) \tilde{\xi}(s') \rangle = \delta(s - s')$ and obtain by comparison with (A.2.3) the equivalent FPE

$$\dot{\tilde{p}}(x, s) = \left[-\partial_x \left(\frac{\tilde{f}(x, s)}{\dot{a}(b(s))} + \alpha \frac{\tilde{g}'(x, s) \tilde{g}(x, s)}{\dot{a}(b(s))} \right) + \frac{1}{2} \partial_x^2 \frac{\tilde{g}(x, s)^2}{\dot{a}(b(s))} \right] \tilde{p}(x, s) \quad (\text{A.2.9})$$

for the PDF $\tilde{p}(x, s) := p(x, b(s))$. This FPE results also from applying the same time transformation directly to (A.2.3) as it should be.

Alternatively, we could also require that in the SDE with transformed time, (A.2.4), the noise must have the correlation function

$$\langle \xi(b(s)) \xi(b(s')) \rangle = \sqrt{\dot{a}(b(s))} \delta(s - s') \quad (\text{A.2.10})$$

in order to have a Gaussian random variable $Z(\Delta s)$ with variance Δs in the integrated SDE, cf. (A.2.2), and to retain the equivalence to a FPE as between (A.2.1) and (A.2.3).

As an example, let us again consider GBM with constant drift as in (A.1.6), but now with the coefficients $a(t) = a/t$ and $b(t) = b/t$. The SDE reads

$$\dot{x}(t) = \frac{a}{t} x(t) + \sqrt{\frac{2b}{t}} x(t) \xi(t) , \quad \alpha\text{-point} . \quad (\text{A.2.11})$$

with δ -correlated $\xi(t)$. By noting $f(x, t) = a/t x$ and $g(x, t) = \sqrt{2b/t} x$, the equivalent FPE from (A.2.3) follows as

$$\dot{p}(x, t) = \left[-\partial_x \left(\frac{a}{t} x + \alpha \frac{2b}{t} x \right) + \partial_x^2 \frac{b}{t} x^2 \right] p(x, t) , \quad (\text{A.2.12})$$

or, by multiplying with t ,

$$t \dot{p}(x, t) = \left[- (a + 2\alpha b) \partial_x x + b \partial_x^2 x^2 \right] p(x, t) . \quad (\text{A.2.13})$$

Transformation to logarithmic time, i.e. $s = a(t) = \ln t$, $t = b(s) = \exp s$ and $\dot{a}(t) = 1/t$, yields the FPE

$$\dot{\tilde{p}}(x, s) = \left[- (a + 2\alpha b) \partial_x x + b \partial_x^2 x^2 \right] \tilde{p}(x, s) \quad (\text{A.2.14})$$

with now time independent coefficients.

The equivalent SDE is accordingly

$$\dot{\tilde{x}}(s) = a x(t) + \sqrt{2b} \tilde{x}(s) \tilde{\xi}(s) , \quad \alpha\text{-point} , \quad (\text{A.2.15})$$

where $\tilde{\xi}(s)$ is again δ -correlated.

On the other hand, if we multiply the SDE with t , we obtain

$$t \dot{x}(t) = a x(t) + \sqrt{2b} x(t) \sqrt{t} \xi(t) , \quad \alpha\text{-point} , \quad (\text{A.2.16})$$

and see that transformation to $s = \ln t$ does not only involve $t \partial_t = \partial_s$ but also $\tilde{\xi}(s) = \sqrt{b(s)} \xi(b(s)) = \sqrt{t} \xi(t)$ in order to reproduce (A.2.15) and $\langle \tilde{\xi}(s) \tilde{\xi}(s') \rangle = \delta(s - s')$.

A.3 Derivation of FPE from SDE

The material presented in this chapter is adapted from the article by Lau and Lubensky [7] and part 4 of the book by Gardiner [4].

MPs $X(t)$ in one continuous degree of freedom can be modelled by stochastic differential equations (SDEs) of the form

$$\dot{x}_t = f(x_t, t) + g(x_t, t) \xi(t) , \quad x(t = t_0) = x_0 \quad (\text{A.3.1})$$

where $x_t = x(t)$ and with the Gaussian noise $\xi(t)$ defined by

$$\langle \xi(t) \rangle = 0 , \quad \langle \xi(t) \xi(t') \rangle = \delta(t - t') . \quad (\text{A.3.2})$$

The noise $\xi(t)$ itself is discontinuous, but its time-integral

$$Z(\Delta t) = \int_t^{t+\Delta t} \xi(t') dt' \quad (\text{A.3.3})$$

is continuous. The random variable $Z(\Delta t)$ is again Gaussian distributed with mean and variance given by

$$\langle Z(\Delta t) \rangle = \int_t^{t+\Delta t} \langle \eta(s) \rangle dt' = 0 , \quad (\text{A.3.4a})$$

$$\begin{aligned} \langle Z(\Delta t)^2 \rangle &= \int_t^{t+\Delta t} \int_t^{t+\Delta t} \langle \xi(t'') \xi(t') \rangle dt'' dt' \\ &= \int_t^{t+\Delta t} \int_t^{t+\Delta t'} \delta(t'' - t') dt'' dt' = \int_t^{t+\Delta t} dt' = \Delta t . \end{aligned} \quad (\text{A.3.4b})$$

Attempting an integration of the SDE (A.3.1) results into

$$\begin{aligned} \int_t^{t+\Delta t} \dot{x}(t') dt' &= x(t + \Delta t) - x(t) \\ &= \int_t^{t+\Delta t} f(x_{t'}, t') dt' + \int_t^{t+\Delta t} g(x_{t'}, t') \xi(t') dt' \end{aligned} \quad (\text{A.3.5a})$$

$$\stackrel{?}{\simeq} f(x_t, t) \Delta t + g(x_t, t) Z(\Delta t) , \quad (\text{A.3.5b})$$

where we encounter in the second line *stochastic integrals*, and the third line is preliminary, as we will see now.

Consider the second stochastic integral involving $\xi(t)$,

$$\mathcal{J}(t, \Delta t) = \int_t^{t+\Delta t} g(x(t'), t') \xi(t') dt' . \quad (\text{A.3.6})$$

We apply the mean-value theorem and write

$$\mathcal{J}(t, \Delta t) = g(x(t_\alpha), t_\alpha) \int_t^{t+\Delta t} \xi(t') dt' , \quad (\text{A.3.7})$$

where $t_\alpha = t + \alpha\Delta t$ with $0 \leq \alpha \leq 1$ and $x(t_\alpha) \simeq x(t) + \alpha\Delta x$ with $\Delta x = x(t + \Delta t) - x(t)$.

In a Riemann integral, the choice of α has no effect as soon as the limit $\Delta t \rightarrow 0$ is taken. But as $\xi(t)$ is discontinuous, we can not omit α from the integration of the SDE arguing that the effect of choosing α will be negligible for a sufficient small value of Δt . We therefore refine the integration of the SDE given in (A.3.5b) by writing

$$x(t + \Delta t) \simeq x(t) + f(x_t + \alpha\Delta x, t_\alpha)\Delta t + g(x_t + \alpha\Delta x, t_\alpha) Z(\Delta t) \quad (\text{A.3.8})$$

and will now explore the effect of α on the statistics of $x(t + \Delta t)$.

First we develop an integration scheme.

We require that the integration scheme has to be in first order of Δt , which is not yet accomplished in (A.3.8), since we know from (A.3.4b) that $Z(\Delta t) = \mathcal{O}(\sqrt{\Delta t})$.

To get (A.3.8) up to order Δt , we expand $f(x + \alpha\Delta x, t_\alpha)$ and $g(x + \alpha\Delta x, t_\alpha)$ in Δx to sufficient order and substitute recursively Δx from (A.3.8),

$$f(x_t + \alpha\Delta x, t_\alpha) = f(x_t, t_\alpha) + \mathcal{O}(\Delta t^{\frac{1}{2}}) \quad (\text{A.3.9a})$$

$$\begin{aligned} g(x_t + \alpha\Delta x, t_\alpha) &= g(x_t, t_\alpha) + g'(x_t, t_\alpha)\alpha\Delta x + \mathcal{O}(\Delta t) \\ &= g(x_t, t_\alpha) + \alpha g'(x_t, t_\alpha)g(x_t, t_\alpha)Z(\Delta t) + \mathcal{O}(\Delta t^{\frac{3}{2}}) \end{aligned} \quad (\text{A.3.9b})$$

where we used that $\Delta x = \mathcal{O}(\sqrt{\Delta t})$. Going with these two expansions back into (A.3.8), we yield the desired numeric integration scheme of linear order in Δt

$$x(t + \Delta t) = x_t + f(x_t, t)\Delta t + g(x_t, t)Z(\Delta t) + \alpha g'(x_t, t)g(x_t, t)Z(\Delta t)^2 . \quad (\text{A.3.10})$$

Here we have dropped the index on t_α , since the stochastic integrals are only stochastic in $x(t)$ and $\xi(t)$, and we assume that $f(x, t)$ and $g(x, t)$ are differentiable in t .

As we see from the expansions in (A.3.9), the choice of α amounts to choosing the point of evaluation in discretising the SDE. That is to say, for instance, $\alpha = 0$ corresponds to the pre-point rule and $\alpha = 1/2$ to the mid-point rule. In other words, if the SDE (A.3.1) is defined as an Itô SDE, we choose in (A.3.10) $\alpha = 0$ to solve the SDE numerically, and for the Stratonovich interpretation we choose $\alpha = 1/2$.

Having in place the integrated SDE (A.3.10) in linear order of Δt , we can derive from it the evolution equation for the PDF $p(x, t)$, known as Fokker-Planck equation (FPE). To this end, we consider an observable $A(x(t))$. We fix $x(t)$ and take $A(x(t+\Delta t))$ as a random variable due to the Gaussian variable $Z(\Delta t)$. The average of $A(x(t+\Delta t))$ is therefore conditioned on the value of $x(t)$ and can be written in terms of the conditional PDF $p(x+\Delta x, t+\Delta t|x, t)$,

$$\langle A(x(t+\Delta t)) \rangle = \int p(x+\Delta x, t+\Delta t|x, t) A(x+\Delta x) d(x+\Delta x) . \quad (\text{A.3.11})$$

On the other hand, we can expand $\langle A(x(t+\Delta t)) \rangle$ in Δt ,

$$\begin{aligned} \langle A(x(t+\Delta t)) \rangle &\simeq \langle A(x(t) + \dot{x}(t)\Delta t) \rangle \\ &\simeq A(x(t)) + A'(x(t)) \langle \dot{x}(t)\Delta t \rangle \\ &\quad + \frac{1}{2}A''(x(t)) \langle \dot{x}(t)^2\Delta t^2 \rangle + \mathcal{O}(\Delta t^3) . \end{aligned} \quad (\text{A.3.12})$$

For the two averages follow by substituting the integrated SDE (A.3.10),

$$\begin{aligned} \langle \dot{x}(t)\Delta t \rangle &\simeq \langle x(t+\Delta t) - x(t) \rangle \\ &\simeq f(x_t, t)\Delta t + g(x_t, t) \langle Z(\Delta t) \rangle + \alpha g'(x_t, t)g(x_t, t) \langle Z(\Delta t)^2 \rangle \\ &= f(x_t, t)\Delta t + \alpha g'(x_t, t)g(x_t, t)\Delta t \end{aligned} \quad (\text{A.3.13a})$$

$$\begin{aligned} \langle (\dot{x}(t)\Delta t)^2 \rangle &\simeq g(x_t, t)^2 \langle Z(\Delta t)^2 \rangle \\ &= g(x_t, t)^2 \Delta t , \end{aligned} \quad (\text{A.3.13b})$$

where we kept only terms of linear order in Δt .

Substituting these averages back into (A.3.12) yields

$$\begin{aligned} \langle A(x(t+\Delta t)) \rangle &\simeq A(x(t)) + A'(x(t)) [f(x_t, t) + \alpha g'(x_t, t)g(x_t, t)] \Delta t \\ &\quad + \frac{1}{2} A''(x(t)) g(x_t, t)^2 \Delta t . \end{aligned} \quad (\text{A.3.14})$$

Note that for $\alpha = 0$ the above formula also derives from Itô's formula in (A.1.5) for the change of variable from $x(t)$ to $A(x(t))$.

The expansion (A.3.14), involving only the observable $A(x(t))$, can be passed on to an equation for $p(x, t)$ by substituting (A.3.11) for the l.h.s., and taking the average with respect to x at time t ,

$$\begin{aligned} &\int A(x+\Delta x) p(x+\Delta x, t+\Delta t) d(x+\Delta x) - \int A(x) p(x, t) dx \\ &= \Delta t \cdot \int \left[A'(x) [f(x_t, t) + \alpha g'(x_t, t)g(x_t, t)] \right. \\ &\quad \left. + \frac{1}{2} A''(x) g(x_t, t)^2 \right] p(x, t) dx . \end{aligned} \quad (\text{A.3.15})$$

Integration by parts and discarding the boundary terms due to the normalisation condition of $p(x, t)$ yields

$$\begin{aligned} &\int A(x+\Delta x) p(x+\Delta x, t+\Delta t) d(x+\Delta x) - \int A(x) p(x, t) dx \\ &= \Delta t \cdot \int A(x) \left[-\partial_x [f(x_t, t) + \alpha g'(x_t, t)g(x_t, t)] \right. \\ &\quad \left. + \frac{1}{2} \partial_x^2 g(x_t, t)^2 \right] p(x, t) dx . \end{aligned} \quad (\text{A.3.16})$$

Since $A(x)$ is arbitrary, and $(x+\Delta x)$ is just an integration variable, we can read off in differential form

$$\begin{aligned} \frac{p(x, t+\Delta t) - p(x, t)}{\Delta t} &= \left[-\partial_x [f(x_t, t) + \alpha g'(x_t, t)g(x_t, t)] \right. \\ &\quad \left. + \frac{1}{2} \partial_x^2 g(x_t, t)^2 \right] p(x, t) \end{aligned} \quad (\text{A.3.17})$$

which in the continuous limit $\Delta t \rightarrow 0$ finally becomes the FPE

$$\dot{p}(x, t) = \left[-\partial_x [f(x_t, t) + \alpha g'(x_t, t)g(x_t, t)] + \frac{1}{2} \partial_x^2 g(x_t, t)^2 \right] p(x, t) . \quad (\text{A.3.18})$$

Note that the FPE depends on α .

The FPE needs to be completed by the initial PDF $p_0(x)$ for the time $t_0 < t$ from which the values x_0 are sampled. The solution of the FPE is then the PDF $p(x, t)$ for x at time t . For the choice $p_0(x) = \delta(x - x_0)$ the solution of the FPE will be the conditional PDF $p(x, t|x_0, t_0)$, from which by

$$p(x, t) = \int p(x, t|x_0, t_0) p_0(x_0) dx_0 \quad (\text{A.3.19})$$

the solution of the FPE with arbitrary initial PDF $p_0(x_0)$ can be obtained. In that sense, $p(x, t|x_0, t_0)$ is the Green's function of the FPE and obeys the same FPE as $p(x, t)$,

$$\begin{aligned} \dot{p}(x, t|x_0, t_0) = & \left[-\partial_x [f(x_t, t) + \alpha g'(x_t, t)g(x_t, t)] \right. \\ & \left. + \frac{1}{2} \partial_x^2 g(x_t, t)^2 \right] p(x, t|x_0, t_0) , \end{aligned} \quad (\text{A.3.20})$$

but without specifying an initial condition.

A set of values for x that follows $p(x, t)$ can in principle be obtained by integrating the SDE (A.3.1) using the scheme (A.3.10) for a certain value of α and in the limit $\Delta t \rightarrow 0$.⁴¹ However, in numeric integrations, only finite Δt are possible, and using the integration scheme (A.3.10) will remain an approximation. Higher order integrations schemes exist, but in the majority of stochastic processes the scheme (A.3.10) is sufficient.

We note that Lau and Lubensky use in [7] the representation of a PDF as the expectation of the δ -function,

$$\begin{aligned} p(x, t|x_0, t_0) &= \int p(x') \delta(x' - x(t; x_0, t_0)) dx' \\ &= \langle \delta(x - x(t; x_0, t_0)) \rangle_{p(x)} , \end{aligned} \quad (\text{A.3.21})$$

where the parametric dependency of $p(x, t|x_0, t_0)$ has been passed on to the random variable $x(t; x_0, t_0)$.

Our derivation of the FPE becomes equivalent to the derivation of Lau and Lubensky by substituting $A(x(t)) = \delta(x - x(t; x_0, t_0))$.

⁴¹or, if possible, by solving the SDE explicitly using α -calculus.

A.4 Derivation of WPI from SDE

The material presented in this chapter follows closely the article by Lau and Lubensky [7].

The aim is to introduce the Wiener path integral (WPI) representation of continuous MPs. A WPI is used to express the conditional PDF as

$$p(x_t, t | x_0, t_0) = \int_{(x_0, t_0)}^{(x_t, t)} \mathcal{D}x(\cdot) P[x(\cdot) | x_0] . \quad (\text{A.4.1})$$

Here, $P[x(\cdot) | x_0]$ is the probability density functional of the path $x(\cdot)$, and $\mathcal{D}x(\cdot)$ is the integration measure in function space. The path integral above is the sum of the probabilities of all paths $x(\cdot)$ that connect a given initial value x_0 at time t_0 with x_t at time t . The notation $x(\cdot)$ emphasises that the whole trajectory is considered, and not, as $x(t')$ might suggest, the value of $x(t)$ at a single time t' . Instead of probability density functional we will also call $P[x(\cdot) | x_0]$ *path probability*.

The WPI above is still only symbolic. The most direct way to concretise the path integral is to discretise time as $t_i = t_0 + i\Delta t$ where Δt is the time step, and also discretise the path $x(\cdot)$ as the sequence (x_1, x_2, \dots, x_N) , where $x_1 = x_0$, $x_N = x_t$, $N = (t - t_0)/\Delta t$ and $x_i = x(t_i)$. Each x_i at time t_i is a random variable and hence follows a PDF $p_i(x_i, t_i)$.

The Markov assumption states that the PDF only depends on the most recent event, and we can write

$$p_i(x_i, t_i) = p(x_i, t_i | x_{i-1}, t_{i-1}) \quad \forall 2 \leq i \leq N , \quad (\text{A.4.2a})$$

$$p_1(x_1, t_1) = p_0(x_1) . \quad (\text{A.4.2b})$$

Hence, the MPs is completely determined by the *propagator* $p(x_{i+1}, t_{i+1} | x_i, t_i)$ and the initial PDF $p_0(x_1)$.

As a direct consequence of the Chapman-Kolmogorov relation (I.1.4), the solution of the conditional FPE can be written as the integration of the product of all propagators with respect to all intermediate variables,

$$p(x_t, t | x_0, t_0) = \int \left[\prod_{i=2}^{N-1} dx_i \right] \prod_{i=1}^{N-1} p(x_{i+1}, t_{i+1} | x_i, t_i) . \quad (\text{A.4.3})$$

The above formula can be viewed as the prototype of a WPI, where we identify the prototypical path probability and integration measure as

$$P[x(\cdot)|x_0] \sim \prod_{i=1}^{N-1} p(x_{i+1}, t_{i+1}|x_i, t_i) , \quad (\text{A.4.4a})$$

$$\mathcal{D}x(\cdot) \sim \prod_{i=2}^{N-1} dx_i . \quad (\text{A.4.4b})$$

The propagator is equivalent to Green's function of the FPE, cf. (A.3.19), which can be obtained from the FPE (A.3.20) for small Δt ([20] p. 73),

$$\begin{aligned} p(x_{i+1}, t_i + \Delta t | x_i, t_i) &\simeq \frac{1}{\sqrt{2\pi\Delta t g(x_i, t_i)^2}} \\ &\times \exp \left[\frac{x_{i+1} - x_i - f(x_i, t_i) - \alpha g'(x_i, t_i)g(x_i, t_i)}{2\Delta t g(x_i, t_i)^2} \right] . \end{aligned} \quad (\text{A.4.5})$$

However, the interpretation of the resulting stochastic integral for the functional $P[x(\cdot)|x_0]$ is ambiguous.

In the following, we will instead build on the SDE discretised in α -point, (A.3.8), to yield a definition of $P[x(\cdot)|x_0]$ and $\mathcal{D}x(\cdot)$ in terms of the discretisation introduced above.

The essence of the derivation is to transform from the random variable $Z(\Delta t)$, of which we know the statistical properties from (A.3.4), to the random variable x_{i+1} . The resulting PDF for x_{i+1} is then the propagator $p(x_{i+1}, t_{i+1}|x_i, t_i)$ used above.

We formulate the mentioned transformation of probability as

$$\mathcal{N}(Z) dZ = p(x_{i+1}, t_{i+1}|x_i, t_i) dx_{i+1} , \quad (\text{A.4.6})$$

where $\mathcal{N}(Z)$ is the PDF of Z . To calculate the Jacobian, we need Z as a function of x_{i+1} . At this point, the underlying SDE enters the calculation by solving the discretised SDE (A.3.8) for Z ,

$$h(x_{i+1}; t_{i+1}, x_i, t_i) := \frac{x_{i+1} - x_i - f_{i_\alpha} \Delta t}{g_{i_\alpha}} = Z . \quad (\text{A.4.7})$$

Here, we take f_{i_α} and g_{i_α} to be evaluated in α -point, that is

$$f_{i_\alpha} := f(x_i + \alpha \Delta x, t_i + \alpha \Delta t) , \quad g_{i_\alpha} := g(x_i + \alpha \Delta x, t_i + \alpha \Delta t) . \quad (\text{A.4.8})$$

The transformation of probability then takes the form

$$p(x_{i+1}, t_{i+1} | x_i, t_i) = \left| \frac{\partial h(x_{i+1}; t_{i+1}, x_i, t_i)}{\partial x_{i+1}} \right| \mathcal{N}(h(x_{i+1}; t_{i+1}, x_i, t_i)) . \quad (\text{A.4.9})$$

The next step is to determine the two factors above which will form the propagator $p(x_{i+1}, t_{i+1} | x_i, t_i)$.

The first factor, using (A.3.8), is readily determined to be

$$\left| \frac{\partial h(x_{i+1}; t_{i+1}, x_i, t_i)}{\partial x_{i+1}} \right| = \frac{1 - \alpha f'_{i_\alpha} \Delta t}{g_{i_\alpha}} - \alpha g'_{i_\alpha} \frac{x_{i+1} - x_i - f_{i_\alpha} \Delta t}{g_{i_\alpha}^2} . \quad (\text{A.4.10})$$

The second factor is best determined by writing the $\mathcal{N}(Z)$ as the expectation of a δ -function

$$\mathcal{N}(h(x_{i+1}; t_{i+1}, x_i, t_i)) = \langle \delta(Z' - h(x_{i+1}; t_{i+1}, x_i, t_i)) \rangle_{\mathcal{N}(Z')} , \quad (\text{A.4.11})$$

in the same fashion as in (A.3.21). Using the Fourier representation of the δ -function, we obtain

$$\begin{aligned} \delta(h(x_{i+1}; t_{i+1}, x_i, t_i) - Z') &= \frac{1}{2\pi} \int \exp [ik h(x_{i+1}; t_{i+1}, x_i, t_i)] \\ &\quad \times \exp [-ik Z'] dk . \end{aligned} \quad (\text{A.4.12})$$

The average $\langle \dots \rangle_{\mathcal{N}(Z')}$ only affects the factor in the second line.

At this point, the statistical properties stated in (A.3.4) are taken into account by substituting for $\mathcal{N}(Z)$ a Gaussian distribution with zero mean and variance Δt and performing the resulting Gaussian integral,

$$\begin{aligned} \left\langle \int \exp [-ik Z'] dk \right\rangle_{\mathcal{N}(Z')} &= \int \mathcal{N}(Z') \int \exp [-ik Z'] dk dZ' \\ &= \frac{1}{\sqrt{2\pi\Delta t}} \int \int \exp \left[-\frac{Z'^2}{2\Delta t} - ik Z' \right] dZ' dk \\ &= \int \exp \left[-\frac{1}{2} k^2 \Delta t \right] dk . \end{aligned} \quad (\text{A.4.13})$$

Combining (A.4.10) with (A.4.11) and (A.4.12), (A.4.7), (A.4.13) and writing $\Delta x = x_{i+1} - x_i$, we obtain

$$p(x_{i+1}, t_{i+1} | x_i, t_i) = \frac{1}{2\pi g_{i_\alpha}} \int \left[1 - \alpha f'_{i_\alpha} \Delta t - \alpha g'_{i_\alpha} \frac{\Delta x - f_{i_\alpha} \Delta t}{g_{i_\alpha}} \right] \times \exp \left[ik \frac{\Delta x - f_{i_\alpha} \Delta t}{g_{i_\alpha}} - \frac{1}{2} k^2 \Delta t \right] dk, \quad (\text{A.4.14})$$

which is already the desired propagator, but not in the desired exponential form (A.4.5).

We could in principle write the prefactor in the rectangular brackets as $\exp \ln[\dots]$ and expand $\ln[\dots]$ to second order to collect also the terms $\Delta x^2 = \mathcal{O}(\Delta t)$. This procedure, however, is considered inconsistent with the concept of path integrals ([7] p. 8).

We therefore rewrite the problematic term, that is the one that involves Δx , as the derivative of the exponential function,

$$\begin{aligned} & -\alpha g'_{i_\alpha} \int \left[\frac{\Delta x - f_{i_\alpha} \Delta t}{g_{i_\alpha}} \right] \exp \left[ik \frac{\Delta x - f_{i_\alpha} \Delta t}{g_{i_\alpha}} - \frac{1}{2} k^2 \Delta t \right] dk \\ &= -\alpha g'_{i_\alpha} \int \exp \left[-\frac{1}{2} k^2 \Delta t \right] (-i \partial_k) \exp \left[ik \frac{\Delta x - f_{i_\alpha} \Delta t}{g_{i_\alpha}} \right] dk \\ &= \alpha i k g'_{i_\alpha} \Delta t \int \exp \left[ik \frac{\Delta x - f_{i_\alpha} \Delta t}{g_{i_\alpha}} - \frac{1}{2} k^2 \Delta t \right] dk, \end{aligned} \quad (\text{A.4.15})$$

where the last line follows by integration by parts and discarding the boundary terms. The remaining prefactor does not involve Δx and can be included into the exponential function by writing it in the form $\exp \ln[\dots]$

and expanding $\ln[\dots]$ to linear order in Δt ,

$$\begin{aligned}
 p(x_{i+1}, t_{i+1} | x_i, t_i) &= \frac{1}{2\pi g_{i_\alpha}} \int \exp \left[ik \frac{\Delta x - f_{i_\alpha} \Delta t}{g_{i_\alpha}} - \frac{1}{2} k^2 \Delta t \right] \\
 &\quad \times (1 - \alpha f'_{i_\alpha} \Delta t + ik g'_{i_\alpha} \Delta t) \, dk \\
 &= \frac{1}{2\pi g_{i_\alpha}} \int \exp \left[ik \frac{\Delta x - f_{i_\alpha} \Delta t}{g_{i_\alpha}} - \frac{1}{2} k^2 \Delta t \right. \\
 &\quad \left. + \ln [1 + \alpha (ik g'_{i_\alpha} - f'_{i_\alpha}) \Delta t] \right] dk \\
 &= \frac{1}{2\pi g_{i_\alpha}} \int \exp \left[ik \frac{\Delta x - f_{i_\alpha} \Delta t}{g_{i_\alpha}} - \frac{1}{2} k^2 \Delta t \right. \\
 &\quad \left. + \alpha (ik g'_{i_\alpha} - f'_{i_\alpha}) \Delta t \right] dk \\
 &= \frac{1}{2\pi g_{i_\alpha}} \int \exp \left[-k^2 \frac{\Delta t}{2} + k \frac{i \Delta t}{g_{i_\alpha}} \left(\frac{\Delta x}{\Delta t} - f_{i_\alpha} + \alpha g'_{i_\alpha} g_{i_\alpha} \right) \right. \\
 &\quad \left. - \alpha f'_{i_\alpha} \Delta t \right] dk . \tag{A.4.16}
 \end{aligned}$$

The resulting Gaussian integral can readily be calculated and we finally end up with⁴²

$$\begin{aligned}
 p(x_{i+1}, t_{i+1} | x_i, t_i) &= \frac{\sqrt{2\pi}}{2\pi g_{i_\alpha} \sqrt{\Delta t}} \exp \left[-\frac{\frac{\alpha f'_{i_\alpha} \Delta t^2}{2} + \frac{\Delta t^2}{4g_{i_\alpha}^2} \left(\frac{\Delta x}{\Delta t} - f_{i_\alpha} + \alpha g'_{i_\alpha} g_{i_\alpha} \right)^2}{\frac{\Delta t}{2}} \right] \\
 &= \frac{1}{\sqrt{2\pi \Delta t g_{i_\alpha}^2}} \exp \left[-\frac{\Delta t}{2g_{i_\alpha}^2} \left(\frac{\Delta x}{\Delta t} - f_{i_\alpha} + \alpha g_{i_\alpha} g'_{i_\alpha} \right)^2 - \alpha \Delta t f'_{i_\alpha} \right] \tag{A.4.17}
 \end{aligned}$$

which is of the expected form in (A.4.5), only that we now have the Jacobian $\alpha \Delta t f'_{i_\alpha}$, and $f(x, t)$ and $g(x, t)$ have to be evaluated in α -point. Note

⁴²Defining $y_i := k/g_{i_\alpha}$ instead of performing the Gaussian integration yields the so called Hubbard-Stratonovich transform of a WPI, cf. [7], which has important applications in field theories.

that for pre-point, $\alpha = 0$, both forms are equivalent.

Having the propagator in place, we can go back to our prototype of a WPI, (A.4.3), and obtain after substituting (A.4.17),

$$\begin{aligned}
 p(x_t, t | x_0, t_0) &= \int \left[\prod_{i=2}^{N-1} dx_i \right] \prod_{i=1}^{N-1} p(x_{i+1}, t_{i+1} | x_i, t_i) \\
 &= \int \left[\prod_{i=2}^{N-1} dx_i \right] \prod_{i=1}^{N-1} \frac{1}{\sqrt{2\pi g_i^2 \Delta t}} \\
 &\quad \times \exp \left[-\frac{\Delta t}{2g_{i_\alpha}^2} \left(\frac{x_{i+1} - x_i}{\Delta t} - f_{i_\alpha} + \alpha g_{i_\alpha} g'_{i_\alpha} \right)^2 \right. \\
 &\quad \left. - \alpha \Delta t f'_{i_\alpha} \right] \\
 &= \frac{1}{\sqrt{2\pi g_N^2 \Delta t}} \int \left[\prod_{i=2}^{N-1} \frac{dx_i}{\sqrt{2\pi g_i^2 \Delta t}} \right] \\
 &\quad \times \exp \left[-\sum_{i=1}^{N-1} \frac{\Delta t}{2g_{i_\alpha}^2} \left(\frac{x_{i+1} - x_i}{\Delta t} - f_{i_\alpha} + \alpha g_{i_\alpha} g'_{i_\alpha} \right)^2 \right. \\
 &\quad \left. - \alpha \Delta t f'_{i_\alpha} \right]. \tag{A.4.18}
 \end{aligned}$$

We are now able to substitute our prototype of the integration measure, (A.4.4b), by the definition

$$\int \mathcal{D}x(\cdot) := \lim_{\substack{N \rightarrow \infty \\ \Delta t \rightarrow 0}} \frac{1}{\sqrt{2\pi \Delta t g_N^2}} \int \left[\prod_{i=2}^{N-1} \frac{dx_i}{\sqrt{2\pi g_i^2 \Delta t}} \right], \tag{A.4.19}$$

and the prototype of the path-probability in (A.4.4a) by

$$P[x(\cdot) | x_0] := \lim_{\substack{N \rightarrow \infty \\ \Delta t \rightarrow 0}} \exp \left[-\Delta t \sum_{i=1}^{N-1} s_i(x_i, x_{i+1}) \right] \tag{A.4.20}$$

with

$$s_i(x_i, x_{i+1}) := \frac{1}{2g_{i_\alpha}^2} \left(\frac{x_{i+1} - x_i}{\Delta t} + f_{i_\alpha} + \alpha g_{i_\alpha} g'_{i_\alpha} \right)^2 - \alpha f'_{i_\alpha}, \tag{A.4.21}$$

In this form, the continuous limit for the path probability can be explicitly performed and we obtain

$$P[x(\cdot)|x_0] = \exp \left[-\mathcal{S}[x(\cdot)] \right] \quad (\text{A.4.22})$$

with the action functional

$$\mathcal{S}[x(\cdot)] := \int_{t_0}^t s(x(\tau), \dot{x}(\tau), \tau) \, d\tau, \quad (\text{A.4.23a})$$

$$s(x, \dot{x}, \tau) := \frac{[\dot{x} - f(x, \tau) + \alpha g'(x, \tau)g(x, \tau)]^2}{2g(x, \tau)^2} + \alpha f'(x, \tau). \quad (\text{A.4.23b})$$

Note that the integral in (A.4.23a) is a stochastic integral, and for discretisation, $f(x, t)$ and $g(x, t)$ have to be discretised in α -point as defined in (A.4.8).

In closing, we remark that from this form of the WPI, the corresponding FPE can be retrieved [7], which brings us full circle with regard to the three equivalent formulations of continuous MPs.

A.5 Overview of SDE, FPE and WPI

We provide an overview of three equivalent descriptions of continuous MPs (MPs), being stochastic differential equations (SDEs), the Fokker-Planck equation (FPE) and Wiener path integrals (WPI), along with a matching first order numerical integration scheme (NUM).

We distinguish the two cases where the MP is initially given by a SDE, or where the MP is initially given by a FPE, and, respectively, the equivalent other forms are desired.

In the same fashion, we also provide the equivalent SDEs in Itô and Stratonovich convention.

SDE Suppose a continuous MP is given by a SDE defined in α -convention ($\alpha = 0$ for Itô and $\alpha = 1/2$ for Stratonovich), then are equivalent

$$(\text{SDE}) \quad \dot{x}_t = f(x_t, t) + g(x_t, t) \xi(t), \quad \alpha\text{-point} \quad (\text{A.5.1a})$$

$$(\text{NUM}) \quad x(t+\Delta t) = x_t + f(x_t, t)\Delta t + g(x_t, t)Z(\Delta t) + \alpha g'(x_t, t)g(x_t, t)Z(\Delta t)^2 \quad (\text{A.5.1b})$$

$$(\text{FPE}) \quad \dot{p}(x, t) = \left[-\partial_x [f(x, t) + \alpha g'(x, t)g(x, t)] + \frac{1}{2} \partial_x^2 g(x, t)^2 \right] p(x, t) \quad (\text{A.5.1c})$$

$$(\text{WPI}) \quad \mathcal{S}[x(\cdot)] = \int_{t_0}^t \frac{[\dot{x} - f(x_\tau, \tau) + \alpha g'(x_\tau, \tau)g(x_\tau, \tau)]^2}{2g(x_\tau, \tau)^2} + \alpha f'(x_\tau, \tau) d\tau, \quad \alpha\text{-point}. \quad (\text{A.5.1d})$$

The index t denotes that t is to be taken as argument. The Gaussian noise ξ has zero mean and is δ -correlated, $\langle \xi(t - t') \rangle = \delta(t - t')$, and according to (A.3.4), $Z(\Delta t)$ is a Gaussian random variable with zero mean and variance Δt . The α -point discretisation is defined in (A.4.8).

According to van Kampen ([19, 5]), when deterministic and stochastic influences have distinguished sources, the SDE is to be taken for $\alpha = 1/2$, in order to retain a clear-cut interpretation of $f(x_t, t)$ as force and $g(x_t, t)\xi(t)$ as noise. Otherwise, the choice of α is a matter of taste.

FPE in Itô-form Suppose a continuous MP is given by a FPE in terms of drift and diffusion,

$$D^{(1)}(x, t) = f(x, t) + \alpha g'(x, t)g(x, t) , \quad (\text{A.5.2a})$$

$$D^{(2)}(x, t) = \frac{1}{2}g(x, t)^2 , \quad (\text{A.5.2b})$$

then are equivalent

$$(\text{FPE}) \quad \dot{p}(x, t) = \left[-\partial_x D^{(1)}(x, t) + \partial_x^2 D^{(2)}(x, t) \right] p(x, t) \quad (\text{A.5.3a})$$

$$(\text{SDE}) \quad \dot{x}_t = D^{(1)}(x, t) - \alpha D^{(2)'}(x_t, t) + \sqrt{2D^{(2)}(x_t, t)} \xi(t) , \quad \alpha\text{-point} \quad (\text{A.5.3b})$$

$$(\text{NUM}) \quad x(t + \Delta t) = x(t) + \left[D^{(1)}(x, t) + (1 - 2\alpha)D^{(2)'}(x_t, t) \right] \Delta t + \sqrt{2D^{(2)}(x_t, t)} Z(\Delta t) + \alpha D^{(2)'}(x_t, t) Z(\Delta t)^2 \quad (\text{A.5.3c})$$

$$(\text{WPI}) \quad S[x(\cdot)] = \int_{t_0}^t \frac{\left(\dot{x}_\tau - D^{(1)}(x, t) + 2(\alpha - 1)D^{(2)'}(x_\tau, \tau) \right)^2}{4D^{(2)}(x_\tau, \tau)} + \alpha(D^{(1)}(x_\tau, \tau) - D^{(2)'}(x_\tau, \tau)) + \alpha(1 - \alpha)D^{(2)''}(x_\tau, \tau) d\tau , \quad \alpha\text{-point} . \quad (\text{A.5.3d})$$

Again, the index t denotes that t is to be taken as argument. The Gaussian noise ξ has zero mean and is δ -correlated, $\langle \xi(t - t') \rangle = \delta(t - t')$, and according to (A.3.4), $Z(\Delta t)$ is a Gaussian random variable with zero mean and variance Δt . The α -point discretisation is defined in (A.4.8).

Note that the SDE in this forms defines the same dynamics regardless the choice of α .

FPE in Stratonovich-form The FPE is often given in the so-called Stratonovich form, that is in terms of force and diffusion,

$$\begin{aligned} F(x, t) &= D^{(1)}(x, t) - D^{(2)'}(x, t) \\ &= f(x, t) + (\alpha - 1)g'(x, t)g(x, t) , \end{aligned} \quad (\text{A.5.4a})$$

$$D(x, t) = D^{(2)}(x, t) = \frac{1}{2}g(x, t)^2 . \quad (\text{A.5.4b})$$

For convenience, we also give the table of equivalent LE and WPI for this case,

$$(\text{FPE}) \quad \dot{p}(x, t) = \left[-\partial_x F(x, t) + \partial_x D(x, t) \partial_x \right] p(x, t) \quad (\text{A.5.5a})$$

$$\begin{aligned} (\text{SDE}) \quad \dot{x}_t &= F(x_t, t) + (1 - \alpha)D'(x_t, t) \\ &\quad + \sqrt{2D(x_t, t)} \xi(t) , \quad \alpha\text{-point} \end{aligned} \quad (\text{A.5.5b})$$

$$\begin{aligned} (\text{NUM}) \quad x(t + \Delta t) &= x(t) + \left[F(x_t, t) + (1 - \alpha)D'(x_t, t) \right] \Delta t \\ &\quad + \sqrt{2D(x_t, t)} Z(\Delta t) + \alpha D'(x_t, t) Z(\Delta t)^2 \end{aligned} \quad (\text{A.5.5c})$$

$$\begin{aligned} (\text{WPI}) \quad S[x(\cdot)] &= \int_{t_0}^t \frac{(\dot{x}_\tau - F(x_\tau, \tau) + (2\alpha - 1)D'(x_\tau, \tau))^2}{4D(x_\tau, \tau)} \\ &\quad + \alpha F'(x_\tau, \tau) + \alpha(1 - \alpha)D''(x_\tau, \tau) d\tau , \quad \alpha\text{-point} . \end{aligned} \quad (\text{A.5.5d})$$

Again, the index t denotes that t is to be taken as argument. The Gaussian noise ξ has zero mean and is δ -correlated, $\langle \xi(t - t') \rangle = \delta(t - t')$, and according to (A.3.4), $Z(\Delta t)$ is a Gaussian random variable with zero mean and variance Δt . The α -point discretisation is defined in (A.4.8).

Note that the SDE in this forms defines the same dynamics regardless the choice of α .

Itô and Stratonovich SDE The two predominantly used interpretations of SDEs are those of Itô ($\alpha = 0$) and Stratonovich ($\alpha = 1/2$). It often is convenient, to switch from a Itô SDE to a Stratonovich one and vice versa. Again, ξ is a Gaussian noise with zero mean and correlation $\langle \xi(t - t') \rangle = \delta(t - t')$. See (A.4.8) for the definition of discretisation in α -point.

The key observation is that a SDE of the form

$$\dot{x}_t = f(x_t, t) - \alpha g'(x_t, t)g(x_t, t) + g(x_t, t) \xi(t) , \quad \alpha\text{-point} , \quad (\text{A.5.6})$$

defines the same dynamics for arbitrary α with $0 \leq \alpha \leq 1$.

For the Itô SDE

$$\dot{x}_t = f(x_t, t) + g(x_t, t) \xi(t) , \quad \text{pre-point} , \quad (\text{A.5.7a})$$

the equivalent Stratonovich SDE reads

$$\dot{x}_t = f(x_t, t) - \frac{1}{2}g'(x_t, t) + g(x_t, t) \xi(t) , \quad \text{mid-point} . \quad (\text{A.5.7b})$$

For the Stratonovich SDE

$$\dot{x}_t = f(x_t, t) + g(x_t, t) \xi(t) , \quad \text{mid-point} , \quad (\text{A.5.8a})$$

the equivalent Itô SDE reads

$$\dot{x}_t = f(x_t, t) + \frac{1}{2}g'(x_t, t) + g(x_t, t) \xi(t) , \quad \text{pre-point} . \quad (\text{A.5.8b})$$

In general, for a SDE defined in α -point

$$\dot{x}_t = f(x, t) + g(x_t, t) \xi(t) , \quad \alpha\text{-point} \quad (\text{A.5.9a})$$

the equivalent SDE in $\tilde{\alpha}$ -point reads

$$\dot{x}_t = f(x, t) + (\alpha - \tilde{\alpha})g'(x, t)g(x, t) + g(x_t, t) \xi(t) , \quad \tilde{\alpha}\text{-point} \quad (\text{A.5.9b})$$